BioMed Research International

Laboratory Medicine

Guest Editors: Mina Hur, Andrew St. John, and Antonio La Gioia

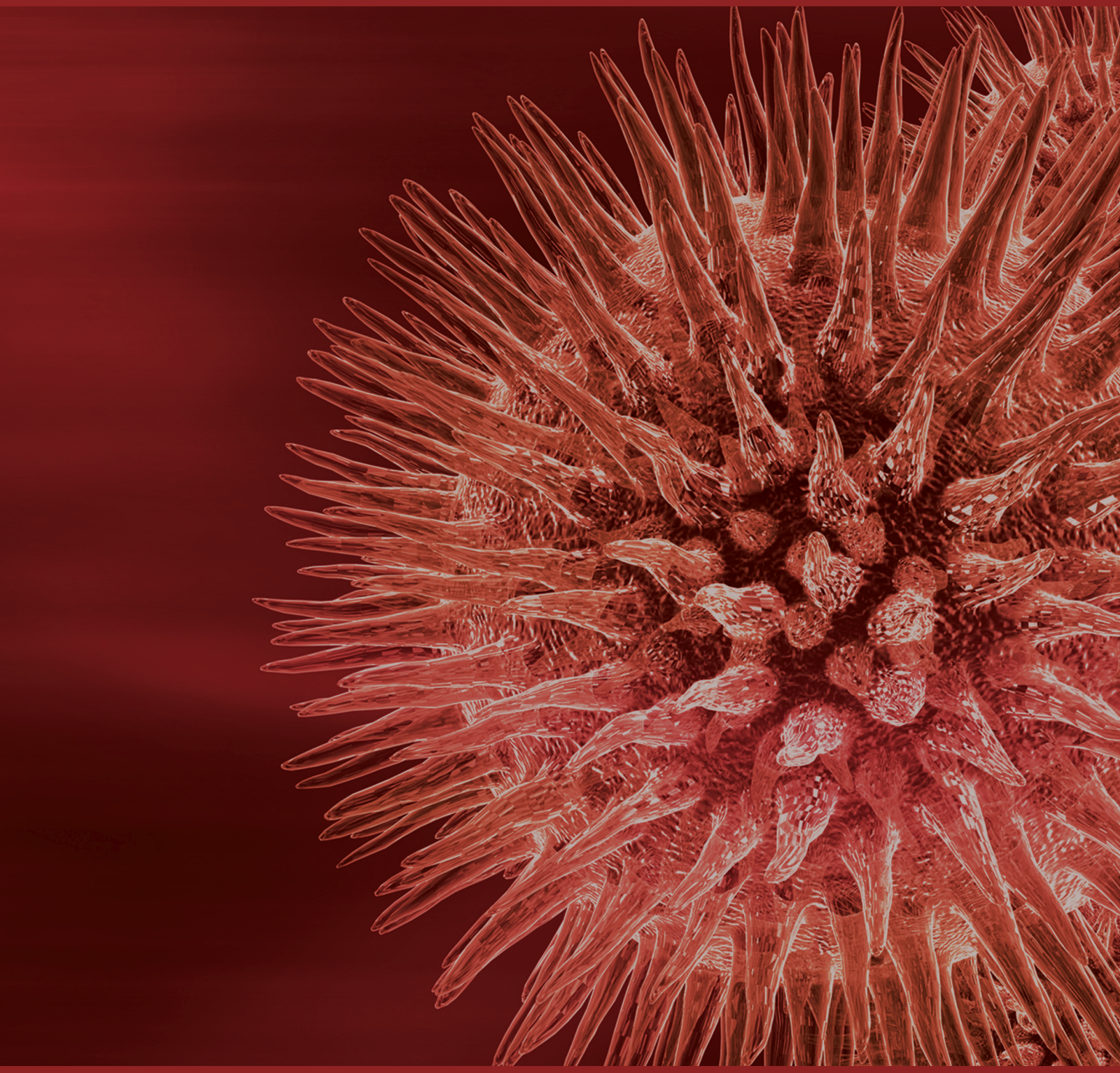

Laboratory Medicine

BioMed Research International

Laboratory Medicine

Guest Editors: Mina Hur, Andrew St. John,
and Antonio La Gioia

Contents

Hindawi Publishing Corporation
BioMed Research International
Volume 2013, Article ID 269194, 2 pages
http://dx.doi.org/10.1155/2013/269194

Editorial
Laboratory Medicine

Mina Hur,[1] Andrew St. John,[2] and Antonio La Gioia[3]

[1] *Department of Laboratory Medicine, Konkuk University School of Medicine, 120-1 Neungdong-ro, Hwayang-dong, Gwangjin-gu, Seoul 143-729, Republic of Korea*
[2] *Australian Research Council, Canberra, ACT, Australia*
[3] *Italian Society of Clinical Biochemistry and Molecular Biology, Milan, Italy*

Correspondence should be addressed to Mina Hur; dearmina@hanmail.net

Received 11 April 2013; Accepted 11 April 2013

Clinical laboratories have a vital role to play in translating research findings into clinically useful measurements. This involves assessment of new procedures to ensure that they are analytically valid and also continually integrating the findings from new studies into routine practice. These important tasks are covered in this special issue on laboratory medicine which includes a wide variety of laboratory-related topics as illustrated by three review articles and 12 research papers. The first review article by D.-H. Ko et al. comprehensively examines the methods available for haptoglobin typing and discusses the characteristics, clinical applications, and limitations of each method. A. Noto et al. describe the role of neutrophil gelatinase-associated lipocalin (NGAL) for managing acute kidney injury and the potential benefits derived from the combined clinical use of urine NGAL and metabolomics in kidney disease. The third review by E. Urrechaga et al. looks at new laboratory biomarkers for hypochromia including their clinical significance and utility in daily practice.

Several papers examine issues in diagnostic hematology, one of the traditional areas of laboratory testing. Y. Nam et al. assess hypercoagulability using a relatively new thrombomodulin-induced thrombin generation assay (TGA) in patients with liver cirrhosis. They show that, although routine coagulation tests did not detect the thrombotic tendency in cirrhosis, the TGA could detect hypercoagulability in cirrhosis. The paper by M. Hur et al. emphasizes that prothrombin time international normalized ratio (INR) measurements by point-of-care testing coagulometers still need to be confirmed with INR measurements in the laboratory. H. R. Lee et al. evaluate the relationship between mean platelet volume (MPV) and characteristics of cord blood (CB) units and shows that MPV may be one of the most useful parameters to assist with making decisions about the priority for processing specimens in the cord blood bank. F. Chongliang et al., in their interesting study on complete blood counts, suggest that a model that uses levels of neutrophils, lymphocytes, and platelets is potentially useful in the objective evaluation of survival time or disease severity in unselected critically ill patients.

Three interesting papers come from the areas of serology/immunology, chemistry, and microbiology. K. Lee et al. evaluate the overall efficacy of reverse sequence screening for syphilis (RSSS) and examine the practical issues associated with the routine investigation of syphilis. The study by M. Han et al. analyzes the degree of concordance between the various multiple allergen simultaneous test assays and a reference method. J. Gervasoni et al. evaluate various assay kits for 25-hydroxyvitamin D2/D3 and show that they have acceptable agreement with liquid chromatography-tandem mass spectrometry.

Five papers deal with the growing area of molecular diagnostics. T. Kaewphinit et al. combined a loop-mediated isothermal amplification method with a chromatographic lateral-flow dipstick and show that it can specifically and rapidly detect the IS6110 gene of *M. tuberculosis*. S. Kim et al. introduced a new allele-specific real-time PCR system for *TPMT* genotyping, which can be used to improve the efficacy and safety of thiopurine treatments in clinical practice. R. Januchowsk et al. analyzed *MDR* gene expression in drug-resistant ovarian cancer cell lines. They suggest that it is

possible to predict cross-resistance to other drugs when the classical *MDR*, which is correlated with P-gp expression, is involved. S. M. Hwang et al. evaluated the human platelet antigen (HPA) genotype and/or the CD109 mRNA expression in various human cell types. They demonstrate that the 4-1BB signal pathway plays a key role in organ transplantation tolerance. Lastly the paper by Y. Shi et al. demonstrates that gene silencing of 4-1BB by RNA interference inhibits the acute rejection in rats with liver transplantation.

We hope that these papers in this special issue of BioMed Research International will help to confirm the important role that clinical laboratories play in translational research and the need to continuously update laboratory practice as new findings and developments appear.

Mina Hur
Andrew St. John
Antonio La Gioia

Hindawi Publishing Corporation
BioMed Research International
Volume 2013, Article ID 754169, 4 pages
http://dx.doi.org/10.1155/2013/754169

Research Article

Mean Platelet Volume Reflect Hematopoietic Potency and Correlated Blood Group O in Cord Blood from Healthy Newborn

Hye Ryun Lee,[1] Jeong Su Park,[2,3] Sue Shin,[2,3,4] Eun Youn Roh,[2,3,4] Jong Hyun Yoon,[2,3,4] Eun Young Song,[2] Byung Jae Kim,[5] and Ju Young Chang[6]

[1] *Department of Laboratory Medicine, Gyeongsang National University Hospital, Gyeongsangnam-do, Jinju 660-702, Republic of Korea*
[2] *Department of Laboratory Medicine, Seoul National University College of Medicine, Seoul 156-707, Republic of Korea*
[3] *Department of Laboratory Medicine, Boramae Hospital, Seoul 156-707, Republic of Korea*
[4] *Seoul Metropolitan Government Public Cord Blood Bank (Allcord), Boramae Hospital, Seoul 156-707, Republic of Korea*
[5] *Department of Obstetrics and Gynecology, Boramae Hospital, Seoul 156-707, Republic of Korea*
[6] *Department of Paediatrics, Boramae Hospital, Seoul 156-707, Republic of Korea*

Correspondence should be addressed to Sue Shin; jeannie@snu.ac.kr

Received 6 November 2012; Revised 11 March 2013; Accepted 11 March 2013

Academic Editor: Andrew St. John

We evaluated the relationship between mean platelet volume (MPV) and characteristics of 10,577 cord blood (CB) units in a public CB bank in Korea. Blood group O has the highest MPV ($P = 0.002$). MPV correlated with CB volume ($r = 0.121$), Hb ($r = 0.377$), WBC ($r = 0.111$), TNCs ($r = 0.110$), CD34+ cell ($r = 0.174$), CD34+ cells/TNCs ($r = 0.157$), gestational age ($r = -0.102$), and birth weight ($r = 0.023$); ($P < 0.001$ in all). MPV may be one of the useful decision parameters of process priority in CB bank.

1. Introduction

Among CB units with similar TNC counts and HLA types, the CD34+ cell count is used to select the best unit [1–3]. To improve the quality of CB units in banks, robust and easy-to-perform tests are needed to predict hematopoietic potency and transplantation outcomes before processing and storing CB.

Mean platelet volume (MPV) has been reported to correlate with TNC and CD34+ cell counts, suggesting that MPV may be useful as a predictor of hematopoietic potency and transplantation outcomes [4]. Therefore, we retrospectively analyzed a large number of CB units to ascertain the relationship between MPV and hematopoietic parameters and other variables, including TNC and CD34+ cell counts, hemoglobin and platelet concentrations, WBC count, and maternal and neonatal factors. These values were also evaluated according to the ABO blood groups of the neonates.

2. Design and Methods

2.1. Subjects and Data Collection. Data from a total of 10,577 CB units that were processed and stored at the Seoul Metropolitan Public Cord Blood Bank (Allcord) from October 2006 through August 2009 were analyzed. The CB units were donated by pregnant Korean women who provided informed consent. The study protocol was approved by the Institutional Review Board of Seoul National University Boramae Hospital (06-2012-64). We used in utero technique from the term healthy infant without any perinatal problems. CB was collected into a collection bag containing 24.5 mL citrate phosphate dextrose adenine-1 as an anticoagulant. Within 24 hours after delivery, the collected CB was transferred to the CB bank in a shipping container at 15°C to 25°C to maintain cell viability according to the standard operating procedures of Allcord. The units containing more than 60 mL CB (excluding anticoagulant) were subject to be processed.

Table 1: Characteristics of mothers and neonates.

Variable	n	%	Mean ± SD	Median	Range
Maternal age (years old)	**10,577**		**30.8 ± 3.5**	**31.0**	**16–49**
<20	20	0.2			
20–24	265	2.5			
25–29	3,561	33.7			
30–34	5,257	49.7			
35–39	1,363	12.9			
≥40	111	1.0			
Gestational age (weeks)	**10,577**		**39.1 ± 1.2**	**39**	**32–42**
<36	57	0.5			
36	165	1.6			
37	669	6.3			
38	2,136	20.2			
39	3,157	29.8			
40	3,361	31.8			
41	1,014	9.6			
42	18	0.2			
Birth weight (kg)	**10,577**		**3.36 ± 0.38**	**3.35**	**1.66–6.70**
≤2.50	118	1.1			
2.51–3.00	1,693	16.0			
3.01–3.50	5,349	50.6			
3.51–4.00	2,956	27.9			
>4.00	461	4.4			
Sex of neonates	**10,577**				
Male	5,456	51.6			
Female	5,121	48.4			
Mode of delivery	**10,571**				
V/D	7,781	73.6			
C/S	2,790	26.4			
ABO blood group of neonates	**10,577**				
A	3,669	34.7			
B	2,854	27.0			
O	2,844	26.9			
AB	1,210	11.4			

V/D: vaginal delivery; C/S: Cesarean section; SD: standard deviation.

Table 2: Characteristics of 10,577 cord blood units.

Variable	Mean ± SD	Median	Range
Volume (mL)	86.0 ± 18.0	83.0	53.9–201.2
Hb (g/dL)	11.7 ± 1.3	11.7	5.4–17.4
WBCs ($\times 10^3/\mu$L)	10.9 ± 3.0	10.4	3.2–31.2
Platelets ($/\mu$L)	207 ± 39	205	72–422
MPV (fL)	9.5 ± 0.6	9.4	7.6–13.2
TNCs ($\times 10^8$/unit)	8.8 ± 3.0	8.3	1.5–32.2
CD34+ cells ($\times 10^6$/unit)	1.15 ± 1.09	0.84	0.02–15.67
CD34+ cells/TNCs (%)	0.123 ± 0.089	0.101	0.007–1.102

Hb: hemoglobin; WBCs: white blood cells; MPV: mean platelet volume; TNCs: total nucleated cells; SD: standard deviation.

The automated blood cell counter (XE-2100; Sysmex, Kobe, Japan) was used to determine the MPV and concentrations of Hb, WBCs, and platelets of all CB units. MPV was calculated by dividing the plateletcrit by the number of platelets. After volume reduction for cryopreservation, the blood was further tested to determine TNC and CD34+ cell counts and ABO blood group, according to the standard operating procedures of Allcord as described elsewhere [5].

Relationships between variables were determined by simple linear regression analysis. These variables were also compared according to ABO blood group by analysis of variance and the Kruskal-Wallis test. All statistical analyses were performed using the Statistical Package for Society Sciences (SPSS) (version 12.0; IBM Corp., Chicago, IL, USA); $P < 0.05$ was considered significant.

3. Results and Discussion

Table 1 shows the characteristics of the mothers (age) and neonates (gestational age, birth weight, sex, mode of delivery, and ABO blood group). Table 2 shows the following characteristics of the 10,577 CB units: volume, concentrations of Hb, WBCs, and platelets MPV from the units before volume reduction process and TNC count, CD34+ cell count, and CD34+ cells/TNCs from the units after the process. Analysis of the 10,577 CB units showed that MPV was positively correlated with CB volume ($r = 0.121$, $P < 0.001$), Hb concentration ($r = 0.377$, $P < 0.001$), and WBC count ($r = 0.111$, $P < 0.001$) but not platelet concentration. In addition, MPV was positively correlated with TNC count ($r = 0.110$, $P < 0.001$), CD34+ cell count ($r = 0.174$, $P < 0.001$), and CD34+ cells/TNCs ($r = 0.157$, $P < 0.001$). No relationship was found between MPV and maternal age ($r = 0.003$, $P = 0.739$). However, MPV was negatively correlated with gestational age ($r = -0.102$, $P < 0.001$) and positively correlated with birth weight ($r = 0.023$, $P = 0.020$). Neonatal gender was not associated with MPV. When we did the multivariate analyses of MPV with CB volume, CD34+ cell count, WBC count, TNC, gestational age, and birth weight, the associations were also significant (see Supplementary Table 1 available online at: http://dx.doi.org/10.1155/2013/754169).

Table 3 shows the characteristics according to the ABO blood group. The birth weight of the neonates and CB values for Hb concentration, platelet concentration, and MPV differed according to ABO blood group. Although neonates with blood type O had the lowest birth weight (P for trend = 0.003), their CB units showed the highest MPV (P for trend = 0.002) and Hb concentration (P for trend < 0.001). In contrast, CB units from neonates with blood type A had the highest platelet concentration (P for trend < 0.001).

The present study shows that the MPV of CB correlates with TNC and CD34+ cell counts and the ratio of CD34+ cells to TNCs in the processed CB units, which is consistent with the results of previous studies [4, 6]. Our study is significant

Table 3: Gestational age, birth weight, cord blood volume, blood cell components, mean platelet volume, and other hematopoietic parameters of the cord blood units according to ABO blood group of neonates.

	A ($n = 3669$)	B ($n = 2854$)	O ($n = 2844$)	AB ($n = 1210$)	P
Gestational age (weeks)	39.1 ± 1.2	39.1 ± 1.2	39.1 ± 1.2	39.1 ± 1.2	0.406
Birth weight (kg)	3.37 ± 0.38	3.35 ± 0.38	3.34 ± 0.37	3.37 ± 0.37	0.003
Volume (mL)	86.3 ± 18.2	85.6 ± 17.8	86.1 ± 18.2	86.0 ± 18.0	0.393
Hb (g/dL)	11.6 ± 1.3	11.7 ± 1.3	11.8 ± 1.3	11.6 ± 1.3	<0.001
WBCs ($\times 10^3/\mu$L)	10.8 ± 3.1	10.9 ± 2.9	11.0 ± 3.1	10.8 ± 3.1	0.092
Platelets ($/\mu$L)	209 ± 39	205 ± 38	206 ± 39	206 ± 38	<0.001
MPV (fL)	9.486 ± 0.607	9.446 ± 0.610	9.507 ± 0.617	9.466 ± 0.616	0.002

SD: standard deviation; Hb: hemoglobin; MPV: mean platelet volume; WBCs: white blood cells; TNCs: total nucleated cells.

because of the large number of CB units analyzed from a Korean CB bank.

We previously reported the relationship between ABO blood group and hematopoietic parameters (TNC count, CD34+ cell count, and CD34+ cells/TNCs) in CB units [5]. CB obtained from neonates with blood type O has higher TNC and CD34+ cell counts and ratio of CD34+ cells to TNCs than neonates with other blood types; therefore, CB units with blood type O may have greater hematopoietic potency. In this study, we also found that neonates with blood type O had significantly higher MPV. However, neonates with blood type A, not neonates of blood type O, had the highest platelet concentration.

In this study, we found that MPV appeared to be inversely correlated with platelet concentration in CB units, but this relationship was not statistically significant. Studies have reported a nonlinear inverse relationship between MPV and platelet count in the peripheral blood of adults [7, 8]. In contrast, a positive correlation has been reported between MPV and platelet concentration in CB units; however, that study analyzed only 167 units [4]. We analyzed a pretty much larger number of CB units in our study (10,577); therefore, we believe there is no proof of relationship between MPV and platelet concentration. Our finding that MPV positively correlated with Hb is consistent with that of a previous study [6]. MPV was also positively correlated with WBC concentration.

MPV was not associated with maternal age or neonatal gender but was negatively correlated with gestational age and positively correlated with birth weight.

Anticoagulants can affect MPV in CB after collection. In particular, EDTA causes time-dependent platelet swelling, which increases MPV [9]. Therefore, it is important to use alternative anticoagulants and reduce the time between collection and analysis. Because MPV changes can be reduced using citrate-based anticoagulants [10, 11], we used collection bags containing the citrate-based anticoagulant CPDA-1. In addition, platelet clumping and early clotting is a concern after ex utero collection of CB. Therefore, we collected CB in utero to better evaluate the relationship between platelet concentration and MPV.

In summary, this study reveals that the MPV of CB units correlates with TNC and CD34+ cell counts and the gestational age and birth weight of neonates. MPV is routinely measured with other blood components using automatic hematologic analyzer before CB processing but is not currently used as a predictor of hematopoietic potency. However, MPV values combined with CB volume limit of 60 mL before processing and TNC and CD34+ cell counts after processing may be useful in the selection of high-quality units for storage.

Authors' Contribution

SS was the principal investigator and takes primary responsibility for the paper. B. J. Kim and J. Y. Chang recruited the cord blood and data. E. Y. Roh, J. H. Yoon, and E. Y. Song coordinated the research. H. R. Lee and J. S. Park wrote the paper and did the statistical analysis.

Conflict of Interests

The authors reported no potential conflict of interests.

Acknowledgments

The authors would like to thank all the staffs of the Allcord for their technical assistance and greatly appreciate the consideration of Korean mothers who voluntarily donate cord blood to the public cord blood bank. This work was supported by the Clinical Research Fund from SMG-SNU Boramae Hospital (03-2008-05).

References

[1] A. R. Migliaccio, J. W. Adamson, C. E. Stevens, N. L. Dobrila, C. M. Carrier, and P. Rubinstein, "Cell dose and speed of engraftment in placental/umbilical cord blood transplantation: graft progenitor cell content is a better predictor than nucleated cell quantity," *Blood*, vol. 96, no. 8, pp. 2717–2722, 2000.

[2] N. Schmitz and J. Barrett, "Optimizing engraftment—source and dose of stem cells," *Seminars in Hematology*, vol. 39, no. 1, pp. 3–14, 2002.

[3] J. E. Wagner, J. N. Barker, T. E. DeFor et al., "Transplantation of unrelated donor umbilical cord blood in 102 patients with malignant and nonmalignant diseases: influence of CD34 cell dose and HLA disparity on treatment-related mortality and survival," *Blood*, vol. 100, no. 5, pp. 1611–1618, 2002.

[4] M. Eskola, S. Rekunen, P. Aroviita et al., "Association of cord blood platelet characteristics and hematopoietic progenitor cells," *Transfusion*, vol. 48, no. 5, pp. 884–892, 2008.

[5] H. R. Lee, J. S. Park, S. Shin et al., "Increased numbers of total nucleated and CD34+ cells in blood group O cord blood: an analysis of neonatal innate factors in the Korean population," *Transfusion*, vol. 52, no. 1, pp. 76–81, 2012.

[6] M. Eskola, S. Juutistenaho, K. Aranko, S. Sainio, and R. Kekomäki, "Association of cord blood platelet count and volume with hemoglobin in healthy term infants," *Journal of Perinatology*, vol. 31, no. 4, pp. 258–262, 2011.

[7] B. J. Bain, "Platelet count and platelet size in males and females," *Scandinavian Journal of Haematology*, vol. 35, no. 1, pp. 77–79, 1985.

[8] J. D. Bessman, "The relation of megakaryocyte ploidy to platelet volume," *American Journal of Hematology*, vol. 16, no. 2, pp. 161–170, 1984.

[9] K. M. Bowles, L. J. Cooke, E. M. Richards, and T. P. Baglin, "Platelet size has diagnostic predictive value in patients with thrombocytopenia," *Clinical and Laboratory Haematology*, vol. 27, no. 6, pp. 370–373, 2005.

[10] M. S. Dastjerdi, T. Emami, A. Najafian, and M. Amini, "Mean platelet volume measurement, EDTA or citrate?" *Hematology*, vol. 11, no. 5-6, pp. 317–319, 2006.

[11] C. B. Thompson, D. D. Diaz, P. G. Quinn, M. Lapins, S. R. Kurtz, and C. R. Valeri, "The role of anticoagulation in the measurement of platelet volumes," *American Journal of Clinical Pathology*, vol. 80, no. 3, pp. 327–332, 1983.

Hindawi Publishing Corporation
BioMed Research International
Volume 2013, Article ID 612032, 6 pages
http://dx.doi.org/10.1155/2013/612032

Review Article

NGAL and Metabolomics: The Single Biomarker to Reveal the Metabolome Alterations in Kidney Injury

A. Noto,[1] F. Cibecchini,[2] V. Fanos,[1] and M. Mussap[2]

[1] *Neonatal Intensive Care Unit, Puericulture Institute and Neonatal Section, University of Cagliari, Via Ospedale 119, 09124 Cagliari, Italy*
[2] *Department of Laboratory Medicine, University Hospital San Martino, Largo Rosanna Benzi 10, 16132 Genova, Italy*

Correspondence should be addressed to M. Mussap; michele.mussap@hsanmartino.it

Received 15 December 2012; Accepted 6 March 2013

Academic Editor: Andrew St. John

Conditions affecting kidney structure and function can be considered acute or chronic, depending on their duration. Acute kidney injury (AKI) is one of a number of acute kidney diseases and consists of an abrupt decline in kidney function after an injury leading to functional and structural changes. The widespread availability of enabling technologies has accelerated the rate of novel biomarker discovery for kidney injury. The introduction of novel biomarkers in clinical practice will lead to better preventative and therapeutic interventions and to improve outcomes of critically ill patients. A number of biomarkers of functional change and cellular damage are under evaluation for early diagnosis, risk assessment, and prognosis of AKI. Neutrophil gelatinase-associated lipocalin (NGAL) has emerged as the most promising biomarker of kidney injury; this protein can be measured by commercially available methods in whole blood, plasma, serum, and urine. Concomitantly, metabolomics appears to be a snapshot of the chemical fingerprints identifying specific cellular processes. In this paper, we describe the role of NGAL for managing AKI and the potential benefits deriving from the combined clinical use of urine NGAL and metabolomics in kidney disease.

1. Introduction

The definition of biomarker makes any characteristic that can be objectively measured and evaluated as an indicator of both normal and pathological processes. This is a general description, which may refer to either a laboratory investigation, carried out in biological samples, or to a functional or imaging test [1]. In medicine, a good biomarker has the ability to increase the performance of the clinical care of a specific disease. Due to this, the significant improvement in the diagnosis, prognosis and/or treatment of the disease has to be demonstrated before accepting a new marker in clinical practice. This is in accordance with the principles of Evidence-Based Laboratory Medicine [2]. Typically, a biomarker can be classified in different subtypes, such as (a) a biomarker that indicates a risk factor, if it identifies a risk of developing a disease; (b) a marker for screening, if it can be used for the assessment of a disease state; (c) a diagnostic index, if it can be used to recognize a state of overt disease; (d) a staging biomarker, if it can be used to stratify patients into different classes of severity of disease; (e) a prognostic index, if it is able to predict the future of the natural history of the morbidity; (f) an index of response to the therapy, if it can be used for monitoring the therapeutic drug. In addition, from the biological point of view, a good "biomarker" should be a protein that originates from the injured cells, and its quantity should be proportional to the mRNA expression. Furthermore, its appearance should be temporally related to the inciting stimulus, and the expression of the biomarker should rapidly decay when the acute phase of injury has terminated [3].

2. Biomarker of Kidney Damage

Given that acute kidney injury (AKI) is associated with significant morbidity and mortality, and because no specific treatment is available to reverse AKI, early recognition and management is paramount. Taking into account that traditional biomarkers such as serum creatinine are very

insensitive and influenced by various extrarenal factors, there is a need to identify new biomarkers of renal cell injury capable to identify additional patients with AKI and the majority of patients at an earlier stage. [4]. In the past, research aimed at evaluating the two main physiological mechanisms underlying the excretory function of the kidney, which are the glomerular filtration and the tubular reabsorption of peptides and proteins. These mechanisms are in fact used to calculate the glomerular filtration rate (GFR); however, they do not always reflect the functional status of the kidney in case of injury [5]. As a matter of fact, a biochemical test should ideally be able to reveal early and specifically the deterioration of the renal function in order to assess the extent of morphofunctional damage. In fact, a correct diagnosis would lead to an appropriate therapy which prevents morbidity and mortality associated with this condition. In the context of renal disease, the use of creatinine, alone is not an accurate measure of renal function since its correlation with the GFR is not linear, its increase over the values of normality occurs after a substantial loss of renal function, and its concentration is reduced in situations such as loss of muscle mass, amputation, chronic organic disease, liver disease, obesity, vegetarian diet, and extremes of age. Moreover, the identification of early AKI is clinically relevant, not by chance that the assessment of risk factors for kidney damage and an early diagnosis of kidney diseases are considered primary targets by the World Health Organization (WHO). Novel urine and serum biomarkers may significantly improve outcome and reduce mortality if they are able to indicate AKI hours after an insult, in comparison with the days it may take serum creatinine to rise substantially. Currently, at least around twenty of candidate biochemical markers of AKI have been studied and proposed in the literature; the most popular investigated biomarker was neutrophil gelatinase-associated lipocalin (NGAL) [5].

3. Neutrophil Gelatinase-Associated Lipocalin (NGAL)

Few years ago, the American Society of Nephrology (ASN) in agreement with the National Health Institute (NHI) selected the AKI as area of interest because it was considered an area which needed a more indepth study. An AKI group was created and subsequently divided into several working subgroups with one of these being the biomarkers group. This group was one of the most significant and successful as it discovered a number of genes and proteins related to the early detection of renal damage. NGAL was one of the genes discovered during AKI [6]. NGAL is an ubiquitous protein of 178 amino acids with a molecular mass of approximately 25 kDa and composed of 8 beta sheets that form a shaped structure. It belongs to the family of lipocalins, which are a family of proteins that transport small hydrophobic molecules, such as steroids and lipids [7]. The lipocalins have been associated with many biological processes, such as inflammation, the transport of pheromones, and the synthesis of prostaglandins [8]. NGAL was initially identified by Allen and Venge in 1989 from human neutrophils, and it is now known that it is expressed at low levels in several human tissues, including kidney, trachea, lungs, stomach, and colon [9]. However, its precise role has been only recently clarified by Paragas et al. (2011), who worked on an experimental model of mouse and was able to point out the production of NGAL in case of kidney damage. Initially, the group developed a reporter mouse using a construct formed by the gene of NGAL associated with a luciferase, which enabled the comparison of the NGAL gene and protein expression *in vivo*. They studied the correlation between NGAL mRNA level produced by the kidney and the protein released from the kidney to the urine in real time. By inducing kidney injury experimentally, the timing and the intensity of NGAL mRNA and protein were correlated and dependent on the degree of kidney damage. In addition, they found that the detection of the injury was possible after 3 hours whereas serum creatine rose after about 12 h, and its production was located in the distal convoluted tubule and the collecting duct while the proximal tubule was involved in the process of plasma NGAL reabsorption [3]. In that regard, Portillia et al. (2009) highlighted the role of NGAL as marker of proximal tubule damage in a population of 40 children developing AKI after cardiac surgery. In this study, they were able to correlate the improper function carried by the proximal tubule with the level of NGAL. They also postulated that acute kidney injury resulting from hypoxic condition could cause disruption of megalin-dependent endocytosis in the renal proximal tubule, resulting in the loss of urinary NGAL and suggesting it as a marker of proximal injury [10]. In agreement with the latter, Kuwabara et al. (2009) published a recent work in which, using an experimental animal model of diabetic nephropathy: the STZ-mice (Streptozotocin, 180 mg/kg of body weight), they were able to underline that, after kidney injury, the primary source of NGAL found in the urine was the glomerular filtrate and the cause of this was the proximal tubule damage. In addition, the NGAL mRNA expression in the kidneys of STZ mice was slightly increased compared to control mice. These findings indicate that urinary NGAL is a biomarker that can reflect damage in glomeruli, proximal tubules [11]. However, the role of NGAL does not seem to be yet fully clarified, as showed in a recent paper by Bagshaw et al. (2010), who demonstrated an additional role of NGAL in AKI complicated by sepsis [12, 13]. The experimental design involved the recruitment of 83 patients, half of which had AKI, while the remainder had sepsis-induced AKI. The purpose of that study was to investigate whether there were significant differences between the plasma and urinary NGAL in patients with AKI complicated by sepsis compared with patients with AKI without sepsis. The results of this study showed that although the values of plasma NGAL (pNGAL) and urine NGAL (uNGAL) were on average higher in patients with sepsis, the value of pNGAL was increased within 12 hours in patients with AKI and sepsis compared with patients with AKI and no sepsis. However, results show no significant differences at 24 and 48 hours. As regards to uNGAL, the patients with AKI and sepsis had a higher value within 24 hours in this case too, but there were no significant differences in later times. In conclusion, relative changes in pNGAL and uNGAL may have diagnostic and/or prognostic

value and should be evaluated in further investigations. These observations suggest there are differential biomarker patterns in septic AKI that may have clinical relevance and prognostic importance. Another key point about the role of NGAL was provided by a recent paper published in 2010 by Grenier et al. The purpose of their study was to investigate the role of NGAL protein in chronic kidney disease (CKD) [14]. CKD is known to be a major concern for public health around the world since it affects up to 20 million people in the USA and between 2 and 3 million people in Italy. Such studies have shown an unambiguous role of NGAL in the early diagnosis of AKI, but this protein has many other functions, some of which are still not well elucidated. The experimental design organized by the group led by Viau started from a mouse model (FVB/N) that developed renal lesions and with which they were able to demonstrate that the NGAL production not only had a role as kidney injury marker, but itself was involved in some way to the progression of the disease. In fact, the severity of the lesions was significantly reduced in the same experimental mouse model in which the gene NGAL/Lcn2 was silenced (NGAL/Lcn2 −/−). These results point out a new important role of NGAL in the progression of CKD.

NGAL can be measured in whole blood, serum, plasma, and urine by several commercially available analytical immunoassays. They include a whole blood point of care immunoassay (Triage NGAL Test, Biosite-Inverness Medical, Waltham, MA, USA), a fully automated immunoturbidimetric assay optimized for measuring urine NGAL on the Architect analytical platform (Abbott Laboratories, Abbott Park, IL, USA) [15], and an enhanced turbidimetric immunoassay for the measurement of NGAL in urine and EDTA plasma (NGAL Test, BioPorto Diagnostics A/S, Gentofte, Denmark). The latter represents an evolution of a previously exiting manual enzyme-linked immunosorbent assay (ELISA), commercialized by the same manufacturer, and can be adapted for use on a variety of automated clinical chemistry analyzers.

Being NGAL a critical component of innate immunity to bacterial infection, it is also expressed during systemic inflammation and sepsis, increasing in the blood stream and, in turn, in urine. Moreover, during systemic inflammation and sepsis, uNGAL significantly increases because of neutrophils accumulation within the tubular lumen. Consequently, uNGAL can increase (a) as a result of a renal tubular damage; (b) in the course of an acute phase response; (c) as the concomitant presence of sepsis with AKI. On the other hand, three isoforms of human NGAL have been isolated: a 25 kDa monomer, a 45 kDa disulfide-linked homodimer, and a 135 kDa heterodimer consisting of a monomer covalently bound with neutrophil gelatinase, also named matrix metalloproteinase (MMP-9) via an intermolecular disulfide bridge. Neutrophils synthesize the monomer and the homodimer, whereas renal tubular epithelial cells synthesize the monomer and, to some extent, the heterodimer [16, 17]. Theoretically, an "ideal" immunoassay capable to distinguish various molecular forms of uNGAL should permit to assess the origin of uNGAL and, ultimately, the pathological process leading to the changes in uNGAL concentration [17]. As a consequence, we could distinguish sepsis-induced uNGAL from AKI-induced uNGAL excretion. Unfortunately, this "ideal" immunoassay does not exist; the cocktail of antibodies used in the current NGAL immunoassays does not distinguish between the isoforms of the protein, and thus there is a need to develop immunoassays with combination of polyclonal and monoclonal antibodies that preferentially recognize monomeric NGAL originating from kidney tubules, which could, hence, be distinguished from the homodimer and, especially, from the monomeric form synthesized by neutrophils due to the different molecular structure and epitope exposure.

4. The New Era of Discovery and Developing Biomarker: The Metabolomics

The advent of metabolomics, in which all of the metabolites in a given tissue or biological fluid are examined (with the caveat that some metabolites will not be detected in any given experiment), is one of the latest advances in the field of omics. The term metabolome was firstly coined in 1998 by Oliver et al. to designate the set of low molecular weight compounds synthesized by an organism [18]. Afterwards, the first draft of the human metabolome was completed on January 23, 2007, and consisted of a database of about 2,500 metabolites [19]. The word metabolomics means to study a particular set of samples from a holistic rather than reductionist point of view. This omics science uses a series of techniques such as proton nuclear magnetic resonance (^{1}H NMR) spectroscopy and gas chromatography-mass spectrometry (GC-MS) which are capable of giving a general profile of all the metabolites present in a set of samples analyzed. The metabolome represents the collection of all metabolites within a biological sample such as urine, blood, and saliva, which are the end products of their gene expression together with the contribution of the environment. From a clinical point of view, the study of the metabolome is comparable to observe a snapshot of a particular biological sample which may reveal new biochemical pattern that could be used for the diagnosis and classification of diseases as well as to improve the understanding of pathophysiological mechanisms. In fact, the metabolomics approach, by providing access to a portion of biomolecular space not covered by other approaches such as proteomics and genomics, offers unique insights into small molecule regulation and signaling. Moreover, this "omics" approach has been successfully used in the fields of physiology, neonatology, pharmacology, toxicology, and nutrition [20–25].

Two strategies configure metabolomics studies: the targeted and the nontargeted approach [26]. The targeted approach is focused on the investigation of several well-defined compounds; it is only used when the target of a drug or disease process is at least partially understood. The nontargeted approach can be defined as a "nonspecific approach"; it allows to investigate both endogenous and exogenous metabolites detectable in a biological fluid or in a tissue. This approach is focused on capturing as much information as possible, providing a functional fingerprint of the physiological and pathological state of the body.

Metabolic fingerprinting describes the unbiased analysis of the metabolome by investigating metabolite patterns in different experimental groups with the subsequent classification of these patterns into a fingerprint [27]. Samples can be classified if the metabolite fingerprints differ between groups. Metabolite identification relies on public databases [28]: the Human Metabolome Database (HMDB, the metabolomic equivalent of GenBank). It is an open access database (http://www.hmdb.ca) providing reference to nuclear magnetic resonance (NMR) and mass spectra, metabolite disease associations, metabolic pathway data, and reference to metabolite concentrations for hundreds of human metabolites from several biofluids [29]. In most cases, proton nuclear magnetic resonance (^{1}H NMR) spectroscopy and MS-based assays are used for metabolic fingerprinting [30]; these techniques require a well-defined sample preparation. Concisely, ^{1}H NMR spectroscopy allows for the simultaneous detection of 20–50 metabolites with an analytical sensitivity ranging 1–10 mmol/L; below this cutoff, the detection and quantification of metabolites is still unreliable, although high field NMR spectroscopy and cryoprobes can improve sensitivity [31]. On the other hand, MS is considered the gold standard in metabolite detection and quantification until now; depending on the metabolite, the sensitivity of MS is in the picomolar and nanomolar range. However, MS should be coupled to an array of separation techniques including gas chromatography (GC) and liquid chromatography (LC); in addition, MS requires longer analytical time (20–60 min for each sample), extensive sample preparation including derivatization, and the limitation to volatile compounds [32]. Other technologies less commonly used for metabolomics are Raman and infrared spectroscopy. Each method has serious drawbacks, such that neither by itself is ideal.

Metabolomics appears to be extremely attractive for research and clinical purposes, because it offers several advantages over genomics, transcriptomics, and proteomics. Firstly, metabolites vary both quantitatively and qualitatively at any given time. Secondly, metabolic response is extremely rapid, and thus it can be measured within a very short time from the start of the process, while transcriptomics and proteomics are "late signals," since their response to a challenge may take hours, days, and sometimes weeks. Thirdly, the metabolome communicates with the environment, being an open system, whereas transcriptomics and proteomics strictly detect endogenous changes. Last but not least, despite the very high overall number of endogenous metabolites (~100,000), the number of major metabolites relevant for clinical diagnostics and drug development has been estimated at 1,400–3,000 molecules [33], which means less data to manipulate and interpret, being genes (~25,000), transcripts (~85,000), and proteins (>10,000,000) greatly outnumbered.

5. The Metabolomics Approach in Kidney Disease

The recent development of the omics technique also reached the field of kidney disease and seems to be promising in offering new target metabolites that may be considered biomarkers in the next future [34, 35]. In a recent paper, the metabolic difference was investigated between populations of healthy adults born with an extremely low birth weight (ELBW) and those born at term appropriate for gestational age (AGA) [36]. The purpose of that work was to verify the presence of metabolites that might be considered as "biomarkers" that can predict the development of diseases in adulthood. The study was conducted on two groups of individuals, and urine samples were collected aseptically from a group of 18 subjects (8 males and 10 females, mean age 24 years, SD: ± 4.27) born ELBW and a group of other 13 (7 males and 6 females, mean age 25 years, SD: ± 5.15) born AGA. These samples were analyzed using the automated uNGAL method on the Architect platform and then by metabolomics (^{1}H-NMR spectrometer Varian 500 MHz, Agilent Technologies). uNGAL concentration showed a significant difference between the ELBW subjects (median 577, range: 32 to 10,224 mg/g urinary creatinine) compared with the AGA group (median 10.6, range: 2.2 to 53, 4 mg/g urinary creatinine) (P value < 0.05). In addition, the ^{1}H-NMR metabolomics analysis, through a mathematical model, was able to correlate the ELBW metabolic profiles with uNGAL concentration; conversely, uNGAL could not be correlated to AGA. This study, for the first time, demonstrated the relevance of the use of the metabolomics technique together with a novel promising marker of renal damage. It is therefore reasonable to consider that further studies are required about the use of both of these techniques, which may underline the potential prognostic value in case of disease such as the chronic kidney diseases. In fact, this finding may contribute to the identification of people who may develop chronic kidney failure in the near future or in adulthood.

6. Conclusion

Increasing knowledge in the science of biology and medicine has accelerated the discovery of novel biomarkers and elucidated their roles in molecular pathways triggered by physiological and/or pathological conditions. Emerging tools, like metabolomics, depend on sophisticated technologies (GC-MS, ^{1}H NMR, etc.), which contribute to the sudden development of new biochemical and molecular tests. On one hand, there is a need to develop new predictive approaches for a preventive medicine that allow the prediction of asymptomatic conditions and for tailored therapeutic management. On the other hand, there is an urgent need to translate these developing methods (epigenomics, metabolomics, etc.) and next generation biomarkers (NGAL, KIM-1, etc.) from bench to bedside in order to improve clinical outcome and quality of care. This challenge can be addressed, for example, using a combined approach between the potential of new biomarkers such as uNGAL and the "next generation" metabolomics technique. However, clinical quality specifications (sensitivity, specificity, positive and negative predictive values, etc.) should be addressed as well as the balance between costs and

benefits, in term of improved patient outcome per dollar (or euro, etc.) spent.

Abbreviations

AKI: Acute kidney injury
GFR: Glomerular filtration rate
NGAL: Neutrophil gelatinase-associated lipocalin
NMR: Nuclear magnetic resonance.

Conflict of Interests

The authors declare that they have no conflict of interests.

References

[1] R. Frank and R. Hargreaves, "Clinical biomarkers in drug discovery and development," *Nature Reviews Drug Discovery*, vol. 2, no. 7, pp. 566–580, 2003.

[2] M. Mussap, A. Noto, F. Cibecchini, and V. Fanos, "Emerging biomarker in neonatal sepsis," *Drugs of the Future*, vol. 37, no. 5, p. 353, 2012.

[3] N. Paragas, A. Qiu, Q. Zhang et al., "The Ngal reporter mouse detects the response of the kidney to injury in real time," *Nature Medicine*, vol. 17, no. 2, pp. 216–222, 2011.

[4] J. V. Bonventre, V. S. Vaidya, R. Schmouder, P. Feig, and F. Dieterle, "Next-generation biomarkers for detecting kidney toxicity," *Nature Biotechnology*, vol. 28, no. 5, pp. 436–440, 2010.

[5] R. G. Fassett, S. K. Venuthurupalli, G. C. Gobe, J. S. Coombes, M. A. Cooper, and W. E. Hoy, "Biomarkers in chronic kidney disease: a review," *Kidney International*, vol. 80, pp. 806–821, 2011.

[6] P. Devarajan, "Neutrophil gelatinase-associated lipocalin: a promising biomarker for human acute kidney injury," *Biomarkers in Medicine*, vol. 4, no. 2, pp. 265–280, 2010.

[7] L. Kjeldsen, A. H. Johnsen, H. Sengelov, and N. Borregaard, "Isolation and primary structure of NGAL, a novel protein associated with human neutrophil gelatinase," *Journal of Biological Chemistry*, vol. 268, no. 14, pp. 10425–10432, 1993.

[8] J. Mishra, M. A. Qing, A. Prada et al., "Identification of neutrophil gelatinase-associated lipocalin as a novel early urinary biomarker for ischemic renal injury," *Journal of the American Society of Nephrology*, vol. 14, no. 10, pp. 2534–2543, 2003.

[9] J. B. Cowland and N. Borregaard, "Molecular characterization and pattern of tissue expression of the gene for neutrophil gelatinase-associated lipocalin from humans," *Genomics*, vol. 45, no. 1, pp. 17–23, 1997.

[10] D. Portilla, C. Dent, T. Sugaya et al., "Liver fatty acid-binding protein as a biomarker of acute kidney injury after cardiac surgery," *Kidney International*, vol. 73, no. 4, pp. 465–472, 2008.

[11] T. Kuwabara, K. Mori, M. Mukoyama et al., "Urinary neutrophil gelatinase-associated lipocalin levels reflect damage to glomeruli, proximal tubules, and distal nephrons," *Kidney International*, vol. 75, no. 3, pp. 285–294, 2009.

[12] S. M. Bagshaw, M. Bennett, M. Haase et al., "Plasma and urine neutrophil gelatinase-associated lipocalin in septic versus non-septic acute kidney injury in critical illness," *Intensive Care Medicine*, vol. 36, no. 3, pp. 452–461, 2010.

[13] A. Viau, K. El Karoui, D. Laouari et al., "Lipocalin 2 is essential for chronic kidney disease progression in mice and humans," *Journal of Clinical Investigation*, vol. 120, no. 11, pp. 4065–4076, 2010.

[14] F. C. Grenier, S. Ali, H. Syed et al., "Evaluation of the ARCHITECT urine NGAL assay: assay performance, specimen handling requirements and biological variability," *Clinical Biochemistry*, vol. 43, no. 6, pp. 615–620, 2010.

[15] L. Cai, J. Rubin, W. Han, P. Venge, and S. Xu, "The origin of multiple molecular forms in urine of HNL/NGAL," *Clinical Journal of the American Society of Nephrology*, vol. 5, no. 12, pp. 2229–2235, 2010.

[16] S. Hatipoglu, E. Sevketoglu, A. Gedikbasi et al., "Urinary MMP-9/NGAL complex in children with acute cystitis," *Pediatric Nephrology*, vol. 26, pp. 1263–1268, 2011.

[17] T. L. Nickolas, C. S. Forster, M. E. Sise et al., "NGAL (Lcn2) monomer is associated with tubulointerstitial damage in chronic kidney disease," *Kidney International*, vol. 82, pp. 718–722, 2012.

[18] S. G. Oliver, M. K. Winson, D. B. Kell, and F. Baganz, "Systematic functional analysis of the yeast genome," *Trends in Biotechnology*, vol. 16, no. 9, pp. 373–378, 1998.

[19] D. S. Wishart, D. Tzur, C. Knox et al., "HMDB: The human metabolome database," *Nucleic Acids Research*, vol. 35, no. 1, pp. D521–D526, 2007.

[20] D. Wishart, "Applications of metabolomics in nutritional science," *Human Metabolome Project*, 2008.

[21] L. Atzori, J. L. Griffin, A. Noto, and V. Fanos, "Metabolomics: a new approach to drug delivery in perinatology," *Current Medicinal Chemistry*, vol. 19, pp. 4654–4661, 2012.

[22] F. C. Marincola, A. Noto, P. Caboni et al., "A metabolomic study of preterm human and formula milk by high resolution NMR and GC/MS analysis: preliminary results," *The Journal of Maternal-Fetal & Neonatal Medicine*, vol. 25, pp. 62–67, 2012.

[23] S. Collino, F. P. Martin, and S. Rezzi, "Clinical Metabolomics paves the way towards future healthcare strategies," *British Journal of Clinical Pharmacology*, vol. 75, no. 3, pp. 619–629, 2012.

[24] J. C. Lindon, J. K. Nicholson, E. Holmes, and J. R. Everett, "Metabonomics: metabolic processes studied by NMR spectroscopy of biofluids," *Concepts in Magnetic Resonance*, vol. 12, no. 5, pp. 289–320, 2000.

[25] D. I. Ellis, W. B. Dunn, J. L. Griffin, J. W. Allwood, and R. Goodacre, "Metabolic fingerprinting as a diagnostic tool," *Pharmacogenomics*, vol. 8, no. 9, pp. 1243–1266, 2007.

[26] U. Christians, J. Albuisson, and J. Klawitter, "The role of metabolomics in the study of kidney diseases and in the development of diagnostic tools," in *Biomarkers in Kidney Disease*, C. L. Edelstein, Ed., pp. 39–100, Elsevier Academic Press, San Francisco, Calif, USA, 2011.

[27] M. Oldiges, S. Lütz, S. Pflug, K. Schroer, N. Stein, and C. Wiendahl, "Metabolomics: current state and evolving methodologies and tools," *Applied Microbiology and Biotechnology*, vol. 76, no. 3, pp. 495–511, 2007.

[28] W. J. Griffiths and Y. Wang, "Mass spectrometry: from proteomics to metabolomics and lipidomics," *Chemical Society Reviews*, vol. 38, no. 7, pp. 1882–1896, 2009.

[29] D. S. Wishart, C. Knox, A. C. Guo et al., "HMDB: a knowledgebase for the human metabolome," *Nucleic Acids Research*, vol. 37, no. 1, pp. D603–D610, 2009.

[30] J. M. Fonville, A. D. Maheir, M. Coen, E. Holmes, J. C. Lindon, and J. K. Nicholson, "Evaluation of full-resolution J-resolved1H NMR projections of biofluids for metabonomics information

retrieval and biomarker identification," *Analytical Chemistry*, vol. 82, no. 5, pp. 1811–1821, 2010.

[31] Z. Pan and D. Raftery, "Comparing and combining NMR spectroscopy and mass spectrometry in metabolomics," *Analytical and Bioanalytical Chemistry*, vol. 387, no. 2, pp. 525–527, 2007.

[32] K. K. Pasikanti, P. C. Ho, and E. C. Y. Chan, "Gas chromatography/mass spectrometry in metabolic profiling of biological fluids," *Journal of Chromatography B*, vol. 871, no. 2, pp. 202–211, 2008.

[33] E. Y. Xu, W. H. Schaefer, and Q. Xu, "Metabolomics in pharmaceutical research and development: metabolites, mechanisms and pathways," *Current Opinion in Drug Discovery and Development*, vol. 12, no. 1, pp. 40–52, 2009.

[34] L. Atzori, R. Antonucci, L. Barberini et al., "1H NMR-based metabolic profiling of urine from children with nephrouropathies," *Frontiers in Bioscience*, vol. 2, pp. 725–732, 2010.

[35] V. Fanos, R. Antonucci, M. Zaffanello, and M. Mussap, "Nenatal drug induced nephrotoxicity: old and next generation biomarkers for early detection and management of neonatal dug-induced nephrotoxicity, with special emphasis on ungal and on metabolomics," *Current Medicinal Chemistry*, vol. 19, pp. 4595–4605, 2012.

[36] L. Atzori, M. Mussap, A. Noto et al., "Clinical metabolomics and urinary NGAL for the early prediction of chronic kidney disease in healthy adults born ELBW," *The Journal of Maternal-Fetal & Neonatal Medicine*, vol. 24, supplement 2, pp. 40–43, 2011.

Hindawi Publishing Corporation
BioMed Research International
Volume 2013, Article ID 926230, 6 pages
http://dx.doi.org/10.1155/2013/926230

Research Article

Detection of *Mycobacterium tuberculosis* by Using Loop-Mediated Isothermal Amplification Combined with a Lateral Flow Dipstick in Clinical Samples

Thongchai Kaewphinit,[1] Narong Arunrut,[2,3] Wansika Kiatpathomchai,[2,3] Somchai Santiwatanakul,[4] Pornpun Jaratsing,[5] and Kosum Chansiri[5]

[1] *Innovative Learning Center, Srinakharinwirot University, Sukhumvit 23, Bangkok 10110, Thailand*
[2] *Centex Shrimp, Faculty of Science, Mahidol University, Bangkok 10400, Thailand*
[3] *National Center for Genetic Engineering and Biotechnology (BIOTEC), National Science and Technology Development Agency, Pathumthani 12120, Thailand*
[4] *Department of Pathology, Faculty of Medicine, Srinakharinwirot University, Sukhumvit 23, Bangkok 10110, Thailand*
[5] *Department of Biochemistry, Faculty of Medicine, Srinakharinwirot University, Sukhumvit 23, Bangkok 10110, Thailand*

Correspondence should be addressed to Thongchai Kaewphinit; thongchaika@swu.ac.th

Received 3 November 2012; Revised 2 February 2013; Accepted 5 February 2013

Academic Editor: Mina Hur

Tuberculosis (TB) is a communicable disease caused by the bacterium *Mycobacterium tuberculosis* (MTB) and is a persistent problem in the developing countries. Loop-mediated isothermal amplification (LAMP) allows DNA to be amplified rapidly at a constant temperature. Here, a LAMP method was combined with a chromatographic lateral-flow dipstick (LFD) to detect IS*6110* gene of *M. tuberculosis* specifically and rapidly. The reaction was optimized at 63°C for 60 min, and the amplified DNA hybridized to an FITC-labeled oligonucleotide probe for 5 min was detected at the LFD test line 5 min after application. Excluding the step of DNA extraction, the test results could be generated approximately within 1 h. In addition to the advantage of short assay time, this technique could avoid the contact of carcinogenic ethidium bromide due to the exclusion of the electrophoresis analysis step. Furthermore, the data indicated that LAMP-LFD could detect *M. tuberculosis* genomic DNA as little as 5 pg. The technique showed a significant specificity since no cross-hybridization to *M. intracellulare* (MIC), *M. fortuitum* (MFT), *M. avium* (MAV), *M. kansasii* (MKS), and *M. gordonae* (MGD) genomic DNAs was observed. In the clinical unknown samples test, the sensitivity of LAMP-LFD was 98.92% and the specificity was 100% compared to those of the standard culture assay. Based on its sensitivity, specificity, rapidity, low cost, and convenience, LAMP-LFD could be applicable for use in both laboratories and epidemiological surveys of MTB.

1. Introduction

TB is an airborne disease caused by the bacterium *Mycobacterium tuberculosis* (MTB). WHO reported that TB is a persistent problem in developing countries and ranks as the second leading cause of death from an infectious disease worldwide after the human immunodeficiency virus (HIV) [1]. This bacterium is a slow-growing bacterium that needs 1-2 months for growing in a culture; however, a rapid and timely diagnosis of tuberculosis is essential to combat this disease. The Ziehl-Neelsen (ZN) stain for direct specimen examination is a conventional diagnostic tool but lacks sensitivity. The tests based on PCR have shown promise for the detection of mycobacteria in clinical samples [2–4], but this amplification process requires additional processing time, reagents, and devices, which affect the cost of the assay. Moreover, PCR analysis needs well-trained personnel.

The LAMP assay allows DNA to be amplified at a constant temperature of 60–65°C [5]. After LAMP, the amplified DNA is normally detected by agarose gel electrophoresis, ethidium bromide staining, and UV transillumination. Due to the use of several primers, LAMP generates a complex mixture

Table 1: Primers and probe used for LAMP of the IS*6110* gene of MTB.

Primer name	Genome position	Sequences 5′-3′
F3	581-597	GCCAGATGCACCGTCGA
B3	759-740	GACACATAGGTGAGGTCTGC
FIP (F1c/TTTT/F2)	664-646/TTTT/604-623	AGCGATCGTGGTCCTG CGG-TTTT-GATGACCAAACTCGGCCTGT
BIP (B1c/TTTT/B2)	682-699/TTTT/738-721	TCCCGCCGATCTCGTCCA-TTTTT-ACCCACAGCCGGTTAGGT
FITC-Probe	665-680	ATCCGGCCACAGCCC

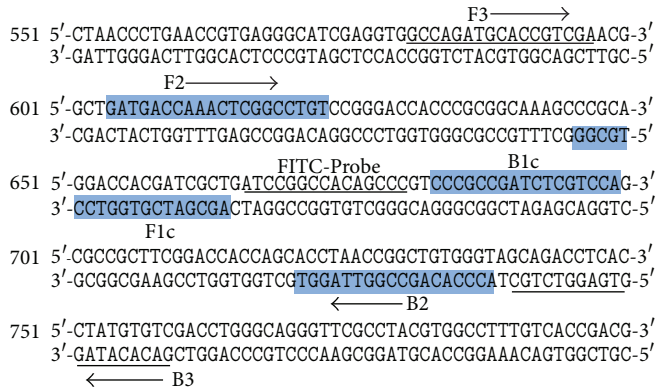

Figure 1: Nucleotide sequence of IS*6110* gene (GenBank accession number: X17348). The primers F3 and B3 were shown as underlined nucleotide sequences and arrows. The FIP (F1c/TTTT/F2) and BIP (B1c/TTTT/B2) inner primers are the shaded boxes and arrows. The FITC-labeled probe sequence is shown in italic and underlined sequences.

of DNA products of different sizes; therefore, gel analysis cannot distinguish specific and nonspecific products. To avoid possible false positive results, the authenticity of LAMP DNA products can be confirmed by restriction endonuclease digestion [5] or by hybridization to specific probes [6]. Later, to further simplify and shorten the time needed to generate LAMP data, a biotin-labeled oligonucleotide probe and an FITC-labeled DNA probe captured by gold-labeled anti-FITC antibody following chromatography on a LFD (Milenia GenLine Hybri Detect) were developed. The techniques were successfully applied in the detection of viruses such as shrimp infectious hypodermal and hematopoietic necrosis virus [7] and shrimp Taura syndrome virus [8]. Using this strategy, the sensitivity is equivalent to that of PCR assay with similar time use of approximately 1 h. Described here was a LAMP-LFD method optimized for the detection of MTB. The sensitivity and specificity of this technique were investigated in comparison to those of a PCR assay.

2. Materials and Methods

2.1. Samples and DNA Extraction. All clinical samples (101 unknown sputum samples) and standard strain (H37RVKK11-20) were provided from the National Tuberculosis Reference Laboratory (NTRL), Bureau of Tuberculosis, Department of Disease Control, Ministry of Public Health, Thailand. DNA was extracted from all clinical samples following the method of Rienthong et al. [9]. Briefly, Sputum unknown samples were decontaminated with N-acetyl-L-cysteine-sodium hydroxide. After centrifugation, the crude cell lysates were suspended in 300 μL of distilled water, killed with heat at 95°C for 20 min in Thermoblock, and then underwent sonification for 15 min at the highest speed in an ultrasonic bath, followed by spinning the samples in a standard centrifuge with an aerosol-tight rotor at approximately 10,000 g for 5 min. The supernatant was used for the LAMP amplification. The total samples of unknown sputum were compared to those of the standard culture assay on Lowenstein-Jensen slants and incubated at 37 °C for 8 weeks. The genomic DNA from the standard (H37RVKK11-20) was prepared following the method of Kaewphinit and coworkers [10]. The concentration and quality of genomic DNA in the LAMP reaction were determined by spectrophotometric analysis at 260 and 280 nm.

2.2. LAMP Primers and PCR Primers. LAMP primers for MTB were designed according to the published sequences of the IS*6110* gene specific for MTB genome (Gen-Bank accession no. X17348) using Primer Explorer version 4 (http://primerexplorer.jp/elamp4.0.0/index.html). The directions and details of the primers are shown in Figure 1 and Table 1. The normal primers and biotin-labeled FIP primer were synthesized by Bio Basic Inc., Canada.

2.3. Optimization of Temperature for LAMP. To determine the optimum temperature for amplification, the LAMP reactions were carried out at 60, 63, and 65°C for 1 h, followed by the analysis of the LAMP products by gel electrophoresis. The reaction mixture contained 2 μM, each of inner primers FIP and BIP, 0.2 μM, each of outer primers F3 and B3, 1.6 mM of dNTP mix (Promega, Madison, WI, USA), 0.5 M of betaine (Sigma-Aldrich, St. Louis, MO, USA), 6 mM of $MgSO_4$, 8U of Bst DNA polymerase (large fragment; New England Biolabs Inc., Beverly, MA, USA), 1X of the supplied buffer, and 50 ng of DNA in a final volume of 25 μL.

2.4. Lateral Flow Dipstick (LFD) Assay. A 5′-FITC-labeled oligonucleotide probe designed according to the IS*6110* gene of MTB between the F1c and B1c primer targets was synthesized by Bio Basic Inc., Canada. As recommended in similar tests [7, 8], 20 picomoles of FITC-labeled probe (FITC-5′-ATCCGGCCACAGCCC-3′) was added to the LAMP reaction and after hybridization at 65°C for 5 min, 8 μL hybridized product was added to 120 μL assay buffer in a new tube, and an LFD was dipped into the mixture for 5 min.

2.5. Sensitivity of LAMP by Gel Electrophoresis and LFD. To determine detection sensitivity limits, 10-fold serial dilutions (10^{-1} to 10^{-6}) of 50 ng of total DNA of MTB (H37RVKK11-20) were used as templates for biotin-labeling LAMP tests performed under optimized conditions. Amplified DNA was detected either by 2% agarose gel electrophoresis and ethidium bromide staining followed by DNA visualization using a UV transilluminator or by the use of LFD as described above.

2.6. Specificity of LAMP-LFD. The specificity of LAMP primers was examined using 50 ng of total DNA extracted from other mycobacterium. These included infectious *M. intracellulare* (MIC), *M. fortuitum* (MFT), *M. avium* (MAV), *M. kansasii* (MKS), and *M. gordonae* (MGD). The biotin-labeled LAMP products were analyzed by 2% agarose gel electrophoresis and by LFD.

2.7. PCR for MTB Detection. Tenfold serial dilutions of 50 ng of total DNA extracted from MTB (H37RVKK11-20) were used as the template for PCR detection of MTB using the Thermal Cycler (Touchgene Gradient, model: FTGRAD2D, Techne Ltd, UK). All reactions were 25 μL volume containing 50 ng of genomic DNA in 10x PCR buffer, 1 μM, each of primers, 100 μM of dNTP, 1.5 mM $MgCl_2$, and 1.5 units of *Taq* DNA polymerase (Invitrogen). PCR was performed by using a DNA thermal cycler for 30 cycles. Each cycle consisted of denaturation at 94°C for 2 min, annealing at 53°C for 1 min, and extension at 72°C for 1 min and a final extension at 72°C for 10 min. PCR amplicon was analyzed by 1.5% agarose gel electrophoresis. The PCR assay was prepared following the method of Kaewphinit and colleagues [10].

2.8. Bacterial DNA Samples Analysis. The LAMP-LFD assays in this study for identification of 101 clinical sputum double-blind samples were detected individually using the LFD assay compared to those of the standard culture assay and AFB smear.

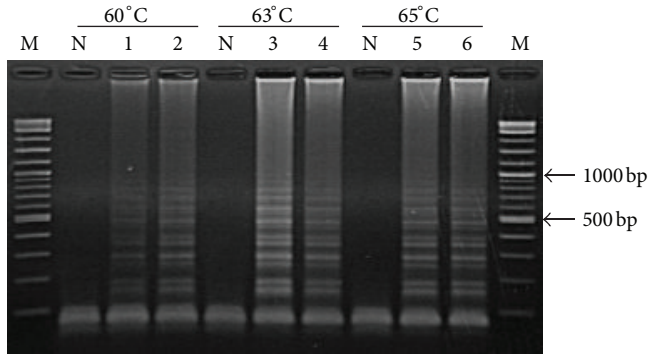

Figure 2: Optimization of biotin labeling LAMP conditions at different temperatures (60, 63, and 65°C) by using 50 ng (lanes 1, 3, and 5) and 5 ng (lanes 2, 4, and 6) of MTB genomic DNA. Lanes M and N represent DNA ladder marker and negative control (no-DNA template), respectively.

3. Results

3.1. Optimization of Reaction Temperature for MTB Detection. When the LAMP was carried out at 60, 63, and 65°C for 60 min with 50 ng of MTB infected samples DNAs (Figure 2), all three temperatures tested generated similar LAMP product patterns with the clearest and strongest bands at 63°C. Based on this, the temperature of 63°C was used for all tests in this study.

3.2. Comparison of LAMP and PCR Sensitivity with Gel Electrophoresis. Using equivalent quantities of DNA extracted from MTB-infected samples as templates at various dilutions, the detection limits for LAMP and PCR were both at 10^{-4} dilution (Figures 3(a) and 3(b)).

3.3. Sensitivity of the Combined LAMP-LFD. The LAMP-LFD detection of MTB showed a limit at 10^{-4} DNA dilution (Figure 3(c)). This corresponded to the detection limit for LAMP or PCR methods followed by electrophoresis, as described above. The detection limit was also similar to those previously reported for hepatopancreatic parvovirus (HPV) detection in black tiger shrimp *Penaeus monodon* [11].

3.4. Specificity of LAMP-Gel Electrophoresis and LAMP-LFD. A specificity test was manipulated by using 50 ng each of MTB genomic DNAs and other mycobacteria (i.e., MIC, MFT, MAV, MKS, and MGD). The data revealed that no cross-reactions were obtained from LAMP-gel electrophoresis (Figure 4(a)) and LAMP-LFD or LFD (Figure 4(b)).

3.5. Bacterial DNA Samples Analysis. A total of 101 clinical sputum double-blind samples using culture and AFB smear test results were confirmed by the NTRL. After LAMP-amplification, all genomic DNAs were hybridized with

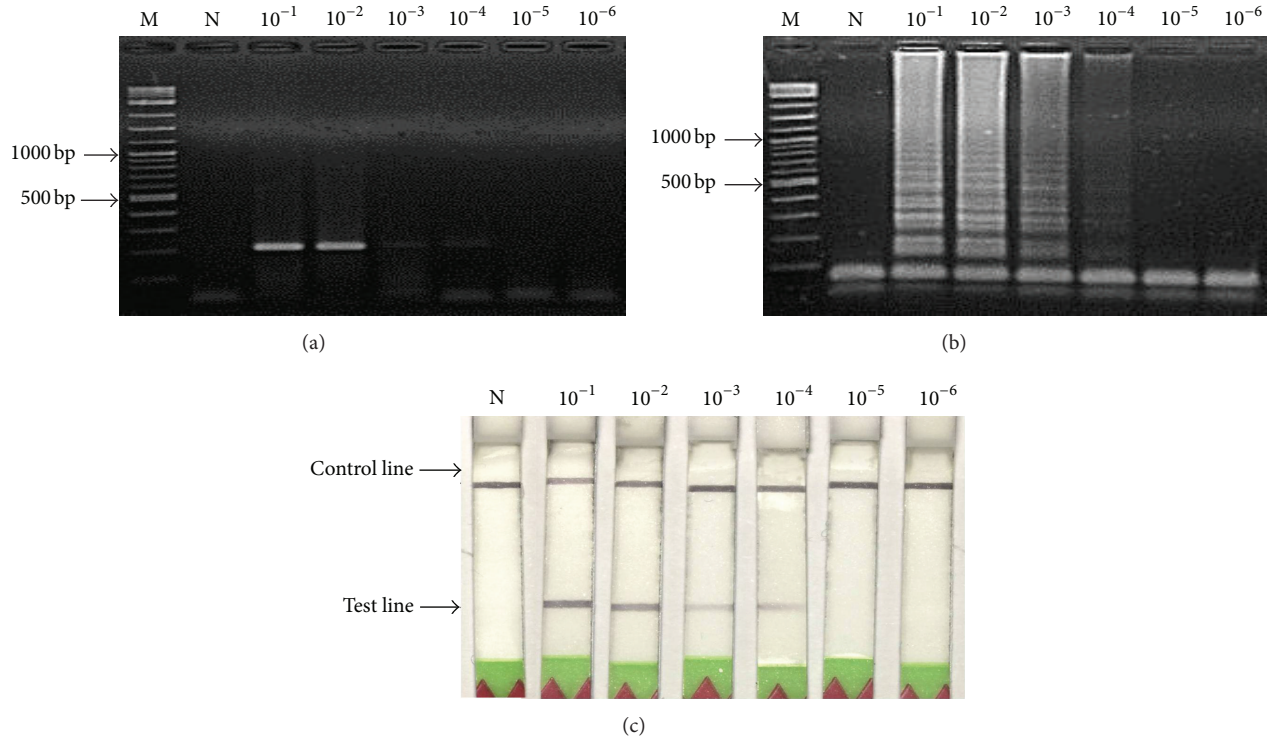

Figure 3: Detection sensitivity data of MTB genomic DNAs at concentration range of 10^{-1} to 10^{-6} dilutions (initial concentration was 50 ng) obtained from (a) PCR, (b) LAMP, and (c) LAMP-LFD. Lanes M and N represent DNA ladder marker and negative control (no-DNA template), respectively.

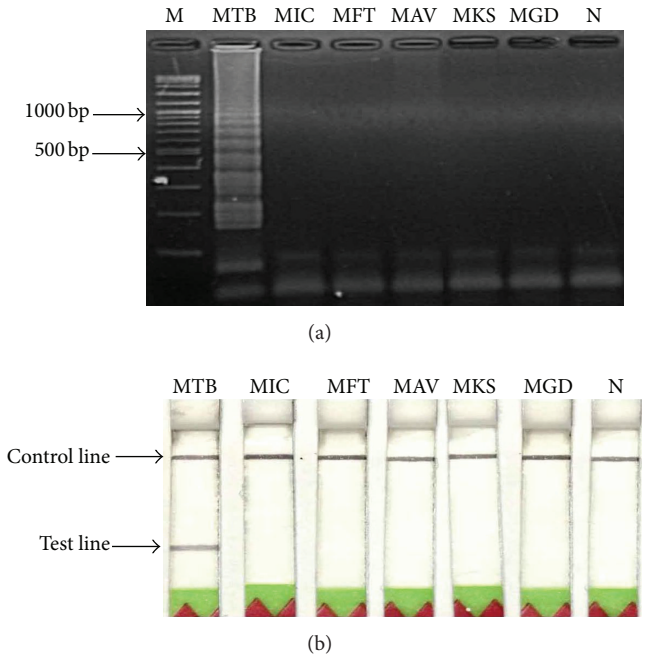

Figure 4: Specificity test data of the LAMP method for MTB using 50 ng each of DNA templates and detection by (a) gel electrophoresis or by (b) LFD. Lane M represents DNA ladder marker. Lanes 1–6 represent DNAs of MTB, MIC, MFT, MAV, MKS, and MGD, respectively. Lane 7 represents negative control (no-DNA template).

a FITC-Probe, and the results were detected by LFD and compared with those obtained from the traditional culture and AFB smear test. In brief, the sensitivity and specificity of this assay for clinical samples' diagnosis of MTB genomic DNAs were 98.92% and 100%, respectively, but the sensitivity of AFB smears test was 80.65%, both methods compared to those of the culture assay (Table 2).

4. Discussion

The LAMP-LFD technique was used for the detection of MTB in clinical double blind samples. In this study, the LAMP method was carried out at 63°C for 60 min, which was faster than typical PCR methods that require 2-3 h for PCR cycling. Referring to the test, no expensive equipment was required and the results could be determined within approximately 1 h (not including DNA preparation time). LAMP-LFD was faster than LAMP-gel electrophoresis (2 h 30 min) and much faster than PCR-gel electrophoresis (3 h 30 min) [12].

The LAMP detection method that targeted a 178 bp sequence of the IS*6110* gene was successfully developed for the detection of MTB, with the sensitivity of the LAMP being comparable to that of common PCR amplification for MTB, which was at the concentration level 5 pg of genomic DNA, a sensitivity higher than that reported previously [13].

In the clinical unknown sample test (Table 2), the sensitivity of the LAMP-LFD was 98.92% (92/93), but AFB

Table 2: Clinical double blind samples identified with LAMP-LFD, tested with specific carrying the IS*6110* gene probes for genotyping, and compared with the culture and AFB smear test.

Culture test*	AFB smear test* AFB grade 3+ (30)	2+ (30)	1+ (15)	— (26)	LAMP-LFD test Positive	Negative
		Positive		Negative		
Positive (93)		75		18	92	1
Negative (8)		0		8	0	8
Total (101)		75		26	92	9

*Culture and AFB smear test results were confirmed by the NTRL, Bureau of Tuberculosis, Department of Disease Control, Ministry of Public Health, Thailand.

smear test was 80.65% (75/93), as compared to those of the culture assay, and the specificity of the LAMP-LFD was 100%. For the one sample containing LFD assay was false negative MTB as compared with those of the culture assay. It was reasoned that possibly only a small amount of bacterial DNA was extracted from sputum samples. When compared to positive cultures, the sensitivity, specificity, positive predictive value, and negative predictive value of the method for MTB diagnosis were higher than that method, and the overall time for the procedure was faster than that reported previously [13, 14]. In addition, the LAMP-LFD assay for detection step confirms the identity of the specific amplicon by hybridization and avoids the use of carcinogens such as ethidium bromide. The test platform can be adapted easily for rapid detection of other mycobacteria agents simply by designing appropriate sets of LAMP primers and specific probes. Since the cost for the LAMP-LFD detection is comparable with that for standard PCR followed by electrophoresis, it constitutes a highly sensitive, safe and rapid alternative for the detection of MTB. Hence, the technique could be applicable for detecting minute amounts of MTB in clinical specimens. According to the specificity test, no cross-reactions to other mycobacteria were observed. This indicated that the LAMP method was specific for MTB. The introduction of LFD for analysis of LAMP amplification products could reduce the time and complications associated with usual detection by electrophoresis. This resulted in a total analysis time (excluding the DNA extraction step) of less than 75 min. The high sensitivity and specificity, the relatively short analysis time, and the use of relatively inexpensive equipment were key advantages of the LAMP-LFD assay. In addition, the technique did not involve the use of carcinogens such as ethidium bromide. The test platform can be adapted easily for rapid detection of other mycobacteria agents simply by designing appropriate sets of LAMP primers and specific FITC probes to be used with the generic LFD employed. According to the sensitivity, specificity, less time consumption, low cost and convenience, LAMP-LFD could be applicable for use in both laboratories and epidemiological surveys of MTB.

Acknowledgments

This work was supported by the Faculty of Medicine, Srinakharinwirot University, no. 335/2554. Also, the authors would like to acknowledge the help of the Bureau of Tuberculosis, Ministry of Public Health, Thailand.

References

[1] WHO, "Global Tuberculosis Report," 2012, http://www.who.int/tb/publications/global_report/gtbr12_main.pdf.

[2] A. Brisson-Noel, B. Gicquel, D. Lecossier, V. Levy-Frebault, X. Nassif, and A. J. Hance, "Rapid diagnosis of tuberculosis by amplification of mycobacterial DNA in clinical samples," *The Lancet*, vol. 2, no. 8671, pp. 1069–1071, 1989.

[3] P. Khandekar, A. G. Amin, P. P. Reddi, J. N. Banwalikar, C. T. Shivannaure, and V. M. Katoch, "Evaluation of PCR based test for the detection of *Mycobacterium tuberculosis* in coded sputum specimens," *Indian Journal of Medical Research*, vol. 100, pp. 167–171, 1994.

[4] V. Sritharan and R. H. Barker Jr., "A simple method for diagnosing M. tuberculosis infection in clinical samples using PCR," *Molecular and Cellular Probes*, vol. 5, no. 5, pp. 385–395, 1991.

[5] T. Notomi, H. Okayama, H. Masubuchi et al., "Loop-mediated isothermal amplification of DNA," *Nucleic Acids Research*, vol. 28, no. 12, article e63, 2000.

[6] Y. Mori, T. Hirano, and T. Notomi, "Sequence specific visual detection of LAMP reactions by addition og cationic polymers," *BMC Biotechnology*, vol. 6, article 3, 2006.

[7] W. Kiatpathomchai, W. Jaroenram, N. Arunrut, S. Jitrapakdee, and T. W. Flegel, "Shrimp Taura syndrome virus detection by reverse transcription loop-mediated isothermal amplification combined with a lateral flow dipstick," *Journal of Virological Methods*, vol. 153, no. 2, pp. 214–217, 2008.

[8] N. Arunrut, P. Prombun, V. Saksmerprome, T. W. Flegel, and W. Kiatpathomchai, "Rapid and sensitive detection of infectious hypodermal and hematopoietic necrosis virus by loop-mediated isothermal amplification combined with a lateral flow dipstick," *Journal of Virological Methods*, vol. 171, no. 1, pp. 21–25, 2011.

[9] D. Rienthong, S. Rienthong, C. Boonin, S. Woraswad, and Y. Kasetjaroen, "Rapid detection for early appearance of rifampin and isoniazid resistance in *Mycobacterium tuberculosis*," *Siriraj Medical Journal*, vol. 61, pp. 49–55, 2009.

[10] T. Kaewphinit, S. Santiwatanakul, C. Promptmas, and K. Chansiri, "Detection of non-amplified *Mycobacterium tuberculosis* genomic DNA using piezoelectric DNA-based biosensors," *Sensors*, vol. 10, no. 3, pp. 1846–1858, 2010.

[11] T. Nimitphak, W. Meemetta, N. Arunrut, S. Senapin, and W. Kiatpathomchai, "Rapid and sensitive detection of *Penaeus monodon* nucleopolyhedrovirus (PemoNPV) by loop-mediated isothermal amplification combined with a lateral-flow dipstick," *Molecular and Cellular Probes*, vol. 24, no. 1, pp. 1–5, 2010.

[12] R. Y. Zhu, K. X. Zhang, M. Q. Zhao et al., "Use of visual loop-mediated isotheral amplification of *rimM* sequence for rapid detection of *Mycobacterium tuberculosis* and *Mycobacterium bovis*," *Journal of Microbiological Methods*, vol. 78, pp. 339–343, 2009.

[13] M. F. Lee, Y. H. Chen, and C. F. Peng, "Evaluation of reverse transcription loop-mediated isothermal amplification in conjunction with ELISA-hybridization assay for molecular detection of *Mycobacterium tuberculosis*," *Journal of Microbiological Methods*, vol. 76, no. 2, pp. 174–180, 2009.

[14] E. Aryan, M. Makvandi, A. Farajzadeh et al., "A novel and more sensitive loop-mediated isothermal amplification assay targeting IS6110 for detection of *Mycobacterium tuberculosis* complex," *Microbiological Research*, vol. 165, no. 3, pp. 211–220, 2010.

Hindawi Publishing Corporation
BioMed Research International
Volume 2013, Article ID 390630, 6 pages
http://dx.doi.org/10.1155/2013/390630

Review Article

A Review of Haptoglobin Typing Methods for Disease Association Study and Preventing Anaphylactic Transfusion Reaction

Dae-Hyun Ko,[1,2] Ho Eun Chang,[2] Taek Soo Kim,[1,2] Eun Young Song,[1] Kyoung Un Park,[1,2] Junghan Song,[1,2] and Kyou Sup Han[1]

[1] *Department of Laboratory Medicine, Seoul National University College of Medicine, Seoul, Republic of Korea*
[2] *Department of Laboratory Medicine, Seoul National University Bundang Hospital, 300 Gumi-dong, Bundang-gu, Seongnam-si, Gyeonggi-do 463-707, Republic of Korea*

Correspondence should be addressed to Kyoung Un Park; m91w95pf@snu.ac.kr

Received 27 November 2012; Accepted 5 February 2013

Academic Editor: Mina Hur

Haptoglobin, the product of the *Hp* gene, is a glycoprotein involved in the scavenging of free hemoglobin. Haptoglobin levels increase or decrease in response to various acquired conditions, and they are also influenced by genetic predisposition. There were 2 major alleles, Hp^1 and Hp^2, and 1 minor allele, Hp^{del}. Many researchers have attempted to study the haptoglobin types and their association with disease; however, no definitive conclusions have been reached yet. It is reported that patients who are genetically deficient in haptoglobin are at risk of anaphylaxis against blood components containing haptoglobin. Haptoglobin genotypes also affect the reference intervals of haptoglobin levels. Many studies have attempted to establish simple and accurate typing methods. In this paper, we have broadly reviewed several methods for haptoglobin typing—phenotyping, Southern blotting, conventional PCR, real-time PCR, and loop-mediated isothermal amplification. We discuss their characteristics, clinical applications, and limitations. The phenotyping methods are time consuming and labor intensive and not designed to detect patients harboring Hp^{del}. The rapid and robust haptoglobin genotyping may help in preventing fatal anaphylactic reactions and in establishing the relationships between the haptoglobin phenotypes and diseases.

1. Introduction

Haptoglobin (Hp) is a plasma glycoprotein and a positive acute-phase reactant [1]. It binds to free hemoglobin, forming hemoglobin-haptoglobin (Hb-Hp) complex. This complex is then removed by macrophages via a cell-surface receptor (CD163) [2]. Haptoglobin can thus prevent tissue damage caused by free hemoglobin and reduce iron loss in hemolytic conditions. From a clinical perspective, haptoglobin is one of the most important indicators of hemolytic anemia.

Recently, many studies have revealed the association between haptoglobin phenotypes and various infections and diseases such as diabetes, cancer, and cardiovascular diseases [1, 3, 4]. However, no definitive conclusions have been made yet, and the results of some earlier studies were inconsistent. This may be because of the relatively small numbers of subjects evaluated and the lack of a simple and robust typing method.

The most important issue in clinical practice concerning haptoglobin is probably anaphylactic transfusion reactions, although this is not a commonly encountered problem. Patients who are genetically deficient in haptoglobin and carry the anti-haptoglobin antibody may experience adverse reactions against the haptoglobin protein in blood products. There have been several reports on this issue [5–8]. Muta et al. reported that even a non-haptoglobin-deficient patient could experience a transfusion reaction caused by the anti-haptoglobin antibody [9]. However, true anhaptoglobinemia

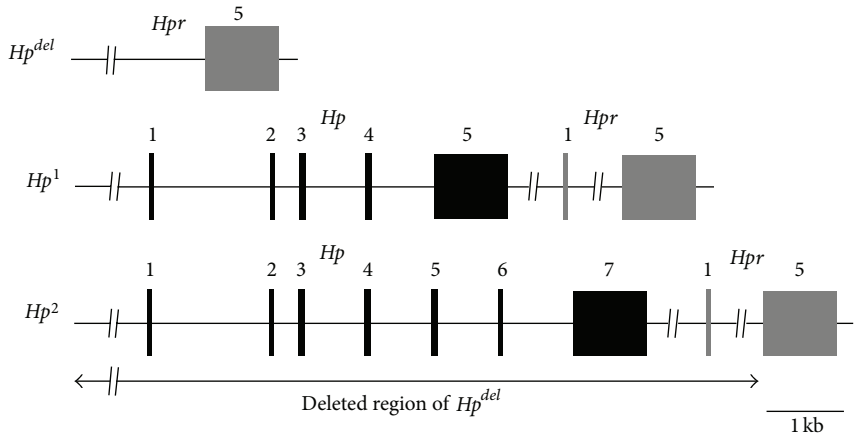

Figure 1: A schematic diagram of the genetic structure of the Hp^1, Hp^2, and Hp^{del} alleles. The Hp^1 allele has 5 exons compared to 7 exons of the Hp^2 allele. Exons 5 and 6 of the Hp^2 allele are the result of an internal duplication of exon 3 and exon 4 of the Hp^1 allele. A deletion spanning from the upstream region of exon 1 of the *Hp* gene to intron 4 of the *Hpr* gene makes the Hp^{del} allele. The black box and the shaded box represent exons of the *Hp* gene and the *Hpr* gene, respectively. The number above each box designates the number of the corresponding exon (see text for details). *Hp*: haptoglobin gene; *Hpr*: haptoglobin-related protein.

cannot be determined on the basis of the haptoglobin level alone because many acquired conditions might lower the haptoglobin concentrations to undetectable levels [10, 11].

Recently, another issue related to haptoglobin typing in clinical practice has been recognized. Haptoglobin types may affect the interpretation of the HbA1c levels in the estimation of glucose controls in diabetes patients, since haptoglobin is involved in hemoglobin turnover [12].

The results of previous studies emphasize the need for a rapid and robust genotyping method for haptoglobin. In this paper, we discuss the haptoglobin typing methods reported till date and reassess their utility in clinical practice.

2. Gene Structure and Alleles of Haptoglobin

There are 2 major alleles of haptoglobin—Hp^1 and Hp^2. Hp^2 is thought to be generated by the internal duplication of 2 exons of Hp^1 [16]. They are inherited in a codominant manner and may combine to result in 3 phenotypes, that is, Hp 1-1, Hp 2-1, and Hp 2-2. In contrast to Hp 1 proteins which exist in dimer forms, Hp 2 proteins can polymerize to form multimers with higher molecular mass [17]. This unique property can be used for haptoglobin phenotyping, as discussed later. Further, haptoglobin types affect the reference interval of haptoglobin levels in the serum; higher ranges are observed when the Hp^1 allele is present and lower ranges when the Hp^2 allele is present [17–19].

The Hp^{del} allele—an unusual allele also designated as Hp^0 in some literatures—is formed by the deletion of a portion of the 5′ flanking region of the *Hp* gene (5170 bp upstream of the exon 1 of *Hp*) to intron 4 of the *Hpr* (haptoglobin-related protein) gene [13, 20]. It is usually found in East and Southeast Asia with allele frequencies of 0.011–0.044 and not yet been reported in other races [13, 18, 21–24]. This allele is responsible for anhaptoglobinemia, which results from homozygosity for the Hp^{del} allele. A schematic diagram of the Hp^1, Hp^2, and Hp^{del} alleles is presented in Figure 1.

Some rare variants of the haptoglobin gene have also been reported with considerable ethnic differences [1]. Most of these variants have been designated on the basis of phenotypic methods, and their genetic mechanisms have not been fully studied. Some of the variants arise from genetic variations in the promoter regions, such as Hp 2-1M [25]. The variant Hp Johnson, also referred to as Hp^3, is thought to result from an additional internal duplication of the Hp^2 allele [26]. Although these alleles are of interest to researchers, their clinical significance has not been sufficiently evaluated. Thus, we will not discuss them in this paper.

Researchers wishing to conduct or design a haptoglobin-genotyping strategy should consider the presence of the *Hpr* gene. The *Hpr* gene is located near the *Hp* gene and contains sequences similar to those of the *Hp* gene. It is thought to originate from duplication and divergence [20, 27]. Primers and/or probes for the *Hp* gene should be carefully constructed to prevent them from binding to similar sequences in the *Hpr* gene.

3. Haptoglobin Phenotyping

As mentioned earlier, haptoglobin types influence the chemical structure of the products of the gene. Individuals homozygous for the Hp^1 allele (Hp 1-1 phenotype) have only Hp 1 dimers in their serum, and individuals harboring 2 Hp^2 alleles (Hp 2-2 phenotype) bear Hp 2 polymers with various sizes. Heterozygotes with both Hp^1 and Hp^2 alleles have Hp 1 dimers and Hp 2-1 polymers as well [17]. These proteins can be separated by gel electrophoresis, isoelectric focusing, chromatography, or ELISA [28–31]. A typical diagram of

Figure 2: Typical electrophoresis patterns of haptoglobin proteins according to their genotypes. Hp 1-1 shows a fast migrating band corresponding to the small Hp 1 dimer, and Hp 2-2 displays multiple slow migrating bands representing polymers consisting of Hp 2 proteins. Hp 2-1 has a fast migrating band and several slow migrating bands.

electrophoresis results is shown in Figure 2. Although these phenotyping methods have been used for a relatively long time and many studies have been conducted based on these methods, they require special equipment and experienced personnel to interpret the results. Furthermore, these techniques are not designed to detect patients harboring the Hp^{del} allele that is, they cannot discriminate true anhaptoglobinemia from conditions of acquired undetectable haptoglobin levels.

4. Haptoglobin Genotyping

4.1. Southern Blotting. As the genetic structures of Hp^1 and Hp^2 alleles were revealed, many researchers have tried to determine haptoglobin genotypes using molecular genetic techniques. Using various restriction enzymes and probes, Southern blotting has been effectively used to determine haptoglobin genotypes [16, 20]. However, this approach is not free from the limitations inherent to the method itself—requirement of a large amount of genomic DNA labor and time consumption and risk of radiation hazards. As more convenient and safe genotyping methods are being developed, the utility of Southern blotting has been steadily decreasing.

4.2. Conventional PCR. Koda et al. used conventional PCR for detecting Hp^{del} allele [13]. They targeted the junction region of the Hp^{del} allele to produce an amplicon of 315 bp. Exon 1 of the *Hp* gene was also amplified as a control (476 bp). The combination of these 2 products can identify individuals homozygous for Hp^{del} (315 bp only), heterozygous for Hp^{del} (315 and 476 bp), and without Hp^{del} (476 bp only). However, this strategy cannot distinguish between the Hp^1 and Hp^2 alleles.

Genotyping methods using conventional strategies for determining the Hp^1 and Hp^2 alleles were suggested by 2 groups. Koch et al. designed 4 primers to distinguish the Hp^1 from the Hp^2 alleles [14]. They suggested 3 protocols for genotyping, each yielding different patterns of PCR products. In the simplest protocols, which used just 1 set of primers, the Hp^1 allele and the Hp^2 allele were amplified to generate bands of 1757 bp and 3481 bp, respectively (protocol 1). In some instances where a band of the Hp^2 allele might not be easily detected due to its large size, another set of primers was applied to create an Hp^2-specific small amplicon of 349 bp (protocol 2). Koch et al. also tried to use all the 4 primers simultaneously to yield an Hp^1-specific band (1757 bp), 3 Hp^2-specific bands (349 bp, 1910 bp, and 1923 bp), and 2 nonspecific products (195 bp and 196 bp) (protocol 3). In the last protocol, an additional unknown band of about 450 bp was observed, which was suspected to be specific for the Hp^2 allele. An approach designed by Carter et al. used a similar scheme to produce a larger amplicon for the Hp^2 allele (4370 bp) and a smaller amplicon for the Hp^1 allele (3000 bp) [15]. However, these protocols could not detect the Hp^{del} allele. It is difficult to infer the presence of the Hp^{del} allele in the heterozygous state, and, since no amplification controls were used in both methods, it is impossible to discriminate the homozygous state for the Hp^{del} from amplification failure.

Park et al. used the strategies explained earlier to determine the haptoglobin genotypes in a Korean population [18]. Appropriate combinations of the methods can successfully detect the various combinations of the *Hp* alleles, such as Hp^1Hp^1, Hp^2Hp^1, Hp^2Hp^2, $Hp^{del}Hp^1$, $Hp^{del}Hp^2$, and $Hp^{del}Hp^{del}$. However, genotyping strategies using conventional PCR require keeping multiple sets of primers and performing tedious postamplification processes, such as electrophoresis. In addition, it is difficult to detect relatively large products over 3 kb, especially in poor amplification conditions. Typical patterns of a conventional PCR corresponding to specific haptoglobin genotypes are shown in Figure 3.

4.3. Real-Time PCR. To overcome the drawbacks of conventional PCR, Soejima et al. have developed a haptoglobin genotyping strategy using real-time PCR [32–34]. According to the typing purpose, two types of detection techniques were used.

In the first protocol using TaqMan probes [32, 33], they designed 3 sets of primers and probes to target the Hp^{del} breakpoint specific for Hp^{del} (Hp^{del}), the breakpoint of the duplication region specific for Hp^2 (HP2), and 5′ region of exon 1 as an internal control (HP5′). Each genotype produced appropriate signals as expected. Subjects who are homozygous for Hp^2 and those harboring Hp^1 and Hp^2 could be discriminated on the basis of the HP2/Hp5′ ratio calculated from the ΔΔCt values. This method could reliably determine the genotypes of the subjects in less than an hour through a single reaction. However, the approach cannot determine some rare variants such as Hp Johnson or Hp 2-1M [26, 32]. Nakamura et al. have applied this real-time PCR method for the genotyping of a Mongolian population [36]. More than 99% (943 of 946) of the subjects could be accurately typed by real-time PCR. In contrast, the haptoglobin genotypes of 3 individuals were misidentified, who were later revealed as having the rare Hp variant, Hp Johnson.

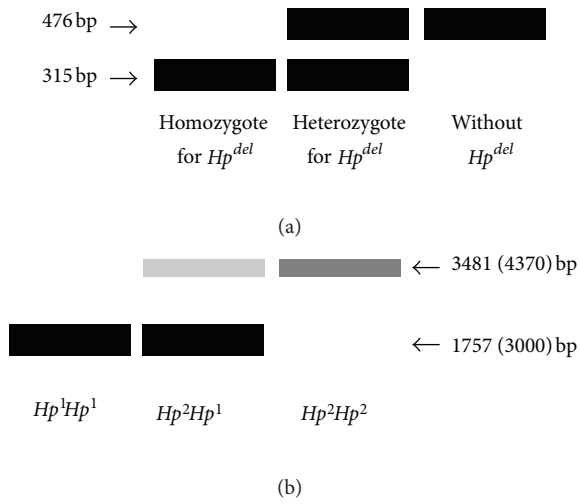

Figure 3: A schematic representation of conventional PCR results for *Hp* genotyping. (a) Gel electrophoresis to distinguish the Hp^{del} allele from other alleles [13]. A band of 315 bp size is specific for the Hp^{del} allele, and a larger band (476 bp) represents the presence of alleles other than Hp^{del} (Hp^1 or Hp^2 alleles). (b) A representative image of PCR products to determine the Hp^1 and Hp^2 genotypes [14, 15]. The amplification of the Hp^2 allele results in a large-sized amplicon (3481 or 4370 bp according to the primer design), and the Hp^1 allele is amplified to produce a relatively smaller band (1757 or 3000 bp). The larger band (>3.0 kb) is very weak and sometimes not detected, especially in the presence of a smaller band (see text for details).

Another method proposed by the same group is a SYBR Green I-based method to detect Hp^{del} allele [34]. This method easily detected Hp^{del} allele via melting curve analysis without using expensive TaqMan probes. But it only discriminated the Hp^{del} allele and the alleles without the deletion, as the Hp^1 and Hp^2 alleles produce the same signals.

They applied both methods to mass screening for pretransfusion testing [34]. Over 2000 patients were examined, and signals from some samples were too weak and cannot be detected, especially in the TaqMan-based method (data not given in the literature). This might be due to the fact that they used diluted blood samples as templates, and duplicate analysis might solve the problem.

4.4. Other Nucleic Acid Amplification Test. Another genetic analysis technique called loop-mediated isothermal amplification (LAMP) was recently developed and applied in many fields [37, 38]. This method can amplify nucleic acids with high degree of sensitivity and specificity in isothermal condition, requiring only a simple heating block or water bath. And a positive reaction can be detected by a simple visual inspection of turbidity. Soejima et al. have developed LAMP method for detection of Hp^{del} allele [35]. This method can efficiently analyze few samples without a sophisticated thermal cycler and detection apparatus. But two reaction tubes are required, and it cannot distinguish Hp^1 and Hp^2 alleles.

The principles and characteristics of various typing methods discussed earlier are summarized in Table 1.

5. Conclusions

Simple and reliable genotyping of haptoglobin is crucial in 4 aspects. (a) Phenotyping is laborious and cannot discriminate between patients with acute hemolytic conditions and those with Hp^{del}. (b) Haptoglobin levels should be interpreted according to the different reference intervals determined by genotypes. (c) Anaphylactic reaction to blood products can be fatal to transfusion recipients with anhaptoglobinemia. (d) Rapid and robust genotyping methods can establish a definite association between a haptoglobin genotype and a disease state.

We have discussed several haptoglobin typing methods. Phenotyping methods have been used for a long time, and a large body of data has been accumulated. Although certain rare and/or newly discovered variants may be identified via phenotyping, this approach does not detect anhaptoglobinemia. Southern blotting is easy to design and intuitive but requires tedious manual work and has the risk of radiation exposure. Conventional PCR can determine haptoglobin genotyping fairly well when appropriately designed. However, multiple primers and reactions are required to distinguish between the Hp^1, Hp^2, and Hp^{del} alleles. Genotyping strategy using real-time PCR using TaqMan probes has been suggested, and it can distinguish 3 alleles in a single reaction. From a perspective of transfusion reaction, to distinguish the Hp^{del} allele from others is important. SYBR Green I-based real-time PCR and LAMP assay have been proposed for this purpose.

To prevent anaphylactic transfusion reactions, distinguishing the Hp^{del} allele from the nondeficient allele is most important. However, discrimination between the Hp^1 and Hp^2 alleles may also be meaningful because they affect the reference interval of haptoglobin and may cause confusion in interpreting haptoglobin levels. Moreover, Muta et al. report a transfusion reaction caused by an anti-haptoglobin antibody in a non-haptoglobin-deficient patient, which suggests the possibility of developing a subtype-specific anti-haptoglobin antibody [9]. Thus, a genotyping method capable of distinguishing between the Hp^1, Hp^2, and Hp^{del} alleles is preferable. Real-time PCR using TaqMan probes developed by Soejima et al. seems to be desirable due to its simplicity and discriminative power, but reaction failure occurs in some samples for unknown reasons.

After reviewing various methods for haptoglobin typing, we conclude that no single method is sufficiently simple and efficient to discriminate between the various alleles of haptoglobin. The need for haptoglobin genotyping, however, is on the rise, and more simple and powerful methods are likely to be developed in the future. In the absence of an ideal method, researchers and/or laboratory physicians should fully comprehend the characteristics and limitations of various approaches used for haptoglobin genotyping and carefully choose 1 or more methods appropriate for their purpose.

Table 1: Characteristics of haptoglobin typing methods.

Method	Typing principle	Advantages	Disadvantages
Phenotyping [28–31]	Structure and size variations in proteins	Used for a long time Large amount of data accumulated Detects rare and/or new variants	Cannot detect Hp^{del} genotype Requires special equipment and trained personnel
Southern blotting [16, 20]	Restriction size variation	Detects Hp^{del} allele May recognize new alleles	Labor and timeconsuming Requires large amount of DNA Risk of radiation hazard
Conventional PCR [13–15, 18]	Size variation of amplified products	Distinguishes between Hp^1, Hp^2, and Hp^{del} alleles under appropriate combinations	Need to keep multiple primer sets Tedious postamplification process Difficult to amplify and detect large-sized products
Real-time PCR using TaqMan probe [32, 33]	Signals from probes reacting to amplified regions and their ratios	Discriminates between Hp^1, Hp^2, and Hp^{del} alleles in a single reaction	Cannot detect rare variants Multiple sets of primers and probes Reaction failure in a large scale study
Real-time PCR using SYBR Green I [34]	Melting curve analysis	Detect Hp^{del} allele effectively	Cannot distinguish between Hp^1 and Hp^2 Reaction failure in a large scale study
Loop-mediated isothermal amplification [35]	Turbidity measurement	Detect Hp^{del} allele effectively No need for a thermal cycler	Cannot distinguish between Hp^1 and Hp^2 Multiple sets of primers and 2 reaction tubes needed Not thoroughly evaluated

References

[1] K. Carter and M. Worwood, "Haptoglobin: a review of the major allele frequencies worldwide and their association with diseases," *International Journal of Laboratory Hematology*, vol. 29, no. 2, pp. 92–110, 2007.

[2] M. Kristiansen, J. H. Graversen, C. Jacobsen et al., "Identification of the haemoglobin scavenger receptor," *Nature*, vol. 409, no. 6817, pp. 198–201, 2001.

[3] H. Van Vlierberghe, M. Langlois, and J. Delanghe, "Haptoglobin polymorphisms and iron homeostasis in health and in disease," *Clinica Chimica Acta*, vol. 345, no. 1-2, pp. 35–42, 2004.

[4] M. Simpson, J. K. Snell-Bergeon, G. L. Kinney et al., "Haptoglobin genotype predicts development of coronary artery calcification in a prospective cohort of patients with type 1 diabetes," *Cardiovascular Diabetology*, vol. 10, p. 99, 2011.

[5] K. Morishita, E. Shimada, Y. Watanabe, and H. Kimura, "Anaphylactic transfusion reactions associated with anti-haptoglobin in a patient with ahaptoglobinemia," *Transfusion*, vol. 40, no. 1, pp. 120–121, 2000.

[6] E. Shimada, K. Tadokoro, Y. Watanabe et al., "Anaphylactic transfusion reactions in haptoglobin-deficient patients with IgE and IgG haptoglobin antibodies," *Transfusion*, vol. 42, no. 6, pp. 766–773, 2002.

[7] N. Shimode, H. Yasuoka, M. Kinoshita et al., "Severe anaphylaxis after albumin infusion in a patient with ahaptoglobinemia," *Anesthesiology*, vol. 105, no. 2, pp. 425–426, 2006.

[8] H. Kim, J. Choi, K. U. Park et al., "Anaphylactic transfusion reaction in a patient with anhaptoglobinemia: the first case in Korea," *Annals of Laboratory Medicine*, vol. 32, no. 4, pp. 304–306, 2012.

[9] T. Muta, M. Ozaki, T. Tokuyama et al., "Anti-haptoglobin antibody detection after febrile non-hemolytic transfusion reactions in a non-haptoglobin-deficient patient," *Transfusion and Apheresis Science*, vol. 41, no. 3, pp. 171–173, 2009.

[10] A. Rougemont, M. Quilici, J. Delmont, and J. P. Ardissone, "Is the HpO phenomenon in tropical populations really genetic?" *Human Heredity*, vol. 30, no. 4, pp. 201–203, 1980.

[11] J. Delanghe, M. Langlois, and M. De Buyzere, "Congenital anhaptoglobinemia versus acquired hypohaptoglobinemia," *Blood*, vol. 91, no. 9, p. 3524, 1998.

[12] K. Suzuki, K. Yagi, R. Oka et al., "Relationships of serum haptoglobin concentration with HbA1c and glycated albumin concentrations in Japanese type 2 diabetic patients," *Clinical Chemistry and Laboratory Medicine*, vol. 47, no. 1, pp. 70–74, 2009.

[13] Y. Koda, Y. Watanabe, M. Soejima et al., "Simple PCR detection of haptoglobin gene deletion in anhaptoglobinemic patients with antihaptoglobin antibody that causes anaphylactic transfusion reactions," *Blood*, vol. 95, no. 4, pp. 1138–1143, 2000.

[14] W. Koch, W. Latz, M. Eichinger et al., "Genotyping of the common haptoglobin Hp 1/2 polymorphism based on PCR," *Clinical Chemistry*, vol. 48, no. 9, pp. 1377–1382, 2002.

[15] K. Carter, D. J. Bowen, C. A. M, and M. Worwood, "Haptoglobin type neither influences iron accumulation in normal subjects nor predicts clinical presentation in HFE C282Y haemochromatosis: phenotype and genotype analysis," *British Journal of Haematology*, vol. 122, no. 2, pp. 326–332, 2003.

[16] N. Maeda, F. Yang, D. R. Barnett, B. H. Bowman, and O. Smithies, "Duplication within the haptoglobin Hp2 gene," *Nature*, vol. 309, no. 5964, pp. 131–135, 1984.

[17] M. R. Langlois and J. R. Delanghe, "Biological and clinical significance of haptoglobin polymorphism in humans," *Clinical Chemistry*, vol. 42, no. 10, pp. 1589–1600, 1996.

[18] K. U. Park, J. Song, and J. Q. Kim, "Haptoglobin genotypic distribution (including Hp0 allele) and associated serum haptoglobin concentrations in Koreans," *Journal of Clinical Pathology*, vol. 57, no. 10, pp. 1094–1095, 2004.

[19] I. Kasvosve, Z. A. R. Gomo, I. T. Gangaidzo et al., "Reference range of serum haptoglobin is haptoglobin phenotype-dependent in blacks," *Clinica Chimica Acta*, vol. 296, no. 1-2, pp. 163–170, 2000.

[20] Y. Koda, M. Soejima, N. Yoshioka, and H. Kimura, "The haptoglobin-gene deletion responsible for anhaptoglobinemia," *American Journal of Human Genetics*, vol. 62, no. 2, pp. 245–252, 1998.

[21] M. Soejima, Y. Koda, J. Fujihara, and H. Takeshita, "The distribution of haptoglobin-gene deletion (Hpdel) is restricted to East Asians," *Transfusion*, vol. 47, no. 10, pp. 1948–1950, 2007.

[22] K. Teye, I. K. E. Quaye, Y. Koda et al., "A-61C and C-101G Hp gene promoter polymorphisms are, respectively, associated with ahaptoglobinaemia and hypohaptoglobinaemia in Ghana," *Clinical Genetics*, vol. 64, no. 5, pp. 439–443, 2003.

[23] S. E. Cox, C. Doherty, S. H. Atkinson et al., "Haplotype association between haptoglobin (Hp2) and Hp promoter SNP (A-61C) may explain previous controversy of haptoglobin and malaria protection," *PLoS ONE*, vol. 2, no. 4, article e362, 2007.

[24] E. Shimada, M. Odagiri, K. Chaiwong et al., "Detection of Hpdel among Thais, a deleted allele of the haptoglobin gene that causes congenital haptoglobin deficiency," *Transfusion*, vol. 47, no. 12, pp. 2315–2321, 2007.

[25] N. Maeda, "DNA polymorphisms in the controlling region of the human haptoglobin genes: a molecular explanation for the haptoglobin 2-1 modified phenotype," *American Journal of Human Genetics*, vol. 49, no. 1, pp. 158–166, 1991.

[26] S. Oliviero, M. DeMarchi, and A. O. Carbonara, "Molecular evidence of triplication in the haptoglobin Johnson variant gene," *Human Genetics*, vol. 71, no. 1, pp. 49–52, 1985.

[27] N. Maeda, "Nucleotide sequence of the haptoglobin and haptoglobin-related gene pair," *Journal of Biological Chemistry*, vol. 260, no. 11, pp. 6698–6709, 1985.

[28] O. Smithies, "Zone electrophoresis in starch gels: group variations in the serum proteins of normal human adults.," *The Biochemical Journal*, vol. 61, no. 4, pp. 629–641, 1955.

[29] A. Alonso, G. Visedo, M. Sancho, and J. Fernandez-Piqueras, "Haptoglobin subtyping by isoelectric focusing in miniaturized polyacrylamide gels rehydrated in presence of 2-mercaptoethanol," *Electrophoresis*, vol. 11, no. 4, pp. 321–324, 1990.

[30] J. Delanghe, K. Allcock, M. Langlois, L. Claeys, and M. De Buyzere, "Fast determination of haptoglobin phenotype and calculation of hemoglobin binding capacity using high pressure gel permeation chromatography," *Clinica Chimica Acta*, vol. 291, no. 1, pp. 43–51, 2000.

[31] N. S. Levy and A. P. Levy, "ELISA for determination of the haptoglobin phenotype," *Clinical Chemistry*, vol. 50, no. 11, pp. 2148–2150, 2004.

[32] M. Soejima and Y. Koda, "TaqMan-based real-time PCR for genotyping common polymorphisms of haptoglobin (HP1 and HP2)," *Clinical Chemistry*, vol. 54, no. 11, pp. 1908–1913, 2008.

[33] M. Soejima and Y. Koda, "Rapid real-time PCR detection of HPdel directly from diluted blood samples," *Clinical Chemistry*, vol. 54, no. 6, pp. 1095–1096, 2008.

[34] M. Soejima, Y. Tsuchiya, K. Egashira, H. Kawano, K. Sagawa, and Y. Koda, "Development and validation of a SYBR Green I-based real-time polymerase chain reaction method for detection of haptoglobin gene deletion in clinical materials," *Transfusion*, vol. 50, no. 6, pp. 1322–1327, 2010.

[35] M. Soejima, K. Egashira, H. Kawano, A. Kawaguchi, K. Sagawa, and Y. Koda, "Rapid detection of haptoglobin gene deletion in alkaline-denatured blood by loop-mediated isothermal amplification reaction," *Journal of Molecular Diagnostics*, vol. 13, no. 3, pp. 334–339, 2011.

[36] H. Nakamura, M. Soejima, L. Munkhtulga, S. Iwamoto, and Y. Koda, "Haptoglobin polymorphism in Mongolian population: comparison of the two genotyping methods," *Clinica Chimica Acta*, vol. 408, no. 1-2, pp. 110–113, 2009.

[37] T. Notomi, H. Okayama, H. Masubuchi et al., "Loop-mediated isothermal amplification of DNA," *Nucleic Acids Research*, vol. 28, no. 12, p. E63, 2000.

[38] Y. Mori and T. Notomi, "Loop-mediated isothermal amplification (LAMP): a rapid, accurate, and cost-effective diagnostic method for infectious diseases," *Journal of Infection and Chemotherapy*, vol. 15, no. 2, pp. 62–69, 2009.

Hindawi Publishing Corporation
BioMed Research International
Volume 2013, Article ID 105319, 4 pages
http://dx.doi.org/10.1155/2013/105319

Research Article

Development of a Prognostic Score Using the Complete Blood Cell Count for Survival Prediction in Unselected Critically Ill Patients

Fang Chongliang,[1] Li Yuzhong,[1,2] Shi Qian,[2] Liu Xiliang,[3] and Liu Hui[2]

[1] *Second Affiliated Hospital of Dalian Medical University, Dalian 116023, China*
[2] *College of Medical Laboratory, Dalian Medical University, Dalian 116044, China*
[3] *Center Hospital of Dalian, Dalian 116033, China*

Correspondence should be addressed to Liu Hui; liuhui60@sina.com

Received 4 November 2012; Revised 30 January 2013; Accepted 30 January 2013

Academic Editor: Antonio La Gioia

Objective. The purpose of this study was to develop a new prognostic scoring system for critically ill patients using the simple complete blood cell count (CBC). *Methods*. CBC measurements in samples from 306 patients in an intensive care unit were conducted with automated analyzers, including levels of neutrophils, lymphocytes, erythrocytes, hemoglobin, and platelets. The time of sampling and the time of death were recorded. Z values were calculated according to the measured values, reference mean values, and standard deviations. The prognostic score was equivalent to the median of the Z value of each of the measured parameters. *Results*. There was a significant correlation between survival time and neutrophil, lymphocyte, and platelet levels ($P < 0.05$). Prognostic scores were calculated from the Z value of these three parameters. Survival times decreased as the prognostic score increased. *Conclusions*. This study suggests that a model that uses levels of neutrophils, lymphocytes, and platelets is potentially useful in the objective evaluation of survival time or disease severity in unselected critically ill patients.

1. Introduction

Although accurate prediction of survival is essential for palliative care, the numerous clinical tools currently available that attempt to determine how long a patient is likely to live remain inappropriate [1, 2]. The clinical significance of studies on survival predictors in critically ill patients is hindered by the difficulty of finding objective and quantitative common predictors of death. On the basis of such studies, performance status, including parameters such as anorexia, weight loss, dysphagia, dyspnea, and cognitive failure, has been found to correlate most strongly with survival [3–5]. However, the nature of this subjective and qualitative data tends to preclude precise specification. Some prognostic scoring systems with performance status, clinical symptoms, and biochemical parameters help to guide accurate prediction, such as the acute physiology and chronic health evaluation (APACHE), yet are considered too complex for general clinical use [6]. Therefore, the prediction of clinical events with laboratory parameters, including complete blood cell count (CBC), has become an increased focus of research. Accumulating evidence indicates that the CBC is an effective predictor of mortality in many disease states, including hematological disease [7–9], neoplasms [10–12], and diseases of the circulatory system [13–15].

Biomarkers in fluids offer the opportunity for more objective and reproducible measurement. They are not only able to provide a reliable and objective basis for screening and for diagnosis, but they can also measure disease severity [16–18]. The CBC demonstrates nonspecific changes in a variety of critical illnesses [19–21]. Therefore, nonspecific changes in the CBC in critically ill patients could be considered a key prognostic factor in the evaluation of survival prediction in these patients [7–15]. Accordingly, it is possible that the CBC

Table 1: Survival time and levels of baseline CBC indicators in critically ill patients.

Group	Survival median day	N	Blood cell count (mean ± SD)				
			Neu	Lym	RBC	HB	Plt
Day 1	1	59	14.0 ± 11.3	2.1 ± 1.9	3.5 ± 1.2	108.1 ± 34.2	140.5 ± 101.8
Day 2	2	64	12.3 ± 6.5	1.4 ± 1.0	3.6 ± 1.2	111.1 ± 38.3	150.3 ± 102.0
Day 3	3	29	9.5 ± 5.6	0.9 ± 0.6	3.7 ± 1.1	111.5 ± 34.8	138.1 ± 75.2
Day 4	4	21	10.6 ± 7.3	1.5 ± 1.3	3.5 ± 1.0	107.3 ± 30.5	152.4 ± 94.1
Day 5	5	34	10.9 ± 7.1	1.2 ± 0.7	3.6 ± 0.8	107.3 ± 26.1	167.0 ± 81.0
Days 6–30	14	38	10.1 ± 5.4	1.2 ± 0.7	3.4 ± 0.7	106.5 ± 22.1	171.8 ± 100.1
Days 31–180	91	37	6.9 ± 4.5	1.4 ± 0.7	3.7 ± 0.8	114.4 ± 22.2	209.9 ± 102.2
Days 181–365	296	24	5.2 ± 3.0	1.6 ± 0.7	4.0 ± 0.8	121.8 ± 28.7	223.3 ± 92.8

Table 2: Relationship between survival time and levels of CBC indicators.

Correlation		Neu	Lym	RBC	HB	Plt
Survival time	r	−0.142	−0.168	0.008	−0.015	0.125
	p	0.012	0.003	0.892	0.788	0.027

could be used as a predictor of survival in unselected critically ill patients. The current study performed a quantitative analysis on changes in the CBC in critically ill patients. Furthermore, we developed a new prognostic scoring system to evaluate survival times with sensitive parameters specifically for critically ill patients.

2. Subjects and Methods

2.1. Subjects. Critically ill patients recruited into this study received treatment in an intensive care unit (ICU) between July 2006 and December 2010 at three hospitals (Second Affiliated Hospital of Dalian Medical University, Center Hospital of Dalian, and Third Hospital of Dalian, China). Inclusion criteria were availability of data on CBCs in medical records and death within one year of CBC measurement. Exclusion criteria were primary diseases from systemic hematological disorders and accidental injuries. A total of 306 subjects were selected (170 males, 136 females; mean age 65.3 ± 15.5 years). The main diseases were cardiovascular and cerebrovascular (n = 69), chronic obstructive pulmonary disease (n = 13), various types of tumors (n = 86), and other diseases (n = 138).

The time of the observation, that is, the CBC measurement, and the time of death were recorded. The date of death was obtained from medical records and residence queries. On the basis of survival time, subjects were divided into 8 groups (Day 1, Day 2, Day 3, Day 4, Day 5, Days 6–30, Days 31–180, and Days 180–365). The study was conducted in accordance with the Declaration of Helsinki, and the study was approved by the Institutional Ethics Committee of Dalian Medical University.

2.2. CBC Data. CBC data was obtained from medical records. CBC measurement, which included levels of neutrophils (Neu, $3.5 \pm 1.2 \cdot 10^9$/L), lymphocytes (Lym, $2.2 \pm 0.6 \cdot 10^9$/L), red blood cells (RBC, $4.5 \pm 0.6 \cdot 10^{12}$/L), hemoglobin (HB, 142 ± 20 g/L), and platelets (Plt, $210 \pm 53 \cdot 10^9$/L), was performed with an automatic analyzer, using standard commercial reagent kits. All the analyzers met the requirements of external quality assessment in Dalian, China.

2.3. Statistical Analysis and Establishment of the Model. Correlation coefficient (Spearman's method) was used to assess the correlation between survival time and biochemical parameters (alpha = 0.05, two-tailed test). The significant indicators were used to set up the prognostic score. On the basis of the reference range, we obtained mean values ($\overline{X}$) and standard deviation (S). The Z values were calculated according to the following formulas, where X is the measured value:

$$\text{Neu, Lym: } Z = (X - \overline{X})/S.$$

$$\text{RBC, HB, Plt: } Z = (\overline{X} - X)/S.$$

The prognostic score was equivalent to the median of the Z value of each of the measured parameters. For Z values of Neu, Lym, and Plt of 1.36, 1.70, and 1.45, respectively, for example, the prognostic score was 1.45.

3. Results

The original data for survival time in this cohort of critically ill patients and levels of Neu, Lym, RBC, HB, and Plt is shown in Table 1. The relationship between survival time and CBC levels as determined by correlation analysis is shown in Table 2. The Neu, Lym, and Plt levels are considered predictors. Prognostic scores were calculated from the Z value of Neu, Lym, and Plt levels, as shown in Table 3. Survival time decreased as the prognostic scores increased.

4. Discussion

Natural death for the majority of people can be considered a process of loss of organ function. Compensatory or stress responses will occur during this process. The CBC contributes to the data used to assess these reactions and potentially offers the opportunity for a more objective measurement [7–15]. Therefore, identification of the CBC in unselected critically ill patients is essential in our understanding

Table 3: Distribution of prognostic scores in different survival time groups.

Group	Score (Quartile)		
	25th	50th	75th
Day 1	0.41	2.12	2.87
Day 2	0.18	1.63	2.62
Day 3	−0.47	1.19	2.25
Day 4	−0.21	0.73	2.35
Day 5	−0.12	0.73	1.62
Days 6–30	−0.08	0.82	1.76
Days 31–180	−0.98	−0.06	0.50
Days 181–365	−0.96	−0.34	0.33

of the impairment and restorative processes that occur during the end of life. In the current study, Neu and Lym levels were negatively correlated with survival time, while Plt level was positively correlated, indicating that these three parameters could have potential in the prediction of survival in critically ill patients.

Theoretically, the three parameters change independently. Abnormal changes in two or three of them can be considered as nonspecific systemic changes that are associated with death, and abnormal changes in a single indicator may be specific. There may be no correlation between a change in a single indicator and the occurrence of death. Thus, we transformed measurement data into Z values in order to assess the comparability of change in measured values. The median of the Z value of each of the measured parameters (prognostic score) can be considered a quantitative evaluation of holistic changes rather than a change in only one indicator.

As data transformation into Z values was conducted according to the reference range of each item, theoretically the score is equivalent to zero, and the higher the observed score, the greater the risk of death. Our results show that survival time decreases as the prognostic score increases, suggesting that a model using Neu, Lym, and Plt levels is potentially useful in the objective evaluation of survival time in critically ill patients.

Multiple analysis is a basic tool for developing a risk model [22–24]. Large populations of several thousand individuals are required to perform the linear multiple regression. Our mathematical model was established on the basis of normal reference ranges rather than multiple analyses. The patients could be considered as a separate validation population. Compared to traditional methods, our method for establishing a mathematical model had a higher efficiency.

We believe that disease severity when patients are admitted to ICU is not easy to determine objectively. Therefore, time of death is a reliable indicator of disease severity. The subjects needed to be standardized, thus rendering the results comparable; thus, subjects were divided on the basis of survival time. Our results showed that the predictive score in the group that survived 181–365 days was close to zero, close to the theoretically normal score. This implied that the score would be zero or close to zero in patients who survive more than 365 days, but this group was not observed in this study.

The hypothesis for this study was that CBC results are associated with imminent death and are unlikely to be related to death occurring in the longer term, as a result of many confounding variables. The current study demonstrates a responsiveness of the CBC to death, within a period of approximately one week, which is consistent with our hypothesis. CBC is a conventional laboratory test and contains much information. Our results may be useful for the development of a validated scoring system for survival prediction or disease severity. Further prospective randomized controlled trial studies are warranted to validate the usefulness of these determinants for accurate survival predictions.

References

[1] J. L. Vincent, S. M. Opal, and J. C. Marshall, "Ten reasons why we should NOT use severity scores as entry criteria for clinical trials or in our treatment decisions," *Critical Care Medicine*, vol. 38, no. 1, pp. 283–287, 2010.

[2] A. Chandra, S. Mangam, and D. Marzouk, "A review of risk scoring systems utilised in patients undergoing gastrointestinal surgery," *Journal of Gastrointestinal Surgery*, vol. 13, no. 8, pp. 1529–1538, 2009.

[3] M. M. Wheeler, "APACHE: an evaluation," *Critical Care Nursing Quarterly*, vol. 32, no. 1, pp. 46–48, 2009.

[4] S. Gripp, S. Moeller, E. Bölke et al., "Survival prediction in terminally ill cancer patients by clinical estimates, laboratory tests, and self-rated anxiety and depression," *Journal of Clinical Oncology*, vol. 25, no. 22, pp. 3313–3320, 2007.

[5] I. Hyodo, T. Morita, I. Adachi, Y. Shima, A. Yoshizawa, and K. Hiraga, "Development of a predicting tool for survival of terminally III cancer patients," *Japanese Journal of Clinical Oncology*, vol. 40, no. 5, Article ID hyp182, pp. 442–448, 2010.

[6] E. Leung, K. McArdle, and L. S. Wong, "Risk-adjusted scoring systems in colorectal surgery," *International Journal of Surgery*, vol. 9, no. 2, pp. 130–135, 2011.

[7] Y. S. Chae, H. Shin, S. K. Sohn et al., "Absolute lymphocyte count at day + 21 predicts survival in patients with early-stage diffuse large B-cell lymphoma treated with rituximab, cyclophosphamide, adriamycin, vincristine and prednisone," *Leukemia & Lymphoma*, vol. 53, no. 9, pp. 1757–1763, 2012.

[8] D. Sun, P. Elson, M. Liedtke et al., "Absolute lymphocyte count at day 28 independently predicts event-free and overall survival in adults with newly diagnosed acute lymphoblastic leukemia," *American Journal of Hematology*, vol. 87, no. 10, pp. 957–960, 2012.

[9] M. M. Patnaik, D. Caramazza, N. Gangat, C. A. Hanson, A. Pardanani, and A. Tefferi, "Age and platelet count are IPSS-independent prognostic factors in young patients with primary myelofibrosis and complement IPSS in predicting very long or very short survival," *European Journal of Haematology*, vol. 84, no. 2, pp. 105–108, 2010.

[10] W. Chua, K. A. Charles, V. E. Baracos, and S. J. Clarke, "Neutrophil/lymphocyte ratio predicts chemotherapy outcomes in patients with advanced colorectal cancer," *British Journal of Cancer*, vol. 104, no. 8, pp. 1288–1295, 2011.

[11] M. Kaneko, H. Nozawa, K. Sasaki et al., "Elevated neutrophil to lymphocyte ratio predicts poor prognosis in advanced colorectal cancer patients receiving oxaliplatin-based chemotherapy," *Oncology*, vol. 82, no. 5, pp. 261–268, 2012.

[12] M. Ishizuka, K. Kubota, J. Kita, M. Shimoda, M. Kato, and T. Sawada, "Usefulness of a modified inflammation-based prognostic system for predicting postoperative mortality of patients undergoing surgery for primary hepatocellular carcinoma," *Journal of Surgical Oncology*, vol. 103, no. 8, pp. 801–806, 2011.

[13] B. Azab, M. Zaher, K. F. Weiserbs et al., "Usefulness of neutrophil to lymphocyte ratio in predicting short-and long-term mortality after NonST-elevation myocardial infarction," *American Journal of Cardiology*, vol. 106, no. 4, pp. 470–476, 2010.

[14] A. De Labriolle, L. Bonello, G. Lemesle et al., "Decline in platelet count in patients treated by percutaneous coronary intervention: definition, incidence, prognostic importance, and predictive factors," *European Heart Journal*, vol. 31, no. 9, pp. 1079–1087, 2010.

[15] J. Núñez, E. Núñez, V. Bodí et al., "Low lymphocyte count in acute phase of ST-segment elevation myocardial infarction predicts long-term recurrent myocardial infarction," *Coronary Artery Disease*, vol. 21, no. 1, pp. 1–7, 2010.

[16] L. Hui, L. Shijun, Z. Xinyu, W. Yuai, and X. Xiaoting, "Objective assessment of stress levels and health status using routinely measured clinical laboratory parameters as biomarkers," *Biomarkers*, vol. 16, no. 6, pp. 525–529, 2011.

[17] L. Hui, W. Yuai, Q. Xia, and Y. Hong, "Serum glucose- and C-reactive protein-based assessment of stress status in a healthy population," *Clinical Laboratory*, vol. 56, no. 5-6, pp. 227–230, 2010.

[18] H. Wang, X. Zhao, G. Luan, X. Liu, and H. Liu, "Nonspecific biochemical changes under different health statuses and a quantitative model based on biological markers to evaluate systemic function in humans," *Clinical Laboratory*, vol. 56, no. 5-6, pp. 223–225, 2010.

[19] O. Trdan, I. Ray-Coquard, G. Chvetzoff et al., "Validation of prognostic scores for survival in cancer patients beyond first-line therapy," *BMC Cancer*, vol. 11, article 95, 2011.

[20] Y. Yoneyama, M. Ito, M. Sugitou, A. Kobayashi, Y. Nishizawa, and N. Saito, "Postoperative lymphocyte percentage influences the long-term disease-free survival following a resection for colorectal carcinoma," *Japanese Journal of Clinical Oncology*, vol. 41, no. 3, pp. 343–347, 2011.

[21] M. Moroni, E. Lombardini, R. Salber et al., "Hematological changes as prognostic indicators of survival: similarities between gottingen minipigs, humans, and other large animal models," *PLoS ONE*, vol. 6, no. 9, Article ID e25210, 2011.

[22] J. Steer, J. Gibson, and S. C. Bourke, "The DECAF Score: predicting hospital mortality in exacerbations of chronic obstructive pulmonary disease," *Thorax*, vol. 67, no. 11, pp. 970–976, 2012.

[23] S. M. Wiseman, J. I. Forrest, J. E. Chan et al., "Factors predictive of 30-day postoperative mortality in HIV/AIDS patients in the era of highly active antiretroviral therapy," *Annals of Surgery*, vol. 256, no. 1, pp. 170–176, 2012.

[24] M. Kolditz, G. Hffken, P. Martus et al., "CAPNETZ study group. Serum cortisol predicts death and critical disease independently of CRB-65 score in community-acquired pneumonia: a prospective observational cohort study," *BMC Infectious Diseases*, vol. 12, article 90, 2012.

Hindawi Publishing Corporation
BioMed Research International
Volume 2013, Article ID 305704, 4 pages
http://dx.doi.org/10.1155/2013/305704

Research Article

Validation of New Allele-Specific Real-Time PCR System for Thiopurine Methyltransferase Genotyping in Korean Population

Sollip Kim,[1] Hye Won Lee,[2] Woochang Lee,[2] Sail Chun,[2] and Won-Ki Min[2]

[1] *Department of Laboratory Medicine, Ilsan Paik Hospital, Inje University College of Medicine, Joowha-ro 170, Ilsanseo-gu, Goyang, Gyeonggi, Republic of Korea*
[2] *Department of Laboratory Medicine, Asan Medical Center, University of Ulsan College of Medicine, 88, Olympic-ro 43-gil, Songpa-gu, Seoul, Republic of Korea*

Correspondence should be addressed to Sail Chun; sailchun@amc.seoul.kr

Received 15 November 2012; Accepted 29 January 2013

Academic Editor: Andrew St. John

Introduction. Thiopurine drugs are metabolized via S-methylation and catalyzed by thiopurine S-methyltransferase (TPMT). Patients with very low TPMT activity are at high risk of fatal bone marrow toxicity when standard doses of thiopurine drugs are administered. *TPMT* genotyping can predict TPMT activity and is not affected by transfusion or red blood cell defects. Here, we report a new allele-specific real-time polymerase chain reaction (PCR) system for thiopurine methyltransferase genotyping that is validated in Korean population. *Materials and Methods*. Three major *TPMT* single-nucleotide polymorphisms (*TPMT* **2*, **3B*, and **3C*) were genotyped using real-time PCR with the allele-specific primers and probes. Internal positive controls were included in each well, and an automatic interpretative algorithm was applied. This system was validated using 244 clinical samples and 2 commercial DNA samples that had been previously genotyped using PCR-direct sequencing. *Results*. All of the obtained results are concordant with those of the reference method. All of the internal positive control reactions were successful. The allele frequency of *TPMT* **3C* was 2.05% (10 of 488 alleles). All of the patients with variant alleles were heterozygotes, and no homozygotes were detected. No *TPMT* **2*, **3A*, or **3B* alleles were observed in this Korean population. *Conclusion*. This rapid, accurate, and user-friendly genotyping system can be readily used to improve the efficacy and safety of thiopurine treatments in clinical practice.

1. Introduction

Thiopurine drugs, such as azathioprine, 6-mercaptopurine, and 6-thioguanine, are used to treat patients with leukemia, inflammatory bowel disease, rheumatic disease, and those who have received an organ transplant [1]. Approximately 30–40% of inflammatory bowel disease patients fail to benefit from this treatment [2]. The crucial factor that explains the interindividual differences, in terms of therapeutic efficacy and adverse reactions, is the variable activity of the thiopurine methyltransferase (TPMT) enzyme, which is involved in the metabolic pathways of these drugs [2]. Approximately 90% of individuals have normal activity, 10% have intermediate activity, and 0.3% have low or undetectable activity [1]. Patients with decreased TPMT activity might experience hematopoietic toxicity, such as myelosuppression, if they are treated with standard thiopurine doses [3, 4]. Dosage reduction can minimize toxicity in these patients [5].

Methods that measure the TPMT activity of red blood cells (RBCs) are available, but these results may be falsely elevated by recent blood transfusions or falsely lowered by RBC aging [6, 7]. On the other hand, *TPMT* genotyping can predict TPMT activity and offers an advantage over phenotypic methods in the aforementioned situations [1, 6, 8]. Compared with wild-type (*TPMT* **1*) homozygotes, individuals with 2 variant alleles demonstrate low or undetectable TPMT activity, while those with one variant allele demonstrate intermediate TPMT activity [1].

Although polymerase-chain-reaction-(PCR-) direct sequencing is considered the gold standard, both the test procedures and the interpretation of the results are time-consuming and labor-intensive. Moreover, four variant

alleles together account for over 95% of the reduced TPMT activity in Caucasian subjects [9]: *TPMT* *2 (rs1800462, c.238G > C, and p.Ala80Pro); *3B (rs1800460, c.460G > A, and p.Ala154Thr); *3C (rs1142345, c.719A > G, and p.Tyr240Cys); *3A (c.460G > A and c.719A > G). The most prevalent variant alleles in the Caucasian population is *TPMT* *3A (10% of this population carries a nonfunctional allele), while *TPMT* *3C predominates in the East Asian population (4.7% of this population) [2].

Therefore, genotyping only the major target regions could be sufficient for preassessment of patients prior to commencing thiopurine drugs. In addition, a faster, high-throughput method is needed for applications in the clinical laboratory. Allele-specific real-time PCR may be a good approach. In this paper, we describe how we developed and validated a new allele-specific real-time PCR system with an automatic interpretative function that can be used to detect *TPMT* genetic polymorphisms for the dose adjustment of thiopurine drugs.

2. Materials and Methods

2.1. Development of the Allele-Specific Real-Time PCR System. Our allele-specific, real-time PCR system was developed based on the use of allele-specific primers and 5′ nuclease probes. Two types of primers were designed in order to specifically detect the desired genotypes: one specific for the wild-type allele and the other for variants [10]. An internal positive control (IPC), *GAPDH*, was added to all of the wells in order to verify successful amplification.

We selected the target *TPMT* single-nucleotide polymorphisms (SNPs) based on thiopurine dosing guidelines [11] and the genotype frequencies that have been reported in Korean populations and elsewhere [12, 13]. After designing several sets of primers using Primer3 (http://primer3.sourceforge.net/), we selected the most efficient primer pairs with the smallest and largest cycle thresholds (Cts) between the wild-type and variant signals. The primer and probe sequences for the real-time PCR system are proprietary information of the manufacturer (Bioneer, Daejeon, South Korea). The real-time PCR reactions were carried out on an Exicycler real-time system (Bioneer).

Each 50 μL reaction mixture included 5 μL of template DNA, *TPMT*-specific primers, dual-labeled fluorogenic 5′ nuclease *TPMT*-specific probes (5′-FAM; 3′-Dabsyl), a dual-labeled fluorogenic 5′ nuclease *GAPDH*-specific IPC probe (5′-TAMRA; 3′-BHQ1), DNA polymerase, dNTPs, and a stabilizer. The amplification protocol included an initial denaturation at 95°C for 10 minutes, followed by 45 cycles of denaturation at 95°C for 20 seconds and annealing and extension at 55°C for 30 seconds. The results were considered successful if the IPC was amplified with a Ct < 30.

To determine the required minimal DNA concentration, various concentrations of DNA samples (100 ng/μL, 30 ng/μL, 10 ng/μL, 5 ng/μL, and 1 ng/μL) were isolated from 5 patients for 3 consecutive days, tested in quadruplicate and compared. To determine the analytical limit of detection, serially diluted variant templates (1×10^7–1×10^2 copies/μL) were tested. An automatic interpretative software program for real-time PCR assays, which was based on Ct differences of 2, was used as previously reported [10].

2.2. Validation of the Allele-Specific Real-Time PCR System. To validate the accuracy of the allele-specific real-time PCR genotyping method, we performed both PCR-direct sequencing and allele-specific real-time PCR using DNA samples from 244 patients who were treated with azathioprine or mercaptopurine. Genomic DNA was extracted from 2 mL of ethylenediaminetetraacetic-acid-(EDTA-) anticoagulated blood using a QIAamp DNA mini kit (Qiagen, Valencia, CA, USA) in accordance with the manufacturer's instructions. In addition, a commercially available *3B genomic DNA (NA09301) sample and *3C genomic DNA (NA03579) sample were also analyzed (Coriell Institute, Camden, NJ, USA). Bidirectional sequencing was conventionally performed on an ABI Prism 3130XL Genetic Analyzer (Applied Biosystems, Foster City, CA, USA). Details regarding the primers used in the sequencing analysis are available upon request.

3. Results

3.1. Development and Establishment of the Allele-Specific Real-Time PCR System. We selected three major target SNPs: *TPMT* c.238G > C (*2); c.460G > A (*3A and *3B); c.719A > G (*3A and *3C). All IPCs were perfectly amplified. We found that all of the target SNPs were successfully amplified using the specifically designed allele-specific primers and the 5′ nuclease probe. At least 5 ng/μL of the template DNA was needed to yield reproducible results. The analytical limit of detection was 1×10^2 copies/reaction for 238G > C and c.460G > A and was 1×10^3 copies/reaction for c.719A > G. A concentration of 1.0 ng/μL corresponded to 1×10^3 copies/μL.

All of the interpreted results of each specimen are summarized in each row, and the results from all of tested samples are displayed in Figure 1(a). In addition, all of the reaction curves generated for the 3 SNPs from the selected samples are simultaneously displayed (Figures 1(b) and 1(c)), allowing easy and convenient visualization of the reaction curves.

3.2. Validation of the Allele-Specific Real-Time PCR System. In all 246 DNA samples (244 patients and 2 commercially available samples), all of the homozygotes demonstrated ΔCt values >8.0, whereas all of the heterozygotes demonstrated ΔCt values <1.0. No ambiguous results were obtained, and all of the data are in agreement with those obtained using the PCR-direct sequencing method. The allele frequency of *TPMT* *3C was 2.05% (10 of 488 alleles). All of the patients with variant alleles were heterozygotes, and no homozygotes were detected. No *TPMT* *2, *3A, or *3B alleles were observed in this Korean population.

4. Discussion

We developed and validated an allele-specific real-time PCR system (Bioneer) that uses an automatic interpretation function for thiopurine dose genotyping. It was used to assess several major SNPs: *TPMT* *2, *3A, *3B, and *3C. Based on the

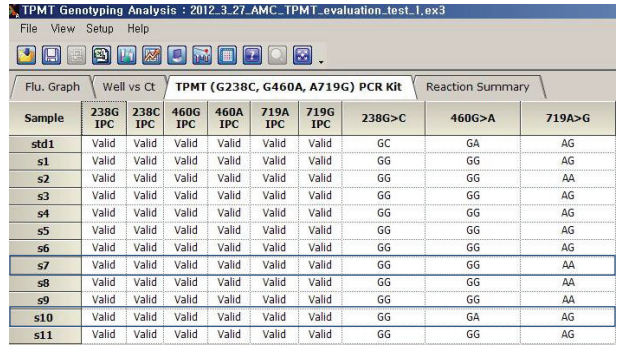

Sample	238G IPC	238C IPC	460G IPC	460A IPC	719A IPC	719G IPC	238G>C	460G>A	719A>G
std1	Valid	Valid	Valid	Valid	Valid	Valid	GC	GA	AG
s1	Valid	Valid	Valid	Valid	Valid	Valid	GG	GG	AG
s2	Valid	Valid	Valid	Valid	Valid	Valid	GG	GG	AA
s3	Valid	Valid	Valid	Valid	Valid	Valid	GG	GG	AG
s4	Valid	Valid	Valid	Valid	Valid	Valid	GG	GG	AG
s5	Valid	Valid	Valid	Valid	Valid	Valid	GG	GG	AG
s6	Valid	Valid	Valid	Valid	Valid	Valid	GG	GG	AG
s7	Valid	Valid	Valid	Valid	Valid	Valid	GG	GG	AA
s8	Valid	Valid	Valid	Valid	Valid	Valid	GG	GG	AA
s9	Valid	Valid	Valid	Valid	Valid	Valid	GG	GG	AA
s10	Valid	Valid	Valid	Valid	Valid	Valid	GG	GA	AG
s11	Valid	Valid	Valid	Valid	Valid	Valid	GG	GG	AG

(a)

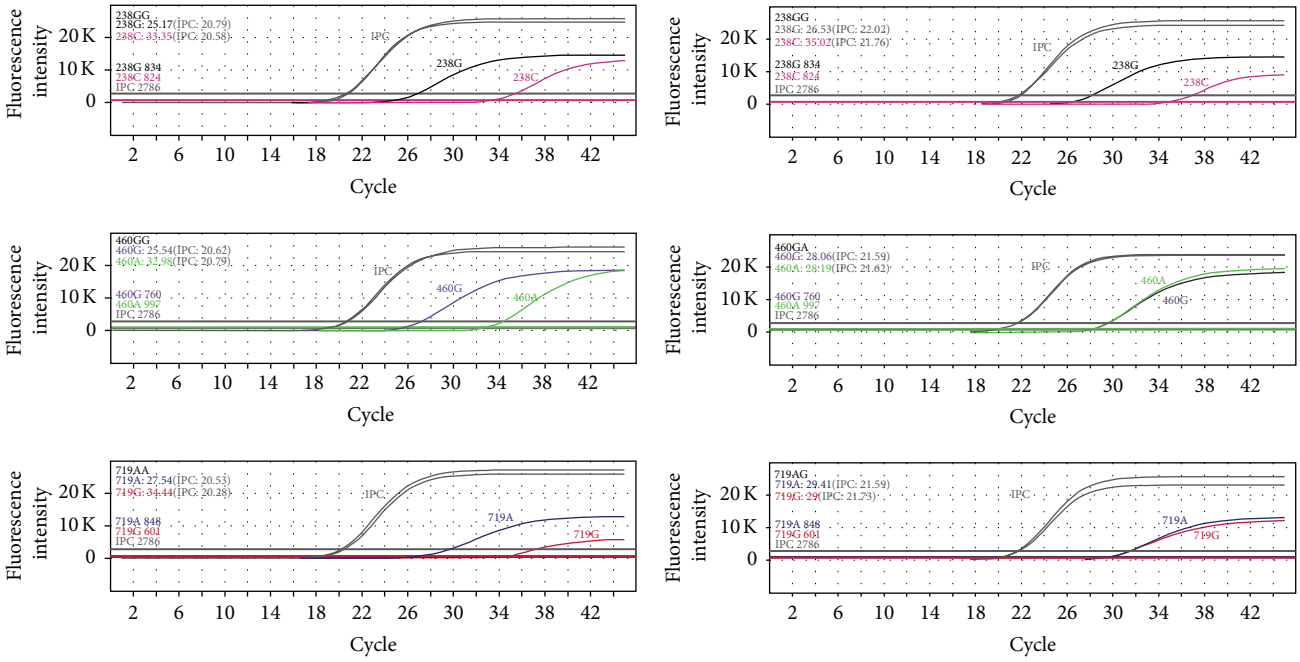

(b) Sample name: s7

(c) Sample name: s10

Figure 1: Examples of the automatically interpreted results. Typical displays are shown. (a) Each row shows all of the interpreted results for the three SNPs of one sample. (b) Simultaneous display of all of the reaction curves for the three SNPs of one wild-type sample. (c) Simultaneous display of all reaction curves for the three SNPs of one sample (460G > A and 719A > G heterozygotes).

thiopurine dosing guidelines [11] and population genotype data [12, 13], we were able to consider the genotyping of these 3 SNPs as sufficient for thiopurine dose adjustment in our population. Although the allele frequency of *6 (c.539A > T and p.Tyr180Phe) has been reported as 1.27% (3 of 256) [14] and 0.25% (2 of 800) in the Korean population [13], *6 is not currently a clinically relevant SNP in the Clinical Pharmacogenetics Implementation Consortium guidelines [11]. Teml et al. [15] recommended using a genotyping strategy to replace the measurement of TPMT activity only if either a complete genetic analysis of all of the currently known functionally relevant TPMT alleles is conducted or if the selection of all of the frequently known alleles in a certain ethnic population is performed. The platform for *TPMT* *6 could be included if data on Korean patients are sufficiently accumulated for the modification of thiopurine dosing guidelines.

To validate our method, we assayed DNA samples from 244 patients and two commercially available genomic DNA samples, the genotypes of which had previously been confirmed using the PCR-direct sequencing method. We found that the results of the two methods were in excellent agreement. Because the SNPs of *TPMT* are variations at the germline level, they theoretically appear with frequencies of 0%, 50%, and 100%. A Ct difference ≥2 between a variant and the wild-type allele indicates a ≥4-fold difference between the amount of wild-type and variant genomic DNA that are present [10]. Therefore, we considered a Ct difference of 2 to be sufficient for distinguishing between wild-type and variant

alleles. We actually found that the Ct differences were ≥8 for all of the homozygotes and <1 for all of the heterozygotes. Hence, none of our findings were inconclusive. We could not validate *TPMT* *2 because of difficulties obtaining adequate samples, and this is a limitation of this study. However, because *TPMT* *2 has been found to be absent in the Korean population [13, 14], this system could be suitable for *TPMT* genotyping of Koreans.

Although real-time PCR requires less time and effort than conventional sequencing, laboratory personnel with little experience may have difficulty interpreting the results. We thus devised an automatic algorithm for the interpretation of real-time PCR results based on the Ct differences [10]. This software can reduce interpretation errors and is timeefficient. In addition, the automatically interpreted results can be connected to a laboratory information system to automatically generate pharmacogenetic interpretation reports, thus saving time and effort in the preparation of laboratory reports. In addition, because our genotyping system is a ready-to-use kit, the time needed for reagent preparation is negligible. In terms of cost, the sequencing method costs $50 per exon, so $150 for three exons per specimen. In contrast, our allele-specific real-time PCR method is expected to cost $50 per specimen; thus, one-third of the cost of the sequencing method.

In conclusion, the system described here allows accurate and timely genotyping in a clinical laboratory setting, allowing the adjustment of the thiopurine dose based on the genotyping results of each patient.

Conflict of Interests

The authors have no conflict of interests to declare.

Acknowledgment

This study was supported by a Grant from the Korean Ministry of Knowledge Economy (Development Project for Regional Industrial Technology no. 70007468).

References

[1] H. L. McLeod and C. Siva, "The thiopurine S-methyltansferase gene locus—implications for clinical pharmacogenomics," *Pharmacogenomics*, vol. 3, no. 1, pp. 89–98, 2002.

[2] S. Haglund, M. Lindqvist, S. Almer, C. Peterson, and J. Taipalensuu, "Pyrosequencing of TPMT alleles in a general Swedish population and in patients with inflammatory bowel disease," *Clinical Chemistry*, vol. 50, no. 2, pp. 288–295, 2004.

[3] J. Colombel, N. Ferrari, H. Debuysere et al., "Genotypic analysis of thiopurine S-methyltransferase in patients with Crohn's disease and severe myelosuppression during azathioprine therapy," *Gastroenterology*, vol. 118, no. 6, pp. 1025–1030, 2000.

[4] W. E. Evans, "Pharmacogenetics of thiopurine S-methyltransferase and thiopurine therapy," *Therapeutic Drug Monitoring*, vol. 26, no. 2, pp. 186–191, 2004.

[5] W. E. Evans, Y. Y. Hon, L. Bomgaars et al., "Preponderance of thiopurine S-methyltransferase deficiency and heterozygosity among patients intolerant to mercaptopurine or azathioprine," *Journal of Clinical Oncology*, vol. 19, no. 8, pp. 2293–2301, 2001.

[6] C. R. Yates, E. Y. Krynetski, T. Loennechen et al., "Molecular diagnosis of thiopurine S-methyltransferase deficiency: genetic basis for azathioprine and mercaptopurine intolerance," *Annals of Internal Medicine*, vol. 126, no. 8, pp. 608–614, 1997.

[7] L. Lennard, T. S. Chew, and J. S. Lilleyman, "Human thiopurine methyltransferase activity varies with red blood cell age," *British Journal of Clinical Pharmacology*, vol. 52, no. 5, pp. 539–546, 2001.

[8] M. V. Relling, M. L. Hancock, G. K. Rivera et al., "Mercaptopurine therapy intolerance and heterozygosity at the thiopurine S-methyltransferase gene locus," *Journal of the National Cancer Institute*, vol. 91, no. 23, pp. 2001–2008, 1999.

[9] L. Colleoni, D. Kapetis, L. Maggi et al., "A new thiopurine S-methyltransferase haplotype associated with intolerance to azathioprine," *Journal of Clinical Pharmacology*, 2012. In press.

[10] S. Kim, H. W. Lee, W. Lee et al., "New allele-specific real-time PCR system for warfarin dose genotyping equipped with an automatic interpretative function that allows rapid, accurate, and user-friendly reporting in clinical laboratories," *Thrombosis Research*, vol. 130, no. 1, pp. 104–109, 2011.

[11] M. V. Relling, E. E. Gardner, W. J. Sandborn et al., "Clinical pharmacogenetics implementation consortium guidelines for thiopurine methyltransferase genotype and thiopurine dosing," *Clinical Pharmacology & Therapeutics*, vol. 89, pp. 387–391, 2011.

[12] H. Cho, H. J. Baek, D. K. Han, S. Y. Bae, H. Kook, and T. J. Hwang, "Genetic polymorphism of thiopurine methyltransferase in children with acute lymphoblastic leukemia," *Clinical Pediatric Hematology-Oncology*, vol. 15, pp. 1–9, 2008.

[13] S. S. Lee, W. Kim, Y. Jang, and J. Shin, "Duplex pyrosequencing of the TPMT∗3C and TPMT∗6 alleles in Korean and Vietnamese populations," *Clinica Chimica Acta*, vol. 398, no. 1-2, pp. 82–85, 2008.

[14] E. Schaeffeler, U. M. Zanger, M. Eichelbaum, S. Asante-Poku, J. Shin, and M. Schwab, "Highly multiplexed genotyping of thiopurine S-methyltransferase variants using MALDI-TOF mass spectrometry: reliable genotyping in different ethnic groups," *Clinical Chemistry*, vol. 54, no. 10, pp. 1637–1647, 2008.

[15] A. Teml, E. Schaeffeler, and M. Schwab, "Pretreatment determination of TPMT—state of the art in clinical practice," *European Journal of Clinical Pharmacology*, vol. 65, no. 3, pp. 219–221, 2009.

Hindawi Publishing Corporation
BioMed Research International
Volume 2013, Article ID 270426, 5 pages
http://dx.doi.org/10.1155/2013/270426

Methodology Report

Total 25-Hydroxyvitamin D Determination by an Entry Level Triple Quadrupole Instrument: Comparison between Two Commercial Kits

Jacopo Gervasoni, Andrea Cocci, Cecilia Zuppi, and Silvia Persichilli

Istituto di Biochimica e Biochimica Clinica, Università Cattolica del Sacro Cuore, Largo A. Gemelli 8, 00168 Rome, Italy

Correspondence should be addressed to Silvia Persichilli; spersichilli@rm.unicatt.it

Received 29 November 2012; Revised 18 January 2013; Accepted 25 January 2013

Academic Editor: Antonio La Gioia

Objective. 25-hydroxyvitamin D_2/D_3 ($25\text{-}OHD_2/D_3$) determination is a reliable biomarker for vitamin D status. Liquid chromatography-tandem mass spectrometry was recently proposed as a reference method for vitamin D status evaluation. The aim of this work is to compare two commercial kits (Chromsystems and PerkinElmer) for $25\text{-}OHD_2/D_3$ determination by our entry level LC-MS/MS. *Design and Methods*. Chromsystems kit adds an online trap column to an HPLC column and provides atmospheric pressure chemical ionization, isotopically labeled internal standard, and 4 calibrator points. PerkinElmer kit uses a solvent extraction and protein precipitation method. This kit can be used with or without derivatization with, respectively, electrospray and atmospheric pressure chemical ionization. For each analyte, there are isotopically labeled internal standards and 7 deuterated calibrator points. *Results*. Performance characteristics are acceptable for both methods. Mean bias between methods calculated on 70 samples was 1.9 ng/mL. Linear regression analysis gave an R^2 of 0.94. $25\text{-}OHD_2$ is detectable only with PerkinElmer kit in derivatized assay option. *Conclusion*. Both methods are suitable for routine. Chromsystems kit minimizes manual sample preparation, requiring only protein precipitation, but, with our system, $25\text{-}OHD_2$ is not detectable. PerkinElmer kit without derivatization does not guarantee acceptable performance with our LC-MS/MS system, as sample is not purified online. Derivatization provides sufficient sensitivity for $25\text{-}OHD_2$ detection.

1. Introduction

Vitamin D (vitD) is is critical for the regulation of calcium and phosphate homeostasis and is implicated in important biological processes [1]. VitD exists in two forms; $vitD_3$ (cholecalciferol) is formed in the skin upon exposure to sunlight; $vitD_2$ (ergocalciferol) is obtained from the ultraviolet irradiation of plants materials. These two vitD forms are metabolized in the liver to give 25-hydroxy vitamin D (25-OHD), further hydrolyzed in the kidney to biologically active metabolite 1,25-dihydroxy vitamin D (1,25-OHD). This last metabolite is difficult to measure, because it is present at extremely low concentrations (15–60 pg/mL), thus, circulating liver metabolites $25\text{-}OHD_2/D_3$ are recognized as markers for vitamin D status [2, 3].

Recently vitD status has been associated with several diseases including cancer cardiovascular disease, diabetes, multiple sclerosis, osteoporosis, rheumatoid arthritis, and chronic pain [4].

Methods for $25\text{-}OHD_3$ and $25\text{-}OHD_2$ determination can be grouped in immunochemical methods (based on radioactive, enzymatic, or chemiluminescence detection) and chromatographic methods (HPLC and LC-MS/MS).

Immunoassay methods are the most used for their rapidity, despite that several studies reported problems of reproducibility and interferences. Recent papers have reviewed performance and limitations of immunochemical, HPLC-based, and liquid chromatography-tandem mass spectrometry (LC-MS/MS) methods [5, 6]. One limitation in the $25\text{-}OHD_2/D_3$ measurement was represented by the lack of reference standards until the development of two ethanol-based calibrators (SRM 2972) and four serum-based calibrators (SRM 972) by the US National Institute of Standards and Technology (NIST). There are two LC-MS/MS methods as

reference methods by the Joint Committee for Traceability in Laboratory Medicine [7, 8].

The release of these standards significantly contributed to increasing the agreement among different LC-MS/MS methods, overcoming the lack of standardization highlighted by the Vitamin D External Quality Assessment Schemes (DEQAS) [9].

The purpose of this work is to compare two commercial kits for 25-OHD_2/D_3 determination by LC-MS/MS with our entry level triple quadrupole instrument.

2. Materials and Methods

Serum samples were obtained from 70 subjects belonging to the hospital staff (40 males, 30 females; 18–60 age range) and submitted to periodical clinical control. All subjects have given their informed consent. Samples were collected and stored at −80°C. When thawed, all samples were analyzed for 25-OHD_2/D_3 by LC-MS/MS with both Chromsystems (Chromsystems Instruments & Chemicals GmbH, Munchen, Germany) and PerkinElmer (Wallac Oy, Turku, Finland) kits.

Water, acetonitrile, and formic acid (LC-MS grade) were purchased from Baker (Mallinckrodt Baker Italy, Milan, Italy).

Analyses were performed using a triple stage quadrupole TSQ Quantum Access (Thermo Fisher, Palo Alto, CA, USA) equipped with APCI source for Chromsystems and for PerkinElmer in nonderivatized mode and with ESI source for PerkinElmer in derivatized mode.

2.1. Chromsystems Assay. In the Chromsystems kit, the preanalytical phase is simplified to only a protein precipitation, because an online trap column concentrates the analytes and separates interfering substances. The trap column is connected to an HPLC column which provides further purification.

Calibration was performed using a lyophilized multilevel serum calibrator set NIST traceable ($n = 6$) of known concentration. Low and high concentration lyophilized sera samples were used as quality controls. $^2H_6$-25(OH)D_3 was used as internal standard (IS) to correct for sample treatment and instrument variability.

Samples, calibrators, and quality controls were prepared according to the manufacturer's instructions. Briefly, to 100 μL of serum sample, 25 μL of precipitation reagent and 200 μL of internal standard were added. After an incubation of 10 minutes, samples were centrifuged at 15000 ×g for 5 minutes, and 200 μL was transferred into the vials. 50 μL was injected into the HPLC-MS/MS system.

Samples were analyzed using an APCI source to maximize sensitivity. The APCI source was working in the positive mode, producing positively charged ions in the form of $[H^+]$ adduct ions. Discharge current was maintained at 7.0 μA; vaporizer temperature was maintained at 400°C with a capillary temperature of 300°C. Gas settings were sheath gas pressure, 40 (arbitrary units); auxiliary gas pressure, 35 (arbitrary units); ion sweep gas pressure, 0 (arbitrary units). Argon was used as collision gas at a collision pressure of 1.5 mTorr.

Table 1: Compounds dependent MS/MS parameters for Chromsystems (a) and for PerkinElmer (b) assays.

(a)

Chromsystems			
Compound	SRM	Collision Energy [eV]	Tube Lens [V]
25(OH)D_3	383.2 → 210.8	23	80
25(OH)D_2	395.2 → 268.8	17	80
25(OH)D_3/D_2 IS	389.3 → 210.8	28	80

(b)

PerkinElmer			
Compound	SRM	Collision Energy [eV]	Tube Lens [V]
25(OH)D_3 Cal	613.4 → 298.1	19	110
25(OH)D_3 IS	610.1 → 310.1	19	110
25(OH)D_3	607.4 → 298.1	19	110
25(OH)D_2 Cal	625.4 → 298.1	17	110
25(OH)D_2 IS	622.4 → 301.1	17	110
25(OH)D_2	619.4 → 298.1	17	110

Mobile phases (A and B) were used independently in isocratic mode with trap column, and analytical column respectively. All materials and reagents were provided by the manufacturers. Total run time was 6.5 minutes.

The selected reaction monitoring (SRM) transitions for each analyte, their respective collision energy, and tube lens values were reported in Table 1(a).

2.2. PerkinElmer Assay. PerkinElmer kit uses a combination of solvent extraction and protein precipitation procedures. This kit can be alternatively used with derivatization, using ESI source, or without derivatization, using APCI. Derivatization improves ionization efficiency and MS/MS signal intensity of the analytes. In our preliminary tests, our entry-level mass spectrometer showed an inadequate sensitivity for quantification of serum 25(OH)D_2 and 25(OH)D_3 using the kit in nonderivatized mode (data not shown). Kit was then used only in derivatized mode. Calibration was performed using 7 calibrator points (charcoal stripped human serum enriched with six increasing levels of $^2H_6$-25(OH)D_2 and $^2H_6$-25(OH)D_3). Three control levels (lyophilized serum added with increasing amount of $^2H_6$-25(OH)D_2 and $^2H_6$-25(OH)D_3) were used as quality controls.

For each analyte specific isotopically labeled internal standards ($^2H_3$-25(OH)D_2 for VitD_2 and $^2H_3$-25(OH)D_3 for VitD_3) were used.

Samples, calibrators, and quality controls were prepared according to the manufacturer's instructions with slightly modifications in order to enhance sensitivity. Briefly, to 150 μL of serum sample, 300 μL of daily precipitation solution (DPS, IS solution in acetonitrile 0.1% formic acid) was added. After an incubation of 10 minutes samples were centrifuged at 15000 ×g for 5 minutes, and 300 μL was transferred into

96 well plates. Samples were placed under a stream of high purity dry nitrogen gas until all the samples were dry. 50 μL of derivatization reagent was added to each wel,l and the plate, covered with aluminum foil, was shaken at 750 rpm for 10 minutes. After removing the aluminum foil 50 μL of quench solution was added to each well, and the plate, covered with aluminum foil, was shaken at 750 rpm for 10 minutes. The plate was loaded onto the autosampler, and 50 μL were injected into the HPLC-MS/MS system.

For derivatizated assay, among the columns proposed, we selected a Waters XBridge C8 (3.5 μm 2.1 × 100 mm) equilibrated with a gradient of water/methanol added with 0.1% formic acid and 0.025% additive (provided by the manufacturer). While, for nonderivatized assay, we used a C18 Beta Basic 5 μm 2.1 × 100 mm column equilibrated with a different gradient of water/methanol added with 0.1% formic acid. Total run time was 9.0 and 6.0 minutes for derivatized and underivatized assays, respectively.

In derivatized assay, the ESI source was working in the positive mode, producing positively charged ions in the form of $[H^+]$ adduct ions. Capillary voltage was maintained at 3800 V, with a capillary temperature of 300°C. Gas settings were sheath gas pressure, 40 (arbitrary units); auxiliary gas pressure, 5 (arbitrary units); ion sweep gas pressure, 0 (arbitrary units). Argon was used as collision gas at a collision pressure of 1.5 mTorr.

The MRM transitions for each analyte, their respective collision energy, and tube lens values were reported in Table 1(b).

In non-derivatizated assay, the APCI source was working in positive mode, producing positively charged ions in the form of $[H^+]$ adduct ions. Discharge current was maintained at 7.0 μA; vaporizer temperature was maintained at 430°C with a capillary temperature of 300°C. Gas settings were sheath gas pressure, 40 (arbitrary units); auxiliary gas pressure, 5 (arbitrary units); ion sweep gas pressure, 0 (arbitrary units). Argon was used as collision gas at a collision pressure of 1.5 mTorr.

2.3. Methods Evaluation. The following parameters were assessed: linearity, limit of quantification (LOQ), limit of detection (LOD), and imprecision.

LOD and LOQ were evaluated by measuring the lower calibration point serially diluted with water.

The imprecision was evaluated using all the quality controls (QCs), three for PerkinElmer and two for Chromsystems. To evaluate within-assay imprecision, each QC was measured ten times in the same analytical run; between-assay imprecision was evaluated by measuring in duplicate the same QC samples for ten consecutive days.

25-OHD_3 values obtained by the LC-MS/MS methods were correlated using linear regression analysis. The bias of results was analyzed according to Bland-Altman [10].

Data acquisition was carried out using the mass spectrometer software (Excalibur 2.0.7, Thermo Fisher, Palo Alto, CA, USA). Quantitative analyses were carried out using Excalibur software for the Chromsystems method and Microsoft Excel 2010 (Microsoft Office 2010) for the PerkinElmer method. Statistical analysis was performed using Microsoft Excel 2010 (Microsoft Office 2010).

3. Results

Figure 1(a) shows, from top to bottom, typical SRM chromatograms of 25-OHD_3, IS ($^2H_6$-25(OH)D_3), and 25-OHD_2 obtained using the Chromsystems kit. The retention time of these analytes is approximately 2.8 min.

Figure 1(b) shows, from top to bottom, typical SRM chromatogram of 25-OHD_3, IS $^2H_3$-25(OH)D_3, 25-OHD_2 and IS $^2H_3$-25(OH)D_2 obtained using the PerkinElmer kit. The retention time is approximately 4.0 min.

In derivatized assay option, chemical modification of the 25-OHD_2 and 25-OHD_3 is achieved by derivatizing them in the extracted serum using 4-Phenyl-1,2,4-triazoline-3,5-dione (PTAD). In this reaction, PTAD is selectively added to the cis-diene double bonds of the 25-OHD_2/D_3 molecules, resulting in the generation of a new chiral center and the subsequent formation of a new pair of 25-OHD_2/D_3 diastereoisomers. Although partially resolved both 6S- and 6R-isomers signals should be finally combined for quantitative determination of 25-OHD_2 and 25-OHD_3 in the samples. This could explain the poor peak shape showed in Figure 1(b).

Both chromatographic runs are without interferences, confirming the high selectivity of these methods.

Performance characteristics are acceptable for both methods. According to manufacturer's instructions the linearity of the PerkinElmer assay is 329 ng/mL for 25-OHD_2 and 314 ng/mL for 25-OHD_3, and the linearity of the Chromsystems assay is 250 ng/mL for both 25-OHD_2 and 25-OHD_3.

LOQ, estimated as the lowest concentration of 25-OHD_3 where the relative uncertainty of a single measurement is reproducible within ±20%, was 3.0 ng/mL for PerkinElmer kit and 4.1 ng/mL for Chromsystems kit.

LOD, defined as the minimum concentration of 25-OHD_3 which gives a signal three times higher than the noise, was 1.6 ng/mL for PerkinElmer kit and 2.6 ng/mL for Chromsystems kit.

LOQ for 25-OHD_2 was 1.4 ng/mL for PerkinElmer kit and 3.0 for Chromsystems kit; the LOD of 25-OHD_2 was 0.5 ng/mL for PerkinElmer kit and 2.3 ng/mL for Chromsystems kit. Since 25-OHD_2 is normally present in very low concentrations (lower than 2.0 ng/mL), its determination is not possible with our entry level instrument using Chromsystems kit. Moreover, also using a slightly more performing instrument, as reported in the package insert of the Chromsystems kit, LOQ (2.4 ng/mL) is not adequate for the quantification of 25-OHD.

Intra-assay imprecision for 25-OHD_3 ranged from 3.6% to 3.7% for Chromsystems and from 4.6% to 4.9% for PerkinElmer. Interassay imprecision for 25-OHD_3 ranged from 4.6% to 4.8% for Chromsystems and from 4.2% to 5.1% for PerkinElmer.

Intra-assay imprecision for 25-OHD_2 ranged from 3.8% to 4.0% for Chromsystems and from 4.5% to 4.8% for PerkinElmer. Interassay imprecision for 25-OHD_2 ranged

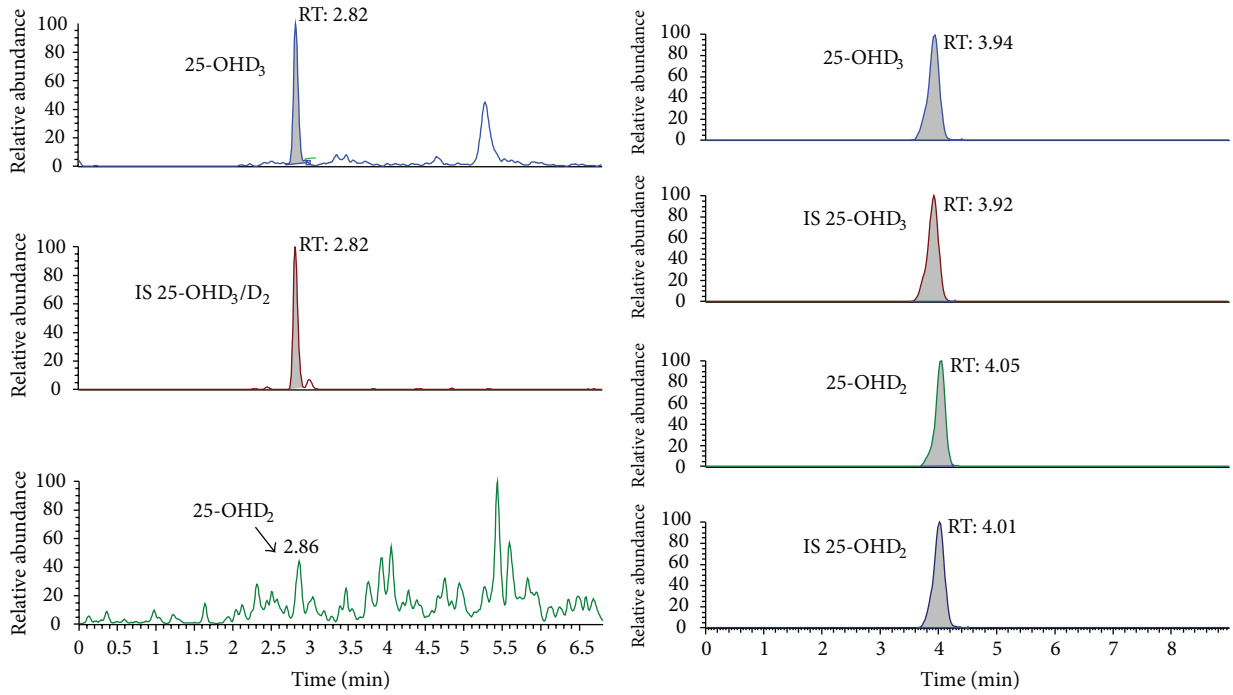

Figure 1: Typical SRM chromatograms of a serum sample (23.4 ng/mL 25-OHD_3 and 25-OHD_2 not detectable) assayed using the Chromsystems kit. The retention time of 25-OHD_2/D_3 is 2.8 minutes (a). Typical SRM chromatogram of a serum sample (21.8 ng/mL 25-OHD_3 and 25-OHD_2 1.6 ng/mL) assayed using the PerkinElmer kit. The retention time is 4.0 min (b).

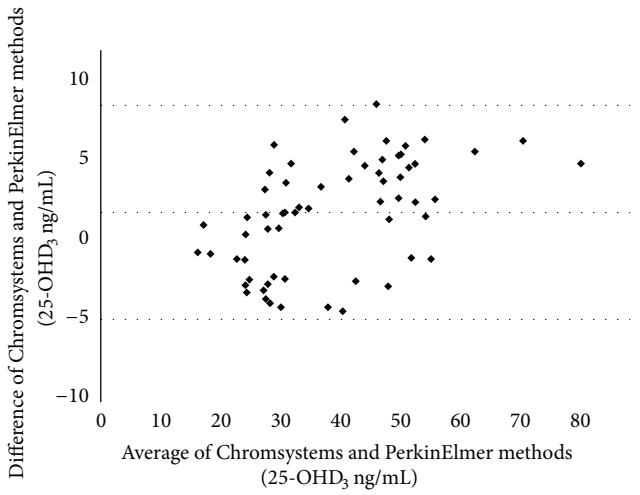

Figure 2: Bland-Altman plots of the differences between 25-OHD_3 values obtained by Chromsystems and PerkinElmer kits. Mean ± 1.96 SD.

from 5.7% to 6.6% for Chromsystems and from 4.3% to 5.1% for PerkinElmer.

Figure 2 shows the Bland-Altman plots of the differences between 25-OHD_3 values obtained with Chromsystems and PerkinElmer methods. Mean bias was 1.9 ng/mL, showing a good agreement between the two methods, confirmed by linear regression analysis (R^2: 0.94; $Y_{\text{Chromsystems}} = 1.15X_{\text{PerkinElmer}} - 8.44$).

4. Conclusion

Using the Chromsystems kit, manual sample preparation is minimized and limited to a simple and effective protein precipitation.

The PerkinElmer kit without derivatization does not guarantee acceptable performance with our LC-MS/MS system, but the manufacturer reports better analytical performance using a more performant instrument. Derivatization is more time consuming but provides sufficient sensitivity for the detection of 25-OHD_2.

Chromsystems kit does not declare neither the type of the column nor the composition of mobile phases, while PerkinElmer does.

In PerkinElmer kit, automated calculation is made highly complicated by the presence of different deuterated standards and cannot be performed by our software.

Several studies indicate the presence of 25-OHD_2/D_3 epimers, particularly 3 epi-25OH-D_2 and 3 epi-25OH-D_3, like potential confounders in 25-OHD_2/D_3 measurements. The presence of these epimers was initially considered relevant only for children younger than one year [11], but recently work showed that the concentration of 25-OHD_2/D_3 epimers may also be significant in adults [12].

For these reasons, both PerkinElmer and Chromsystems provide an alternative kit that permits to discriminate and quantify 25-OHD_2/D_3 epimers.

Therefore as a future perspective, we intend to clarify the possible role of epimers in adults using LC-MS/MS methods able to separate the less biologically active 25-OHD_2/D_3 epimers.

References

[1] M. F. Holick, "Vitamin D deficiency," *The New England Journal of Medicine*, vol. 357, pp. 266–281, 2007.

[2] K. M. Seamans and K. D. Cashman, "Existing and potentially novel functional markers of VitD status: a systematic review," *The American Journal of Clinical Nutrition*, vol. 89, pp. 1997S–2008S, 2009.

[3] D. B. Endres and R. K. Rude, "Bone and mineral metabolism," in *Tietz Textbook of Clinical Chemistry and Molecular Diagnostics*, C. A. Burtis, E. A. Ashwood, and D. E. Bruns, Eds., Elsevier Saunders, St. Louis, Mo, USA, 4th edition, 2006.

[4] M. F. Holick, "Vitamin D status: measurement, interpretation, and clinical application," *Annals of Epidemiology*, vol. 19, no. 2, pp. 73–78, 2009.

[5] A. M. Wallace, S. Gibson, A. de la Hunty, C. Lamberg-Allardt, and M. Ashwell, "Measurement of 25-hydroxyvitamin D in the clinical laboratory: Current procedures, performance characteristics and limitations," *Steroids*, vol. 75, no. 7, pp. 477–488, 2010.

[6] H. W. Moon, J. H. Cho, M. Hur, J. Song et al., "Comparison of four current 25-hydroxyvitamin D assays," *Clinical Biochemistry*, vol. 45, pp. 326–330, 2012.

[7] S. S. C. Tai, M. Bedner, and K. W. Phinney, "Development of a candidate reference measurement procedure for the determination of 25-hydroxyvitamin D_3 and 25-hydroxyvitamin D_2 in human serum using isotope-dilution liquid chromatography tandem mass spectrometry," *Analytical Chemistry*, vol. 82, no. 5, pp. 1942–1948, 2010.

[8] H. C. M. Stepman, A. Vanderroost, K. Van Uytfanghe, and L. M. Thienpont, "Candidate reference measurement procedures for serum 25-hydroxyvitamin D_3 and 25-hydroxyvitamin D_2 by using isotope-dilution liquid chromatography-tandem mass spectrometry," *Clinical Chemistry*, vol. 57, no. 3, pp. 441–448, 2011.

[9] C. J. Farrell, S. Martin, B. McWhinney, I. Straub, P. Williams, and M. Herrmann, "State-of-the-art vitamin D assays: a comparison of automated immunoassays with liquid chromatography-tandem mass spectrometry methods," *Clinical Chemistry*, vol. 58, pp. 531–542, 2012.

[10] J. M. Bland and D. G. Altman, "Comparing methods of measurement: why plotting difference against standard method is misleading," *The Lancet*, vol. 346, no. 8982, pp. 1085–1087, 1995.

[11] R. J. Singh, R. L. Taylor, G. S. Reddy, and S. K. G. Grebe, "C-3 epimers can account for a significant proportion of total circulating 25-hydroxyvitamin D in infants, complicating accurate measurement and interpretation of vitamin D status," *Journal of Clinical Endocrinology and Metabolism*, vol. 91, no. 8, pp. 3055–3061, 2006.

[12] G. Lensmeyer, M. Poquette, D. Wiebe, and N. Binkley, "The C-3 epimer of 25-hydroxyvitamin D_3 is present in adult serum," *The Journal of Clinical Endocrinology & Metabolism*, vol. 97, pp. 163–168, 2012.

Hindawi Publishing Corporation
BioMed Research International
Volume 2013, Article ID 603786, 8 pages
http://dx.doi.org/10.1155/2013/603786

Review Article

Biomarkers of Hypochromia: The Contemporary Assessment of Iron Status and Erythropoiesis

Eloísa Urrechaga,[1] Luís Borque,[2] and Jesús F. Escanero[2]

[1] *Laboratory Hospital Galdakao-Usansolo, 48960 Galdakao, Biscay, Spain*
[2] *Department of Pharmacology and Physiology, Faculty of Medicine, University of Zaragoza, 50009 Zaragoza, Spain*

Correspondence should be addressed to Eloísa Urrechaga; eloisa.urrechagaigartua@osakidetza.net

Received 4 December 2012; Accepted 28 January 2013

Academic Editor: Antonio La Gioia

Iron status is the result of the balance between the rate of erythropoiesis and the amount of the iron stores. Direct consequence of an imbalance between the erythroid marrow iron requirements and the actual supply is a reduction of red cell hemoglobin content, which causes hypochromic mature red cells and reticulocytes. The diagnosis of iron deficiency is particularly challenging in patients with acute or chronic inflammatory conditions because most of the biochemical markers for iron metabolism (serum ferritin and transferrin) are affected by acute phase reaction. For these reasons, interest has been generated in the use of erythrocyte and reticulocyte parameters, available on the modern hematology analyzers. Reported during blood analysis routinely performed on the instrument, these parameters can assist in early detection of clinical conditions (iron deficiency, absolute, or functional; ineffective erythropoiesis, including iron restricted or thalassemia), without additional cost. Technological progress has meant that in recent years modern analyzers report new parameters that provide further information from the traditional count. Nevertheless these new parameters are exclusive of each manufacturer, and they are patented. This is an update of these new laboratory test biomarkers of hypochromia reported by different manufactures, their meaning, and clinical utility on daily practice.

1. Advances in Basic Science

The control of iron homeostasis acts at both the cellular and the systemic level and involves a complex system of different cell types, transporters, and signals. To maintain systemic iron homeostasis, communication between cells that absorb iron from the diet (duodenal enterocytes), consume iron (mainly erythroid precursors), and store iron (hepatocytes and tissue macrophages) must be tightly regulated [1].

In the last 10 years, understanding of the regulation of iron homeostasis has changed substantially. A small peptide hormone, hepcidin, emerged as the central regulator of iron absorption, plasma iron levels, and iron distribution. The hormone controls the iron homeostasis and acts by inhibiting iron flows into plasma from macrophages involved in recycling of senescent erythrocytes, duodenal enterocytes engaged in the absorption of dietary iron, and hepatocytes that store iron [2].

The same factors that influence dietary iron absorption, that is, iron stores, erythropoietic activity, hemoglobin, oxygen content, and inflammation, also regulate the expression of hepcidin by hepatocytes.

Hepcidin reduces the quantity of circulating iron by limiting the egress of the metal from both intestinal and macrophage cells and is the key for the regulation of systemic iron homeostasis [3].

2. Iron Status

Absolute iron deficiency is defined as a decreased total iron body content. Iron deficiency anemia (IDA) occurs when iron deficiency is sufficiently severe to diminish erythropoiesis and cause the development of anemia.

Distinction between IDA and other entities in the differential diagnosis of anemia, especially anemia that accompanies infection, inflammation, and cancer, commonly

termed anemia of chronic disease (ACD), to distinguish ACD from the combined state IDA/ACD is a daily challenge for clinicians and laboratory professionals [4].

It has long been known that inflammation can mimic some aspects of iron deficiency by impairing the utilization of existing iron stores for red cell production and inducing an iron-sequestration syndrome and low serum iron. The molecular mechanisms that underlie the redistribution of iron during inflammation center on the cytokine-stimulated overproduction of hepcidin.

Functional iron deficiency describes a state where the total iron content of the body is normal or even elevated, but the iron is "locked away" and unavailable for the production of red blood cells. Iron becomes limiting for erythropoiesis, but generally the resulting anemia is not severe [2].

The laboratory diagnosis of absolute iron deficiency has been based on low serum iron, low percent transferrin saturation (TSAT), and low ferritin [5]. The limitations of using transferrin saturation reflect those of serum iron, that is, wide diurnal variation and low specificity. It is also reduced in inflammatory disease [6, 7].

On the other hand, as ferritin is an acute phase reactant, its serum levels may be elevated in the presence of chronic inflammation, infection, malignancy, and liver disease, making ferritin somewhat less than an ideal test for determining iron deficiency [8].

Serum transferrin receptor (sTfR) is not affected by inflammation [9] which would make sTfR a more reliable test than serum ferritin when inflammation is present. sTfR and the derived sTfR/log ferritin (ferritin index) are reliable markers of iron deficiency in mixed situations [10].

A particular case of ACD is represented by anemia of chronic kidney disease (CKD). Anemia is one of the most characteristic manifestations of CKD. The most well-known cause is inadequate production of erythropoietin, but there are also other causes leading to impaired erythropoiesis (reduced proliferative activity of erythroid precursors in bone marrow, reduced survival of red cells, and decreased iron availability), contributing to anemia [11, 12].

3. The Clinician's Need for Reliable Laboratory Tests

Recombinant human erythropoietin (rHuEpo) for the treatment of CKD and patients with anemia related to cancer has been available since 1989. However, rHuEpo therapy results in functional iron deficiency due to insufficient iron stores for the accelerated erythropoiesis [13].

Iron deficiency is the main cause of suboptimal response to erythropoietin in dialysis patients. Maintenance iron supplementation is required to successfully treat anemia. Long-term orally administered iron therapy is limited by noncompliance, gastrointestinal side effects, insufficient absorption, and drug interaction; intravenous iron compounds are used to treat dialysis patients who become iron deficient [14].

Monitoring erythropoietin treated patients' iron status is important to detect iron deficiency and avoid the adverse effects of iron medication [15].

The most important question regarding anemia therapy in these patients is which are the best parameters to assess the iron available for erythropoiesis, and the need for predictors and indicators of effectiveness has not abated [16, 17].

Interest has been generated in the use of erythrocyte and reticulocyte new indices available on the modern analyzers based on flow cytometry technology.

In 2004, European Best Practice Guidelines suggested an hemoglobin (Hb) target of 110 g/L [18]; the assessment of anemia in CKD patients should include the laboratory measurement of the following parameters:

(i) Hb concentration, to assess the degree of anemia;

(ii) red blood cell indices (mean cell volume MCV, mean cell hemoglobin MCH), to assess the type of anemia;

(iii) absolute reticulocyte count, to assess erythropoietic activity;

(iv) serum ferritin concentration, to assess iron stores;

(v) functional iron available for erythropoiesis:

  (a) percentage of hypochromic red cells (Siemens);
  (b) transferrin saturation;
  (c) reticulocyte hemoglobin content (Siemens);

(vi) plasma C-reactive protein, to assess inflammation.

Two parameters are exclusive of one-manufacturer's counters.

Direct consequence of an imbalance between the erythroid marrow iron requirements and the actual supply is a reduction of red cell hemoglobin content, which causes hypochromic mature red cells and reticulocytes. The modern hematological parameters contribute to the advanced study of the anemia and depend on the technology employed; the debate about other parameters with the same clinical meaning and potential utility as reticulocyte hemoglobin content and percentage of hypochromic red cells reported by Siemens analyzers is open.

4. The Advance of Technology

The hemogram is one of the more required tests by the clinicians, the analysis nowadays is totally automated, and the correct interpretation of the results requires to reunite the knowledge about the characteristics of the equipment and the clinical meaning of the results. The suppliers contribute innovations, providing new parameters that can help the clinicians to make a diagnosis in a fast, cheap, and useful manner [19].

The professionals of the clinical laboratory must obtain the maximum yield of the new technologies obtaining as much information as possible.

Automated blood cell counters have changed substantially during the last 20 years. Technological progress has meant that in recent years modern analyzers, fully automated, have been available. These analyzers report new parameters that provide further information from the traditional count;

Table 1: The new biomarkers of hypochromia now reported by the analyzers of different manufacturers.

Parameter	Abbreviation (unit)	Company
Hypochromic RBC	Hypo (%)	Siemens
Reticulocyte Hb content	CHr (pg)	Siemens
Hypochromic RBC	%HPO (%)	Abbott
Reticulocyte Hb content	MCHr (pg)	Abbott
Hypochromic RBC	Hypo He (%)	Sysmex
Reticulocyte Hb equivalent	Ret He (pg)	Sysmex
Low Hb density	LHD (%)	Beckman Coulter

RBC: red blood cells; Hb: hemoglobin.

this information must be evaluated to prove the potential clinical utility in different clinical situations.

Each company applies the technology in a different way in the analyzers, and for this reason these new parameters are exclusive of each manufacturer, and they are patented. Table 1 summarizes the RBC extended parameters now reported by the different analyzers.

Flow cytometry provides information about individual cell characteristics. This is in contrast to previous measurements of MCV, MCH, and MCHC which only calculate mean values for the total red cell population.

Modern counters can provide information about the reticulocyte counts but also about the characteristics of these cells (size or Hb content), related to the quality of the erythropoiesis, giving information of the current erythropoietic activity of the bone marrow.

Reticulocytes are immature red blood cells with a life span of only 1 to 2 days. When these are first released from the bone marrow, measurement of their hemoglobin content or volume can reflect the amount of iron immediately available for erythropoiesis.

Red blood cells (RBCs) are continuously produced in the bone marrow; when a state of iron deficiency proceeds and the iron stores progressively decrease, mean cell volume (MCV), mean cell hemoglobin (MCH), and red blood cell count (RBC) tend to decline. In iron deficient erythropoiesis, synthesis of Hb molecules is severely impaired leading to the production of erythrocytes with low Hb concentration (hypochromic cells). Because of their long-life span of approximately 3 months, several cohorts of normochromic and increasingly hypochromic red cells coexist in the peripheral blood leading to anisocytosis; red cell distribution width (RDW) reflects the variation of size of the red cells.

Anisocytosis and anisochromia are related concepts but not identical; RBCs undergo a rapid reduction in volume and hemoglobin in the few days after release from the bone marrow; in healthy individuals (and patients with mild disease) the characteristics of the population can be stable. But in clinical setting such as IDA the production of reticulocytes appears to be counterbalanced by delayed clearance of old cells, and the natural evolution of the red cells is altered [20].

MCV is the mean of the volumes of all erythrocytes; RDW refers to the variety of volumes present in the red cell population, so the contribution of marginal-sized subsets to the calculated mean value can be assessed.

This is not the case for Hb content. MCH is calculated from red blood cell count and Hb and represents the average; the percentage of RBC subsets can give complementary information of the contribution of cell with extreme values of Hb (hypochromic and hyperchromic cells) to the mean values, reflecting the fluctuations of iron availability to the erythron in the previous weeks.

The assessment of the erythrocyte subsets is an added information can be useful, as it reflects the situation of the whole of RBC.

5. Siemens (Siemens Healthcare Diagnostics, Deerfield, IL, USA)

Applying flow cytometry technology, the detection of two light-scatter signals allows the independent measurements of cell-by-cell characteristics of volume and hemoglobin concentration; on the reticulocyte channel of ADVIA analyzers immature red cells are stained based on their RNA content using the stain Oxazine 750.

The hypochromic red cells (referred to as %Hypo) and CHr (reticulocyte hemoglobin content) are reported by the Siemens ADVIA 120 hematology analyzer (Siemens Medical Solutions Diagnostics, Tarrytown, NY, USA). Reticulocyte Hb content (CHr) and the percentage of hypochromic red blood cells (%Hypo) reflect iron availability and are reliable markers of functional iron deficiency [21, 22].

The measurement of CHr is a direct assessment of the incorporation of iron into Hb and thus an estimate of the recent functional availability of iron to the erythron; due to the life span of the reticulocytes CHr is a sensitive indicator of iron deficient erythropoiesis, cutoff 28-29 pg [23, 24].

rHuEpo is effective in stimulating production of red blood cells, but without an adequate iron supply to bind to heme, and the red blood cells will be hypochromic, low in Hb concentration. Thus, in states of iron deficiency, a significant percentage of red blood cells leaving the bone marrow will have a low Hb concentration. By measuring the percentage of RBCs with Hb concentration <280 g/L, iron deficiency can be detected. Hypochromic red cells percentages have been correlated with iron deficiency. %Hypo is reported by Siemens Advia 120 hematology analyzer based on the optical cell-by-cell hemoglobin measurement.

The measurement of %Hypo (defined as the percentage of red blood cells with Hb concentration less than 280 g/L) is a sensitive method for quantifying the hemoglobinization of mature red cells. Because of the long circulating life span of mature erythrocytes %Hypo values are related to iron status in the last 2-3 months and have been recognised as an indicator of iron deficiency [25–27]. %Hypo < 5% is considered normal. Two different criteria, more specifically, %Hypo > 5% and >10% have been used. %Hypo > 10%, has been more commonly used for defining absolute iron deficiency and functional iron deficiency [18].

CHr and %Hypo have been used as a diagnostic tool, together with biochemical markers, to distinguish IDA from

ACD, and are incorporated to the guidelines for the monitoring of recombinant human erythropoietin rHuEpo therapy [18, 28–31]. These red blood cell and reticulocyte indices have also been recognized as reliable markers of iron deficiency on physiological conditions, where the demand for iron increases (children, women at child bearing age, pregnancy) [27, 32, 33].

The transition from the normal iron-replete state to the development of iron deficiency anemia is a sequential process: depletion of the storage iron compartment, followed by its exhaustion and the consequent initiation of depletion of the functional iron compartment. Normal Hb level does not exclude lack of iron storage, because individuals with normal body iron stores must lose a large amount of body iron during a long period before the Hb falls [34].

Nonanemic iron deficiency is sometimes termed "latent iron deficiency" or "depleted iron stores." Reticulocyte-derived parameters can be useful in this context because they give information regarding the actual iron supply and the quality of the erythropoiesis within 2 days.

CHr could be a sensitive marker to detect early the negative balance between body iron content and the demand for erythropoiesis, before the mature cell indices or even Hb move below the reference intervals, improving the diagnostic algorithms [35–38].

The size of iron stores in blood donors can be also evaluated with confidence by means of CHr [39–41].

6. Abbott (Abbott Diagnostics, Santa Clara, CA, USA)

The flow-cytometric optical technology for RBC parameters measurement was first made available by the Technicon Company in their H* series of instruments, later followed by the Advia hematology analyzers (Bayer Diagnostics, presently Siemens Healthcare Diagnostics, Deerfield, IL, USA). As a consequence, many of the data reported in the literature have been generated using these analyzers. In 2010, Abbott Diagnostics introduced extended RBC parameters on the CELL-DYN Sapphire analyzer. The technology used in this instrument is multiangle laser light scattering by single cell, sphered RBC, and relies on the Mie theory, like what the Advia analyzers do. Therefore, it was anticipated that there would exist a very high level of agreement between the extended RBC parameters of both types of analyzer. Although the parameters measured are identical, the manufacturers use slightly different nomenclature (Table 1).

Mie theory describes the mathematics of light diffraction by spherical objects; in this case the red cells are transformed into isovolumetric spheres. When using monochromatic (laser) light, diffraction is only a function of the size and the refractive index of the object (related to its internal structure).

CELL-DYN Sapphire extended RBC parameters are produced collecting data of light in 3 different angles and in the reticulocyte channel of the fluorescence signal.

Mathematical models in the software use these scatter signals for calculating, for each individual cell, estimates of cellular volume (V) and cellular Hb concentration (CHC); these parameters can be specifically calculated for reticulocytes, too mean cellular volume of reticulocytes (MCVr) and mean cellular Hb content of reticulocytes (MCHr).

The whole RBC population can be classify considering the Hb concentration:

%HPO is the percentage of hypochromic RBC with CHC < 280 g/L,

%HPR the percentage the percentage of hyperchromic RBC, CHC > 410 g/L.

It has been published the new extended RBC parameters as measured on CELL-DYN Sapphire show a high degree of correlation with those of the Advia analyzers, although the absolute values may differ [42, 43]. This renders it necessary to establish instrument-specific reference ranges and clinical decision values [44, 45].

The reference intervals for %HPO and MCHr have been established, 0–4.8% and 28.5–34.5 pg, respectively [44], and the median in patients with no anemia (2.7% for %HPO and 29.9 pg for MCHr), are already published [43].

Although the numerical values do differ from the Advia parameters because of differences in technology, their clinical utility seems to be rather comparable [43].

7. Sysmex (Sysmex Corporation, Kobe, Japan)

Sysmex XE analyzers (Sysmex Corporation, Kobe, Japan) employ flow cytometry technology. In the reticulocyte channel blood cells are stained by a polymethine dye, specific for RNA/DNA. A bi-dimensional distribution of forward scattered light and fluorescence is presented as a scattergram, indicating mature red cells and reticulocytes. Forward scatter correlates with erythrocyte and reticulocyte Hb content, the so-called RBC Hb equivalent (RBC He), reticulocyte Hb equivalent (Ret He).

Measurements of Ret He provide useful information in diagnosing anemia, iron-restricted erythropoiesis, and functional iron deficiency and response to iron therapy during rHuEpo therapy [46–49]; Ret He, generated by all Sysmex XE analyzers (Sysmex Corporation, Kobe, Japan), has been recognised as a direct assessment of the incorporation of iron into erythrocyte Hb and a direct estimate of the recent functional availability of iron, thus provides the same information as CHr [50–52]. Twenty-nine pg is the cutoff value that defines deficient erythropoiesis. Ret He correlates with CHr with the same clinical meaning [53–55].

The role inflammation impairing the utilization of existing iron stores has been explained previously; recent articles focus on critically ill patients and the attempts to introduce Ret He in the transfusion area improving the management of anemic patients in critical conditions [56, 57]. The iron sequestration in the macrophages could be an evolutionary mechanism of defense against determined pathogens of high virulence [1]; impairment of reticulocyte Hb content can be considered as a consequence of infection and activation of mechanisms of immunity [58].

Derived from RBC Hb equivalent (RBC He), the Sysmex XE 5000 analyzer reports the percentages of hypochromic red

cells; %Hypo He indicates the percentage of hypochromic red cells with an Hb content less than 17 pg. Reference intervals are already published [59].

Recent studies confirm the clinical reliability of %Hypo He as marker of iron availability [60] and the assessment of functional iron deficiency in hemodialysis patients [61]; 2.7% is the cutoff value which defines iron deficiency in those patients [62].

8. Beckman Coulter (Beckman Coulter Inc. Miami, FL, USA)

Beckman Coulter (Beckman Coulter Inc. Miami, FL, USA) applies the Volume Conductivity Scatter technology to this field and new parameters are now available on the LH series analyzers.

Low hemoglobin density (LHD%) derives from the traditional mean cell hemoglobin concentration (MCHC), using the following mathematical sigmoid transformation:

$$\text{LHD\%} = 100 * \sqrt{1 - \left(\frac{1}{1 + e^{1.8(30 - \text{MCHC})}}\right)}. \quad (1)$$

MCHC is an inclusive measure of both the availability of iron over the preceding 90–120 days and of the proper introduction of iron into intracellular Hb. In the same way LHD% is related to iron availability and the Hb content of the mature red cells.

In this equation defining LHD%, in addition to the standard sigmoid function, a square root is applied to further enhance numerical resolution in the lower end region, to improve the differentiation between the normal and the abnormal among the blood samples having relatively low values of LHD%.

The reference range and the values of LHD% in normal population have been established, 1.0–4.0%, and the correlation with %Hypo values and its clinical usefulness in the study of iron status have been assessed [63].

LHD% is a reliable parameter for the detection of iron deficiency in patients with anemia in the presence of inflammation [64], recognizes subsets of patients, and therefore improves the diagnosis and management of anemia; LHD% > 6.0% suggests iron deficiency [65, 66].

9. Summary

The official National Institutes of Health definition of a biomarker is "a characteristic that is objectively measured and evaluated as an indicator of normal biologic processes, pathogenic processes, or pharmacologic response to a therapeutic intervention" [67]. More generally, a biomarker is a laboratory measurement that can be used to measure the progress of disease or the effects of treatment, as the new RBC extended parameters can do and is proved in the published studies selected in the reference section.

The percentage of hypochromic erythrocytes and the reticulocyte Hb content, reported by the modern analyzers, expand information at a cellular level:

(1) provide Hb content information on red cells;

(2) monitor changes in Hb incorporation into erythron;

(3) are more sensitive than indirect Biochemical measurements.

Operational Efficiency:

(i) rapid and automated;
(ii) rapid information to Clinicians of iron status;
(iii) faster response to changes from therapy;
(iv) financial justification.

Aids clinicians in

(i) assessing true status of iron;
(ii) detect functional iron deficiency, patients who can benefit from therapy;
(iii) differential diagnosis.

10. Conclusions

Several findings in the field of iron metabolism and erythropoiesis are modifying the traditional concepts on anemia. These findings point out the need for reliable diagnostic tests that are able to allow the better evaluation of the causes underlying apparently similar clinical conditions, implying a stronger collaboration between laboratory professionals and clinicians in order to optimize patient treatment.

Anemia is defined as a decrease concentration of Hb in the blood, cutoff depending on age and gender, but isolated Hb measurement has both low specificity and low sensitivity. The latter can be improved by including measures of iron-deficient erythropoiesis.

The biomarkers of hypochromia provide information about the iron supply and are reliable markers of iron restricted erythropoiesis in complex clinical situations.

An appropriate combination of laboratory tests gives evidence of iron depletion, reflects iron restricted red cells production, and so will help to establish a correct assessment of the iron status and thus the appropriate treatment.

Disclosure

The authors alone are responsible for the content of the paper. None of the authors has accepted any funding or support from an organization that may in any way gain or lose financially from the information that this paper contributes.

Conflict of Interests

The authors report no conflict of interests.

Acknowledgment

The author would like to highlight the contribution of Consolidated Research Group, Clinical Biochemistry and Sports, Autonomous Government of Aragon to the edition of the paper.

References

[1] D. W. Swinkels, M. C. H. Janssen, J. Bergmans, and J. J. M. Marx, "Hereditary hemochromatosis: genetic complexity and new diagnostic approaches," *Clinical Chemistry*, vol. 52, no. 6, pp. 950–968, 2006.

[2] T. Ganz and E. Nemeth, "Iron sequestration and anemia of inflammation," *Seminars in Hematology*, vol. 46, no. 4, pp. 387–393, 2009.

[3] R. E. Fleming and B. R. Bacon, "Orchestration of iron homeostasis," *The New England Journal of Medicine*, vol. 352, no. 17, pp. 1741–1744, 2005.

[4] G. Weiss and L. T. Goodnough, "Anemia of chronic disease," *The New England Journal of Medicine*, vol. 352, no. 10, pp. 1011–1023, 2005.

[5] L. T. Goodnough, B. Skikne, and C. Brugnara, "Erythropoietin, iron, and erythropoiesis," *Blood*, vol. 96, no. 3, pp. 823–833, 2000.

[6] A. Mast, "The clinical utility of peripheral blood tests in the diagnosis of iron deficiency anemia," *Bloodline*, vol. 1, pp. 7–9, 2001.

[7] D. Coyne, "Iron indices: what do they really mean?" *Kidney International Supplements*, no. 101, pp. S4–S8, 2006.

[8] K. Kalantar-Zadeh, R. A. Rodriguez, and M. H. Humphreys, "Association between serum ferritin and measures of inflammation, nutrition and iron in haemodialysis patients," *Nephrology Dialysis Transplantation*, vol. 19, no. 1, pp. 141–149, 2004.

[9] C. Beerenhout, O. Bekers, J. P. Kooman, F. M. van der Sande, and K. M. L. Leunissen, "A comparison between the soluble transferrin receptor, transferrin saturation and serum ferritin as markers of iron state in hemodialysis patients," *Nephron*, vol. 92, no. 1, pp. 32–35, 2002.

[10] B. S. Skikne, "Serum transferrin receptor," *The American Journal of Hematology*, vol. 83, no. 11, pp. 872–875, 2008.

[11] G. Weiss, "Iron metabolism in the anemia of chronic disease," *Biochimica et Biophysica Acta*, vol. 1790, no. 7, pp. 682–693, 2009.

[12] C. E. Lankhorst and J. B. Wish, "Anemia in renal disease: diagnosis and management," *Blood Reviews*, vol. 24, no. 1, pp. 39–47, 2010.

[13] I. Cavill and I. C. Macdougall, "Functional iron deficiency," *Blood*, vol. 82, no. 4, article 1377, 1993.

[14] I. C. Macdougall, "Poor response to erythropoietin: practical guidelines on investigation and management," *Nephrology Dialysis Transplantation*, vol. 10, no. 5, pp. 607–614, 1995.

[15] R. A. Zager, A. C. M. Johnson, S. Y. Hanson, and H. Wasse, "Parenteral iron formulations: a comparative toxicologic analysis and mechanisms of cell injury," *The American Journal of Kidney Diseases*, vol. 40, no. 1, pp. 90–103, 2002.

[16] J. B. Wish, "Assessing iron status: beyond serum ferritin and transferrin saturation," *Clinical Journal of the American Society of Nephrology*, vol. 1, pp. S4–S8, 2006.

[17] E. Katodritou, K. Zervas, E. Terpos, and C. Brugnara, "Use of erythropoiesis stimulating agents and intravenous iron for cancer and treatment-related anaemia: the need for predictors and indicators of effectiveness has not abated," *British Journal of Haematology*, vol. 142, no. 1, pp. 3–10, 2008.

[18] F. Locatelli, P. Aljama, P. Bárány et al., "Revised European best practice guidelines for the management of anaemia in patients with chronic renal failure," *Nephrology Dialysis Transplantation*, vol. 19, supplement 2, pp. ii1–ii47, 2004.

[19] M. Buttarello and M. Plebani, "Automated blood cell counts: state of the art," *The American Journal of Clinical Pathology*, vol. 130, no. 1, pp. 104–116, 2008.

[20] J. M. Higgins and L. Mahadevan, "Physiological and pathological population dynamics of circulating human red blood cells," *Proceedings of the National Academy of Sciences of the United States of America*, vol. 107, pp. 20587–20592, 2010.

[21] P. Cullen, J. Söffker, M. Höpfl et al., "Hypochromic red cells and reticulocyte haemglobin content as markers of iron-deficient erythropoiesis in patients undergoing chronic haemodialysis," *Nephrology Dialysis Transplantation*, vol. 14, no. 3, pp. 659–665, 1999.

[22] C. Thomas and L. Thomas, "Biochemical markers and hematologic indices in the diagnosis of functional iron deficiency," *Clinical Chemistry*, vol. 48, no. 7, pp. 1066–1076, 2002.

[23] A. E. Mast, M. A. Blinder, Q. Lu, S. Flax, and D. J. Dietzen, "Clinical utility of the reticulocyte hemoglobin content in the diagnosis of iron deficiency," *Blood*, vol. 99, no. 4, pp. 1489–1491, 2002.

[24] C. Brugnara, "Iron deficiency and erythropoiesis: new diagnostic approaches," *Clinical Chemistry*, vol. 49, no. 10, pp. 1573–1578, 2003.

[25] I. C. Macdougall, "Merits of percentage hypochromic red cells as a marker of functional iron deficiency," *Nephrology Dialysis Transplantation*, vol. 13, no. 4, pp. 847–849, 1998.

[26] C. Bovy, A. Gothot, J. M. Krzesinski, and Y. Beguin, "Mature erythrocyte indices: new markers of iron availability," *Haematologica*, vol. 90, no. 4, pp. 549–551, 2005.

[27] C. Bovy, A. Gothot, P. Delanaye, X. Warling, J. M. Krzesinski, and Y. Beguin, "Mature erythrocyte parameters as new markers of functional iron deficiency in haemodialysis: sensitivity and specificity," *Nephrology Dialysis Transplantation*, vol. 22, no. 4, pp. 1156–1162, 2007.

[28] S. Kotisaari, J. Romppanen, I. Penttilä, and K. Punnonen, "The Advia 120 red blood cell and reticulocyte indices are useful in diagnosis of iron-deficiency anemia," *European Journal of Haematology*, vol. 68, no. 3, pp. 150–156, 2002.

[29] "National kidney foundation, kidney disease outcomes quality initiative NKF-K/DOQI clinical practice guideline and clinical practice recommendations for anemia in chronic kidney disease," *The American Journal of Kidney Disease*, vol. 47, no. 5, supplement 3, pp. S11–S145, 2006.

[30] F. Locatelli, A. Covic, K. U. Eckardt, A. Wiecek, and R. Vanholder, "Anaemia management in patients with chronic kidney disease: a position statement by the anaemia working group of European renal best practice (ERBP)," *Nephrology Dialysis Transplantation*, vol. 24, no. 2, pp. 348–354, 2009.

[31] L. T. Goodnough, E. Nemeth, and T. Ganz, "Detection, evaluation, and management of iron-restricted erythropoiesis," *Blood*, vol. 116, no. 23, pp. 4754–4761, 2010.

[32] M. Ervasti, S. Kotisaari, S. Heinonen, and K. Punnonen, "Use of advanced red blood cell and reticulocyte indices improves the accuracy in diagnosing iron deficiency in pregnant women at term," *European Journal of Haematology*, vol. 79, no. 6, pp. 539–545, 2007.

[33] M. Ervasti, S. Kotisaari, U. Sankilampi, S. Heinonen, and K. Punnonen, "The relationship between red blood cell and reticulocyte indices and serum markers of iron status in the cord blood of newborns," *Clinical Chemistry and Laboratory Medicine*, vol. 45, no. 8, pp. 1000–1003, 2007.

[34] P. Suominen, K. Punnonen, A. Rajamäki, and K. Irjala, "Serum transferrin receptor and transferrin receptor-ferritin index identify healthy subjects with subclinical iron deficits," *Blood*, vol. 92, no. 8, pp. 2934–2939, 1998.

[35] N. Stoffman, C. Brugnara, and E. R. Woods, "An algorithm using reticulocyte hemoglobin content (CHr) measurement in

screening adolescents for iron deficiency," *Journal of Adolescent Health*, vol. 36, no. 6, pp. 529–533, 2005.

[36] C. Ullrich, A. Wu, C. Armsby et al., "Screening healthy infants for iron deficiency using reticulocyte hemoglobin content," *The Journal of the American Medical Association*, vol. 294, no. 8, pp. 924–930, 2005.

[37] M. Shaker, P. Jenkins, C. Ullrich, C. Brugnara, B. T. Nghiem, and H. Bernstein, "An economic analysis of anemia prevention during infancy," *Journal of Pediatrics*, vol. 154, no. 1, pp. 44–49, 2009.

[38] C. Ramakers, D. A. A. van der Woude, J. M. Verzijl, J. M. A. Pijnenborg, and E. M. van Wijk, "An added value for CHr and MCV in the diagnosis of iron deficency in postpartum anemic women," *International Journal of Laboratory Hematology*, vol. 34, no. 5, pp. 510–516, 2012.

[39] H. Radtke, T. Meyer, U. Kalus et al., "Rapid identification of iron deficiency in blood donors with red cell indexes provided by Advia 120," *Transfusion*, vol. 45, no. 1, pp. 5–10, 2005.

[40] V. Nadarajan, P. Sthaneshwar, and G. I. Eow, "Use of red blood cell indices for the identification of iron deficiency among blood donors," *Transfusion Medicine*, vol. 18, no. 3, pp. 184–189, 2008.

[41] M. J. Semmelrock, R. B. Raggam, K. Amrein et al., "Reticulocyte hemoglobin content allows early and reliable detection of functional iron deficiency in blood donors," *Clinica Chimica Acta*, vol. 413, no. 7-8, pp. 678–682, 2012.

[42] S. H. Kang, H. K. Kim, C. K. Ham, D. S. Lee, and H. I. Cho, "Comparison of four hematology analyzers, CELL-DYN Sapphire, ADVIA 120, Coulter LH 750, and Sysmex XE-2100, in terms of clinical usefulness," *International Journal of Laboratory Hematology*, vol. 30, no. 6, pp. 480–486, 2008.

[43] A. A. M. Ermens, J. J. M. L. Hoffmann, M. Krockenberger, and E. M. van Wijk, "New erythrocyte and reticulocyte parameters on CELL-DYN Sapphire; analytical and preanalytical aspects," *International Journal of Laboratory Hematology*, vol. 34, no. 3, pp. 274–282, 2012.

[44] J. J. M. L. Hoffmann, N. M. A. van den Broek, and J. Curvers, "Reference intervals of extended erythrocyte and reticulocyte parameters," *Clinical Chemistry and Laboratory Medicine*, vol. 50, no. 5, pp. 941–948, 2012.

[45] O. Costa, G. van Moer, K. Jochmans, J. Jonckheer, S. Damiaens, and M. de Waele, "Reference values for new red blood cell and platelet parameters on the Abbott Diagnostics Cell-Dyn Sapphire," *Clinical Chemistry and Laboratory Medicine*, vol. 50, no. 5, pp. 967–969, 2012.

[46] M. Buttarello, V. Temporin, R. Ceravolo, G. Farina, and P. Bulian, "The new reticulocyte parameter (RET-Y) of the Sysmex XE 2100: its use in the diagnosis and monitoring of posttreatment sideropenic anemia," *The American Journal of Clinical Pathology*, vol. 121, no. 4, pp. 489–495, 2004.

[47] C. Canals, A. F. Remacha, M. P. Sardá, J. M. Piazuelo, M. T. Royo, and M. Angeles Romero, "Clinical utility of the new Sysmex XE 2100 parameter—reticulocyte hemoglobin equivalent—in the diagnosis of anemia," *Haematologica*, vol. 90, no. 8, pp. 1133–1134, 2005.

[48] C. Brugnara, B. Schiller, and J. Moran, "Reticulocyte hemoglobin equivalent (Ret He) and assessment of iron-deficient states," *Clinical and Laboratory Haematology*, vol. 28, no. 5, pp. 303–308, 2006.

[49] C. Thomas, A. Kirschbaum, D. Boehm, and L. Thomas, "The diagnostic plot: a concept for identifying different states of iron deficiency and monitoring the response to epoetin therapy," *Medical Oncology*, vol. 23, no. 1, pp. 23–36, 2006.

[50] L. Thomas, S. Franck, M. Messinger, J. Linssen, M. Thomé, and C. Thomas, "Reticulocyte hemoglobin measurement—comparison of two methods in the diagnosis of iron-restricted erythropoiesis," *Clinical Chemistry and Laboratory Medicine*, vol. 43, no. 11, pp. 1193–1202, 2005.

[51] O. David, A. Grillo, B. Ceoloni et al., "Analysis of red cell parameters on the Sysmex XE 2100 and ADVIA 120 in iron deficiency and in uraemic chronic disease," *Scandinavian Journal of Clinical and Laboratory Investigation*, vol. 66, no. 2, pp. 113–120, 2006.

[52] M. Garzia, A. Di Mario, E. Ferraro et al., "Reticulocyte hemoglobin equivalent: an indicator of reduced iron availability in chronic kidney diseases during erythropoietin therapy," *Laboratory Hematology*, vol. 13, no. 1, pp. 6–11, 2007.

[53] A. E. Mast, M. A. Blinder, and D. J. Dietzen, "Reticulocyte hemoglobin content," *The American Journal of Hematology*, vol. 83, no. 4, pp. 307–310, 2008.

[54] M. MacOni, L. Cavalca, P. Danise, F. Cardarelli, and M. Brini, "Erythrocyte and reticulocyte indices in iron deficiency in chronic kidney disease: comparison of two methods," *Scandinavian Journal of Clinical and Laboratory Investigation*, vol. 69, no. 3, pp. 365–370, 2009.

[55] N. Miwa, T. Akiba, N. Kimata et al., "Usefulness of measuring reticulocyte hemoglobin equivalent in the management of haemodialysis patients with iron deficiency," *International Journal of Laboratory Hematology*, vol. 32, no. 2, pp. 248–255, 2010.

[56] G. Préfontaine, M. Darveau, C. Ahnadi et al., "Reticulocyte hemoglobin content in 13 critically ill patients: a preliminary study," *Transfusion Alternatives in Transfusion Medicine*, vol. 10, no. 4, pp. 182–188, 2008.

[57] R. Fernández, I. Tubau, J. Masip, L. Muñoz, I. Roig, and A. Artigas, "Low reticulocyte hemoglobin content is associated with a higher blood transfusion rate in critically ill patients: a cohort study," *Anesthesiology*, vol. 112, no. 5, pp. 1211–1215, 2010.

[58] M. Schoorl, D. Snijders, M. Schoorl, W. G. Boersma, and P. C. M. Bartels, "Temporary impairment of reticulocyte hemoglobin content in subjects with community adquired pneumonia," *International Journal of Laboratory Hematology*, vol. 34, no. 4, pp. 390–395, 2012.

[59] E. Urrechaga, L. Borque, and J. F. Escanero, "Potential utility of the new sysmex XE 5000 red blood cell extended parameters in the study of disorders of iron metabolism," *Clinical Chemistry and Laboratory Medicine*, vol. 47, no. 11, pp. 1411–1416, 2009.

[60] E. Urrechaga, L. Borque, and J. F. Escanero, "Percentage of hypochromic erythrocytes as potential marker of iron availability," *Clinical Chemistry and Laboratory Medicine*, vol. 50, no. 4, pp. 685–687, 2012.

[61] E. Urrechaga, L. Borque, and J. F. Escanero, "Erythrocyte and reticulocyte indices in the assessment of erythropoiesis activity and iron availability," *International Journal of Laboratory Hematology*.

[62] M. Buttarello, R. Pajola, E. Novello et al., "Diagnosis of iron deficiency in patients undergoing hemodialysis," *The American Journal of Clinical Pathology*, vol. 133, no. 6, pp. 949–954, 2010.

[63] E. Urrechaga, "The new mature red cell parameter, low haemoglobin density of the Beckman-Coulter LH750: clinical utility in the diagnosis of iron deficiency," *International Journal of Laboratory Hematology*, vol. 32, no. 1, pp. e144–e150, 2010.

[64] E. Urrechaga, L. Borque, and J. F. Escanero, "Erythrocyte and reticulocyte indices on the LH 750 as potential markers of functional iron deficiency," *Anemia*, vol. 2010, Article ID 625919, 7 pages, 2010.

[65] E. Urrechaga, L. Borque, and J. F. Escanero, "Low Hemoglobin Density (LHD %) potential marker of iron availability," *International Journal of Laboratory Hematology*, vol. 34, no. 1, pp. 47–51, 2012.

[66] E. Urrechaga, L. Borque, and J. F. Escanero, "Assessing iron status in CKD patients: new Laboratory parameters," in *Chronic Kidney Disease*, M. Gööz, Ed., pp. 225–250, InTech, Zagreb, Croatia, 1st edition, 2012.

[67] A. S. Ptolemy and N. Rifai, "What is a biomarker? Research investments and lack of clinical integration necessitate a review of biomarker terminology and validation schema," *Scandinavian Journal of Clinical and Laboratory Investigation*, vol. 70, no. s242, pp. 6–14, 2010.

Hindawi Publishing Corporation
BioMed Research International
Volume 2013, Article ID 856754, 6 pages
http://dx.doi.org/10.1155/2013/856754

Research Article

Coagulation Proteins Influencing Global Coagulation Assays in Cirrhosis: Hypercoagulability in Cirrhosis Assessed by Thrombomodulin-Induced Thrombin Generation Assay

Nam Youngwon,[1] Ji-Eun Kim,[1,2] Hae Sook Lim,[1] Kyou-Sup Han,[1] and Hyun Kyung Kim[1,2]

[1] *Department of Laboratory Medicine, Seoul National University College of Medicine, 101 Daehak-ro, Jongno-gu, Seoul 110-744, Republic of Korea*
[2] *Cancer Research Institute, Seoul National University College of Medicine, 101 Daehak-ro, Jongno-gu, Seoul 110-744, Republic of Korea*

Correspondence should be addressed to Hyun Kyung Kim; lukekhk@snu.ac.kr

Received 22 October 2012; Revised 3 January 2013; Accepted 24 January 2013

Academic Editor: Mina Hur

Background. Liver disease is accompanied by profound hemostatic disturbances. We investigated the influences of pro- and anticoagulation factors on global coagulation tests including prothrombin time (PT), activated partial thromboplastin time (aPTT), and thrombin generation assay (TGA) in cirrhosis. We also investigated whether cirrhotic patients exhibit hypo- or hypercoagulability using the TGA. *Methods*. The TGA was performed on a calibrated automated thrombogram, given lag time, endogenous thrombin potential (ETP), and peak thrombin in 156 cirrhotic patients and 73 controls. *Results*. PT was determined according to the factor (F) II, FV, FVII, FIX, and protein C levels. We observed that aPTT was dependent on FII, FIX, and FX levels. The ETP was dependent on FII, antithrombin, and protein C with 5 pM tissue factor (TF) stimulation, and FIX and protein C at 1 pM TF. The ETP ratio with 1 pM TF increased significantly in cirrhosis, indicating hypercoagulability, whereas that with 5 pM TF did not increase in cirrhosis. *Conclusion*. PT and the TGA are sensitive to protein C levels. Even with prolonged PT, the TGA can detect hypercoagulability in cirrhosis. Further studies should evaluate global coagulation status in cirrhosis patients using the newly devised TGA system.

1. Introduction

Prothrombin time (PT) and activated partial thromboplastin time (aPTT) are widely used in clinical laboratories as routine screening tests of the coagulation system. However, these tests cannot accurately predict hemorrhagic risk and vary among individuals [1]. Recently, there has been increasing evidence that thrombin generation provides useful information on the coagulation status. The thrombin generation assay (TGA) is a global coagulation test that measures the total amount of thrombin production triggered by tissue factor (TF) in plasma using an automated calibrated thrombogram. The resultant thrombogram has been validated as a good indicator of thrombotic and hemorrhagic conditions [2, 3].

Liver disease is accompanied by profound disturbances in the hemostatic system due to reduced plasma levels of pro- and anticoagulation factors synthesized by the liver [4]. Thus, the global effect of liver disease on hemostasis is very complex in that patients with advanced liver disease can experience bleeding or even thrombosis. In clinical practice, cirrhosis is generally accompanied by prolonged PT and aPTT due to impaired synthesis of most coagulation factors. Therefore, PT is widely used to predict bleeding risk in cirrhosis. However, despite PT prolongation, patients with cirrhosis seldom exhibit clinical bleeding events; hence, the PT may not accurately reflect the global hemostatic activity affected by various decreased levels of pro- and anticoagulation factors in cirrhosis. Several recent reports suggest that cirrhotic patients exhibit normal intact thrombograms as a result of acquired protein C deficiency despite prolonged PT [5–7]. However, the effect of protein C deficiency in cirrhosis remains unclear. Moreover, no existing report discusses how the individual

levels of pro- and anticoagulant factors influence global coagulation test results in cirrhotic patients, including PT, aPTT, and TGA.

In this study, we have investigated the influence of coagulation and anticoagulation factors on 3 global coagulation tests, that is, PT, aPTT, and TGA, in a population of patients with cirrhosis. We also investigated whether patients with cirrhosis exhibit hypo- or hypercoagulability using TGA stimulated by 2 different concentrations of TF.

2. Materials and Methods

2.1. Study Population. In total, 156 adult patients with cirrhosis were included in the present study. Cirrhosis was diagnosed based on the clinical, laboratory, or radiologic findings. Exclusion criteria were inherited bleeding or thrombotic disorders, warfarin or heparin use within 7 days of blood collection, or body weight < 30 kg. The severity of cirrhosis was estimated according to the model for end-stage liver disease (MELD) score. The MELD score was used for evaluation of cirrhosis severity and calculated as follows: MELD score $-10[0.957\ln(\text{creatinine, mg/dL}) + 0.378\ln(\text{bilirubin, mg/dL}) + 1.12\ln(\text{INR}) + 0.643]$. Peripheral venous blood samples were collected in commercially available tubes containing 0.109 M sodium citrate (Becton Dickinson, San Jose, CA, USA). The plasma was separated by centrifuging whole blood at 1550 ×g for 15 min within 2 h of blood collection. The aliquots of plasma were stored at −80°C.

Seventy-three healthy adults for whom the coagulation screening tests were requested in routine health checkups were included as controls. The study protocol was reviewed and approved by the Institutional Review Board of Seoul National University College of Medicine.

2.2. Thrombin Generation Assay. Thrombin generation in TF-triggered platelet-poor plasma (PPP) was measured by the calibrated automated thrombogram method (Thrombinoscope BV, Maastricht, The Netherlands) as described previously [8]. Briefly, 20 μL reagent containing TF with final concentration of 5 or 1 pM (PPP reagent 5 pM and PPP reagent low, resp.; Thrombinoscope BV) and phospholipids or thrombin calibrators were dispensed into each well of round-bottom 96-well plates, and 80 μL test plasma was added. In the same batch run, thrombomodulin (TM; Haematologic Technologies, Essex Junction, VT, USA) was added to the test plasma. The final concentration of TM was 5 nM for 5 pM TF stimulation and 2.5 nM for 1 pM TF stimulation. After the addition of 20 μL fluorogenic substrate in hydroxyethyl-piperazineethanesulfonic acid (HEPES) buffer with $CaCl_2$, the fluorescent signal was read in a Fluoroskan Ascent fluorometer (Thermo Labsystems OY, Helsinki, Finland). Thrombin generation curves were subsequently calculated with Thrombinoscope software version 3.0.0.29 (Thrombinoscope BV) and analyzed using parameters that describe the initiation, propagation, and termination phases of thrombin generation, namely, the lag time, endogenous thrombin potential (ETP), and peak thrombin concentration (peak thrombin). The lag time is equivalent to the clotting time and was defined as the time required to reach one-sixth of the peak height, which is the measure of the initiation phase. The peak height was defined as the maximum thrombin concentration. ETP is the area under the thrombin generation curve and represents the total amount of thrombin generated. The ETP ratio was calculated by dividing "ETP with TM" by "ETP without TM" multiplied by 100. Because TM is an anticoagulant, TM addition triggers the reduction of ETP value. Therefore, the ETP ratio reflects increased resistance to the anticoagulant action of TM. In other words, the increased ETP ratio represents hypercoagulability that resists anticoagulant activity of TM. In each plate containing an aliquot of control plasma (POOL NORM, Diagnostica Stago, France), the interassay and intra-assay coefficients of variation (CV) of ETP were 2.6% and 5.2%, respectively.

2.3. Conventional Coagulation Tests. Coagulation tests including PT, aPTT, and factor assays were performed on an automated coagulation analyzer (ACL TOP, Beckman Coulter, Fullerton, CA, USA). PT, aPTT, and fibrinogen were measured with clotting method by using HemosIL RecombiPlasTin, SynthASil, and HemosIL Fibrinogen-C XL reagents, respectively (Instrumentation Laboratory SpA, Milan, Italy). Coagulation factors were assayed by a PT-based clotting assay using HemosIL RecombiPlasTin reagent for factor (F) II, FV, FVII, and FX as well as an aPTT-based clotting assay using SynthASil reagent for FVIII and FIX. Antithrombin and protein C levels were determined by chromogenic assays (HemosIL liquid antithrombin and HemosIL Protein C, resp.; Instrumentation Laboratory SpA), and protein S activity was measured by clotting assay (HemosIL Free Protein S, Instrumentation Laboratory SpA).

2.4. Statistical Analysis. Continuous variables were compared using the Mann-Whitney U test and Kruskal-Wallis analysis. Meanwhile, categorical variables were compared using the χ^2 test. Correlations are expressed as Pearson's coefficients. Multiple linear regression analysis was performed to assess the relative effects of coagulation and anticoagulation factors on thrombin generation, PT, and aPTT. The adjusted R^2 and standardized regression coefficients (β) of the independent variables were calculated for each model. All analyses were carried out using SPSS version 12.0 (SPSS Inc., Chicago, IL, USA). The level of significance was set at $P < 0.05$.

3. Results

3.1. Effects of Pro- and Anticoagulation Factors on Global Coagulation Tests. The clinical and laboratory characteristics of the controls and patients are shown in Table 1. There were no significant differences between the controls and patients with respect to age, gender, WBC, or creatinine. Compared with the controls, PT and aPTT were significantly prolonged in the patients with cirrhosis (Table 1). Similarly, anticoagulation factors, including antithrombin, protein C, and protein S, were lower in the cirrhosis patients.

In the multiple linear regression analysis using data of cirrhotic patients (Table 2), the β value of FII for PT as

Table 1: Clinical and laboratory characteristics of the patients and controls.

		Cirrhotic patients				
	Controls (n = 73)	Total (n = 156)	MELD < 20 (n = 78)	MELD 20–25 (n = 37)	MELD > 25 (n = 41)	**P value
Age (years)	54 (50–62.50)	57.5 (52–66.75)	55 (50–67)	59 (57–68.5)	57 (47–65)	0.050
Gender						
Male	43 (58.9%)	99 (63.5%)	52 (65.8%)	23 (62.2%)	25 (61.0%)	0.852
Female	30 (41.1%)	57 (36.5%)	27 (34.2%)	14 (37.8%)	16 (39.0%)	
Etiology of cirrhosis						
ALD		16 (10.3%)	6 (7.7%)	3 (8.1%)	7 (17.1%)	
HCV		4 (2.6%)	2 (2.6%)	0 (0.0%)	2 (22.0%)	
HBV		16 (10.3%)	13 (16.7%)	0 (0.0%)	3 (56.1%)	0.406
Cryptogenic		40 (25.6%)	26 (33.3%)	12 (32.4%)	2 (4.9%)	
HCV and HCC		20 (12.8%)	6 (7.7%)	7 (18.9%)	7 (0.0%)	
HBV and HCC		60 (38.5%)	25 (32.1%)	15 (40.5%)	20 (0.0%)	
Child-Pugh B		84 (53.8%)	65 (82.3%)	13 (35.1%)	6 (14.6%)	<0.001
Child-Pugh C		72 (46.2%)	13 (16.5%)	24 (64.9%)	35 (85.4%)	<0.001
AST (IU/L)	25.0 (19.0–30.0)	49.5* (31.3–95.3)	37.0 (28.0–63.0)	47.0 (29.0–80.5)	100.0 (48.0–295.0)	<0.001
ALT (IU/L)	24.0 (19.0–34.0)	32.5* (20.0–68.8)	28.0 (19.0–53.0)	23.0 (18.0–39.0)	64.0 (26.5–107.5)	0.001
ALP (IU/L)	50.0 (43.0–61.0)	99.0* (70.3–153.0)	92.0 (67.0–139.0)	97.0 (69.0–121.5)	122.0 (90.5–254.0)	0.004
WBC ($\times 10^9$/L)	4.95 (4.28–5.85)	5.22 (3.60–12.10)	5.30 (3.49–9.20)	4.24 (3.27–4.59)	12.09 (5.20–18.84)	<0.001
Platelet ($\times 10^9$/L)	233 (203–282)	154*(48–128)	90 (61–187)	59 (41–87)	64 (44–88)	<0.001
Bilirubin (mg/dL)	1.0 (0.8–1.3)	3.2* (1.2–14.4)	1.7 (0.8–3.0)	5.7 (1.6–14.0)	18.0 (14.3–28.1)	<0.001
Albumin (g/L)	4.2 (4.0–4.3)	2.9* (2.5–3.3)	3.0 (2.9–3.5)	2.5 (2.4–3.3)	2.6 (2.4–2.9)	<0.001
Creatinine (mg/dL)	0.94 (0.79–1.02)	0.92 (0.67–1.26)	0.77 (0.62–0.95)	0.94 (0.60–1.40)	1.27 (0.96–2.24)	<0.001
PT (s)	10.9 (10.5–11.4)	23.1* (13.7–27.0)	66.0 (38.0–83.0)	32.0 (28.0–38.0)	35.0 (26.0–38.5)	<0.001
aPTT (s)	30.5 (29.2–33.0)	39.5* (33.4–48.3)	34.2 (30.3–44.4)	41.3 (38.5–57.2)	45.5 (39.2–64.3)	<0.001
Antithrombin (%)	107.7 (97.7–113.7)	47.6* (21.3–68.5)	59.9 (51.6–92.2)	24.3 (15.0–47.0)	21.1 (12.0–28.0)	<0.001
Protein C (%)	113.6 (103.7–122.0)	32.8* (13.6–53.1)	48.7 (36.0–65.5)	13.9 (10.8–37.2)	14.6 (11.4–20.3)	<0.001
Protein S (%)	93.7 (81.7–102.3)	54.5* (43.2–68.6)	54.9 (44.3–75.4)	49.2 (39.6–59.8)	55.9 (44.5–73.8)	0.213

*The Mann-Whitney U test was used between controls and total patients of cirrhosis.
**The Kruskal-Wallis test was used for continuous variables and χ^2 test for discrete variables among three cirrhosis subgroups.
Data are expressed as the median (interquartile range) for continuous variables and number (percentage) for categorical variables unless indicated otherwise.
ALD: alcoholic liver disease; HCV: hepatitis C virus; HBV: hepatitis B virus; PBC: primary biliary cirrhosis; PSC: primary sclerosing cholangitis; AST: aspartate aminotransferase; ALT: alanine aminotransferase; ALP: alkaline phosphatase; WBC: white blood cell count; PLT: platelet count; INR: international normalized ratio; PT: prothrombin time; aPTT: activated partial thromboplastin time; MELD: model of end-stage liver disease.

a dependent variable was −0.413; this means that when FII increases by 1 SD (i.e., 33.7), the PT decreases by 0.413. The significant negative determinants of PT results according to the β values were FII, FV, FVII, and FIX. Interestingly, protein C was a significant positive determinant of PT. Meanwhile, aPTT was mainly dependent on FII, FIX, and FX.

In the TGA, the significant positive determinants of lag time were fibrinogen, protein C, protein S, and, to a lesser extent, FV with both 1 and 5 pM TF. With both 1 and 5 pM TF, FIX and protein C were the strongest positive and negative determinants of peak thrombin, respectively. With 5 pM TF, ETP was positively determined by FII and negatively determined by antithrombin and protein C; meanwhile, with 1 pM TF, ETP was positively determined by FIX and negatively determined by protein C alone.

3.2. Hypercoagulability Expressed as ETP Ratio in Cirrhosis. The ETP ratio with 1 pM TF stimulation was significantly higher in patients than that in controls (Figure 1(a)), whereas there was no significant difference between groups with 5 pM TF (Figure 1(b)).

When the patients were subdivided into 3 groups according to their model of end-stage liver disease (MELD) scores (i.e., low, middle, and high), the ETP ratio with 1 pM TF was significantly increased at both group with <20 of MELD and group with 20–25 of MELD, compared with that of controls. However, the ETP ratio of group with >25 of MELD was not significantly increased, compared with that of group with 20–25 of MELD (Figure 2(a)). A similar pattern was observed with peak thrombin ratio (Figure 2(b)). In contrast, the lag time ratio decreased gradually until the middle range of MELD scores (Figure 2(c)).

4. Discussion

Patients with cirrhosis exhibit impaired coagulation function. These hemostatic changes can be measured using conventional global coagulation assays such as the PT and aPTT.

Table 2: Multivariate regression analysis of the determinants of global coagulation tests in cirrhosis ($n = 156$).

	SD	PT	aPTT	Lag time		Peak thrombin		ETP	
				5 pM TF	1 pM TF	5 pM TF	1 pM TF	5 pM TF	1 pM TF
		β	β	β	β	β	β	β	β
(Adjusted R^2)		0.779	0.633	0.491	0.394	0.509	0.348	0.465	0.265
Fibrinogen	111.9	0.092	−0.005	0.640†	0.602†	0.032	−0.219*	−0.044	−0.200
FII	33.7	−0.413*	−0.659*	−0.311	−0.434	0.455*	0.005	1.339†	0.427
FV	22.6	−0.146*	0.027	0.166*	0.106	0.123	0.015	0.000	−0.081
FVII	39.1	−0.297†	0.089	−0.241	−0.004	0.051	0.127	−0.233	0.098
FVIII	60.6	0.038	−0.179	0.029	0.102	−0.047	−0.083	0.133	−0.097
FIX	35.3	−0.291*	−0.680†	−0.145	−0.281	0.614†	0.990†	0.183	0.717†
FX	34.4	−0.150	0.507*	−0.210	−0.216	0.077	0.265	0.233	0.119
Antithrombin	53.6	0.041	−0.088	0.023	0.026	0.001	−0.057	−0.227*	−0.158
Protein C	44.4	0.301*	−0.025	0.364*	0.466*	−0.657†	−0.846†	−0.796†	−1.093†
Protein S	25.8	0.019	−0.041	0.281†	0.256*	0.019	−0.121	−0.099	−0.027

Data are expressed as standardized regression coefficients (β). $^{*}P < 0.05$; $^{\dagger}P < 0.001$.
F: factor; PT: prothrombin time; aPTT: activated partial thromboplastin time; ETP: endogenous thrombin potential; TF: tissue factor.

However, recent reports suggest the TGA is superior for assessing coagulation status because it involves more physiological systems and measures total thrombin generation over time [5–7]. Although these global coagulation assays are available in clinical laboratories, there was no data thus far about the influence of pro- and anticoagulation factors on PT, aPTT, or TGA in cirrhosis.

The results show that the levels of FII, FV, FVII, and FIX significantly influenced the PT. Because the liver synthesizes all coagulation factors except FVIII, PT prolongation is expected in cirrhosis. However, it is unknown whether anticoagulant proteins such as protein C and protein S, which decreased in cirrhosis, influence the PT. Interestingly, our study revealed that protein C levels influence the PT, indicating that protein C plays a role in PT prolongation via the inactivation of FV and FVIII in the PT system *in vitro*, similar to coagulation *in vivo*. To our knowledge, there has been no report about the effect of protein C on PT value. Since patients with cirrhosis exhibit decreased levels of both coagulation and anticoagulation factors, decreased levels of coagulation factors may prolong the PT, while decreased anticoagulation factors may shorten the PT. Therefore, PT prolongation may not be prominent in cirrhosis unlike changes in other liver function markers. Since PT is a component of the Child-Pugh score as well as the MELD score, which is the most commonly used marker to assess the severity of liver disease [9], it is important for physicians to understand that PT is dependent on protein C as well as coagulation factors.

The aPTT was mainly dependent on FII, FIX, and FX levels. However, anticoagulation factors did not affect the aPTT. Therefore, the aPTT is not a useful test for detecting overall coagulation potential in cirrhosis. Another report states that the aPTT is not a good predictor of hemorrhage either [1].

In our TGA experiments, the lag time of the TGA was positively determined by fibrinogen and anticoagulants including protein C and protein S. It is reasonable that the increased protein C and protein S levels prolong the lag time. The fibrinogen is thought to make the lag time reduced. However, our results show that fibrinogen level paradoxically affect the prolongation of lag time. Since fibrinogen is a well-known acute phase protein [10], this fibrinogen level may be increased in inflammatory status of cirrhotic patients. After all, the increased fibrinogen levels are accompanied by the reduced levels of other coagulation factors in cirrhotic patients. Therefore, the fibrinogen may reflect the other coagulation factors in statistical analysis. In other words, the increased fibrinogen seems to prolong the lag time on the specimen that had low levels of other coagulation factors.

Peak thrombin was significantly dependent on FIX and protein C levels. Dielis et al. [11] reported the influence of coagulation factors on peak thrombin in healthy individuals, in which the main determinants of ETP at 1 pM TF were fibrinogen, FXII, tissue factor pathway inhibitor, and antithrombin. Because their study was based on data of healthy individuals, the determinants of ETP may be quite different from results of our cirrhotic population. In our results, ETP was highly dependent on protein C. Regarding the result, it is noteworthy that protein C levels consistently affected the 3 parameters of the TGA. Thus, the TGA appears to be sensitive to protein C levels. Therefore, the TGA is expected to be a good global assay for estimating overall coagulation activity, especially in clinical conditions with low protein C levels, such as cirrhosis and acquired or congenital protein C deficiency.

Thrombotic events can paradoxically occur in cirrhotic patients even if clinically prolonged PT results are considered to suggest hemorrhagic tendency. Tridopi et al. [4] report that cirrhosis patients exhibit hypercoagulability according to the ETP ratio with 1 pM TF stimulation. In the present study, we investigated the ETP ratio with both 1 and 5 pM TF stimulations to evaluate cirrhotic hypercoagulability. As expected, the ETP ratio with 1 pM TF stimulation was higher in patients with cirrhosis than that in controls, whereas there was no difference between groups with 5 pM TF stimulation. The TF concentration used in the original test was 5 pM;

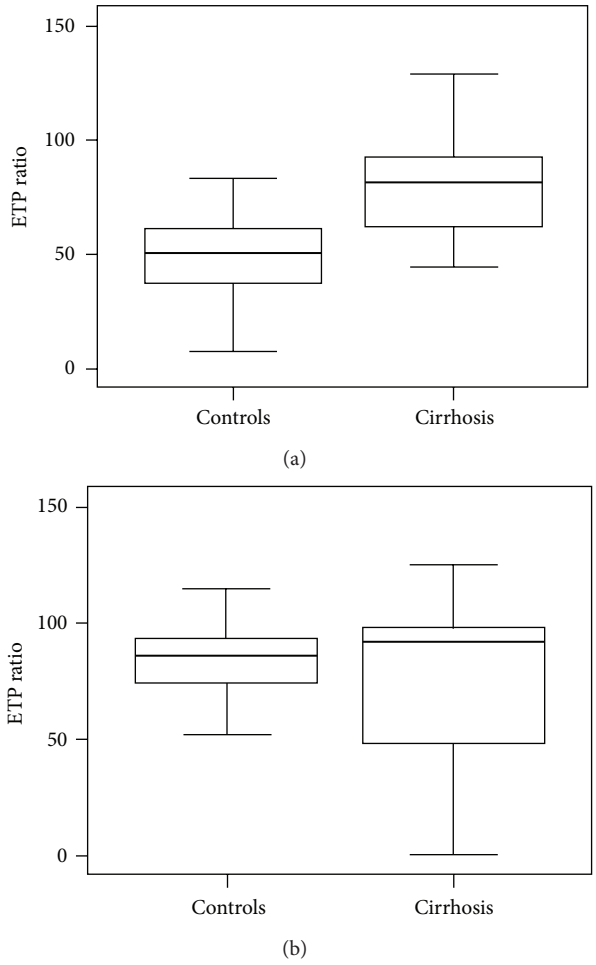

Figure 1: Endogenous thrombin potential (ETP) ratios of healthy controls ($n = 73$) and cirrhotic patients ($n = 156$). The ETP ratio was calculated by dividing "ETP with thrombomodulin (TM)" by "ETP without TM" multiplied by 100. The concentrations of TM were 2.5 nM for 1 pM tissue factor stimulation and 5 nM for 5 pM tissue factor stimulation. (a) With 1 pM tissue factor stimulation, the ETP ratio was significantly higher in the patients with cirrhosis ($P < 0.001$). (b) With 5 pM tissue factor stimulation, there was no significant difference in the ETP ratio between the controls and patients with cirrhosis.

meanwhile, the 1 pM TF concentration was used to increase sensitivity to FVIII, FIX, and FXI [12]. Since hypercoagulability in cirrhosis is considered to be due to increased FVIII and decreased protein C levels [13], the ETP ratio with 1 pM TF stimulation is thought to be higher in cirrhosis. On the contrary, the ETP ratio with 5 pM TF stimulation was not sensitive to FVIII concentration; therefore, it cannot be used to detect the hypercoagulability of cirrhosis. This finding suggests that the original TF concentration of 5 pM is not an appropriate stimulation for ETP to assess the hypercoagulability of cirrhotic patients.

The ETP ratio represents enhanced resistance to the anticoagulant action of thrombomodulin. We demonstrated that the ETP ratio with 1 pM TF stimulation increased gradually with respect to the MELD score until a score of 25. However,

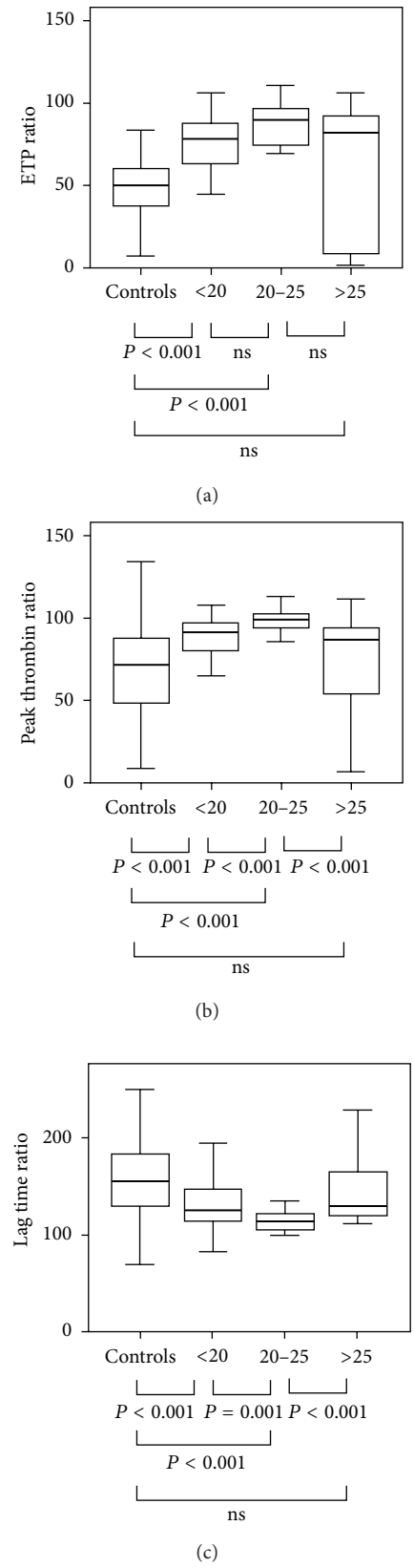

Figure 2: (a) The endogenous thrombin potential (ETP) ratio, (b) peak thrombin ratio, and (c) lag time ratio with 1 pM tissue factor stimulation according to the model of end-stage liver disease (MELD) scores of cirrhotic patients and controls.

the ETP ratio of the patients with MELD scores > 25 was not more than that in those with low MELD scores. A similar pattern was observed with the peak thrombin time, while the opposite pattern was observed with the lag time ratio. Further studies using larger patient groups with MELD scores > 25 are required to confirm whether this hypercoagulability is mainly confined to patients with low to middle MELD scores.

A limitation of the present study is that contact activation may affect the TGA assay *in vitro* [14]. Avoiding contact inhibition in clinical practice is not feasible, because a special tube with a high cost and short shelf life must be used to inhibit contact activation. Moreover, the physiological roles of contact factors *in vivo* remain unclear. Therefore, the present results merely demonstrate the usefulness of TGA as a practical test in clinical laboratory settings.

5. Conclusions

In conclusion, both coagulation and anticoagulation factors affect the results of global coagulation assays such as the PT and TGA. Of note, protein C levels strongly affect the PT and all parameters of the TGA. Patients with cirrhosis exhibit hypercoagulability in terms of their ETP ratio with 1 pM TF stimulation despite their prolonged PT. Although routine coagulation tests such as the PT and aPTT do not detect the thrombotic tendency in cirrhosis, the TGA can detect hypercoagulability in cirrhosis. It would be interesting to evaluate the global coagulation status using the newly devised TGA system in cirrhosis patients in the future.

Conflict of Interests

The authors declare no conflict of interests.

Authors' Contribution

N. Yongwon and J.-E. Kim contributed equally to this work.

Acknowledgment

This study was supported by a Grant from the Korean Health Technology R&D Project, Ministry of Health & Welfare, Republic of Korea (A120659).

References

[1] C. S. Kitchens, "To bleed or not to bleed? Is that the question for the PTT?" *Journal of Thrombosis and Haemostasis*, vol. 3, no. 12, pp. 2607–2611, 2005.

[2] S. J. Lewis, E. Stephens, G. Florou et al., "Measurement of global haemostasis in severe haemophilia a following factor VIII infusion," *British Journal of Haematology*, vol. 138, no. 6, pp. 775–782, 2007.

[3] V. Regnault, S. Béguin, D. Wahl, E. de Maistre, H. Coenraad Hemker, and T. Lecompte, "Thrombinography shows acquired resistance to activated protein C in patients with lupus anticoagulants," *Thrombosis and Haemostasis*, vol. 89, no. 2, pp. 208–212, 2003.

[4] A. Tripodi, F. Salerno, V. Chantarangkul et al., "Evidence of normal thrombin generation in cirrhosis despite abnormal conventional coagulation tests," *Hepatology*, vol. 41, no. 3, pp. 553–558, 2005.

[5] A. Gatt, A. Riddell, V. Calvaruso, E. G. Tuddenham, M. Makris, and A. K. Burroughs, "Enhanced thrombin generation in patients with cirrhosis-induced coagulopathy," *Journal of Thrombosis and Haemostasis*, vol. 8, no. 9, pp. 1994–2000, 2010.

[6] A. Tripodi, "How to implement the modified international normalized ratio for cirrhosis (INRliver) for model for end-stage liver disease calculation," *Hepatology*, vol. 47, no. 4, pp. 1423–1424, 2008.

[7] A. Tripodi, M. Primignani, V. Chantarangkul et al., "An imbalance of pro- versus anti-coagulation factors in plasma from patients with cirrhosis," *Gastroenterology*, vol. 137, no. 6, pp. 2105–2111, 2009.

[8] H. C. Hemker, P. Giesen, R. Al Dieri et al., "Calibrated automated thrombin generation measurement in clotting plasma," *Pathophysiology of Haemostasis and Thrombosis*, vol. 33, no. 1, pp. 4–15, 2003.

[9] P. S. Kamath, R. H. Wiesner, M. Malinchoc et al., "A model to predict survival in patients with end-stage liver disease," *Hepatology*, vol. 33, no. 2, pp. 464–470, 2001.

[10] H. K. Kim, D. S. Lee, S. H. Kang, J. Q. Kim, S. Park, and H. I. Cho, "Utility of the fibrinogen/C-reactive protein ratio for the diagnosis of disseminated intravascular coagulation," *Acta Haematologica*, vol. 117, no. 1, pp. 34–39, 2007.

[11] A. W. J. H. Dielis, E. Castoldi, H. M. H. Spronk et al., "Coagulation factors and the protein C system as determinants of thrombin generation in a normal population," *Journal of Thrombosis and Haemostasis*, vol. 6, no. 1, pp. 125–131, 2008.

[12] K. E. Brummel-Ziedins, R. L. Pouliot, and K. G. Mann, "Thrombin generation: phenotypic quantitation," *Journal of Thrombosis and Haemostasis*, vol. 2, no. 2, pp. 281–288, 2004.

[13] A. Tripodi, M. Primignani, L. Lemma et al., "Detection of the imbalance of procoagulant versus anticoagulant factors in cirrhosis by a simple laboratory method," *Hepatology*, vol. 52, no. 1, pp. 249–255, 2010.

[14] R. Luddington and T. Baglin, "Clinical measurement of thrombin generation by calibrated automated thrombography requires contact factor inhibition," *Journal of Thrombosis and Haemostasis*, vol. 2, no. 11, pp. 1954–1959, 2004.

Hindawi Publishing Corporation
BioMed Research International
Volume 2013, Article ID 946403, 5 pages
http://dx.doi.org/10.1155/2013/946403

Research Article

Human Platelet Antigen Genotyping and Expression of CD109 (Human Platelet Antigen 15) mRNA in Various Human Cell Types

Sang Mee Hwang,[1,2] Mi Jung Kim,[2] Ho Eun Chang,[2] Yun Ji Hong,[1,2] Taek Soo Kim,[1,2] Eun Young Song,[1] Kyoung Un Park,[1,2] Junghan Song,[1,2] and Kyou-Sup Han[1]

[1] *Department of Laboratory Medicine, Seoul National University College of Medicine, Seoul 110-744, Republic of Korea*
[2] *Department of Laboratory Medicine, Seoul National University Bundang Hospital, 173-82 Gumiro, Bundanggu, Gyeonggido, Seongnam 463-707, Republic of Korea*

Correspondence should be addressed to Kyoung Un Park; m91w95pf@snu.ac.kr

Received 12 December 2012; Revised 7 January 2013; Accepted 8 January 2013

Academic Editor: Mina Hur

CD109 gene encodes a glycosylphosphatidylinositol-linked glycoprotein found in a subset of platelets and endothelial cell, and human platelet antigen (HPA) 15 is found on CD109. We evaluated the HPA genotype and/or the CD109 mRNA expression on two peripheral blood stem cells (PBSC), two peripheral bloods (PB), 12 granulocyte products, natural killer (NK)-92, B-lymphocyte (CO88BV59-1), K-562 leukemia cell line, human embryonic stem cell (hESC), and human fibroblasts (HF). HPA genotyping was performed by SNaPshot assay and CD109 mRNA expression was evaluated by real-time PCR with SYBR green and melting curve analysis. Genotype HPA-15a/-15a was found in PBSC#1 and two granulocyte products, and HPA-15a/-15b was found in PBSC#2, eight granulocyte products, NK-92, K-562, hESC, and HF, and HPA-15b/-15b was found in two granulocyte products. CD109 mRNA expression was highly increased in HF and increased in CD34+ and CD34− PBSCs and some granulocyte products, compared to the PB. However, the increase of expression level varied among the PBSC and granulocyte products. The CD109 mRNA expression of NK-92, K-562, hESC, and CO 88BV59-1 was not detected. HPA genotype was evaluated in various cells and the expression of CD109, which contains HPA 15, was different among cell lines and high in HF and PBSCs.

1. Introduction

The CD109 gene encodes a glycosylphosphatidylinositol linked glycoprotein, that is, a member of the alpha2-macroglobulin/complement family of thioester-containing proteins [1]. CD109 is expressed on platelets, activated T-cells, and endothelial cells [2] and has gained clinical attention due to the association of antibodies to CD109 with alloimmune thrombocytopenia and posttransfusion purpura [3]. Depending on a single nucleotide polymorphism at nucleotide of coding CD109 gene, human platelet antigen (HPA)-15a, and HPA-15b alleles are defined [4], and anti-HPA-15 antibodies may develop and cause clinical consequences. Moreover, CD109 mRNA transcript has been studied in various cancers and is found to be highly expressed in squamous cell carcinomas and melanomas [5–7]. CD109 has been reported as a TGF-β coreceptor with high affinity for the TGF-β subtype and inhibiting TGF-β signaling in vitro, thus has been studied as a therapeutic target for diseases in which TGF-β may play a pathophysiological role and a key to elucidate pathogenesis of certain cancers [6, 8]. Thus, CD109 mRNA expression has been studied in some cells and tissues [9–11]. However, the studies of the CD109 mRNA expression have been limited to few cell types thus we have evaluated mRNA expression in a wider variety of cell types and cell lineages including common cell lines. The cell types or cell lineages included in this study are peripheral blood stem cells (PBSC), granulocyte products, natural killer

(NK)-92 cell line, B-lymphocyte cell line (CO 88BV-59-1), K-562 leukemia cell line, human embryonic stem cell (hESC), and human fibroblasts (HF). In addition, the genotype of different HPAs including the HPA 15, which is included in the CD109, was also characterized.

2. Materials and Methods

2.1. Materials. PBSC or granulocytes were collected by Cobe Spectra (Terumo BCT, Lakewood, USA) in two patients for PBSC and 12 patients for granulocyte products with informed consent. CliniMACS Cell separation system (Miltenyi Biotec, Bergisch Gladbach, Germany) was used to obtain CD34 enriched and depleted population of PBSC. PB prior to PBSC or granulocyte collection was also collected from donors.

Three cell lines including NK-92, B-lymphocyte CO88BV59-1, and K-562 leukemia cell lines were used in this study. Human NK-92 cell line was purchased from the American Type Culture Collection (ATCC CRL-2407, Rockville, MD) and maintained in alpha MEM medium supplemented with 12.5% horse serum, 12.5% fetal bovine serum (FBS), 0.2 mM myoinositol, 0.1 mM 2-mercaptoethanol, 0.02 mM folic acid, and recombinant human interleukin-2 (Proleukin, Prometheus, San Diego, CA). CO 88BV59-1 (CRL-10624, ATCC) and K-562 (ATCC) were maintained in RPMI-1640 (Invitrogen, Carlsbad, CA, USA), 10% FBS (Invitrogen).

Other cell types including hESC (SNUhES12 from Institute of Reproductive Medicine and Population in Seoul National University Medical Research Center) and HF (Modern Cell & Tissue Technology, Seoul, Korea) were maintained in RPMI-1640 with 10% FBS. Mouse embryonic fibroblast (MEF) (CF-1 MEF, Modern Cell & Tissue Technology) was also included as a negative control for PCR amplification. Different cells or cell lines were kept at 37°C, 5% CO_2.

2.2. Human Platelet Antigen Genotyping. HPA genotyping was performed for HPA-1, -2, -3, -4, -5, -6, -7, -8, -9, -13, and -15 using SNaPshot assay. Excluding the B-lymphocyte CO 88BV59-1 cell line, all of the cells or cell lines were included in the HPA genotyping. DNA was extracted using QIAamp DNA Blood mini kit (Qiagen). The primers for amplification were used as previously described [12]. PCR was performed with 100 ng of DNA, 0.4 μM for each primer, 0.625 U of *Taq* polymerase (Takara Bio Inc., Otsu, Japan), 10X buffer of 2.5 μL, 2.0 μL of 2.5 mM dNTPs, and 16.0 μL of distilled water. Thermocycling was performed as follows. Initial denaturation was carried out at 95°C for 10 minutes, amplification for 35 cycles at 94°C for 30 seconds, 55°C for 30 seconds, and 72°C for 1 minute and extension at 72°C for 7 minutes. Amplified PCR products were purified using the ExoSAP purification kit (ExoSap-it, Affymetrix, Cleveland, OH, USA). SNaPshot analysis was performed using an ABI PRISM SNaPshot Multiplex kit (Applied Biosystems, Foster City, CA, USA). Two sets of SNaPshot reaction were performed. The first set included the reaction for HPA-1, -2, -3, -4, and -9, and the second reaction was for HPA-5, -6, -7, -8, -13, -15. The sequences of the SNaPshot primers are shown in Table 1.

Table 1: SNaPshot primer sequences.

HPA type	Sense primer	Fragment size (bp)
Set 1		
HPA-1	5′-ggtcacagcgaggtgagccc-3′	20
HPA-2	5′-N_2gatgcccccagggctcctga-3′	30
HPA-3	5′-N_5aatgggggaggggctgggg-3′	39
HPA-9	5′-N_7cactcctttgccccccccag-3′	47
HPA-4	5′-N_9caagctggccacccagatgc-3′	56
Set 2		
HPA-5	5′-gagtctacctgtttactatcaaa-3′	23
HPA-6	5′-N_3caggacgaatgcagccccc-3′	31
HPA-7	5′-N_5aggccaaggtgcgaggctgt-3′	40
HPA-8	5′-N_7atacctgcaaccgttactgc-3′	48
HPA-13	5′-N_9aaggttaacattttcagtaa-3′	56
HPA-15	5′-N_{11}caaattcttggtaaatcctg-3′	64

N: Poly(dGACT) tail.

The multiplex SNaPshot reaction was performed in a final volume of 10 μL, containing 50 ng of each template, 5.0 μL of the SNaPshot multiplex ready reaction mix, and 4 μM of each SNaPshot primers for HPA-1, -2, -3, -4, -5, -6, -7, -9, and 10 μM of primers for HPA-8, -13, and -15. Cycling conditions were 25 cycles of 96°C for 10 seconds, 50°C for 5 seconds, and 60°C for 30 seconds. SNaPshot products were treated with shrimp alkaline phosphatase, separated using 0.15 μL of GeneScan-120 LIZ size standard with a ABI PRISM 3100 Genetic Analyzer, and data were analyzed using the GeneMapper Analysis Software version 2.0 (Applied Biosystems).

2.3. CD109 mRNA Expression. RNA was isolated from all of the cells included in the study with High Pure RNA Isolation kit (Roche, Mannheim, Germany) and reverse transcribed (SuperScript III Reverse Transciptase, Invitrogen). cDNA was amplified using a real-time PCR with the Light Cycler FastStart DNA Master SYBR Green I kit (Roche) in a LightCycler 2.0 (Roche). The following primer sequences were used for detecting expression of CD109 mRNA relative to β_2-microglobulin: the forward primer for CD109 was 5′-TAGCAGTCCACATGTCCGAAAGCA-3′ and the reverse primer was 5′-AACCAGTAGCCACCCAAGAAGTGA-3′ and the forward primer for β_2-microglobulin was 5′-AGATGAGTATGCCTGCCGTGTGAA-3′ and the reverse primer was 5′-TGCGGCATCTTCAAACCTCCATGA-3′. PCR was performed with 2 μL of cDNA, 0.2 μM of each primer, 2 μL of 10X mixture, and 12.8 μL of distilled water. Thermocycling was performed as follows: initial denaturation was carried out at 94°C for 10 minutes, amplification for 40 cycles at 94°C for 10 seconds, 58°C for 10 seconds, and 72°C for 15 seconds. Melting curve analysis was performed for 1 cycle at 95°C for 5 seconds, 65°C for 30 seconds, and 99°C for 0 seconds with a ramp rate of 0.2°C per seconds and 40°C for 30 seconds. Expression of CD109 was compared using β_2-microglobulin as the reference gene and the PB from donors of PBSC included in the study as the control. In case of cell lines, PB of PBSC#2 was used as a reference.

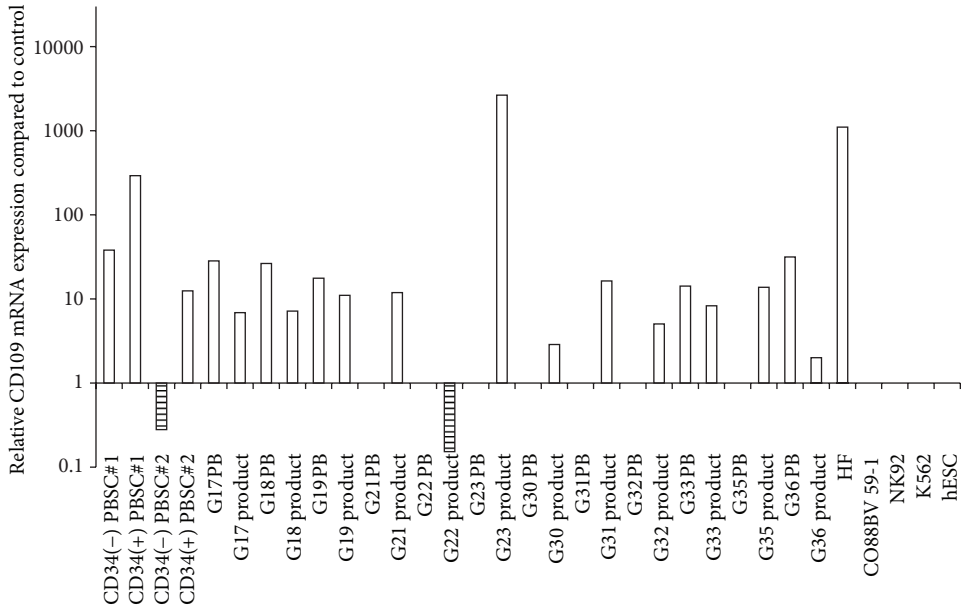

Figure 1: Comparison of CD109 mRNA expression results relative to the expression of those from peripheral blood (PB) of a PBSC donor. The expression of control PB is set as 1.0. The samples with no bar depict specimens with no detectable CD109 mRNA expression.

The relative gene expression was calculated by the modified $2^{-\Delta\Delta Ct}$ method [13].

3. Result

3.1. Human Platelet Antigen Genotyping. The results of HPA-1, -2, -3, -4, -5, -6, -7, -8, -9, -13, and -15 genotyping of different cell lines and cells are shown in Table 2. For HPA-15, genotype HPA-15a/-15a was found in PBSC#1 and two granulocyte products, genotype HPA-15a/-15b was found in PBSC#2, eight granulocyte products, NK-92, K-562, hESC, and HF, and genotype HPA-15b/-15b was found in two granulocyte products.

3.2. CD109 mRNA Expression. The expression of CD109 mRNA was detected in PB of PBSC donors, PBSC products including CD34 enriched and depleted populations, HF, PB of five granulocyte donors, and all of the granulocyte products. However, CD109 mRNA expression was not detected in the PB of seven granulocyte donors, NK-92, K-562, and CO 88BV59-1 cell lines (Figure 1).

The expressions of PBSCs were compared to the PB of donors prior to PBSC collection. CD34+ enriched population showed higher expression of CD109 mRNA compared to the product prior to enrichment. PBSC#1 products showed higher CD109 mRNA expression than PBSC#2 products. The CD34+ percentage and count of CD34+ enriched population was higher in PBSC#1 (86.7%, 741.1/μL) than for PBSC#2 (74.4%, 355.5/μL). The CD109 mRNA expression of other cell lines and cells were compared to the expression of the PB of PBSC donors. HF showed markedly increased CD109 mRNA expression. For granulocyte products, only PB of five donors showed detectable level of mRNA expression. However, all of the granulocyte products were detected with CD109 mRNA expression. Depending on the donors, the CD109 mRNA expression of the product was higher in PB prior to granulocyte collection in five donors but the expression was higher in the granulocyte product in the remaining seven donors.

4. Conclusion

Genotyping of human platelet antigen including HPA 15, which is located in CD109, was performed on different cells and cell lines. There have been no previous reports on the HPA genotype of cell lines, NK-92, CO 88BV59-1 B-lymphocyte, K-562 leukemia, cell lines, and cells including HF and hESC. K-562 is a cell line made from a chronic myeloid leukemia patient [14] and showed HPA-1a/HPA-1b genotype, which is found rarely in Koreans [15]. All the other cells showed genotypes that were frequently found in Koreans [15, 16].

The expression of CD109 mRNA expression was also determined in different cell types and cell lines. Consistent to the previous reports on expression of CD109 on CD34+ hematopoietic stem cells [17], we were able to find high expression of CD109 mRNA on CD34+ enriched population compared to the PB prior to PBSC collection. However, the CD34 depleted population also showed detectable CD109 mRNA expression but lower than PB of PBSC donors. This may be because PB of PBSC donors have significantly high level of hematopoietic stem cells recruited to the PB with prior treatment of granulocyte-colony stimulating factors. Thus, the relative mRNA expression may be different when compared to the PB from normal donors without prior G-CSF treatment. Interestingly, CD34+ products of a donor

Table 2: Human platelet antigen genotype results by SNaPshot assay.

Cell types	HPA-1 (176T > C)	HPA-2 (482C > T)	HPA-3 (2621T > G)	HPA-4 (506G > A)	HPA-5 (1600G > A)	HPA-6 (1544G > A)	HPA-7 (1297C > G)	HPA-8 (1984C > T)	HPA-9 (2602G > A)	HPA-13 (2483C > T)	HPA-15 (2108C > A)
NK-92	T/T	C/C	T/G	G/G	G/A	G/G	C/C	C/C	G/G	C/C	C/A
K-562	C/T	C/C	T/G	G/G	G/G	G/G	C/C	C/C	G/G	C/C	C/A
hESC	T/T	C/C	T/G	G/G	G/G	G/G	C/C	C/C	G/G	C/C	C/A
HF	T/T	C/C	T/G	G/G	G/G	G/A	C/C	C/C	G/G	C/C	C/A
PBSC product #1	T/T	C/C	T/G	G/G	G/G	G/G	C/C	C/C	G/G	C/C	C/A
PBSC product #2	T/T	C/C	T/G	G/G	G/G	G/G	C/C	C/C	G/G	C/C	C/C
Granulocyte G17	T/T	C/C	T/G	G/G	G/A	G/G	C/C	C/C	G/G	C/C	C/A
Granulocyte G18	T/T	C/C	T/G	G/G	G/G	G/G	C/C	C/C	G/G	C/C	C/A
Granulocyte G19	T/T	C/C	T/T	G/G	G/G	G/G	C/C	C/C	G/G	C/C	C/A
Granulocyte G21	T/T	C/C	T/T	G/G	G/G	G/G	C/C	C/C	G/G	C/C	C/A
Granulocyte G22	T/T	C/T	T/T	G/G	G/G	G/G	C/C	C/C	G/G	C/C	C/C
Granulocyte G23	T/T	C/T	T/T	G/G	G/G	G/G	C/C	C/C	G/G	C/C	A/A
Granulocyte G30	T/T	C/C	T/T	G/G	G/A	G/G	C/C	C/C	G/G	C/C	C/C
Granulocyte G31	T/T	C/C	T/G	G/G	G/G	G/G	C/C	C/C	G/G	C/C	C/A
Granulocyte G32	T/T	C/T	T/G	G/G	G/A	G/G	C/C	C/C	G/G	C/C	C/A
Granulocyte G33	T/T	C/T	T/G	G/G	G/G	G/G	C/C	C/C	G/G	C/C	A/A
Granulocyte G35	T/T	C/C	T/G	G/G	G/G	G/G	C/C	C/C	G/G	C/C	C/A
Granulocyte G36	T/T	C/T	T/T	G/G	G/G	G/G	C/C	C/C	G/G	C/C	C/A

with higher percentage and count of CD34 enriched population showed higher expression of CD109 mRNA. Further analysis of CD34+ cells in different products may explain the CD109 mRNA expression level as well. HF, which is also known to have CD109 protein expression [18, 19] showed very high expression of CD109 mRNA. In a previous study, the level of CD109 mRNA expression was compared with normal fibroblasts and scleroderma skin fibroblasts and showed no significant difference [19]. In our study, the mRNA expression of HF was compared to the PB of a PBSC donor and was very high. The CD109 mRNA expression of NK-92, CO 88BV 59-1, and K-562 cell lines were not detected. There have been reports on the expression of CD109 on activated T-lymphocytes [20, 21], but no reports have been made on B-lymphocytes and NK cells.

This was the first study to genotype HPA in various known cell lines and different cells. Moreover, the mRNA expression of CD109 studied in each cell types and was found to be high in PBSCs, some granulocyte products and HF compared to the PB but was not detected in NK cell line, B-lymphocyte cell line, and hESC.

Acknowledgments

This research was supported by the Basic Science Research Program through the National Research Foundation of Korea (NRF) funded by the Ministry of Education, Science and Technology (2010-0024014) and by a Grant 03-2010-006 from the Seoul National University Bundang Hospital Research Fund.

References

[1] M. Lin, D. R. Sutherland, W. Horsfall et al., "Cell surface antigen CD109 is a novel member of the α2 macroglobulin/C3, C4, C5 family of thioester-containing proteins," *Blood*, vol. 99, no. 5, pp. 1683–1691, 2002.

[2] D. R. Sutherland, E. Yeo, A. Ryan, G. B. Mills, D. Bailey, and M. A. Baker, "Identification of a cell-surface antigen associated with activated T lymphoblasts and activated platelets," *Blood*, vol. 77, no. 1, pp. 84–93, 1991.

[3] K. Ertel, M. Al-Tawil, S. Santoso, and H. Kroll, "Relevance of the HPA-15 (Gov) polymorphism on CD109 in alloimmune thrombocytopenic syndromes," *Transfusion*, vol. 45, no. 3, pp. 366–373, 2005.

[4] A. C. Schuh, N. A. Watkins, Q. Nguyen et al., "A tyrosine703serine polymorphism of CD109 defines the Gov platelet alloantigens," *Blood*, vol. 99, no. 5, pp. 1692–1698, 2002.

[5] Y. Ohshima, I. Yajima, M. Y. Kumasaka et al., "CD109 expression levels in malignant melanoma," *Journal of Dermatological Science*, vol. 57, no. 2, pp. 140–142, 2010.

[6] S. Hagiwara, Y. Murakumo, T. Sato et al., "Up-regulation of CD109 expression is associated with carcinogenesis of the squamous epithelium of the oral cavity," *Cancer Science*, vol. 99, no. 10, pp. 1916–1923, 2008.

[7] M. Hashimoto, M. Ichihara, T. Watanabe et al., "Expression of CD109 in human cancer," *Oncogene*, vol. 23, no. 20, pp. 3716–3720, 2004.

[8] A. A. Bizet, K. Liu, N. Tran-Khanh et al., "The TGF-β co-receptor, CD109, promotes internalization and degradation of TGF-β receptors," *Biochimica et Biophysica Acta*, vol. 1813, no. 5, pp. 742–753, 2011.

[9] P. M. Hernández-Campo, J. Almeida, S. Matarraz, M. de Santiago, M. L. Sánchez, and A. Orfao, "Quantitative analysis of the expression of glycosylphosphatidylinositol-anchored proteins during the maturation of different hematopoietic cell compartments of normal bone marrow," *Cytometry B*, vol. 72, no. 1, pp. 34–42, 2006.

[10] M. Hasegawa, S. Hagiwara, T. Sato et al., "CD109, a new marker for myoepithelial cells of mammary, salivary, and lacrimal glands and prostate basal cells," *Pathology International*, vol. 57, no. 5, pp. 245–250, 2007.

[11] K. W. Finnson, B. Y. Tam, K. Liu et al., "Identification of CD109 as part of the TGF-β receptor system in human keratinocytes," *FASEB Journal*, vol. 20, no. 9, pp. 1525–1527, 2006.

[12] X. Xu, F. Zhu, Y. Ying et al., "Simultaneous genotyping of human platelet antigen-1 to 17w by polymerase chain reaction sequence-based typing," *Vox Sanguinis*, vol. 97, no. 4, pp. 330–337, 2009.

[13] T. D. Schmittgen and K. J. Livak, "Analyzing real-time PCR data by the comparative CT method," *Nature Protocols*, vol. 3, no. 6, pp. 1101–1108, 2008.

[14] C. B. Lozzio and B. B. Lozzio, "Human chronic myelogenous leukemia cell line with positive Philadelphia chromosome," *Blood*, vol. 45, no. 3, pp. 321–334, 1975.

[15] D. H. Seo, S. S. Park, D. W. Kim, K. Furihata, I. Uenof, and K. S. Han, "Gene frequencies of eight human platelet-specific antigens in Koreans," *Transfusion Medicine*, vol. 8, no. 2, pp. 129–132, 1998.

[16] H. O. Kim, Y. Jin, T. S. Kickler, K. Blakemore, O. H. Kwon, and P. F. Bray, "Gene frequencies of the five major human platelet antigens in African American, white, and Korean populations," *Transfusion*, vol. 35, no. 2, pp. 863–867, 2003.

[17] L. J. Murray, E. Bruno, N. Uchida et al., "CD109 is expressed on a subpopulation of CD34+ cells enriched in hematopoietic stem and progenitor cells," *Experimental Hematology*, vol. 27, no. 8, pp. 1282–1294, 1999.

[18] B. Y. Tam and A. Philip, "Transforming growth factor-β receptor expression on human skin fibroblasts: dimeric complex formation of type I and type II receptors and identification of glycosyl phosphatidylinositol-anchored transforming growth factor-β binding proteins," *Journal of Cellular Physiology*, vol. 176, no. 3, pp. 553–564, 1998.

[19] X.-Y. Man, K. W. Finnson, M. Baron, and A. Philip, "CD109, a TGF-β co-receptor, attenuates extracellular matrix production in scleroderma skin fibroblasts," *Arthritis Research and Therapy*, vol. 14, no. 3, Article ID R144, 2012.

[20] A. Haregewoin, K. Solomon, R. C. Hom et al., "Cellular expression of a GPI-linked T cell activation protein," *Cellular Immunology*, vol. 156, no. 2, pp. 357–370, 1994.

[21] C. Brashem-Stein, D. Nugent, and I. D. Bernstein, "Characterization of an antigen expressed on activated human T cells and platelets," *Journal of Immunology*, vol. 140, no. 7, pp. 2330–2333, 1988.

Hindawi Publishing Corporation
BioMed Research International
Volume 2013, Article ID 192738, 11 pages
http://dx.doi.org/10.1155/2013/192738

Research Article

Gene Silencing of 4-1BB by RNA Interference Inhibits Acute Rejection in Rats with Liver Transplantation

Yang Shi,[1] Shuqun Hu,[1] Qingwei Song,[1] Shengcai Yu,[1] Xiaojun Zhou,[2] Jun Yin,[2] Lei Qin,[2] and Haixin Qian[2]

[1] *Department of General Surgery, The Affiliated Hospital of Xuzhou Medical College, Xuzhou, Jiangsu 221002, China*
[2] *Department of General Surgery, The First Affiliated Hospital of Soochow University, Suzhou, Jiangsu 215006, China*

Correspondence should be addressed to Haixin Qian; qianhaixin228@126.com

Received 5 September 2012; Accepted 18 December 2012

Academic Editor: Andrew St. John

The 4-1BB signal pathway plays a key role in organ transplantation tolerance. In this study, we have investigated the effect of gene silencing of 4-1BB by RNA interference (RNAi) on the acute rejection in rats with liver transplantation. The recombination vector of lentivirus that contains shRNA targeting the 4-1BB gene (LV-sh4-1BB) was constructed. The liver transplantation was performed using the two-cuff technique. Brown-Norway (BN) recipient rats were infected by the recombinant LVs. The results showed that gene silencing of 4-1BB by RNAi downregulated the 4-1BB gene expression of the splenic lymphocytes *in vitro*, and the splenic lymphocytes isolated from the rats with liver transplantation. LV-sh4-1BB decreased the plasma levels of liver injury markers including AST, ALT, and BIL and also decreased the level of plasma IL-2 and IFN-γ in recipient rats with liver transplantation. Lentivirus-mediated delivery of shRNA targeting 4-1BB gene prolonged the survival time of recipient and alleviated the injury of liver morphology in recipient rats with liver transplantation. In conclusion, our results demonstrate that gene silencing of 4-1BB by RNA interference inhibits the acute rejection in rats with liver transplantation.

1. Introduction

Costimulatory pathways between antigen-presenting cells (APCs) and Tcells play a crucial role in T-cells activation and alloimmune responses [1, 2]. 4-1BB is a member of the tumor necrosis factor receptor superfamily. The functions of receptor mainly as a costimulatory molecule in T lymphocytes. 4-1BB is expressed in activated T cells and antigen presenting cells such as dendritic cells [3]. 4-1BB/4-1BB ligand (4-1BBL) signaling provides T-cells activation with costimulation, that is, dependent or independent of CD28 [4]. 4-1BB can supply sufficient costimulatory signals for T-cells activation [5]. Under the condition of repeated antigen stimulation, the downregulationg expresion of CD28 protein in activated T cells results in activation-induced celll death (AICD), whereas very few 4-1BB molecules may supply sufficient costimulatory signals to sustain T-cells activation and inhibit AICD [6].

As we all know, the liver transplantation is an effective therapy for end-stage liver disease. But the transplantation rejective response is a formidable problem after liver transplantation, especially acute rejection which is the main cause of early dysfunction and transplantation failure [7]. The incidence rate of acute rejection after liver transplantation is up to 50% to 70% [8]. The acute rejection after the organ transplantation is mainly caused by the activation of the immune system in the host. During the acute rejection, T cells are the most important effectors involved in antigen recognition, lymphcyte proliferation and differentiation, and immune regulation, cytolysis. 4-1BB plays a critical role in allograft rejection [9, 10]. Our previous study illuminated that the blockade of the 4-1BB/4-1BBL costimulatory pathway with 4-1BBL monoclonal antibody decreased the acute rejection in rat with liver transplantation [11].

RNA interference- (RNAi-) mediated gene silencing can be generated by the expression of a vector-mediated RNAi anywhere in the genome and is already being tested as a potential therapy in clinical trials for a number of diseases [12, 13]. The viral-based vectors have been developed as an

Table 1: Sense and antisense oligomers of shRNA targeting the 4-1BB gene of rats.

shRNA symbol	Target sequence	Start position	shRNA strand
shRNA1	GCTGTTACAAC ATGGTGGTCA	11	sense 5′-CACCGCTGTTACAACATGGTGGTCATTCAAGAGATGA CCACCATGTTGTAACAGCTTTTTTG-3′ antisense 5′-ACCTTGATTCCAACGGTAACCATCATCTCTTGAAGGA TACCTTCAAGCATTCCGGAGGATTA-3′
shRNA2	GCAGTAAATAC CCTCCGGTCT	110	sense 5′-CACCGCAGTAAATACCCTCCGGTCTTTCAAGAGAAG ACCGGAGGGTATTTACTGCTTTTTTG -3′ antisense 5′-AACCCCTAGGGCTTAAGCAATCCAGTCTCTTGAACCA TTTGGCACTTAAGCCATTGACTGAC-3′
shRNA3	GCAGAGTGTGT CAAGGCTATT	191	sense 5′-CACCGCAGAGTGTGTCAAGGCTATTTCAAGAGAAT AGCCTTCGAGCACACTCTGCTTTTTTG -3′ antisense 5′-AGGTTACCGGGATCCTTGAACAATACTCTTGAACA ACCCGGTTTACCAAATACCGGAATTGG-3′
shRNANC	ATTGGACCAAG TGGTTCATAGC		sense 5′-CCTGACGATTAAGGACTAGGTCAGCTTCAAGAGACCC CTTAAAGCTTTCGGACGTCGCGAAC-3′ antisense 5′-AAGTACCAACTACATCTGGGAACTTCTCTTGAAACCC TGAATGGGTCATCGTAACTACAAC-3′

alternative strategy of gene therapy. Therefore, the aim of present study was to investigate the effect of gene silencing of 4-1BB by RNA interference on the acute rejection in rats with liver transplantation.

2. Materials and Methods

2.1. Lentiviral Vectors. The design of siRNA was performed according to the previously published guidelines by using the Ambion siRNA-finding software [14]. To minimize off-target effects, a BLAST homology search was systematically performed to ensure that a single-mRNA sequence was targeted. Replication-deficient, self-inactivating lentiviral vectors pcDNA-CMV-sh4-1BB-Lentivector (LV-sh4-1BB) and the empty vector (LV-NC) were generated as follows. As shown in Table 1, the target sequence of siRNA sequences targeting 4-1BB of rat (GenBank: NM-001025773) and control were as follows: shRNA1 (11–31), GCTGTTACAACATGGTGGTCA; shRNA2 (110–130), GCAGTAAATACCCTCCGGTCT; shRNA3 (191–211), GCAGAGTGTGTCAAGGCTATT; nonsilencing siRNA, ATTGGACCAAGTGGTTCATAGC. The oligonucleotides were designed according to the structure of the siRNA sense strand-loop-siRNA antisense strand. The siRNA sequences targeting 4-1BB of rat were shown in Table 1. The oligonucleotides were synthesized and used for the construction of pcDNA-CMV-sh4-1BB-Lentivector. A negative control (LV-NC) with DNA oligos targeting 4-1BB of rat was also designed.

The shRNAs were cloned into lentiviral work vector pcDNA-CMV-Lentivector (Shanghai GeneChem Co. Ltd., Shanghai, China), which was linearized using restriction endonucleases BamH I and Pst I. All constructs were verified by sequence analysis. The recombinant lentiviral vectors were designated as LV-sh4-1BB1, LV-shP4-1BB2, LV-shP4-1BB3, and LV-NC. The recombinant work vector and package plasmids were cotransduced into 293T cells using Lipofectamine 2000 (Invitrogen, Carlsbad, CA, USA) for generating the lentivirus. After the cells were cultivated for 48 h, the culture medium was collected, concentrated by ultracentrifugation, aliquoted, and stored at −80°C until used. Virus titer is the number of cells expressing green fluorescent protein (GFP) multiplied by the corresponding dilution. The titer of lentivirus was determined by hole-by-dilution titer assay. The final titer of recombinant virus was 2×10^9 transducing units (TU)/mL.

2.2. 293T-Cell Culture and Transduction. The 293T packaging cell line (Academy of Life Science, Shanghai, China) was cultivated in Dulbecco's modified Eagle's medium (DMEM) (Invitrogen, Carlsbad, CA, USA) supplemented with 10% fetal bovine serum (FBS) (Invitrogen, Carlsbad, CA, USA), 100 mg/mL streptomycin and 100 U/mL penicillin at 37°C in a humidified incubator containing 5% CO_2. Cells were seeded in 24-well plates at 50–70% confluence 24 h prior to transduction. To analyze the transduction efficiency, 293T cells were gated to determine the percentage of GFP-positive cells. Cells with >85% viability were cultivated for additional experiments.

2.3. T-Lymphocytes Isolation, Culture, and Transduction. Spleens were harvested from Brown-Norway (BN) rats

(Animal Center of Soochow University, Suzhou, China) euthanazed by cervical dislocation. The procedures were performed according to the local guidelines for animal research approved by the Administrative Committee of Experimental Animal Care and Use of Soochow University. Single-cell suspensions were prepared by forcing tissue through a fine wire mesh using a syringe plunger followed by repeated pipetting in culture medium. RBC depletion involved cell lysis in 5 mL lysing buffer [0.14 moL/L NH_4Cl, 0.017 moL/L Tris-base (pH 7.5)] for 5 min at 20°C followed by three washes in ice-cold medium. To activated T cell, phytohemagglutinin (50 μg/mL) was added in the culture medium [15].

The T lymphocytes from BN rats were cultivated in RPMI 1640 culture medium (Invitrogen, Carlsbad, CA, USA) supplemented with 10% fetal calf serum (FCS) (Invitrogen, Carlsbad, CA, USA). Transient transduction was performed using Lipofectamine 2000 (Invitrogen, Carlsbad, CA, USA) according to the manufacturer's instructions in six- or 12-well plates with cells at 70–90% confluence.

2.4. Real-Time Quantitative PCR Analysis. Total RNA was extracted by using Trizol reagent (Invitrogen, Carlsbad, CA, USA) according to the manufacturer's instructions. Briefly, the splenic lymphocyte was treated with 1.5 mL Trizol reagent and kept at room temperature for 5 min. After the cells were incubated with 600 μL chloroform for 3 min, the total RNA was centrifuged for 20 min at 12,000 g and 4°C. The total RNA was precipitated with 1000 μL isopropanol. After incubation of 10 min at room temperature, the RNA was precipitated for 10 min at 16.000 g and 4°C. The resulting RNA-pellet was washed with 2000 μL isopropanol. The concentration of RNA was assessed photometrically at 260 nm. The reactions were run on a Roche light Cycler Run 5.32 Real-Time PCR System (Bio-Rad, Hercules, CA, USA) with the following cycle conditions: 95°C for 15 sec, 45 cycles at 95°C for 10 sec, and at 60°C for 30 sec. Melt curve analyses of all real-time PCR products were performed and shown to produce a single-DNA duplex. Quantitative measurements were determined using the $\Delta\Delta$ Ct method and expression of β-actin was used as the internal control. The mRNA expression of the control group was expressed as 100%. Fold-induction of mRNA expression was calculated [16]. The sequences of the 4-1BB gene primers were as follows: forward primer, 5′-GTGTCAAGGCTATTTCAG-3′; reverse primer, 5′-AGACCACGTCTTTCTCC-3′. the product was 275 bp. β-Actin served as a control for normalization. The primers were as follows: forward primer, 5′-CCTCATGAAGATCCTGACCG-3′; reverse primer, 5′-AGCCAGGGCAGTAATCTCCT-3′. The product was 488 bp.

2.5. Western Blot Analysis. The splenic lymphocytes were collected. Cells were washed with cold phosphate-buffered saline (PBS) containing 2 mmoL/L EDTA and lysed with denaturing SDS-PAGE sample buffer using standard methods. Protein extract was prepared. The protein concentration in supernatant was determined by the BCA assay. The final concentration of protein in each sample was adjusted to 2 mg/mL. Protein lysates were separated by 12% SDS-PAGE and transferred onto polyvinylidene fluoride membrane (Millipore, Bedford, MA). The membranes were blocked with 5% skim milk for 1 h at 37°C. Then the membranes were incubated with rabbit anti-4-1BB monoclonal antibody (dilution at 1 : 200) and anti-β-actin antibody (dilution at 1 : 300) (Santa Cruz Biotechnology, Santa Cruz, CA, USA) at 48°C overnight. After the membranes were washed three times with Tris-buffered saline, they were incubated with horseradish peroxidase (HRP)—conjugated goat anti-rabbit immunoglobulin G (IgG) antibody (dilution at 1 : 1,000) (Santa Cruz) at room temperature for 4 h. Immunoreactivity was detected by enhanced chemiluminescence (ECL). The band density was measured with Quantity One analysis software (Bio-Rad, Hercules, CA, USA), and the quantification of 4-1BB to β-actin levels was done by densitometry analysis [17].

2.6. Animals and Rat Liver Transplantation Models. Inbred male Lewis (LEW) and BN rats weighing 200–250 g were purchased from the Vital River Laboratories (Beijing, China). All animals were housed under conditions of constant temperature (22°C) and humidity in a specific-pathogen-free facility. The rats were fed with the commercial rat chow pellets. Male LEW rats were used as the liver donors and BN rats as the recipients.

Orthotopic liver transplantation was performed using the "two-cuff technique" as previously described [11, 18]. Briefly, the donors and recipients were anesthetized with the ether. The suprahepatic vena cava was reconstructed using continuous 8-0 polypropylene sutures. The hepatic artery was not reconstructed. The portal vein was reanastomosed using a polyethylene cuff (8F). When the anastomosis of the portal vein and suprahepatic vena cava was completed, the liver was reperfused. The anastomosis of the infrahepatic vena cava was then completed by the same cuff technique (6F). The bile duct was anastomosed with an intraluminal polyethylene stent (22G). The transplantation procedure required less than 60 min, during which the portal vein was clamped for 13 to 15 min. The procedures were performed according to the local guidelines for animal research approved by the Administrative Committee of Experimental Animal Care and Use of Soochow University.

2.7. Experimental Animal Grouping. Sixty four BN rats were randomly divided into four groups: sham group (S), liver transplantation model group (M), LV-sh4-1BB1 group (LV-sh4-1BB1), and LV-NC group (LV-NC). The rats of the sham and model group were injected 1 mL saline via the dorsal penis vein, respectively, before operation. The rats of the LV-sh4-1BB1 group and LV-NC group were injected 1 mL recombinant LVs and empty LVs via the dorsal penis vein, respectively, before liver transplantation.

On the 7th day after transplantation, 8 rats in each group were killed by cervical dislocation. The lymphocytes were obtained from spleen and used for measurement of 4-1BB expression by real-time RT-PCR and Western blot analysis. Blood samples were gathered by the inferior vena cava and used for biochemistry tests and cytokine assay. The liver lobes were excised to study the pathological changes. The remanent

rats in each group were used to recored the survival time of posttransplantation.

2.8. Analysis of Plasma Liver Function Markers and Cytokines. On the 7th day after transplantation, serum aspartate transaminase (AST), alanine aminotransferase (ALT), lactate dehydrogenase (LDH), and bilirubin (BIL) were measured by using the automatic biochemical meter (TMS1024, Tokyo Bokei, Japan). The concentrations of interleukin-2 (IL-2), IL-10, and interferon-γ (IFN-γ) in plasma were tested using enzyme-linked immunosorbent assay (ELISA) kits (Biosource International, Inc. Camarillo, CA, USA). All the procedures were performed according to the instruction of the manufacturers.

2.9. Histological and Morphometric Analysis of Liver Grafts. On the 7th day posttransplantation, recipient rats were sacrificed. The grafted liver samples were fixed in 10% formalin and embedded in paraffin. Five micrometer thick sections were affixed to slides, deparaffinized, and stained with hematoxylin and eosin. The severity of acute rejection was assessed in a blinded fashion with a rejection activity index (RAI) according to Banff criterion [11, 19, 20].

Grafted livers were fixed in 4% glutaraldehyde, dehydrated with ethanol, and then embedded in Epon812. Liver sections were sliced and stained with uranium lead. Microstructure was read using Hitachi H-600 electron microscopy (Hitachi, Japan).

2.10. Statistical Analysis. Data are presented as mean ± standard deviation (SD). The statistical evaluation of differences in recipient survival was performed using the log rank test applied to Kaplan-Meier plots. All other statistical comparisons among groups were conducted using analysis of variance (ANOVA) with subsequent Dunnett's t-test. Significance was defined as $P < 0.05$.

3. Results

3.1. PCR Identification of Constructed shRNA Expression Plasmids and Titer Determination and Packaging of the Lentiviral Vector. The pcDNA-CMV-Lentivector 4-1BB shRNA expression plasmids were identified using a restriction endonuclease digestion. The lengths of pcDNA-CMV-Lentivector is 7.8 kb and pcDNA-CMV-Lentivector contains BamH I and Pst I two restriction sites. The product of pcDNA-CMV-Lentivector is linear large fragment after the double enzyme. The product of the recombination vector of lentivirus containing shRNA targeting the 4-1BB gene were two fragments, one was 7.8 kb and the other was 326 bp. As shown in Figure 1, results of DNA sequencing were as expected. The recombination vector of lentivirus encoding the specially designed shRNA against the 4-1BB gene was named pcDNA-CMV-sh4-1BB-Lentivector (LV-sh4-1BB). The empty vector was used as blank-control and named pcDNA-CMV-Lentivector (LV-BC). The negative-control shRNA was named LV-NC.

Forty-eight hours after cotransfection of the three-plasmid lentiviral vector into 293T cells, strong green fluorescence was observed using an inverted fluorescence microscope. After a single exposure of 293T cells to the lentivirus, a high percentage (>90%) of transfectants expressed GFP at 48 h after the transduction, indicating a high and stable transduction of the lentiviral vector system (data not shown).

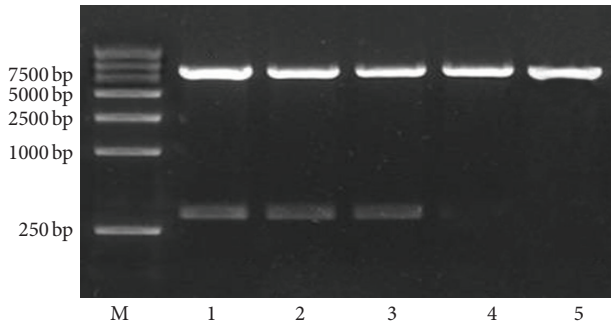

Figure 1: The identification of constructed shRNA expression plasmids by restriction enzyme. Lane 1: LV-sh4-1BB1; lane 2: LV-sh4-1BB2; lanes 3: LV-sh4-1BB3; lanes 4: empty pcDNA-CMV-Lentivector (blank-control); 5: negative-control shRNA (LV-NC).

3.2. Efficiency of Lentiviral Transfection into the Splenic Lymphocytes. To demonstrate the efficiency of siRNA delivery into the splenic lymphocytes, the splenic lymphocytes were infected by LV-sh4-1BB and LV-NC labeled with GFP. Successful lentiviral transfection was evidenced by green fluorescence under fluorescence microscopy 72 h after transduction (Figure 2).

3.3. Lentivirus-Mediated Delivery of shRNA Inhibits 4-1BB Expression in the Splenic Lymphocytes In Vitro. The mRNA expression of 4-1BB in the splenic lymphocytes was measured by real-time PCR 72 h after transduction. As shown in Figure 3(a), the mRNA expression of 4-1BB in the splenic lymphocytes was decreased approximately 96.8%, 94.1, and 95.2%, respectively, by LV-sh4-1BB1, LV-sh4-1BB2, and LV-sh4-1BB3 transduction compared to the empty LV-NC (all $P < 0.05$). These results indicated that the mRNA sequences corresponding to the 4-1BB gene shRNA were specific RNAi targets.

Western blot analysis was performed 72 h after transduction. The results showed that LV-sh4-1BB1, LV-sh4-1BB2, and LV-sh4-1BB3 induced an 85.3%, 84.6, and 84.5% downregulation of the 4-1BB protein level, respectively, compared with the empty LV-NC (all $P < 0.05$) (Figures 3(b) and 3(c)). So among three 4-1BB siRNAs, LV-sh4-1BB1 was selected as the best performing siRNA for use in the next study.

3.4. Lentivirus-Mediated Delivery of shRNA Targeting 4-1BB Gene Downregulated the 4-1BB Expression of the Splenic Lymphocytes Isolated from the Rats with Liver Transplantation. To evaluate the inhibition of 4-1BB mRNA expression in the splenic lymphocytes isolated from the recipient rats, real-time PCR was performed 7 days after transduction. As shown in Figure 4(a), the mRNA expression of 4-1BB in the model of liver transplantation group was significantly

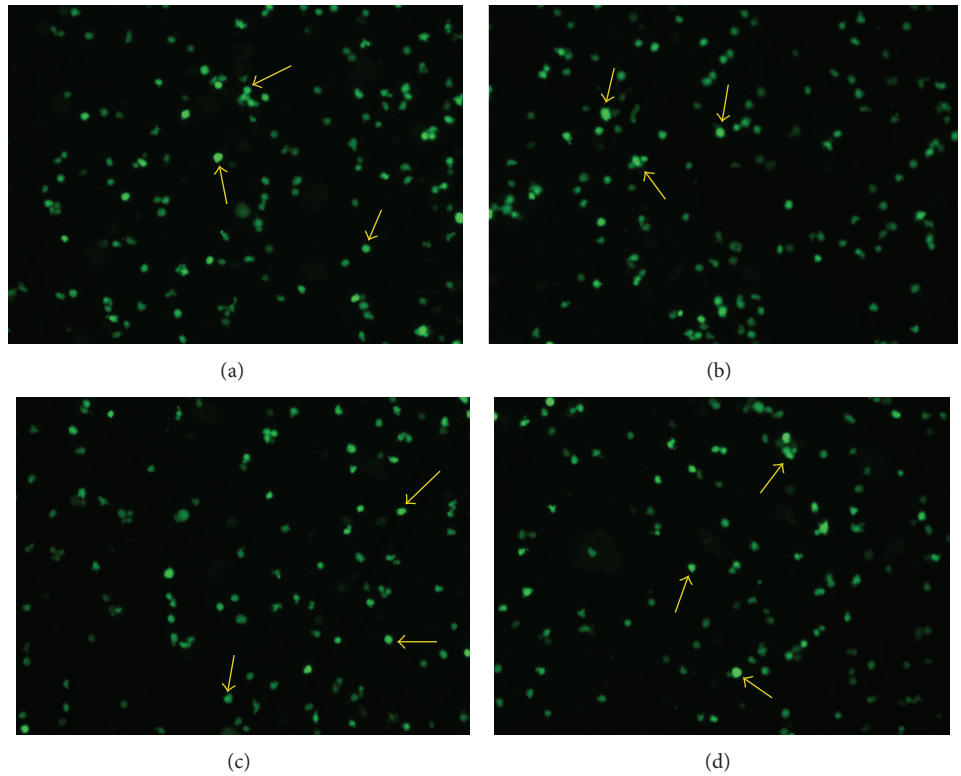

Figure 2: Representative fluorescence microscopy images of splenic lymphocytes 72 h after transduction with pcDNA-CMV-sh4-1BB-Lentivector1-3 (LV-sh4-1BB1-3) (a–c) and negative-control shRNA group (LV-NC) (d) (×100). Arrows indicate GFP fluorescence in the splenic lymphocytes.

Table 2: The levels of AST, LDH, ALT, and T-BIL in plasma of BN recipients rats 7 days after liver transplantation.

Groups	ALT (U/L)	AST (U/L)	LDH (U/L)	T-BIL (mg/L)
Sham (Control)	292.43 ± 32.41	428.39 ± 34.66	859.34 ± 94.36	75.39 ± 8.12
Model	580.52 ± 51.96$^{\#}$	738.11 ± 75.63$^{\#}$	1404.65 ± 168.74$^{\#}$	83.94 ± 9.53
LV-NC	577.21 ± 61.14	784.7 ± 47.85	1553.19 ± 125.83	84.38 ± 10.46
LV-sh4-1BB1	333.26 ± 39.92*	457.7 ± 43.61*	942.81 ± 83.17*	76.84 ± 8.43

The recombination vector of lentivirus containing shRNA targeting the 4-1BB gene was constructed. The liver transplantation was performed using the two-cuff technique. BN recipient rats were infected by the recombinant LVs. The blood samples were gathered 7 days after liver transplantation. The liver function markers were tested by using the automatic biochemical meter. Model: liver transplantation model group; LV-NC: negative-control shRNA group; LV-sh4-1BB1: pcDNA-CMV-sh4-1BB-Lentivector1 group. Data were expressed as means ± SD, $n = 8$. $^{\#}P < 0.05$ compared with the sham (control) group; $^{*}P < 0.05$ compared with the LV-NC group.

upregulated compared with the sham group ($P < 0.05$). LV-sh4-1BB1 transduction resulted in a 91.8% reduction of 4-1BB mRNA expression compared to the LV-NC groups ($P < 0.05$). Western blot analysis was performed 7 days after transduction. The results showed that the protein expression of 4-1BB was significantly upregulated in the model of liver transplantation group compared with the sham group ($P < 0.05$). LV-sh4-1BB1 transduction resulted in a 90.3% reduction of 4-1BB protein expression compared to the LV-NC groups ($P < 0.05$) (Figures 4(b) and 4(c)).

3.5. Lentivirus-Mediated Delivery of shRNA Targeting 4-1BB Gene Prolonged Recipient Survival in Rats with Liver Transplantation. As shown in Figure 5, the survival time of BN recipients rats after liver transplantation was significantly increased in LV-sh4-1BB1 group compared with the LV-NC group ($P < 0.05$). The mean survival time (MST) of rats in LV-NC group was 12 days (range 8–14 days) and the MST of rats in LV-sh4-1BB1 group was 34.5 days (range 15–48 days). 12-day survival rate was 62.5% and 100.0% in LV-NC and LV-sh4-1BB1 group, respectively.

3.6. Lentivirus-Mediated Delivery of shRNA Targeting 4-1BB Gene Decreased the Level of Liver Function Damage in Recipient Rats with Liver Transplantation. As shown in Table 2, compared with the sham group, the plasma concentrations of AST, LDH, and ALT in liver transplantation model group were significantly increased 7 days after liver transplantation ($P < 0.05$). But the plasma concentrations of AST, LDH, and ALT in LV-sh4-1BB1 group were significantly

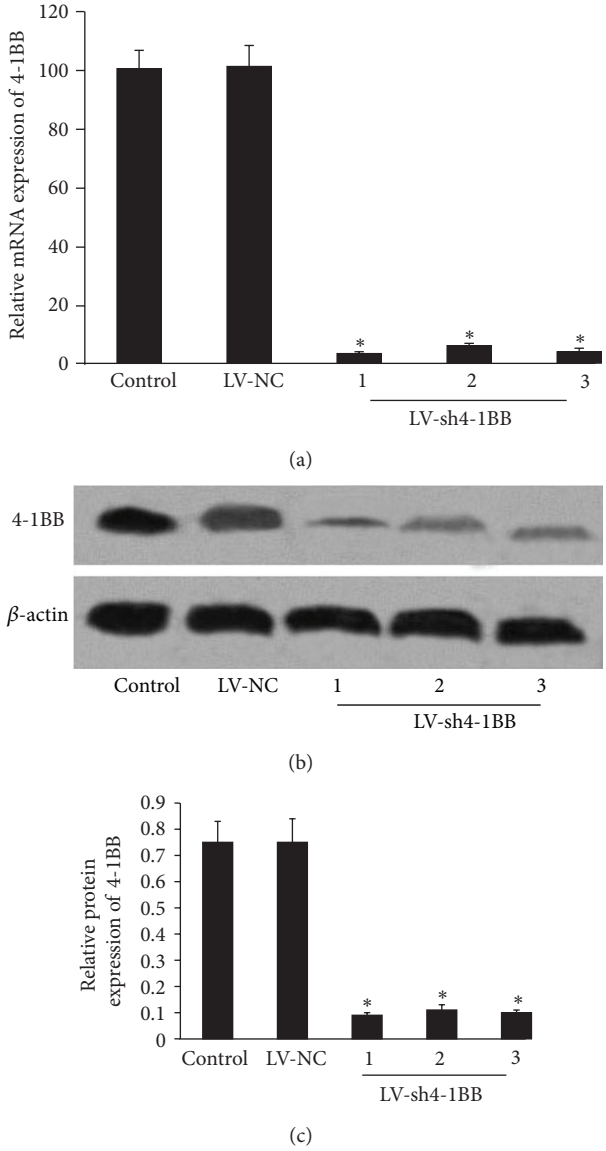

Figure 3: Effect of 4-1BB siRNA transduction on the expression of 4-1BB in the splenic lymphocytes. The recombination vector of lentivirus containing shRNA targeting the 4-1BB gene was constructed. Lymphocytes from BN rats were infected by recombinant LVs. ddH_2O was used as the control. (a) Real-time PCR analysis of the mRNA level of 4-1BB gene in the splenic lymphocytes 72 h after transduction. (b and c) The protein level of 4-1BB gene in the splenic lymphocytes was showed by Western blot analysis 72 h after transduction. β-actin was used as an internal standard. LV-NC: negative-control shRNA group; LV-sh4-1BB1-3: pcDNA-CMV-sh4-1BB1-3-Lentivector group. Data were expressed as means ± SD. $^{*}P < 0.05$ compared with the LV-NC group.

decreased compared to the LV-NC group 7 days after liver transplantation ($P < 0.05$).

3.7. Lentivirus-Mediated Delivery of shRNA Targeting 4-1BB Gene Decreased the Level of Plasma IL-2, IL-10, and IFN-γ in Rats with Liver Transplantation. The concentrations of plasma IL-2 and IFN-γ in liver transplantation model group

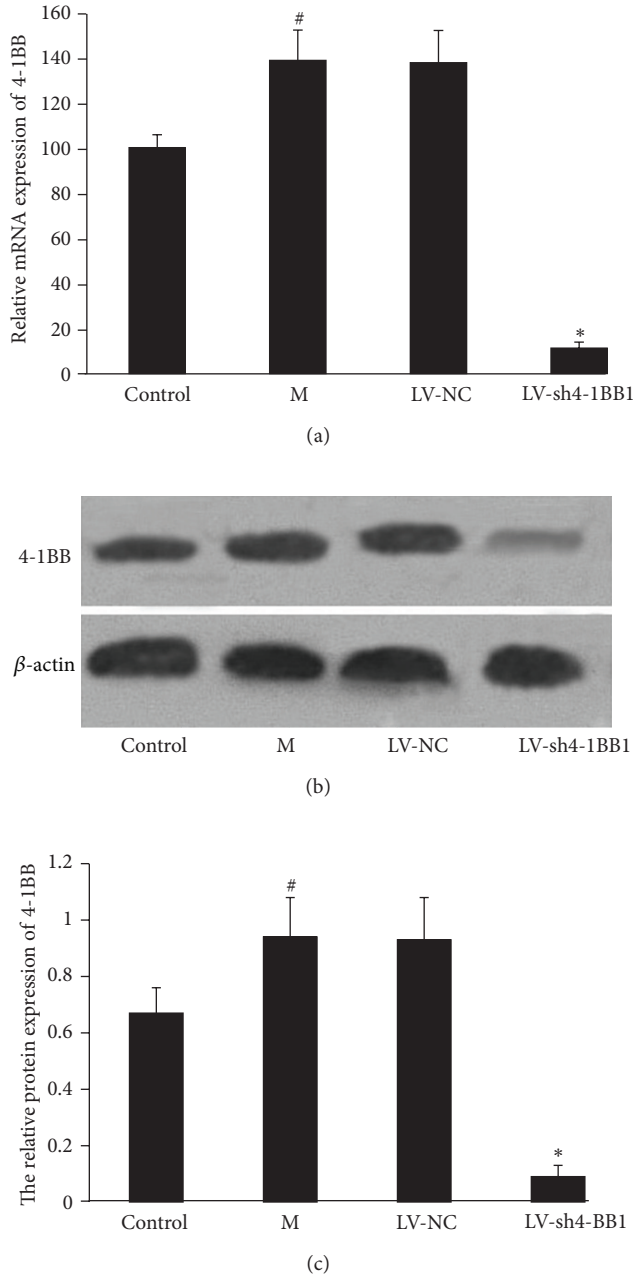

Figure 4: Effect of lentivirus-mediated delivery of shRNA targeting 4-1BB gene on 4-1BB expression of the splenic lymphocytes isolated from the recipient rats with liver transplantation. The recombination vector of lentivirus contains shRNA targeting the 4-1BB gene was constructed. The liver transplantation was performed using the two-cuff technique. BN recipient rats were infected by the recombinant LVs. The splenic lymphocytes from the recipient rats were gathered 7 days after transduction. Sham was used as the control. (a) Real-time PCR analysis of the mRNA level of 4-1BB gene in the splenic lymphocytes 7 days after transduction. (b and c) The protein level of 4-1BB gene in the splenic lymphocytes was showed by Western blot analysis 7 days after transduction. β-actin was used as an internal standard. M: the liver transplantation group; LV-NC: negative-control shRNA group; LV-sh4-1BB1: pcDNA-CMV-sh4-1BB1-Lentivector group. Data were expressed as means ± SD. $^{\#}P < 0.05$ compared with the sham (control) group; $^{*}P < 0.05$ compared with the LV-NC group.

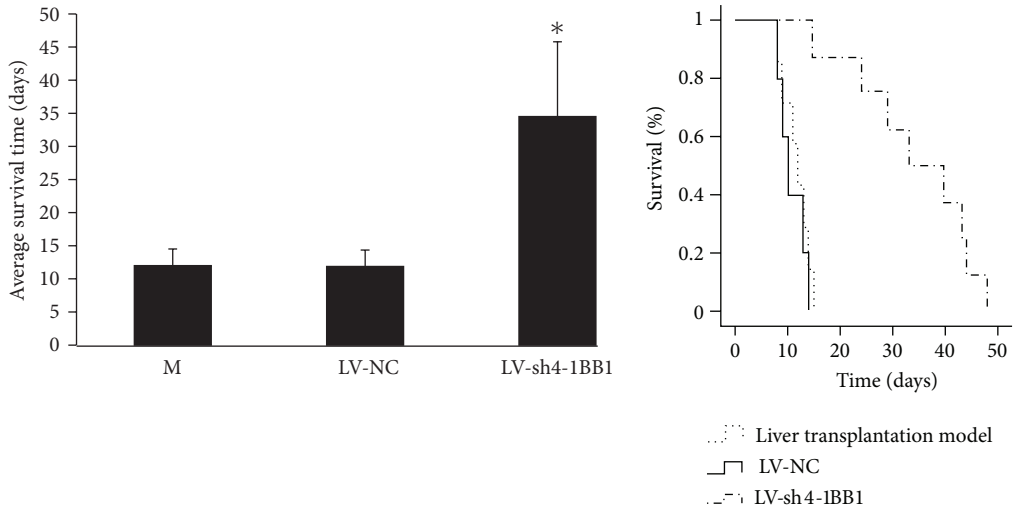

(a) (b)

Figure 5: Effect of lentivirus-mediated delivery of shRNA targeting 4-1BB gene on the survival time in BN recipients rats after liver transplantation. The recombination vector of lentivirus contains shRNA targeting the 4-1BB gene (LV-sh4-1BB1) was constructed. The liver transplantation was performed using the two-cuff technique. BN recipient rats were infected by the recombinant LVs. The survival time of recipients rats was recorded and the percentage of survival was calculated. M: the liver transplantation model group; LV-NC: negative-control shRNA group; LV-sh4-1BB1: pcDNA-CMV-sh4-1BB1-Lentivector group. Data were expressed as means ± SD, $n = 8$. $^{*}P < 0.05$ compared with the LV-NC group.

Table 3: The levels of IL-2, IL-10, and IFN-γ in plasma of BN recipients rats 7 days after liver transplantation.

Groups	IL-2 (pg/mL)	IL-10 (pg/mL)	IFN-γ (pg/mL)
Sham (Control)	71.32 ± 8.67	16.85 ± 2.03	52.49 ± 6.75
Model	139.15 ± 13.73$^{\#}$	15.47 ± 1.27	86.2 ± 8.27$^{\#}$
LV-NC	142.86 ± 16.58	18.35 ± 2.06	80.3 ± 11.64
LV-sh4-1BB1	78.05 ± 8.64*	16.59 ± 1.85	57.86 ± 8.33*

The recombination vector of lentivirus contains shRNA targeting the 4-1BB gene was constructed. The liver transplantation was performed using the two-cuff technique. BN recipient rats were infected by the recombinant LVs. The blood samples were gathered 7 days after liver transplantation. The concentrations of interleukin-2 (IL-2), IL-10, and interferon-γ (IFN-γ) in plasma were tested using enzyme-linked immunosorbent assay (ELISA). Model: liver transplantation model group; LV-NC: negative-control shRNA group; LV-sh4-1BB1: pcDNA-CMV-sh4-1BB-Lentivector1 group. Data were expressed as means ± SD, $n = 8$. $^{\#}P < 0.05$ compared with the sham (control) group; $^{*}P < 0.05$ compared with the LV-NC group.

were significantly increased 7 days after liver transplantation compared with the sham group. However, the plasma concentrations of plasma IL-2 and IFN-γ in LV-sh4-1BB1 group were significantly decreased compared with the LV-NC group 7 days after liver transplantation ($P < 0.05$) (Table 3).

3.8. Lentivirus-Mediated Delivery of shRNA Targeting 4-1BB Gene Alleviated the Injury of Liver Morphology in Recipient Rats with Liver Transplantation. As shown in Figure 6, the severe portal lymphocyte infiltration, the injuries of the portal area and interlobular bile duct, cholangitis, and bridged necrosis in liver parenchyma were observed detected 7 days after liver transplantation in the liver transplantation model group. The rejection was significantly inhibited in the LV-sh4-1BB1 group compared with the LV-NC group. Mild-to-moderate portal inflammatory infiltration, lower grade of endothelialitis, mild bile duct injuries, and no evident hepatocyte necrosis were detected 7 days after liver transplantation in the LV-sh4-1BB1 group.

The histological grade in Banff score in liver transplantation model group was significantly increased 7 days after liver transplantation compared with the sham control group (7.11 ± 0.78 versus 5.17 ± 0.68, $P < 0.05$) (Figure 7). Compared with the LV-NC group, the histological grade in Banff score in LV-sh4-1BB1 group was significantly decreased 7 days after liver transplantation (7.15 ± 0.84 versus 5.89 ± 0.79, $P < 0.05$).

Electron micrographs showed that a typical early stage apoptosis of hepatocytes, swollen mitochondria, and dilatation of endoplasmic reticulum were observed in a majority of hepatocytes 7 days after liver transplantation in liver transplantation model group. But these phenomenons were not observed in LV-sh4-1BB1 group (Figure 8).

4. Discussion

The orthotopic liver transplantation has become the most effective therapy for the patients with end-stage liver disease. However, organ rejection is a thorny problem after transplantation, especially acute rejection which is the main cause

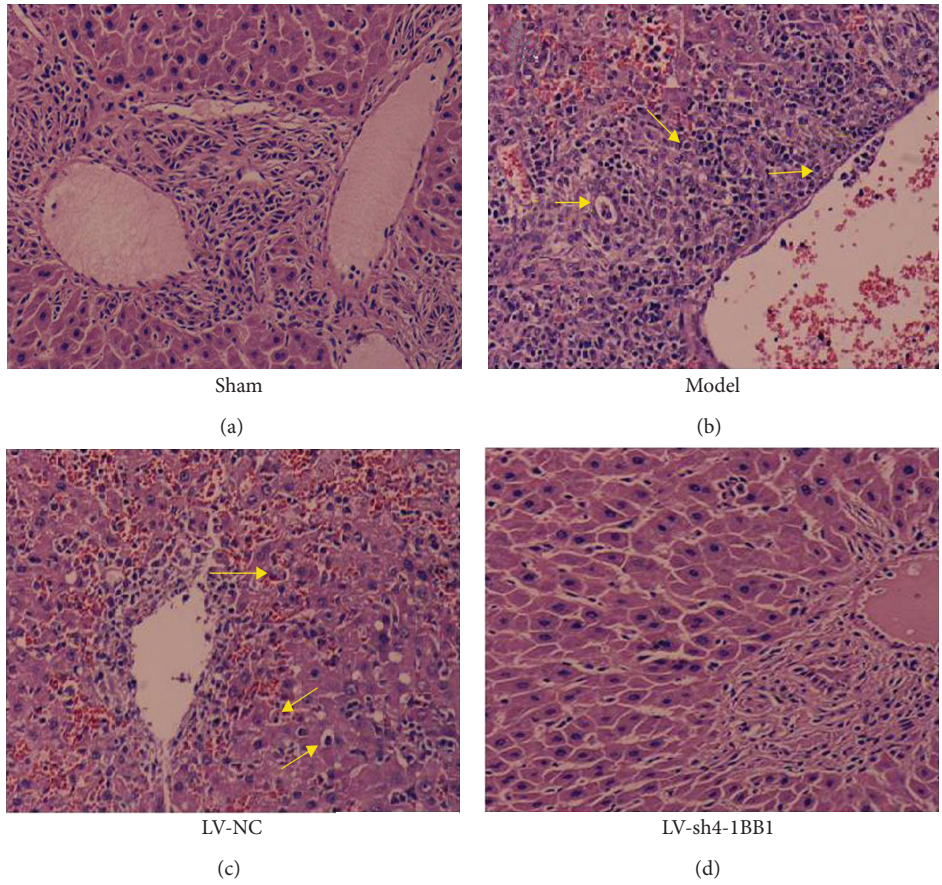

Figure 6: The pathology of liver in recipient rats with liver transplantation (HE, original magnification ×400). The recombination vector of lentivirus contains shRNA targeting the 4-1BB gene was constructed. The liver transplantation was performed using the two-cuff technique. BN recipient rats were infected by the recombinant LVs. The pathology of liver in recipient rats was observed by H-E staining 7 days after liver transplantation. Model: liver transplantation model group; LV-NC: negative-control shRNA group; LV-sh4-1BB1: pcDNA-CMV-sh4-1BB1-Lentivector group.

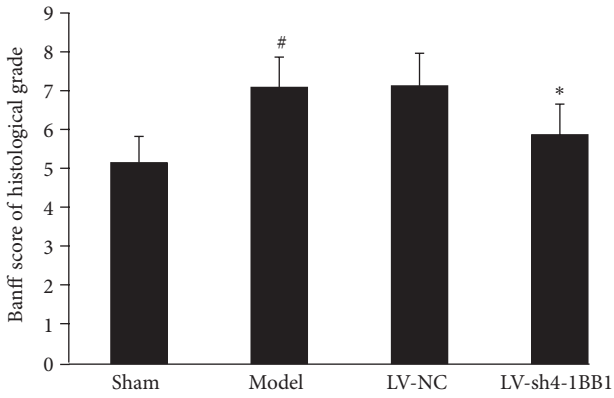

Figure 7: The Banff score of histological grade. Model: liver transplantation model group; LV-NC: negative-control shRNA group; LV-sh4-1BB1: pcDNA-CMV-sh4-1BB1-Lentivector group. Data were expressed as means ± SD, $n = 8$. $^{\#}P < 0.05$ compared with the sham group; $^{*}P < 0.05$ compared with the LV-NC group.

of early dysfunction and retransplantation [21]. Therefore, it is very important to search new and effective methods to prevent and inhibit the organ rejection response in organ transplantation.

Transplantation rejective response is principally mediated by T cells in the peripheral circulation and a variety of inflammatory stimuli that induce T cells to infiltrate the transplanted tissue [22]. $CD4^+$ T cells secrete a number of cytokines which may induce cell infiltration in the graft after allogeneic recognition, and $CD8^+$ T cells are involved in the direct cytotoxicity towards the liver graft [23]. Deletion, anergy, regulation/suppression, ignorance, or induction of activation induced T-cell death will be ways to suppress acute rejection and induce immune tolerance [24].

4-1BB is a family member of tumor necrosis factor receptor. 4-1BB is an important T-cell costimulatory molecule and expressed in activated cytolytic and helper T cells, as well as natural killers (NK) cells. The ligand of 4-1BB (4-1BBL) is expressed in B cells, macrophages, and dendritic cells. 4-1BB signaling preferentially promotes the proliferation and survival of $CD8^+$ T cells and promotes the production of IL-2 in $CD4^+$ T cells and prevents activation-induced cell death. 4-1BB is involved in the activation and survival of $CD4^+$, $CD8^+$, and NK cells [25]. The activation of T cells in the absence of costimulation is futile because T cells deprived of costimulatory signals enter a state of unresponsiveness or anergy.

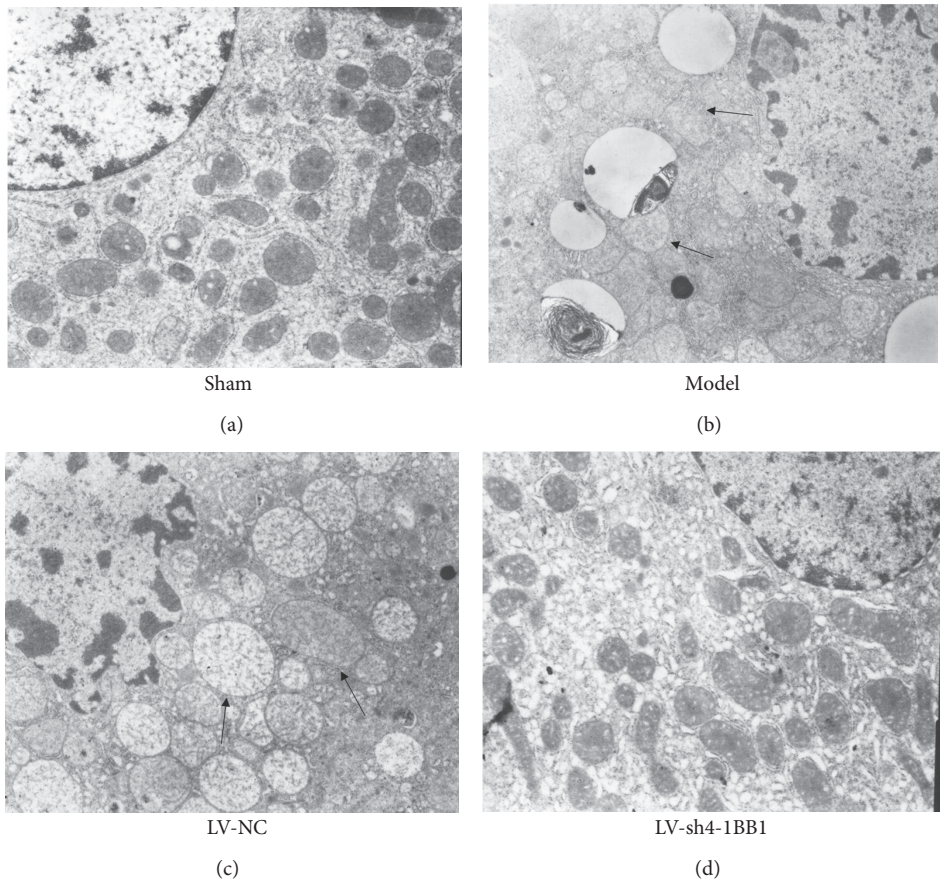

Figure 8: The electron micrographs of liver in recipient rats with liver transplantation (original magnification ×12000). The recombination vector of lentivirus contains shRNA targeting the 4-1BB gene was constructed. The liver transplantation was performed using the two-cuff technique. BN recipient rats were infected by the recombinant LVs. The ultrastructure of liver in recipient rats was observed by electron microscope 7 days after liver transplantation. Model: liver transplantation model group; LV-NC: negative-control shRNA group; LV-sh4-1BB1: pcDNA-CMV-sh4-1BB1-Lentivector group.

The interaction of 4-1BB and 4-1BBL can activate an important costimulatory pathway which plays the diverse and important roles in immune response and organ transplantation tolerance. The previous studies showed that blocking the 4-1BB/4-1BBL signal pathway might modulate the secretion of Th1/Th2 cytokines and prolong the survival of the grafts [26]. It was reported that administration of agonistic anti-4-1BB monoclonal antibody (mAB) prevented the development of various autoimmune and nonautoimmune conditions *in vivo* [27, 28]. Our previous results also suggested the blockade of the 4-1BB/4-1BBL costimulatory pathway with 4-1BBL monoclonal antibody attenuated the acute rejection in recipient rats with the liver transplantation [11].

RNAi-based gene silencing is more rapid and cost-effective compared with the gene knockout techniques. RNA interference (RNAi) is a powerful tool to induce loss-of-function phenotypes by posttranscriptional silencing of gene expression. Viral delivery of short hairpin RNA (shRNA) expression cassettes allows efficient transduction in tissues such as immunological cell *in vivo* [29]. The knockdown of gene expression has been achieved using lentiviral vector constructs that express shRNAs within vector-infected cells. The lentiviral vector system provided useful tools for elucidating gene function by analysis of loss-of-function phenotypes and for exploring the application of RNAi in gene therapy [30]. In our study, The recombination vector of lentivirus containing shRNA targeting the 4-1BB gene was successfully constructed. The liver transplantation was performed using the two-cuff technique. BN recipient rats were infected by the recombinant LVs. The results showed that gene silencing of 4-1BB by RNA interference downregulated the 4-1BB gene expression of the splenic lymphocytes isolated from the recipient rats with liver transplantation. Our results also showed that lentivirus-mediated delivery of shRNA targeting 4-1BB gene prolonged the survival time of recipient rats. These results suggested that the silencing of 4-1BB gene by RNA interference was successful in the recipient rats and useful for the liver transplantation.

The acute transplantation rejective response is the important cause of retransplantation and is principally mediated by T cells [31]. Cytokines including IL-2, IL-10, and INF-γ can accelerate the T-cell mediated immune response, while IL-4, 5, and 6 can be helpful for B-cell mediated humoral immunity. Increase of cytokines is the marker of the

acute transplantation rejective response [32, 33]. Our results showed that gene silencing of 4-1BB by RNA interference decreased the levels of plasma IL-2 and INF-γ seven days after liver transplantation. These illuminated that gene silencing of 4-1BB inhibited the T cell-mediated acute rejection in recipient rats with liver transplantation.

Histopathology is the gold standard for diagnosing graft rejection after transplantation [34]. There are the infiltration of inflammatory cells to portal area including activated lymphocytes, neutrophils and acidophils, inflammation of endotheliocytes under the portal vein and central vein, and the inflammation and injury of the bile duct in the acute rejection of liver transplantation [35, 36]. The dysfunction of the liver should be observed in the acute rejection of liver transplantation. In our study, the results showed that gene silencing of 4-1BB by RNA interference decreased the plasma levels of liver injury markers including AST, ALT, and BIL and alleviated the injury of liver morphology in recipient rats with liver transplantation. Our experiment strongly suggested gene silencing of 4-1BB by RNA interference prevented the liver injury induced by the acute rejection in rats with liver transplantation.

In conclusion, we have demonstrated that gene silencing of 4-1BB by RNA interference inhibits the acute rejection in rats with liver transplantation and it is a promising strategy to prevent progression of graft rejection.

References

[1] J. J. Goronzy and C. M. Weyand, "T-cell co-stimulatory pathways in autoimmunity," *Arthritis Research and Therapy*, vol. 10, no. 1, article S3, 2008.

[2] M. Kornete and C. A. Piccirillo, "Critical co-stimulatory pathways in the stability of Foxp3$^+$ Treg cell homeostasis in type I diabetes," *Autoimmunity Reviews*, vol. 11, no. 2, pp. 104–111, 2011.

[3] A. Palazón, I. Martínez-Forero, A. Teijeira et al., "The HIF-1α hypoxia response in tumor-infiltrating T lymphocytes induces functional CD137 (4-1BB) for immunotherapy," *Cancer Discovery*, vol. 2, no. 7, pp. 608–623, 2012.

[4] D. Teschner, G. Wenzel, E. Distler et al., "In vitro stimulation and expansion of human tumour-reactive CD8$^+$ cytotoxic t lymphocytes by anti-CD3/CD28/CD137 magnetic beads," *Scandinavian Journal of Immunology*, vol. 74, no. 2, pp. 155–164, 2011.

[5] J. A. Hernandez-Chacon, Y. Li, R. C. Wu et al., "Costimulation through the CD137/4-1BB pathway protects human melanoma tumor-infiltrating lymphocytes from activation-induced cell death and enhances antitumor effector function," *Journal of Immunotherapy*, vol. 34, no. 3, pp. 236–250, 2011.

[6] H. W. Chen, C. H. Liao, C. Ying, C. J. Chang, and C. M. Lin, "Ex vivo expansion of dendritic-cell-activated antigen-specific CD4$^+$ T cells with anti-CD3/CD28, interleukin-7, and interleukin-15: potential for adoptive T cell immunotherapy," *Clinical Immunology*, vol. 119, no. 1, pp. 21–31, 2006.

[7] C. Stefanidis, G. Callebaut, W. Ngatchou et al., "The role of biventricular assistance in primary graft failure after heart transplantation," *Hellenic Journal of Cardiology*, vol. 53, no. 2, pp. 160–162, 2012.

[8] M. Glanemann, G. Gaebelein, N. Nussler et al., "Transplantation of monocyte-derived hepatocyte-like cells (NeoHeps) improves survival in a model of acute liver failure," *Annals of Surgery*, vol. 249, no. 1, pp. 149–154, 2009.

[9] T. Asai, B. K. Choi, P. M. Kwon et al., "Blockade of the 4-1BB (CD137)/4-1BBL and/or CD28/CD80/CD86 costimulatory pathways promotes corneal allograft survival in mice," *Immunology*, vol. 121, no. 3, pp. 349–358, 2007.

[10] B. J. Huang, H. Yin, Y. F. Huang et al., "Gene therapy using adenoviral vector encoding 4-1BBIg gene significantly prolonged murine cardiac allograft survival," *Transplant Immunology*, vol. 16, no. 2, pp. 88–94, 2006.

[11] L. Qin, H. G. Guan, X. J. Zhou, J. Yin, J. Lan, and H. X. Qian, "Blockade of 4-1BB/4-1BB ligand interactions prevents acute rejection in rat liver transplantation," *Chinese Medical Journal*, vol. 123, no. 2, pp. 212–215, 2010.

[12] N. Wu, A. B. Yu, H. B. Zhu, and X. K. Lin, "Effective silencing of Sry gene with RNA interference in developing mouse embryos resulted in feminization of XY gonad," *Journal of Biomedicine and Biotechnology*, vol. 2012, Article ID 343891, 11 pages, 2012.

[13] T. Yang, B. Zhang, B. K. Pat, M. Q. Wei, and G. C. Gobe, "Lentiviral-mediated RNA interference against TGF-beta receptor type II in renal epithelial and fibroblast cell populations in vitro demonstrates regulated renal fibrogenesis that is more efficient than a nonlentiviral vector," *Journal of Biomedicine and Biotechnology*, vol. 2010, Article ID 859240, 12 pages, 2010.

[14] K. Ui-Tei, Y. Naito, F. Takahashi et al., "Guidelines for the selection of highly effective siRNA sequences for mammalian and chick RNA interference," *Nucleic Acids Research*, vol. 32, no. 3, pp. 936–948, 2004.

[15] Y. C. Kuo, S. C. Weng, C. J. Chou, T. T. Chang, and W. J. Tsai, "Activation and proliferation signals in primary human T lymphocytes inhibited by ergosterol peroxide isolated from Cordyceps cicadae," *British Journal of Pharmacology*, vol. 140, no. 5, pp. 895–906, 2003.

[16] L. A. Muscarella, V. Guarnieri, M. Coco et al., "Small deletion at the 7q21.2 locus in a CCM family detected by real-time quantitative PCR," *Journal of Biomedicine and Biotechnology*, vol. 2010, Article ID 854737, 7 pages, 2010.

[17] C. S. Kim, J. G. Kim, B. J. Lee et al., "Deficiency for costimulatory receptor 4-1BB protects against obesity-induced inflammation and metabolic disorders," *Diabetes*, vol. 60, no. 12, pp. 3159–93168, 2011.

[18] T. Hori, L. B. Gardner, F. Chen et al., "Impact of hepatic arterial reconstruction on orthotopic liver transplantation in the rat," *Journal of Investigative Surgery*, vol. 25, no. 4, pp. 242–252, 2012.

[19] A. J. Demetris, K. P. Batts, A. P. Dhillon et al., "Banff schema for grading liver allograft rejection: an international consensus document," *Hepatology*, vol. 25, no. 3, pp. 658–663, 1997.

[20] M. H. Sanei, T. D. Schiano, C. Sempoux, C. Fan, and M. I. Fiel, "Acute cellular rejection resulting in sinusoidal obstruction syndrome and ascites postliver transplantation," *Transplantation*, vol. 92, no. 10, pp. 1152–1158, 2011.

[21] B. Fosby, T. H. Karlsen, and E. Melum, "Recurrence and rejection in liver transplantation for primary sclerosing cholangitis," *World Journal of Gastroenterology*, vol. 18, no. 1, pp. 1–5, 2012.

[22] S. Gras, L. Kjer-Nielsen, Z. Chen, J. Rossjohn, and J. McCluskey, "The structural bases of direct T-cell allorecognition: implications for T-cell-mediated transplant rejection," *Immunology and Cell Biology*, vol. 89, no. 3, pp. 388–395, 2011.

[23] I. Pérez-Flores, A. Sánchez-Fructuoso, J. L. Santiago et al., "Intracellular ATP levels in CD4$^+$ lymphocytes are a risk marker of rejection and infection in renal graft recipients," *Transplantation Proceedings*, vol. 41, no. 6, pp. 2106–2108, 2009.

[24] R. J. McKallip, Y. Do, M. T. Fisher, J. L. Robertson, P. S. Nagarkatti, and M. Nagarkatti, "Role of CD44 in activation-induced cell death: CD44-deficient mice exhibit enhanced T cell response to conventional and superantigens," *International Immunology*, vol. 14, no. 9, pp. 1015–1026, 2002.

[25] B. K. Choi, J. S. Bae, E. M. Choi et al., "4-1BB-dependent inhibition of immunosuppression by activated $CD4^+$, $CD25^+$ T cells," *Journal of Leukocyte Biology*, vol. 75, no. 5, pp. 785–791, 2004.

[26] K. Xu, C. Li, X. Pan, and B. Du, "Study of relieving graft-versus-host disease by blocking CD137-CD137 ligand costimulatory pathway in vitro," *International Journal of Hematology*, vol. 86, no. 1, pp. 84–90, 2007.

[27] J. Kim, W. S. Choi, S. La et al., "Stimulation with 4-1BB (CD137) inhibits chronic graft-versus-host disease by inducing activation-induced cell death of donor $CD4^+$ T cells," *Blood*, vol. 105, no. 5, pp. 2206–2213, 2005.

[28] S. Ganguly, J. Liu, V. B. Pillai, R. S. Mittler, and R. R. Amara, "Adjuvantive effects of anti-4-1BB agonist Ab and 4-1BBL DNA for a HIV-1 Gag DNA vaccine: different effects on cellular and humoral immunity," *Vaccine*, vol. 28, no. 5, pp. 1300–1309, 2010.

[29] V. A. Meliopoulos, L. E. Andersen, K. F. Birrer et al., "Host gene targets for novel influenza therapies elucidated by high-throughput RNA interference screens," *The FASEB Journal*, vol. 26, no. 4, pp. 1372–1386, 2012.

[30] T. H. Hutson, E. Foster, J. M. Dawes, R. Hindges, R. J. Yáñez-Muñoz, and L. D. Moon, "Lentiviral vectors encoding short hairpin RNAs efficiently transduce and knockdown LINGO-1 but induce an interferon response and cytotoxicity in central nervous system neurones," *Journal of Gene Medicine*, vol. 14, no. 5, pp. 299–315, 2012.

[31] M. L. del Rio, J. Kurtz, C. Perez-Martinez, A. Ghosh, J. A. Perez-Simon, and J. I. Rodriguez-Barbosa, "B- and T-lymphocyte attenuator targeting protects against the acute phase of graft versus host reaction by inhibiting donor anti-host cytotoxicity," *Transplantation*, vol. 92, no. 10, pp. 1085–1093, 2011.

[32] G. Chen, J. Mi, M. Z. Xiao, and Y. R. Fu, "PDIA3 mRNA expression and IL-2, IL-4, IL-6, and CRP levels of acute kidney allograft rejection in rat," *Molecular Biology Reports*, vol. 39, no. 5, pp. 5233–35238, 2012.

[33] M. H. Karimi, S. Daneshmandi, A. A. Pourfathollah et al., "Association of IL-6 promoter and IFN-γ gene polymorphisms with acute rejection of liver transplantation," *Molecular Biology Reports*, vol. 38, no. 7, pp. 4437–4443, 2011.

[34] P. Kulkarni, M. S. Uppin, A. K. Prayaga, U. Das, and K. V. D. Murthy, "Renal allograft pathology with C4d immunostaining in patients with graft dysfunction," *Indian Journal of Nephrology*, vol. 21, no. 4, pp. 239–244, 2011.

[35] Y. Sanada, K. Mizuta, T. Urahashi et al., "Co-occurrence of nonanastomotic biliary stricture and acute cellular rejection in liver transplant," *Experimental and Clinical Transplantation*, vol. 10, no. 2, pp. 176–179, 2012.

[36] J. I. Wyatt, "Liver transplant pathology—messages for the non-specialist," *Histopathology*, vol. 57, no. 3, pp. 333–341, 2010.

Hindawi Publishing Corporation
BioMed Research International
Volume 2013, Article ID 269347, 5 pages
http://dx.doi.org/10.1155/2013/269347

Research Article

Characterization of Sera with Discordant Results from Reverse Sequence Screening for Syphilis

Kyunghoon Lee, Hyewon Park, Eun Youn Roh, Sue Shin, Kyoung Un Park, Myoung Hee Park, and Eun Young Song

Department of Laboratory Medicine, College of Medicine, Seoul National University, Seoul 110-744, Republic of Korea

Correspondence should be addressed to Eun Young Song; eysong1@snu.ac.kr

Received 16 October 2012; Revised 30 November 2012; Accepted 30 November 2012

Academic Editor: Antonio La Gioia

Reverse sequence screening for syphilis (RSSS) (screening with treponemal tests, followed by confirmation with nontreponemal tests) has been increasingly adopted. CDC recommends confirmation of discordant results (reactive EIA/CIA and nonreactive nontreponemal test) with *Treponema pallidum* particle agglutination assay (TP-PA). We characterized sera with discordant results from RSSS with Architect Syphilis TP CIA. Among 15,713 screening tests using Architect Syphilis TP at Seoul National University Gangnam Center between October 2010 and May 2011, 260 (1.7%) showed reactive results. Rapid plasma reagin (RPR) and TP-PA were performed on 153 available sera among them. On sera with discordant results between Architect Syphilis TP and TP-PA, INNO-LIA Syphilis Score and FTA-ABS were performed. Among 153 sera, RPR was nonreactive in 126 (82.4%). Among them, TP-PA was positive in 103 (81.7%), indeterminate (±) in 7 (5.6%), and negative in 16 (12.7%). Out of 16 CIA(+)/RPR(−)/TP-PA(−) sera, INNO-LIA Syphilis Score and/or FTA-ABS were negative on 14 sera. Out of 7 CIA(+)/RPR(−)/TP-PA(±) sera, INNO-LIA Syphilis Score and FTA-ABS were positive/reactive in 6 sera. RSSS with confirmation by TP-PA on sera with discordant results between Architect Syphilis TP and RPR effectively delineated those discordant results and could be successfully adopted for routine checkup for syphilis.

1. Introduction

Because *Treponema pallidum*, which causes syphilis, cannot be cultured *in vitro*, serologic tests are the most frequently used methods to diagnose syphilis on suspected persons. These serologic tests are traditionally classified as "nontreponemal" and "treponemal". Nontreponemal tests such as rapid plasma reagin (RPR) and venereal disease research laboratory (VDRL) detect antibodies directed against lipoidal antigens. Treponemal tests such as fluorescent treponemal antibody absorbed (FTA-ABS) test, *Treponema pallidum* particle agglutination assay (TP-PA), enzyme immunoassay (EIA), and chemiluminescence immunoassay (CIA) detect antibodies against individual or a mixture of specific *T. pallidum* proteins [1].

Whereas the traditional syphilis screening algorithm involves confirmation of reactive nontreponemal tests by treponemal tests in USA [2], it was recommended that a treponemal test should be used as a screening test followed by another type of treponemal test to confirm a reactive screening test in Europe [3, 4]. Recently, the Centers for Disease Control and Prevention (CDC) acknowledges the use of the reverse sequence screening for syphilis (RSSS) (treponemal tests for screening with confirmation of reactive results by nontreponemal tests) in addition to the traditional screening algorithm for syphilis [5, 6]. Specimens with reactive EIA/CIA results should be reflexively tested with a nontreponemal test (e.g., RPR or VDRL). If test results are discordant (reactive EIA/CIA, nonreactive RPR/VDRL), the specimen should be tested reflexively using the TP-PA test as a confirmatory treponemal test [6].

Although the TP-PA test was recommended as a most suitable second treponemal test for confirmation [6] considering its high sensitivity and specificity [7], the resolution and interpretation of those discordant sera (reactive EIA/CIA, nonreactive RPR/VDRL) are still challenging [8]. Some data

showed there may not be a statistically significant difference in the performance of TP-PA and other treponemal tests [9]. Fourteen out of 26 discordant sera in syphilis screening in UK (reactive screening EIA and negative TP-PA) showed either reactive FTA-ABS or INNO-LIA syphilis score [10]. The aim of our study was to evaluate the overall efficacy of RSSS with Architect syphilis TP (Abbott, Wiesbaden, Germany) as a screening test and also to evaluate the accuracy of TP-PA test as a confirmation test on the discordant sera of RSSS.

2. Materials and Methods

2.1. Tests for Syphilis Screening and Confirmation. A total of 15,713 syphilis screening tests were performed using Architect Syphilis TP (Abbott, Wiesbaden, Germany)—an automated chemiluminescence immunoassay (CIA) at the Seoul National University Hospital Healthcare System Gangnam Center between 1 October 2010 and 31 May 2011. Two-hundred-sixty sera (1.7%) showed reactive results. Among them, 153 sera with sufficient amount of residual sera for additional tests were included in our study. Those sera were tested by RPR (Beckton Dickinson, Sparks, MD, USA) and with TP-PA (Fujirebio Inc., Tokyo, Japan) as a confirmatory second treponemal test. For 26 sera with discordant results among Architect Syphilis TP and TP-PA, the INNO-LIA syphilis score (Innogenetics, Gent, Belgium) and FTA-ABS (Scimedx, Denville, NJ, USA) test were performed to evaluate the utility of TP-PA.

All the tests were performed and interpreted in accordance with the manufacturers' instructions delineated in the kit inserts. The Architect Syphilis TP is a chemiluminescent microparticle immunoassay for the quantitative detection of *T. pallidum*-specific antibodies using recombinant TP antigens such as TpN15, TpN17, and TpN47. RPR card antigen suspension is a carbon particle cardiolipin antigen which detects "reagin", an antibody-like substance present in serum or plasma. The TP-PA uses gelatin particle carriers sensitized with purified *T. pallidum* (Nichols strain). Definite large ring with a rough multiform outer margin and peripheral agglutination was interpreted as "positive", particles concentrated in the shape of a button in the center of the well as "negative", and particles concentrated in the shape of a compact ring with a smooth round outer margin as "indeterminate" according to the instruction of manufacturer.

The FTA-ABS detects circulating antibodies against the etiologic agent of syphilis, *T. pallidum*. The primary reaction involves antibodies which attach to antigens along the surface and internal structure of the microorganism. The INNO-LIA syphilis score is based on the enzyme immunoassay principle in which TpN47, TpN17, and TpN15 recombinant proteins and TmpA synthetic peptide are coated as discrete lines onto a nylon strip with plastic backing. Sera with more than 2 positive bands were interpreted as "positive" and sera with 1 positive band with a minimum intensity of 1 were interpreted as "indeterminate". This study was approved by the institutional review board of Seoul National University Hospital (H-1104-127-360).

Table 1: INNO-LIA syphilis score and FTA-ABS test results of 23 discordant sera between CIA and TP-PA results.

TP-PA	INNO-LIA syphilis score results (N)	FTA-ABS results (N)
RPR(−)/TP-PA(−) ($N = 16$)	Positive (1)	Reactive (1)
	Indeterminate (5)	Reactive (1) Non-reactive (4)
	Negative (10)	Non-reactive (10)
RPR(−)/TP-PA(±) ($N = 7$)	Positive (6)	Reactive (6)
	Indeterminate (1)	Non-reactive (1)
RPR(+)/TP-PA(−) ($N = 1$)	Negative (1)	Non-reactive (1)
RPR(+)/TP-PA(±) ($N = 2$)	Positive (2)	Reactive (2)

CIA: chemiluminescence immunoassay, RPR: rapid plasma regain, TP-PA: *Treponema pallidum* particle agglutination assay, FTA-ABS: fluorescent treponemal antibody absorbed, N: number, ±: indeterminate.

2.2. Statistical Analysis. Mann-Whitney U test was used to compare the S/CO value of Architect Syphilis TP according to the results of RPR, TP-PA, or INNO-LIA syphilis score assays. ROC curve analysis of S/CO value of Architect Syphilis TP compared to TP-PA results was performed. All analyses used SPSS 18.0 statistical software (SPSS Inc., Chicago, IL, USA). P values < 0.05 were considered significant.

3. Results

Among the 153 available sera with CIA screening reactive results, RPR was reactive in 27 (17.6%) and nonreactive in 126 (82.4%) sera. Among the 126 CIA(+)/RPR(−) sera, TP-PA was positive in 103 (81.7%), indeterminate in 7 (5.6%), and negative in 16 (12.7%) sera. Among the 27 CIA(+)/RPR(+) sera, TP-PA was positive in 24 (88.9%), indeterminate in 2 (7.4%), and negative in 1 (3.7%) sera (Figure 1).

On 16 CIA(+)/RPR(−)/TP-PA(−) sera, the INNO-LIA syphilis score was positive in 1, indeterminate in 5, and negative in 10 (Table 1). For the 1 serum with INNO-LIA syphilis score positive results, FTA-ABS result was also reactive. And for the 10 sera with INNO-LIA syphilis score negative results, FTA-ABS results were all nonreactive. For the rest indeterminate 5 sera, FTA-ABS was reactive in 1 and nonreactive in 4. On 7 CIA(+)/RPR(−)/TP-PA(indeterminate) sera, both INNO-LIA syphilis score and FTA-ABS were positive/reactive in 6 sera and negative/nonreactive in 1 serum. On 1 CIA(+)/RPR(+)/TP-PA(−) serum, both INNO-LIA syphilis score and FTA-ABS were negative/nonreactive. On 2 CIA(+)/RPR(+)/TP-PA(indeterminate) sera, both INNO-LIA syphilis score and FTA-ABS were positive/reactive (Table 1).

On 153 sera in our study, the signal to cut-off ratio (S/CO) value of Architect Syphilis TP in RPR reactive group ($N = 27$) was significantly higher than in RPR nonreactive group ($N = 126$) ($P < 0.001$) (Figure 2). On 126 discordant sera (Architect Syphilis TP reactive/RPR non-reactive), the S/CO value of TP-PA positive group ($N = 103$) was significantly higher than the S/CO value of TP-PA negative

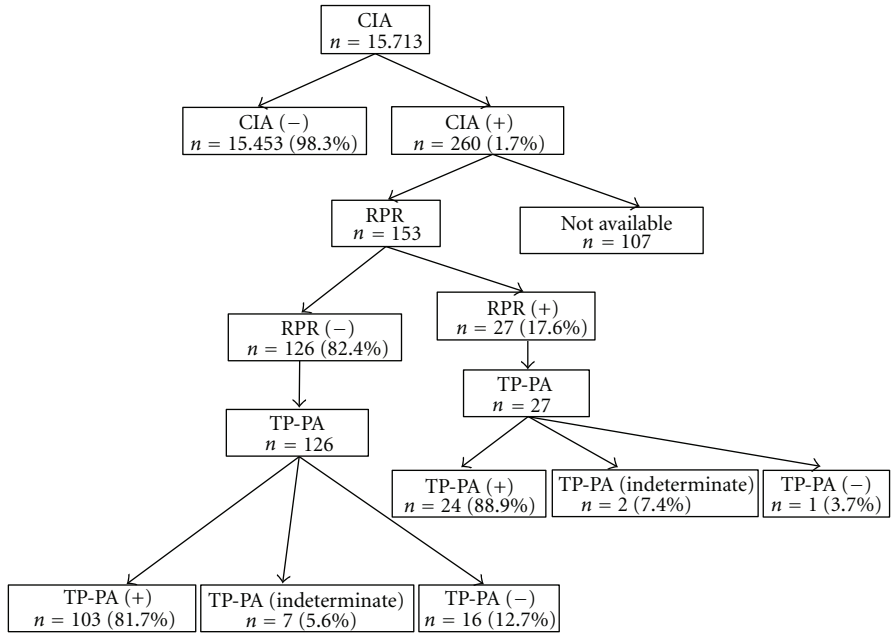

Figure 1: Results of reverse sequence screening algorithms for syphilis using chemiluminescence immunoassay (CIA) for initial screening, rapid plasma reagin (RPR) test, and *Treponema pallidum* particle agglutination assay (TP-PA) for confirmation.

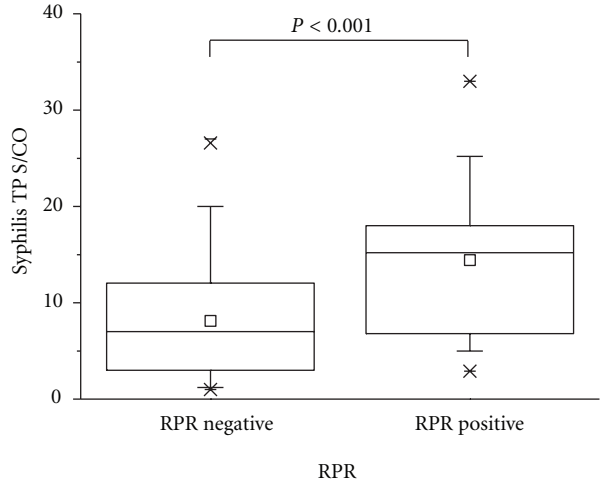

Figure 2: S/CO values of Architect Syphilis TP on 126 RPR(−) and 27 RPR(+) sera.

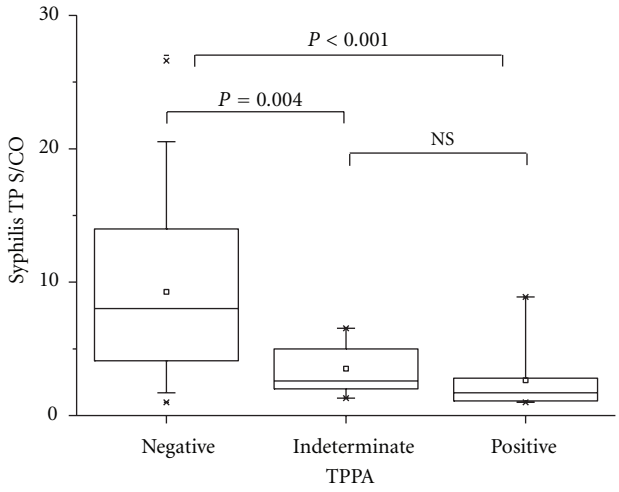

Figure 3: S/CO values of Architect Syphilis TP on 126 CIA(+)/RPR(−) sera according to TP-PA-positive ($N = 103$), indeterminate ($N = 7$), and negative ($N = 16$) results. NS: not significant.

group ($n = 16$) ($P < 0.001$) and the TP-PA indeterminate group ($N = 7$) ($P = 0.004$) (Figure 3). On 23 discordant sera between Architect Syphilis TP and RPR/TP-PA (Syphilis TP reactive/RPR nonreactive/TP-PA indeterminate or negative), the S/CO values of Syphilis TP in INNO-LIA syphilis score-positive ($N = 7$), indeterminate ($N = 6$), and negative ($N = 10$) was not statistically different (Figure 4).

For prediction of TP-PA results with S/CO value of Architect Syphilis TP, S/CO value of 3.1 showed good sensitivity (82.7%) and specificity (87.5%) with highest diagnostic efficacy (Figure 5). With the cut-off of S/CO 3.1, among 126 CIA(+)/RPR(−) sera, 32 sera would have been retested with TP-PA, and 2 sera would have been falsely reported as reactive. With the cut-off of S/CO 9.0, 82 sera would have been retested with TP-PA, and no sera would have been falsely reported as reactive. The area under the curve (95% CI) of S/CO value of Architect Syphilis TP was 0.872 (0.782–0.963).

4. Discussion

The efficiency of reverse sequence screening for syphilis (RSSS) could be dependent on the performance of screening treponemal test. Architect syphilis TP assay has been known

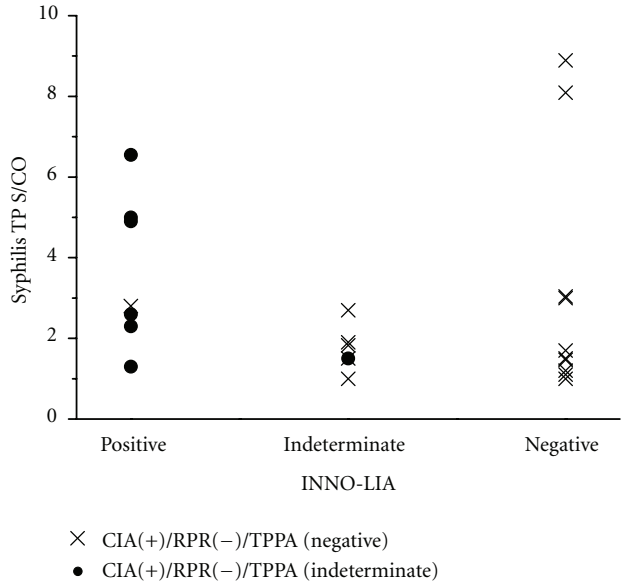

Figure 4: S/CO values of Architect Syphilis TP of 23 discordant sera between CIA and RPR/TP-PA according to the results of INNO-LIA syphilis score.

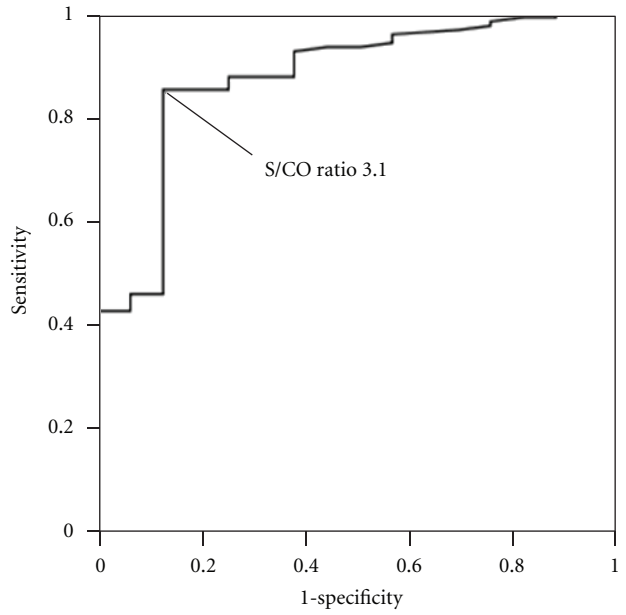

Figure 5: ROC curve of Architect Syphilis TP for prediction of TP-PA results on 126 CIA(+)/RPR(−) sera. The diagnostic sensitivity and specificity are 82.7% and 87.5% for an S/CO ratio of 3.1. The area under the curve (95% CI) is 0.872 (0.782–0.963).

to have an excellent sensitivity and specificity [11, 12]. In our study, from the RSSS using the Architect Syphilis TP CIA as a screening assay, the positive rate of CIA was 1.7% in our low-prevalence population, and the proportion of TP-PA-negative sera among 153 CIA-reactive sera was 10.5% (16/153). In USA, using two EIA assays (Trep-Chek, Trep-Sure EIA kit) and Liaison CIA assay as screening assays, the positive rate of CIA was 2.3% in low-prevalence population, and the proportion of TP-PA-negative sera among 2984 EIA/CIA-reactive sera was 24.7% (737/2984) [6]. Another study in Israel conducted on 12,235 low-prevalence population (4.0% positive rate of screening test) using Architect Syphilis TP as a screening test showed TP-PA-negative rate of 28.3% among 491 Architect Syphilis TP-reactive sera (139/491) [13]. TP-PA-negative rate was slightly lower in our study than in previous reports. It could be due to the difference of study population, prevalence of disease, or performance of screening assays detecting previously treated infection, but should be analyzed in further studies.

For the characterization of discordant sera between CIA and RPR, on 16 CIA(+)/RPR(−)/TP-PA(−) sera, 14 sera was INNO-LIA syphilis score and/or FTA-ABS nonreactive. On 7 CIA(+)/RPR(−)/TP-PA indeterminate sera, 6 sera was INNO-LIA syphilis score and FTA-ABS positive/reactive. Generally, TP-PA showed good performance to delineate discordant sera between CIA and RPR, although, TP-PA-indeterminate results should be confirmed with other treponemal tests. It supports the role of TP-PA in RSSS algorithms suggested by CDC considering the high performance of TP-PA.

The increase of costs by RSSS has been reported recently [14]. To decrease the cost of confirmation test using TP-PA, we analyzed the S/CO value of Architect Syphilis TP correlates with the result of TP-PA. For HCV EIA/CIA, high S/CO value has been reported to be strongly associated with high positive predictive value [15, 16]. CDC recommended with high S/CO value, which shows 95% positive predictive value, there is no need for further confirmation test using RIBA or HCV-RNA test [17]. In our study, from the ROC analysis compared to TP-PA results, cut-off using S/CO of 3.1 on Architect Syphilis TP assay showed highest efficacy (sensitivity 82.7%, specificity 87.5%). With the cut-off of S/CO 3.1, among 126 CIA(+)/RPR(−) sera, 32 sera would have been retested with TP-PA, and 2 sera would have been falsely reported as reactive, which would have been most cost-effective.

5. Conclusions

RSSS with confirmation by TP-PA on sera with discordant results between Architect Syphilis TP and RPR effectively delineated those discordant results and could be successfully adopted for routine checkup for syphilis. S/CO value of 3.1 on Architect Syphilis TP cost-effectively discriminated those sera which need further confirmations with TP-PA assays.

Conflict of Interests

The authors declare that they have no conflict of interests.

References

[1] S. A. Larsen, B. M. Steiner, and A. H. Rudolph, "Laboratory diagnosis and interpretation of tests for syphilis," *Clinical Microbiology Reviews*, vol. 8, no. 1, pp. 1–21, 1995.

[2] K. A. Workowski and S. Berman, "Centers for Disease Control and Prevention. Sexually transmitted diseases treatment guidelines, 2010," *Morbidity and Mortality Weekly Report*, vol. 59, no. 12, pp. 1–113, 2010.

[3] P. French, M. Gomberg, M. Janier et al., "IUSTI: 2008 European guidelines on the management of Syphilis," *International Journal of Sexually Transmitted Disease and Acquired Immunodeficiency Syndrome*, vol. 20, no. 5, pp. 300–309, 2008.

[4] M. Kingston, P. French, B. Goh et al., "UK national guidelines on the management of Syphilis 2008," *International Journal of Sexually Transmitted Disease and Acquired Immunodeficiency Syndrome*, vol. 19, no. 11, pp. 729–740, 2008.

[5] T. Peterman, J. Schillinger, S. Blank et al., "Centers for Disease Control and Prevention. Syphilis testing algorithms using treponemal tests for initial screening -four laboratories, New York City, 2005-2006," *Morbidity and Mortality Weekly Report*, vol. 57, no. 32, pp. 872–875, 2008.

[6] Centers for Disease Control and Prevention, "Discordant results from reverse sequence Syphilis screening-five laboratories, United States, 2006–2010," *Morbidity and Mortality Weekly Reports*, vol. 60, no. 5, pp. 133–137, 2011.

[7] M. J. Cole, K. R. Perry, and J. V. Parry, "Comparative evaluation of 15 serological assays for the detection of syphilis infection," *European Journal of Clinical Microbiology and Infectious Diseases*, vol. 26, no. 10, pp. 705–713, 2007.

[8] M. J. Binnicker, "Which algorithm should be used to screen for syphilis?" *Current Opinion in Infectious Disease*, vol. 25, no. 1, pp. 79–85, 2012.

[9] M. J. Binnicker, D. J. Jespersen, and L. O. Rollins, "Treponema-specific tests for serodiagnosis of syphilis: comparative evaluation of seven assays," *Journal of Clinical Microbiology*, vol. 49, no. 4, pp. 1313–1317, 2011.

[10] P. A. C. Maple, D. Ratcliffe, and E. Smit, "Characterization of *Treponema pallidum* particle agglutination assay-negative sera following screening by treponemal total antibody enzyme immunoassays," *Clinical and Vaccine Immunology*, vol. 17, no. 11, pp. 1718–1722, 2010.

[11] H. Young, J. Pryde, L. Duncan, and J. Dave, "The Architect Syphilis assay for antibodies to Treponema pallidum: an automated screening assay with high sensitivity in primary syphilis," *Sexually Transmitted Infections*, vol. 85, no. 1, pp. 19–23, 2009.

[12] J. Kim, W. H. Kim, C. Cho et al., "Evaluation of automated Architect Syphilis TP as a Diagnostic Laboratory Screening Test for Syphilis," *Korean Journal of Laboratory Medicine*, vol. 28, no. 6, pp. 475–482, 2008.

[13] D. Lipinsky, L. Schreiber, V. Kopel et al., "Validation of reverse sequence screening for syphilis," *Journal of Clinical Microbiology*, vol. 50, no. 4, p. 1501, 2012.

[14] K. Owusu-Edusei Jr., T. A. Peterman, and R. C. Ballard, "Serologic testing for syphilis in the United States: a cost-effectiveness analysis of two screening algorithms," *Sexually Transmitted Diseases*, vol. 38, no. 1, pp. 1–7, 2011.

[15] A. M. Contreras, C. M. Tornero-Romo, J. G. Toribio et al., "Very low hepatitis C antibody levels predict false-positive results and avoid supplemental testing," *Transfusion*, vol. 48, no. 12, pp. 2540–2548, 2008.

[16] K. K. Y. Lai, M. Jin, S. Yuan, M. F. Larson, J. A. Dominitz, and D. D. Bankson, "Improved reflexive testing algorithm for hepatitis C infection using signal-to-cutoff ratios of a hepatitis C virus antibody assay," *Clinical Chemistry*, vol. 57, no. 7, pp. 1050–1056, 2011.

[17] M. J. Alter, W. L. Kuhnert, and L. Finelli, "Centers for Disease Control and Prevention. Guidelines for laboratory testing and result reporting of antibody to hepatitis C virus," *Morbidity and Mortality Weekly Reports*, vol. 52, no. 3, pp. 1–16, 2003.

Hindawi Publishing Corporation
BioMed Research International
Volume 2013, Article ID 241763, 10 pages
http://dx.doi.org/10.1155/2013/241763

Research Article

MDR Gene Expression Analysis of Six Drug-Resistant Ovarian Cancer Cell Lines

Radosław Januchowski,[1] Karolina Wojtowicz,[1] Patrycja Sujka-Kordowska,[1] Małgorzata Andrzejewska,[1] and Maciej Zabel[1,2]

[1] *Department of Histology and Embryology, Poznań University of Medical Sciences, 61-781 Poznań, Poland*
[2] *Department of Histology and Embryology, Wrocław Medical University, 50-368 Wrocław, Poland*

Correspondence should be addressed to Radosław Januchowski; rjanuchowski@wp.pl

Received 18 September 2012; Accepted 21 November 2012

Academic Editor: Antonio La Gioia

Ovarian cancer is the leading cause of death among gynaecological malignancies. Multiple drug resistance makes cancer cells insensitive to chemotherapy. In this study, we developed six primary ovarian cancer cell lines (W1MR, W1CR, W1DR, W1VR, W1TR, and W1PR) resistant to drugs such as methotrexate, cisplatin, doxorubicin, vincristine, topotecan, and paclitaxel. A chemosensitivity assay MTT test was performed to assess drug cross-resistance. Quantitative real-time polymerase chain reaction and Western blot were also performed to determine mRNA and protein expression of genes involved in chemoresistance. We observed high cross-resistance to doxorubicin, vincristine, and paclitaxel in the cell lines resistant to these agents. We also found a significant correlation between resistance to these drugs and increased expression of P-gp. Two different mechanisms of topotecan resistance were observed in the W1TR and W1PR cell lines. We did not observe any correlation between MRP2 transcript and protein levels. Cell lines resistant to agents used in ovarian cancer treatment remained sensitive to methotrexate. The main mechanisms of drug resistance were due to P-gp expression in the doxorubicin, vincristine, and paclitaxel resistant cell lines and BCRP expression in the topotecan resistant cell line.

1. Introduction

Ovarian cancer represents the most common cause of death among gynaecological malignancies in Europe and North America. The average 5-year survival rate is approximately 40%; however, patients with advanced disease (stages III and IV) have a significantly lower survival rate of only 10%–20% [1]. A high percentage of mortality results from low diagnosis. Most ovarian cancers are diagnosed when the disease has progressed to the advanced stages III or IV, according to the FIGO classification.

Regardless of the stage of the disease, the first line of treatment includes a combined chemotherapeutic regimen of platinum and taxane [2]. Unfortunately, approximately 80% of patients with advanced ovarian cancer who respond well after obtaining the first line of treatment will still have a recurrence and will require continuation of treatment. The second line of chemotherapy usually includes taxane derivatives as well as cisplatin, topotecan, doxorubicin, and gemcitabine [3–7]. The 15%–35% of patients' response to most drugs introduced as a second-line of chemotherapeutic regimen.

Drug resistance is the main cause of ineffective chemotherapy in patients. Several data have been published regarding various cellular mechanisms of drug resistance [8–10]. The most significant and prevalent mechanism of drug resistance is provided by the ability of cancer cells to actively expel the therapeutic agents from the cell via transport proteins. This form of drug resistance is called multiple drug resistance (MDR). MDR development occurs when cancer cells become insensitive to not only the primary cytostatic drug used but also to other pharmaceutical agents that bear no chemical similarities to the structure of cytostatic drugs. Many types of cancers show significant primary resistance to cytostatics, while others acquire characteristics of MDR during chemotherapy. The development of MDR leads to the

ineffectiveness of the agent, thereby preventing its further use for treatment [11]. The proteins most implicated in this process belong to the ABC family. These transmembrane proteins use the energy from the hydrolysis of ATP to actively remove drugs from the cell [12]. The critical ABC protein glycoprotein P (P-gp) is encoded by the ABCB1 (multidrug resistance protein 1-MDR1) gene [12, 13]. As expected, P-gp expression is the highest in tumours derived from tissues that normally express P-gp. However, in many other tumours, the expression of P-gp is induced by chemotherapy. This protein is able to actively remove approximately 20 cytostatic drugs from the cell, including [11] paclitaxel [14], doxorubicin [15], and vincristine [16].

Another gene responsible for MDR is MRP1 (MDR-related protein 1; ABCC1). This gene was first described in the non-P-gp MDR small-cell lung carcinoma cell line [12, 17]. MRP1 and P-gp have great similarities in both structure and drug resistance, with the exception of taxanes, which are poor substrates for MRP1. The second member of the multidrug resistance protein (MRP; ABCC) family, MRP2, which is also designed as the canalicular multiorganic anion transporter (CMOAT), is involved in bilirubin glucuronide transport and confers resistance to MRP1 substrates and cisplatin [18]. The role of this protein in the resistance of ovarian cancer to cisplatin has been described in several studies [19, 20]. Another important MDR protein, breast cancer resistance protein BCRP (ABCG2), was cloned from a mitoxantrone-resistant subline of the breast cancer cell line MCF-7 [21]. BCRP lends resistance to many cytostatics, including mitoxantrone and topotecan [12, 22]. Its role in the resistance of ovarian cancer to topotecan is well described [23]. LRP/MVP lung resistance-related protein/major vault protein is an example of a protein involved in MDR that does not belong to the ABC family [24]. It has been reported that LRP expression is correlated with *in vitro* resistance to anticancer drugs such as etoposide, doxorubicin, paclitaxel, and cisplatin [25, 26]. LRP overexpression predicts a poor response to chemotherapy in acute myeloid leukaemia and ovarian carcinoma [12].

The current knowledge on the development of drug resistance is based largely on research on drug sensitive/resistant cell lines. During the last few decades, many such cell lines were developed [27, 28]. However, the research was usually limited to 1 or 2 cell resistant lines. In this study, we developed six drug-resistant cell lines from one parental ovarian cancer cell line. We used drugs commonly used for first-line ovarian cancer treatment (paclitaxel and cisplatin), drugs used for the second line of chemotherapeutic treatment (topotecan and doxorubicin), and drugs that are generally not standard for the treatment of ovarian cancer (methotrexate and vincristine). The objective of our research was to compare the development of drug resistance to cytostatics from the first and the second lines of chemotherapy treatment because they have different mechanisms of action. Additionally, the goal of our study was to compare the cross-resistance between cell lines developed in the presence of these drugs, examine the expression of five genes responsible for the development of MDR, and determine a correlation between the establishments of drug resistance to any treatment with the expression of MDR genes.

2. Materials and Methods

2.1. Reagents and Antibodies. Methotrexate, cisplatin, doxorubicin, vincristine, topotecan, and paclitaxel were obtained from Sigma (St. Louis, MO). RPMI-1640 medium, foetal bovine serum, antibiotic-antimycotic solution, and L-glutamine were also purchased from Sigma (St. Louis, MO). A Cell Proliferation Kit I (MTT) was purchased from Roche Diagnostics GmbH (Mannheim, Germany). Mouse anti-MRP1 monoclonal antibody (Ab) (IU2H10), goat anti-MRP2 polyclonal (Ab) (H-17), rabbit anti-ABCG2 polyclonal Ab (H-70), rabbit anti-GADPH polyclonal Ab (FL-335), donkey anti-goat horseradish peroxidase (HRP)-conjugated Ab, goat anti-mouse HRP-conjugated Ab, and goat anti-rabbit HRP-conjugated Ab were purchased from Santa Cruz Biotechnology (Santa Cruz, CA). Mouse monoclonal anti-P-glycoprotein Ab (C219) and mouse monoclonal anti-MVP/LRP Ab (MVP 37) were obtained from Alexis Biochemicals (Lörrach, Germany).

2.2. Cell Lines and Cell Culture. The primary human ovarian cancer cell line W1 was established in our department (December 2009) from tissue obtained from an untreated patient diagnosed with ovarian cancer. Sublines resistant to methotrexate (W1MR; W1 methotrexate resistant), cisplatin (W1CR; W1 cisplatin resistant), doxorubicin (W1DR; W1 doxorubicin resistant), vincristine (W1VR; W1 vincristine resistant), topotecan (W1TR; W1 topotecan resistant), and paclitaxel (W1PR; W1 paclitaxel resistant) were generated by exposure of the W1 line to incremental increasing concentrations of each drug. The cells were seeding in the concentration of 10 thousand cells/cm^2 in 25 cm^2 flask. Media were supplemented with relevant drug. Initial drugs exposure were at a concentration of MTX 2 ng/mL, CIS 20 ng/mL, Dox 10 ng/mL, Vin 0,5 ng/mL, TOP 0,5 ng/mL, and PAC 1 ng/mL with the cell line exposed three times for 3-day periods during a 3–6-week period allowing for growth recovery between cycles. After the completion of three cycles of drug, the dose was doubled, and the procedure was repeated until the final drug levels were achieved. The final concentration of each drug was MTX 28 ng/mL, CIS 1000 ng/mL, DOX 100 ng/mL, WIN 10 ng/mL, TOP 24 ng/mL, and PAC 1100 ng/mL according to Dietel et al. (1993) [29]. These consternations were twofold greater than the concentration in the plasma 2 hours after intravenous administration [29]. All cell lines were maintained as a monolayer in complete medium [RPMI 1640 medium supplemented with 10% (v/v) foetal bovine serum, 2 pM L-glutamine, penicillin (100 units/mL), streptomycin (100 units/mL) and amphotericin B (25 μg/mL)] at 37°C in a 5% CO_2 atmosphere.

2.3. Drug Sensitivity Assay. The drug sensitivity of the W1 cell line and the drug resistant cell lines were confirmed by the MTT cell survival assay. Briefly, all cell lines were seeded at a density of 5,000 cells/well in 96-well plates. The cells were allowed to grow for 48 hours and subsequently

Table 1: Oligonucleotide sequences used for Q-PCR analysis.

Transcript	Sequence (5′-3′ direction)	ENST number (http://www.ensembl.org/)	Product size (bp)
ABCB1	TGACAGCTACAGCACGGAAG TCTTCACCTCCAGGCTCAGT	00000265724	131 bp
ABCC1	GAGAGTTCCAAGGTGGATGC AGGGCCCAAAGGTCTTGTAT	00000399410	149 bp
ABCC2	TACCAATCCAAGCCTCTACC AGAATAGGGACAGGAACCAG	00000370449	104 bp
ABCG2	TTCGGCTTGCAACAACTATG TCCAGACACACCACGGATAA	00000237612	128 bp
LRP	TGAGGAGGTTCTGGATTTGG TGCACTGTTACCAGCCACTC	00000357402	135 bp
GADPH	GAAGGTGAAGGTCGGAGTCA GACAAGCTTCCCGTTCTCAG	00000229239	199 bp
β-actin	TCTGGCACCACACCTTCTAC GATAGCACAGCCTGGATAGC	00000331789	169 bp
HRPT1	CTGAGGATTTGGAAAGGGTG AATCCAGCAGGTCAGCAAAG	00000298556	156 bp
β2M	CGCTACTCTCTCTTTCTGGC ATGTCGGATGGATGAAACCC	00000558401	133 bp

treated with fresh medium supplemented with or without increasing concentrations of drugs and incubated for 72 h at 37°C. After 72 h of exposure, 10 μL of the MTT labelling reagent was added to the medium (the final concentration of MTT was 0.5 mg/mL), and the cells were incubated for an additional 4 h. Following this process, 100 μL of solubilisation solution was added to each well. The absorbance of each sample was measured in a microplate reader at 570 nm with a reference wavelength of 720 nm, according to the manufacturer's protocol. The negative control was conducted using cell-free culture medium containing both the MTT reagent and solubilisation solution. The experiments were repeated three times, and each concentration in a given experiment was tested in duplicates. Cell viability was expressed as a percentage of the untreated control (means ± SEM).

2.4. Examination of ABCB1 Gene Expression by Using Q-PCR. Changes in ABCB1, ABCC1, ABCC2, ABCG2 and LRP gene expression in the W1 and drug-resistant cell lines were examined. RNA was isolated using the Gene Matrix Universal RNA purification Kit (EURx Ltd.), as described by the manufacturer's protocol. Reverse transcription was performed using the M-MLV reverse transcriptase (Invitrogen) as described in the manufacturer's protocol using a thermal cycler (Veriti 96 well Thermal Cycler). 2 μg of RNA was used to cDNA synthesis. Real-time PCR was performed using the Eppendorf PCR System (Mastercycler realplex^4), Maxima SYBR Green/ROX qPCR Master Mix (Fermentas) and sequence-specific primers, as indicated in Table 1. Glyceraldehyde-3-phosphate dehydrogenase (GADPH), β-actin, hypoxanthine-guanine phosphoribosyltransferase 1 (HRPT1) and beta-2-microglobulin (β2M) served as the normalising genes (geometric mean) against which changes in the examined genes expression were compared. Gene expression was analysed using the relative quantification (RQ) method. RQ estimates the difference at the level of gene expression against a calibrator (W1 drug sensitive line) (RQ of the calibrator = 1). The W1 cell line was used as the calibrator. The analysis was conducted employing the standard formula: $RQ = 2^{-\Delta\Delta Ct}$ (where $\Delta\Delta Ct = \Delta Ct$ for the sample (drug-resistant line) $-\Delta Ct$ for the calibrator (drug sensitive line)). The graphs were made using Sigma Plot.

For amplification, 12,5 μL of Maxima SYBR Green/ROX qPCR Master Mix (Fermentas), 1 μL of each primer (Oligo, Warsaw, Poland) (Table 1), 9,5 μL of water, and 1 μL of cDNA solution were mixed together. One RNA sample of each preparation was processed without RT-reaction to provide a negative control in subsequent PCR. Sample amplification included a hot start (95°C, 15 minutes) followed by 50 cycles of denaturation at 95°C for 15 seconds, annealing at 60°C for 30 seconds, and extension at 72°C for 30 seconds. After amplification, Melt Curve analysis was performed to analyze product melting temperature. The amplification products were also resolved by 3% agarose gel electrophoresis and visualized by ethidium bromide staining.

2.5. SDS-PAGE and Western Blot Analysis of P-gp, MRP1, MRP2, BCRP, LRP. Cells (1×10^6 cells/50 μL lysis buffer) were lysed in buffer containing 20 mM Tris-HCl (pH 7.5), 100 mM NaCl, 5 mM EDTA, Protein Inhibitor Cocktail (ROCHE) and 1% Triton X-100 for 60 min at 4°C. The lysates were centrifuged at 12000 ×g for 15 min at 4°C, and protein concentration was determined using the Bio-Rad (Hercules, CA) protein assay system. Thirty micrograms of the protein was resuspended in a solution of 40 μL of 200 mM Tris-HCl (pH 6.8), 5% SDS, 10% glycerol, 0.25% 2-mercaptoethanol, and 0.1% bromophenol blue. The resuspended protein was loaded into each well and separated on a 7% Tris-glycine

Table 2: Summary of cell line cross-resistance to drug treatment.

Cell line	IC50 (ng/mL)					
	Methotrexate	Cisplatin	Doxorubicin	Vincristine	Topotecan	Paclitaxel
W1	7.02 (5.85–8.58) 1	253 (231–270) 1	20.8 (20.5–21.1) 1	1.85 (1.82–1.87) 1	4.19 (3.55–4.95) 1	3.54 (3.47–3.65) 1
W1MR	970 (858–1086) 138↑***	168 (161–174) 0.66↓**	17.0 (12.4–21.5) 0.82	1.53 (1.42–1.60) 0.83↓**	2.72 (2.55–2.81) 0.65↓*	3.19 (2.77–3.73) 0.90
W1CR	9.00 (6.80–8.12) 1.28	1991 (1630–2470) 7.87↑***	23.3 (20.5–24.5) 1.12	2.57 (1.66–3.53) 1.39	5.66 (5.07–6.55) 1.35	4.43 (3.43–5.55) 1.25
W1DR	6.00 (5.90–6.60) 0.85	258 (213–337) 1.02	215 (165–248) 10.3↑***	106 (30.5–131) 57.3 ↑**	6.4 (5.67–7.44) 1.52↑*	109 (76.6–152) 30.8↑***
W1VR	7.53 (6.10–9.70) 1.07	320 (243–422) 1.26	132 (92–167) 6.35↑***	45.3 (24.4–65.6) 24.5 ↑***	6.35 (4.69–7.74) 1.52	64.8 (44.6–85.6) 18.3↑***
W1TR	39 (22–67) 5.55↑*	374 (285–451) 1.48	30.9 (21.6–33.9) 1.49	2.34 (1.68–3.10) 1.26	83.9 (70.9–98) 20.0↑***	4.24 (3.92–4.86) 1.20
W1PR	7.53 (5.9–8.4) 1.07	383 (366–413) 1.51↑**	4241 (3136–5624) 204↑***	1155 (548–2100) 624↑***	80.2 (72.5–92.8) 19.1↑***	2268 (1868–2788) 641↑***

IC50 mean is indicated for each drug. The drug resistance in W1 cell line was assigned as 1. Underlined values indicate multiplicities of resistance with respect to W1 cell line. $^{*}P < 0.05$; $^{**}P < 0.01$; $^{***}P < 0.001$.

gel using the SDS-PAGE technique. The proteins were transferred to a PVDF membrane and blocked with 5% milk in TBS/Tween (0.1 M Tris-HCl, 0.15 M NaCl, 0.1% Tween 20), followed by immunodetection with either mouse anti-P-gp Ab (C219) at 1 : 500 dilution, mouse anti-MRP1 Ab (IU2H10) at 1 : 500 dilution, goat anti-MRP2 Ab (H-17) at 1 : 500 dilution, rabbit anti-ABCG2 Ab (H-70) at 1 : 500 dilution, or mouse anti-MVP/LRP (MVP37) Ab at 1 : 500 dilution with the appropriate HRP-conjugated secondary Ab. Chemiluminescence detection of the bands was performed using the enhanced chemical luminescence (ECL) kit and Hyperfilm ECL from Amersham (Piscataway, NJ). The Western blot was quantified by densitometry analysis of the band intensity in the autoradiogram using the GelDoc-It Imaging System and the Vision WorkLS software. To normalise protein loading of the lanes, the membranes were stripped and reblotted with rabbit anti-GADPH Ab (FL-335) at 1 : 500 dilution, donkey anti-goat HRP-conjugated Ab, and goat anti-rabbit HRP-conjugated Ab.

3. Results

3.1. Characteristics of W1 and W1 Sublines. The W1MR, W1CR, W1DR, W1VR, W1TR, and W1PR drug-resistant variant sublines of the W1 human ovarian cancer line were all established by the stepwise selection of W1 cells cultured in growth media with increasing drug concentrations. To determine the sensitivity of the W1 and drug-resistant W1 sublines to methotrexate, cisplatin, doxorubicin, vincristine, topotecan, and paclitaxel, cells were treated with different concentrations of each drug for 72 h. The dose-dependent effect of methotrexate on W1 and the drugs-resistant cell lines were observed (Figure 1(a) and Table 2). The W1, W1CR, W1DR, W1VR, and W1PR cell lines were all sensitive to methotrexate treatment. At this concentration (14 ng/mL), the W1MR cell line was not sensitive, while the W1TR cell line displayed partial resistance to methotrexate treatment.

The response of cell lines to cisplatin treatment was also observed (Figure 1(b)). Compared to the other lines, the W1CR cell line was more resistant to cisplatin. The IC50 analysis (Table 2) showed statistically significant changes in W1PR and W1MR cell lines, where an increase and decrease of resistance, respectively, were conferred relative to the W1 cell line.

The effect of doxorubicin, vincristine, and paclitaxel on the cell lines was investigated (Figures 1(c), 1(d), and 1(f)). We observed a high cross-resistance between the W1DR, W1VR, and W1PR cell lines to doxorubicin, vincristine, and paclitaxel drugs. The W1DR and W1VR cell lines shared similar levels of resistance to doxorubicin, vincristine, and paclitaxel. In contrast, the W1PR cell line appeared more resistant to doxorubicin and vincristine than the actual lines developed in the presence of doxorubicin and vincristine (Table 2).

The cell lines W1TR and W1PR were resistant to topotecan and shared a similar dose-dependent response profile

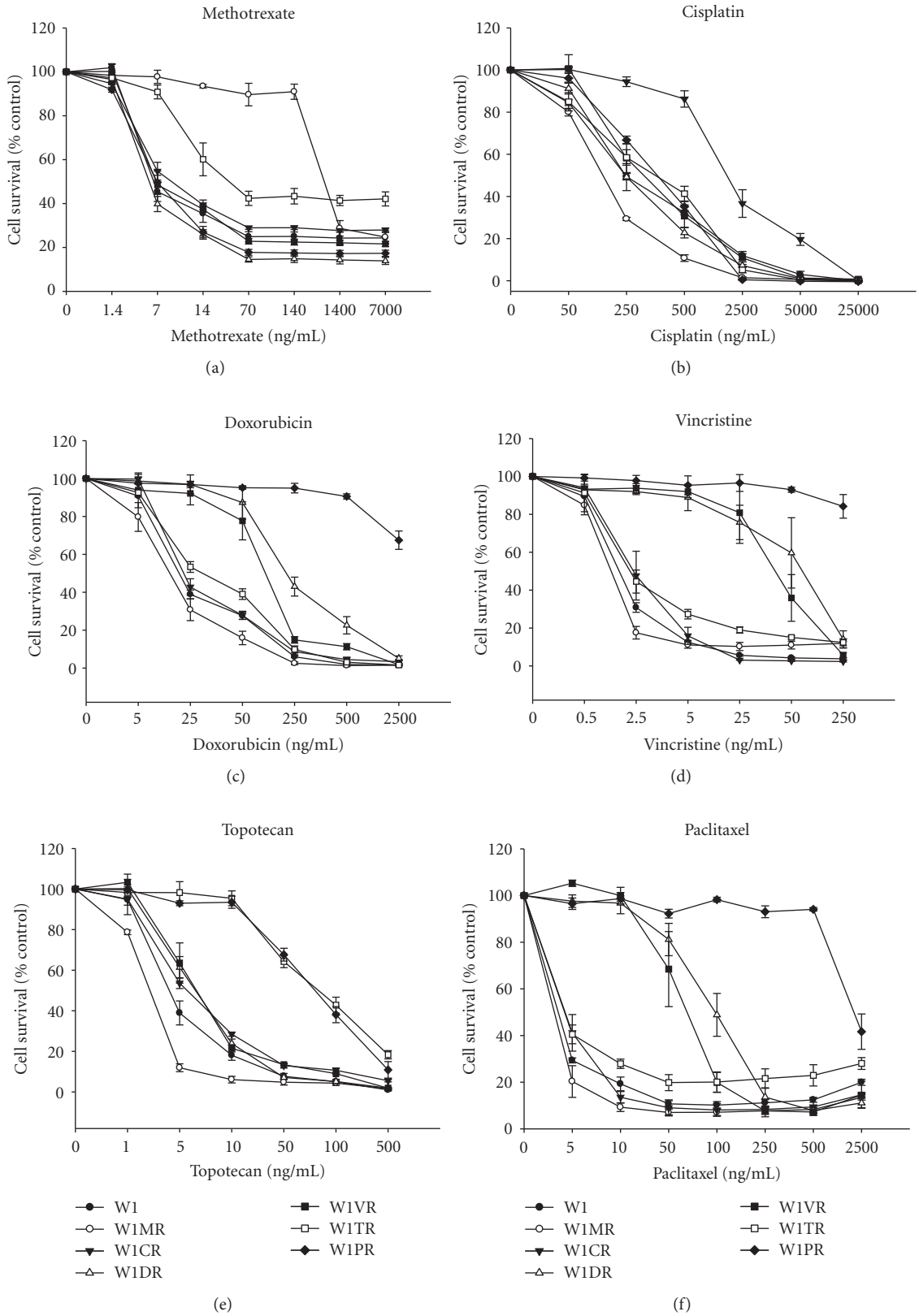

Figure 1: MTT cell survival assay. W1, W1MR, W1CR, W1DR, W1VR, W1TR, and W1PR cells were seeded at density of 5000 cells/well in 96-well plates and treated with or without increasing concentration of methotrexate (a), cisplatin (b), doxorubicin (c), vincristine (d), topotecan (e), and paclitaxel (f), at 37°C for 72 h, and viability of cells was determined. The experiments were repeated three times, and each concentration was tested in triplicate in each experiment. Viability was expressed as a percent on an untreated control (mean ± SEM).

Table 3: Correlation between transcript level and IC50 for cytostatic drugs (Pearson correlation—R^2).

Gene	Cytostatic drug					
	Methotrexate	Cisplatin	Doxorubicin	Vincristine	Topotecan	Paclitaxel
MDR1	0.06	0.03	0.96***	0.97***	0.3	0.96***
MRP2	0.99***	0.06	0.05	0.05	0.09	0.05
BCRP	0.02	0.01	0.03	0.04	0.44	0.03

Values were considered significant at *** $P < 0.001$.

Table 4: Correlation between protein levels and IC50 for cytostatic drugs (Pearson correlation—R^2).

Gene	Cytostatic drug					
	Methotrexate	Cisplatin	Doxorubicin	Vincristine	Topotecan	Paclitaxel
MDR1	0.0549	0.0278	0.9483***	0.9658***	0.3067	0.9486***
MRP2	0.088	0.1529	0.225	0.2388	0.4828	0.254
BCRP	0.0276	0.0019	0.0432	0.0499	0.4059	0.0442

*** $P < 0.001$.

(Figure 1(e)). Other cell lines were also topotecan sensitive, but the W1MR cell line exhibited the greatest sensitivity (Table 2).

3.2. Gene Expression Analysis in Drug-Resistant Ovarian Cancer Cell Lines. To determine whether the development of drug-resistance in the variant sublines of the W1 parental line is associated with increased expression of genes involved in MDR, expression of the following mRNA levels was assessed: MDR1, MRP1, MRP2, BCRP, and LRP. We did not observe statistically significant changes in the MRP1 or LRP transcript levels between the cell lines (Figures 2(b) and 2(e)).

The transcript level of MDR1 significantly increased in the doxorubicin, vincristine, and paclitaxel (W1DR, W1VR and W1PR) resistant cell lines ($P < 0.001$). In contrast, the MDR1 transcript level significantly decreased in the methotrexate-resistant cell line (Figure 2(a)) ($P < 0.01$).

The MRP2 transcript level was significantly higher in the methotrexate-resistant cell line ($P < 0.001$) and significantly lower in the paclitaxel-resistant cell line ($P < 0.01$) (Figure 2(c)).

BCRP expression increased in the vincristine ($P < 0.01$) and topotecan ($P < 0.001$) resistant cell lines. However, expression of BCRP was variable in these two cell lines. We observed approximately sixfold higher transcript levels in the W1VR cells, and expression in the W1TR cells increased by a factor of more than 1,000. In contrast, the expression of BCRP in the W1PR cells significantly decreased ($P < 0.01$) (Figure 1(d)).

3.3. Western Blot Analysis. Western blot analysis (Figure 3) of the P-gp and BCRP proteins validated the transcript expression results. We observed increased expression of P-gp protein in the cell line resistant to paclitaxel, pronounced expression in the cell lines resistant to doxorubicin and some expression in the cell line resistant to vincristine; we observed a very high correlation between transcript and protein levels. We observed an increased expression of the BCRP protein in the topotecan resistant cells. In contrast, the protein levels of MRP2 did not correlate with its transcript levels. We found increased MRP2 expression in the W1MR cell line; however, the expression was higher in the W1CR and W1DR cell lines. Expression of MRP2 in the W1VR and W1TR cell lines was lower than in control, while it was barely detectable in the W1PR line. Expression of MRP1 in W1CR, W1DR, and W1TR was lower than that in control. We observed very stable level of LRP protein in all investigated cell lines.

3.4. Correlation between Chemosensitivity and Gene Expression in the Cell Lines. To assess whether expression of MDR genes was correlated with resistance to a specific drug treatment, correlation analyses of MDR1, MRP2, and BCRP with IC50 levels for methotrexate, cisplatin, doxorubicin, vincristine, topotecan, and paclitaxel were performed. We observed a high degree of correlation between the MDR1 transcript and protein and resistance to doxorubicin, vincristine and paclitaxel (Tables 3 and 4). Similarly, a high correlation was observed between resistance to methotrexate and MRP2 transcript level (Table 3). However, we did not find any correlation between the MRP2 protein level and IC50 for any of the drugs in our study (Table 4). In spite of the high transcript and protein levels of BCRP in the W1TR cell line, we did not observe a correlation between BCRP expression and resistance to topotecan treatment (Tables 3 and 4).

4. Discussion

In our study, we compared development of multiple drug resistance to the parental W1 ovarian cancer cell line in response to cytostatic agents used in ovarian cancer chemotherapy, all of which have different mechanisms of action. The drug cross-reactivity study showed that the parental W1 cell line was sensitive to all investigated drugs with IC50 below their therapeutic concentration [29]. Comparisons between our drug-resistant cell lines, which were

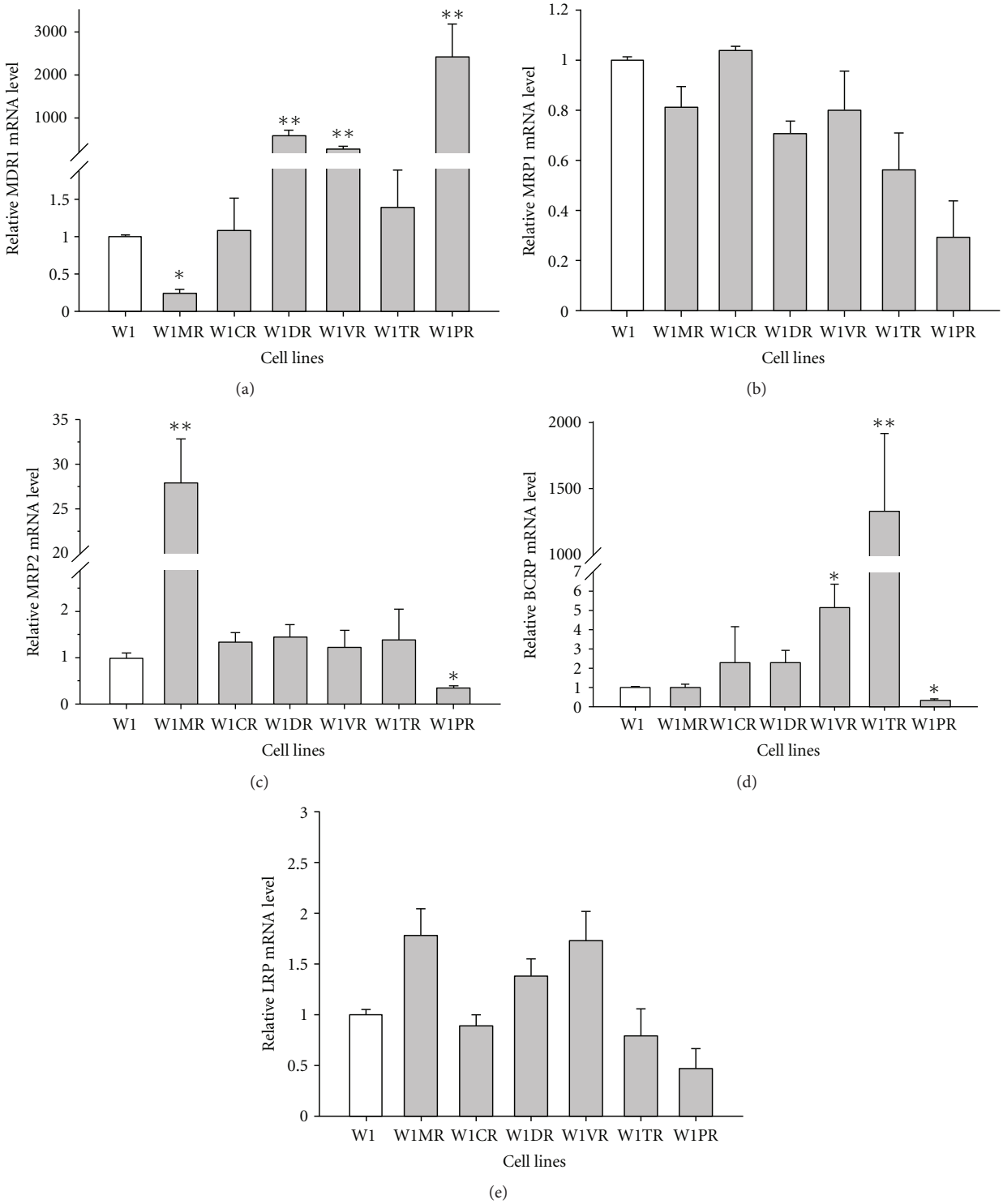

Figure 2: Expression analysis (Q-PCR) of MDR1 (a), MRP1 (b), MRP2 (c), BCRP (d), and LRP (e) genes. The figure presents relative gene expression in resistant cell lines (grey bars) with respect to the W1 cell line (white bars) assigned as 1. Values were considered significant at $^{*}P < 0.01$ and $^{**}P < 0.001$.

generated from drugs that are commonly used as chemotherapy to treat ovarian cancer, revealed that only the W1TR cell line showed partial cross-resistance to methotrexate. The remaining cell lines were methotrexate sensitive. Importantly, because our results showed that cell lines resistant to drugs used in the first and the second line of ovarian cancer treatment remained sensitive to methotrexate, it can be considered a suitable alternative agent for the treatment of

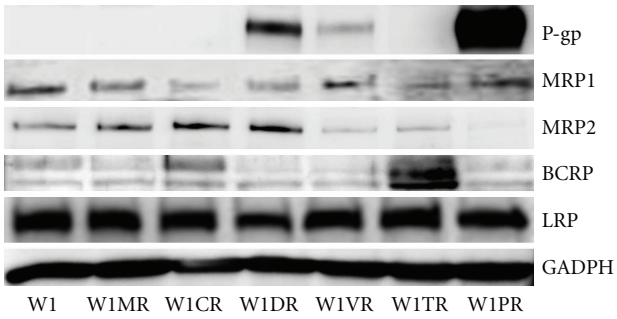

Figure 3: P-gp, MRP1, MRP2, BCRP, and LRP protein expression in W1 and drug-resistant cell lines. The cellular proteins were separated using 7% page and transferred to PVDF, and the membrane was immunoblotted with either primary Ab or HRP-conjugated secondary Ab.

ovarian cancer. Of course these results should be confirmed on established ovarian cancer cell lines.

The drug most commonly prescribed in ovarian cancer treatment is cisplatin [30]. In our results, we did not observe any cross-resistance between the W1CR line and other cell lines resistant to cisplatin. The lack of cross-resistance between cisplatin and other drugs used in ovarian cancer chemotherapy validates the use of cisplatin as a first-line chemotherapeutic agent.

A similar pattern of cross-resistance to doxorubicin, vincristine, and paclitaxel has been observed in the investigated cell lines. The cell lines studied here can be divided in two groups: sensitive to the tested drugs (W1, W1MR, W1CR, and W1TR) and those resistant to the drugs (W1DR, W1VR, and W1PR). These results may have been expected because cross-resistance between cell lines resistant to these drugs has frequently been documented in the literature [31–33]. Furthermore, cross-resistance between the W1DR and W1PR cell lines suggest that doxorubicin is not a recommended second-line cytostatic drug in patients who have developed resistance to paclitaxel as first-line chemotherapy.

The W1PR line has shown a similar pattern of response to the topotecan like topotecan-resistant cell line, W1TR; however, the W1TR line showed no resistance to paclitaxel. Here, we observed only a one-sided cross-resistance, suggesting that topotecan may not serve as a good cytostatic for ovarian cancer treatment because resistance to paclitaxel has already developed. Therefore, topotecan might be better applied as a drug for first-line chemotherapy. The best recognised protein responsible for MDR is P-gp, encoded by the ABCB1 (MDR1) gene. We observed high levels of the transcript and the protein in cell lines resistant to doxorubicin, vincristine and paclitaxel. This observation is consistent with published data showing that P-gp has broad substrate specificity, including natural products such as anthracyclines, vinca alkaloids, and taxanes [8, 12–16, 34]. Both the transcript and protein levels of P-gp exhibited a strong correlation with IC50 for doxorubicin, vincristine, and paclitaxel in W1DR, W1VR, and W1PR cell lines. This result suggests that P-gp played a critical role in resistance to these drugs in the investigated cell lines.

The lack of correlation between the transcript and protein levels of MRP2 may result from increased transcription or increased transcript stability caused by methotrexate treatment. It is also possible that there exists another so far not described MRP2 isoform, and the difference between the transcript and protein levels may reflect different MRP2 isoforms. Regardless, we observed a pronounced correlation between the MRP2 transcript level and methotrexate resistance in our cell lines. This correlation suggests that MRP2 plays a critical role in methotrexate resistance in the investigated cell lines, which is also consistent with several previously published data showing a correlation between MRP2 expression and methotrexate resistance [35, 36]. High MRP2 expression has been observed in cell lines resistant to cisplatin [19, 37]. In our research, we did not observe an increase in the MRP2 transcript or protein level in the cisplatin resistant cell line, which may be due to the fact that MRP2 protein is not the only protein responsible for cisplatin resistance. Glutathione [38], glutathione metabolising enzymes [39], and metallothioneins [40] are also responsible for resistance to cisplatin. The differences in the transcript and protein levels of MRP2 and the role of MRP2 in the resistance of the investigated cell lines require further investigation.

High BCRP transcript and protein levels in the topotecan resistant cell line have been well established [23, 41, 42] and have been subsequently confirmed by our results. Increased BCRP transcript in the W1VR cell line was not expected because vincristine is not a substrate of BCRP. However, BCRP expression increased only sixfold in comparison to over a thousandfold increase in the W1TR line, for which BCRP protein level was not altered. The topotecan resistant cell line was shown to be partially resistant to methotrexate; this resistance may be a direct result of high levels of BCRP expression because methotrexate is a substrate for BCRP. We have observed two different mechanisms of topotecan resistance. The W1TR cell line developed the "classical" topotecan resistance, based on increased BCRP expression [23, 41, 42]. Additionally, we have observed a similar dose-dependent response pattern to topotecan in the paclitaxel resistant cell line, in spite of its low BCRP expression, which may be due to the high levels of P-gp expression in the W1PR cell line. Published reports have suggested that high levels of P-gp expression play a significant role in topotecan resistance [43]. However, two other cell lines with high expression of P-gp, W1DR and W1VR, demonstrated a sensitivity to topotecan. Accordingly, how much of a role MDR1 plays in topotecan resistance and whether other proteins are involved in this drug resistance mechanism must be evaluated. For example, it has been shown that MRP4 plays a role in topotecan resistance [44]. Therefore, the resistance of the W1PR cell line to topotecan requires further investigation.

Contrary to other published results, we observed methotrexate sensitivity in our cell lines expressing high levels of P-gp. According to previously published reports, methotrexate is a substrate for P-gp [45], but our cell lines that have high expression of P-gp (W1DR, W1VR, and W1PR) were all methotrexate sensitive. These seemingly contradictory results may be explained by studies that

showed that P-gp is an efficient methotrexate transporter in cells that were deficient in the methotrexate carrier [46, 47].

5. Conclusions

In summary, some of mechanisms of drug resistance are well known, and our results suggest that it is possible to predict cross-resistance to other drugs when the classical MDR, which is correlated with P-gp expression, is involved. Cases of other resistances such as topotecan, methotrexate, and cisplatin resistance appear to be more complex, and further analyses of MDR development must be explored. Our results confirm that cisplatin is an effective drug for first-line chemotherapy in ovarian cancer treatment. The efficacy of topotecan and doxorubicin as the second lines of chemotherapy may be limited because of their cross-resistance with paclitaxel, which is used as a first line of chemotherapeutic treatment. Therefore, methotrexate may be considered to be an alternative therapy for ovarian cancer treatment because no cross-resistance was observed in our cell lines.

Conflict of Interests

The authors declare that they have no conflict of interests including employment, consultancies, stock ownership, honoraria, paid expert testimony, patent applications/registrations, and grants or other funding.

Acknowledgments

The authors would like to thank Dr. Michał W. Łuczak, Department of Biochemistry and Molecular Biology, Poznań University of Medical Sciences for helpful discussions and insight into this paper. This study was supported by Grant no. N N401 204139 from the National Science Centre.

References

[1] R. J. Kurman, *Blaustein's Pathology of the Female Genital Tract*, Springer, New York, NY, USA, 5th edition, 2002.

[2] The ICON and AGO Collaborators, "Paclitaxel plus platinum-based chemotherapy versus conventional platinum-based chemo-therapy in women with relapsed ovarian cancer: the ICON4/AGO-OVAR-2.2 trial," *Lancet*, vol. 361, pp. 2099–2106, 2003.

[3] J. Pfisterer, M. Plante, I. Vergote et al., "Gemcitabine plus carboplatin compared with carboplatin in patients with platinum-sensitive recurrent ovarian cancer: an intergroup trial of the AGO-OVAR, the NCIC CTG, and the EORTC GCG," *Journal of Clinical Oncology*, vol. 24, no. 29, pp. 4699–4707, 2006.

[4] E. Pujade-Lauraine, S. Mahner, J. Kaern, M. Gebski, P. Heywood, and A. Vasey, "A randomized, phase III study of carboplatin and pegylated liposomal doxorubicin versus carboplatin and paclitaxel in relapsed platinum-sensitive ovarian cancer (OC): CALYPSO study of the Gynecologic Cancer Intergroup (GCIG)," *Journal of Clinical Oncology*, vol. 27, no. 18, abstract LBA5509, 2009.

[5] J. Sehouli, D. Stengel, G. Oskay-Oezcelik et al., "Nonplatinum topotecan combinations versus topotecan alone for recurrent ovarian cancer: results of a phase III study of the North-Eastern German Society of Gynecological Oncology Ovarian Cancer Study Group," *Journal of Clinical Oncology*, vol. 26, no. 19, pp. 3176–3182, 2008.

[6] D. G. Mutch, M. Orlando, T. Goss et al., "Randomized phase III trial of gemcitabine compared with pegylated liposomal doxorubicin in patients with platinum-resistant ovarian cancer," *Journal of Clinical Oncology*, vol. 25, no. 19, pp. 2811–2818, 2007.

[7] G. Ferrandina, M. Ludovisi, D. Lorusso et al., "Phase III trial of gemcitabine compared with pegylated liposomal doxorubicin in progressive or recurrent ovarian cancer," *Journal of Clinical Oncology*, vol. 26, no. 6, pp. 890–896, 2008.

[8] A. A. Stavrovskaya, "Cellular mechanism of multidrug resistance of tumor cells," *Biochemistry*, vol. 65, no. 1, pp. 95–106, 2000.

[9] M. M. Gottesman, "Mechanisms of cancer drug resistance," *Annual Review of Medicine*, vol. 53, pp. 615–627, 2002.

[10] G. D. Kruh, "Introduction to resistance to anticancer agents," *Oncogene*, vol. 22, no. 47, pp. 7262–7264, 2003.

[11] T. Ozben, "Mechanisms and strategies to overcome multiple drug resistance in cancer," *FEBS Letters*, vol. 580, no. 12, pp. 2903–2909, 2006.

[12] G. D. Leonard, T. Fojo, and S. E. Bates, "The role of ABC transporters in clinical practice," *Oncologist*, vol. 8, no. 5, pp. 411–424, 2003.

[13] C. H. Choi, "ABC transporters as multidrug resistance mechanisms and the development of chemosensitizers for their reversal," *Cancer Cell International*, vol. 5, article 30, 2005.

[14] A. Abolhoda, A. E. Wilson, H. Ross, P. V. Danenberg, M. Burt, and K. W. Scotto, "Rapid activation of MDR1 gene expression in human metastatic sarcoma after in vivo exposure to doxorubicin," *Clinical Cancer Research*, vol. 5, no. 11, pp. 3352–3356, 1999.

[15] A. M. Al-Katib, M. R. Smith, W. S. Kamanda et al., "Bryostatin 1 down-regulates mdr1 and potentiates vincristine cytotoxicity in diffuse large cell lymphoma xenografts," *Clinical Cancer Research*, vol. 4, no. 5, pp. 1305–1314, 1998.

[16] A. Podolski-Renić, T. Andelković, J. Banković, N. Tanić, S. Ruždijić, and M. Pešić, "The role of paclitaxel in the development and treatment of multidrug resistant cancer cell lines," *Biomedicine and Pharmacotherapy*, vol. 65, no. 5, pp. 345–353, 2011.

[17] S. P. C. Cole, G. Bhardwaj, J. H. Gerlach et al., "Overexpression of a transporter gene in a multidrug-resistant human lung cancer cell line," *Science*, vol. 258, no. 5088, pp. 1650–1654, 1992.

[18] O. Fardel, E. Jigorel, M. Le Vee, and L. Payen, "Physiological, pharmacological and clinical features of the multidrug resistance protein 2," *Biomedicine and Pharmacotherapy*, vol. 59, no. 3, pp. 104–114, 2005.

[19] P. Surowiak, V. Materna, I. Kaplenko et al., "ABCC2 (MRP2, cMOAT) can be localized in the nuclear membrane of ovarian carcinomas and correlates with resistance to cisplatin and clinical outcome," *Clinical Cancer Research*, vol. 12, no. 23, pp. 7149–7158, 2006.

[20] A. D. Guminski, R. L. Balleine, Y. E. Chiew et al., "MRP2 (ABCC2) and cisplatin sensitivity in hepatocytes and human ovarian carcinoma," *Gynecologic Oncology*, vol. 100, no. 2, pp. 239–246, 2006.

[21] L. Austin Doyle, W. Yang, L. V. Abruzzo et al., "A multidrug resistance transporter from human MCF-7 breast cancer cells," *Proceedings of the National Academy of Sciences of the United States of America*, vol. 95, no. 26, pp. 15665–15670, 1998.

[22] R. W. Robey, O. Polgar, J. Deeken, K. W. To, and S. E. Bates, "ABCG2: determining its relevance in clinical drug resistance," *Cancer and Metastasis Reviews*, vol. 26, no. 1, pp. 39–57, 2007.

[23] M. Maliepaard, M. A. Van Gastelen, L. A. De Jong et al., "Overexpression of the BCRP/MXR/ABCP gene in a topotecan-selected ovarian tumor cell line," *Cancer Research*, vol. 59, no. 18, pp. 4559–4563, 1999.

[24] G. L. Scheffer, A. B. Schroeijers, M. A. Izquierdo, E. A. C. Wiemer, and R. J. Scheper, "Lung resistance-related protein/major vault protein and vaults in multidrug-resistant cancer," *Current Opinion in Oncology*, vol. 12, no. 6, pp. 550–556, 2000.

[25] C. M. Laurencot, G. L. Scheffer, R. J. Scheper, and R. H. Shoemaker, "Increased LRP Mrna expression is associated with the MDR phenotype in intrinsically resistant human cancer cell lines," *International Journal of Cancer*, vol. 72, pp. 1021–1026, 1997.

[26] W. Berger, L. Elbling, and M. Micksche, "Expression of the major vault protein LRP in human non-small-cell lung cancer cells: activation by short-team exposure to antineoplastic drugs," *International Journal of Cancer*, vol. 88, pp. 293–300, 2000.

[27] B. C. Behrens, T. C. Hamilton, and H. Masuda, "Characterization of a cis-diamminedichloroplatinum(II)-resistant human ovarian cancer cell line and its use in evaluation of platinum analogues," *Cancer Research*, vol. 47, no. 2, pp. 414–418, 1987.

[28] E. Dolfini, T. Dasdia, G. Arancia et al., "Characterization of a clonal human colon adenocarcinoma line intrinsically resistant to doxorubicin," *British Journal of Cancer*, vol. 76, no. 1, pp. 67–76, 1997.

[29] M. Dietel, U. Bals, B. Schaefer, I. Herzig, H. Arps, and M. Zabel, "In vitro prediction of cytostatic drug resistance in primary cell cultures of solid malignant tumours," *European Journal of Cancer Part A*, vol. 29, no. 3, pp. 416–420, 1993.

[30] B. T. Hennessy, R. L. Coleman, and M. Markman, "Ovarian cancer," *Lancet*, vol. 374, pp. 371–382, 2009.

[31] R. J. Raggers, I. Vogels, and G. Van Meer, "Multidrug-resistance P-glycoprotein (MDR1) secretes platelet-activating factor," *Biochemical Journal*, vol. 357, no. 3, pp. 859–865, 2001.

[32] M. M. Ho, A. V. Ng, S. Lam, and J. Y. Hung, "Side population in human lung cancer cell lines and tumors is enriched with stem-like cancer cells," *Cancer Research*, vol. 67, no. 10, pp. 4827–4833, 2007.

[33] M. H. G. P. Raaijmakers, E. P. L. M. De Grouw, B. A. Van Der Reijden, T. J. M. De Witte, J. H. Jansen, and R. A. P. Raymakers, "ABCB1 modulation does not circumvent drug extrusion from primitive leukemic progenitor cells and may preferentially target residual normal cells in acute myelogenous leukemia," *Clinical Cancer Research*, vol. 12, no. 11 I, pp. 3452–3458, 2006.

[34] M. M. Gottesman, T. Fojo, and S. E. Bates, "Multidrug resistance in cancer: role of ATP-dependent transporters," *Nature Reviews Cancer*, vol. 2, no. 1, pp. 48–58, 2002.

[35] M. L. H. Vlaming, Z. Pala, A. Van Esch et al., "Functionally overlapping roles of Abcg2 (Bcrp1) and Abcc2 (Mrp2) in the elimination of methotrexate and its main toxic metabolite 7-hydroxymethotrexate in vivo," *Clinical Cancer Research*, vol. 15, no. 9, pp. 3084–3093, 2009.

[36] M. L. H. Vlaming, Z. Pala, A. Van Esch et al., "Impact of Abcc2 (Mrp2) and Abcc3 (Mrp3) on the in vivo elimination of methotrexate and its main toxic metabolite 7-hydroxymethotrexate," *Clinical Cancer Research*, vol. 14, no. 24, pp. 8152–8160, 2008.

[37] B. Liedert, V. Materna, D. Schadendorf, J. Thomale, and H. Lage, "Overexpression of cMOAT (MRP2/ABCC2) is associated with decreased formation of platinum-DNA adducts and decreased G2-arrest in melanoma cells resistant to cisplatin," *Journal of Investigative Dermatology*, vol. 121, no. 1, pp. 172–176, 2003.

[38] T. Ishikawa and F. Ali-Osman, "Glutathione-associated cis-diamminedichloroplatinum(II) metabolism and ATP-dependent efflux from leukemia cells. Molecular characterization of glutathione-platinum complex and its biological significance," *Journal of Biological Chemistry*, vol. 268, no. 27, pp. 20116–20125, 1993.

[39] H. Kase, S. Kodama, E. Nagai, and K. Tanaka, "Glutathione S-transferase π immunostaining of cisplatin-resistant ovarian cancer cells in ascites," *Acta Cytologica*, vol. 42, no. 6, pp. 1397–1402, 1998.

[40] K. Kasahara, Y. Fujiwara, K. Nishio et al., "Metallothionein content correlates with the sensitivity of human small cell lung cancer cell lines to cisplatin," *Cancer Research*, vol. 51, no. 12, pp. 3237–3242, 1991.

[41] C. H. Yang, E. Schneider, M. L. Kuo, E. L. Volk, E. Rocchi, and Y. C. Chen, "BCRP/MXR/ABCP expression in topotecan-resistant human breast carcinoma cells," *Biochemical Pharmacology*, vol. 60, no. 6, pp. 831–837, 2000.

[42] M. Ishii, M. Iwahana, I. Mitsui et al., "Growth inhibitory effect of a new camptothecin analog, DX-8951f, on various drug-resistant sublines including BCRP-mediated camptothecin derivative-resistant variants derived from the human lung cancer cell line PC-6," *Anti-Cancer Drugs*, vol. 11, no. 5, pp. 353–362, 2000.

[43] U. Vanhoefer, M. R. Müller, R. A. Hilger et al., "Reversal of MDR1-associated resistance to topotecan by PAK-200S, a new dihydropyridine analogue, in human cancer cell lines," *British Journal of Cancer*, vol. 81, no. 8, pp. 1304–1310, 1999.

[44] M. Leggas, M. Adachi, G. L. Scheffer et al., "Mrp4 confers resistance to topotecan and protects the brain from chemotherapy," *Molecular and Cellular Biology*, vol. 24, no. 17, pp. 7612–7621, 2004.

[45] M. D. Norris, D. de Graaf, M. Haber, M. Kavallaris, J. Madafiglio, and J. Gilbert, "Involvement of MDR1 P-glycoprotein in multifactorial resistance to methotrexate," *International Journal of Cancer*, vol. 65, pp. 613–619, 1996.

[46] A. J. Gifford, M. Kavallaris, J. Madafiglio, L. H. Matherly, B. W. Stewart, and M. Haber, "P-glycoprotein-mediated methotrexate resistance in CCRF-CEM sublines deficient in methotrexate accumulation due to a point mutation in the reduced folate carrier gene," *International Journal of Cancer*, vol. 78, pp. 176–181, 1998.

[47] D. De Graaf, R. C. Sharma, E. B. Mechetner, R. T. Schimke, and I. B. Roninson, "P-glycoprotein confers methotrexate resistance in 3T6 cells with deficient carrier-mediated methotrexate uptake," *Proceedings of the National Academy of Sciences of the United States of America*, vol. 93, no. 3, pp. 1238–1242, 1996.

Hindawi Publishing Corporation
BioMed Research International
Volume 2013, Article ID 340513, 6 pages
http://dx.doi.org/10.1155/2013/340513

Research Article

Comparison of Three Multiple Allergen Simultaneous Tests: RIDA Allergy Screen, MAST Optigen, and Polycheck Allergy

Minje Han, Sue Shin, Hyewon Park, Kyoung Un Park, Myoung Hee Park, and Eun Young Song

Department of Laboratory Medicine, Seoul National University College of Medicine and Seoul National University Hospital, Seoul 110-744, Republic of Korea

Correspondence should be addressed to Eun Young Song; eysong1@snu.ac.kr

Received 12 October 2012; Revised 14 November 2012; Accepted 19 November 2012

Academic Editor: Mina Hur

We compared the performances of 3 Multiple Allergen Simultaneous Test (MAST) assays: RIDA Allergy Screen (R-Biopharm, Darmstadt, Germany), MAST Optigen allergy system (Hitachi Chemical Diagnostics, Mountain View, CA), and Polycheck Allergy (Biocheck GmbH, Munster, Germany). Forty sera that tested positive with the RIDA Allergy Screen (20 for food and 20 for inhalant panel) were subjected to MAST Optigen and Polycheck Allergy. For 26 available sera with discrepant results, 62 ImmunoCAP allergen-specific IgE tests (Pharmacia Diagnostics, Uppsala, Sweden) were performed. Percent agreements (kappa value) were 87.6% (0.59) and 91.3% (0.60) between RIDA and MAST; 89.9% (0.55) and 88.3% (0.46) between RIDA and Polycheck; and 86.8% (0.51) and 90.6% (0.61) between MAST and Polycheck. Compared with ImmunoCAP, agreements (kappa value) of inhalant and food panels were 51.7% (0.04) and 33.3% (−0.38) for RIDA; 60.7% (0.27) and 81.8% (0.59) for MAST; and 65.5% (0.26) and 45.5% (0.07) for Polycheck. The agreements between RIDA, MAST, and Polycheck and ImmunoCAP-positivity were 45.7%, 88.2%, and 28.6%, respectively, and the agreements for ImmunoCAP-negativity were 37.0%, 51.9%, and 88.9%. MAST Optigen showed better agreement with ImmunoCAP than other assays in the food panel. Better sensitivity of MAST Optigen and better specificity of Polycheck Allergy were suspected.

1. Introduction

For the diagnosis of allergy, presence of allergen-specific immunoglobulin E (IgE) is usually established either by in vivo allergen skin tests or by in vitro allergen-specific IgE measurements [1, 2]. Although, in vivo skin test has been widely used to detect allergen-specific IgE. It is not a quantitative test and is difficult to be standardized [3]. Therefore, detection of allergen-specific IgE is important for the diagnosis of allergy [1, 2]. Since the development and improvement of fluorescent enzyme immunoassay, the ImmunoCAP system (Pharmacia Diagnostics AB, Uppsala, Sweden) has been widely accepted as a reference method of allergen-specific IgE measurement because of its reliability, reproducibility, and good accordance with allergen skin test. However, individual ImmunoCAP test can only detect IgE against a single allergen, making it quite expensive to use in a clinical setting [4].

Therefore, several multiple allergen simultaneous tests (MAST) were developed, which can detect more than 30 allergen-specific IgE [5–8]. However, allergen-specific IgE assays are often modified as manufacturers improve allergens or change reagents to optimize test performance, affecting the diagnostic performance of those assays. MAST Optigen (Hitachi Chemical Diagnostics, Mountain View, CA, USA), upgraded version of MAST CLA (Hitachi Chemical Diagnostics, Mountain View, CA, USA), and Polycheck Allergy (Biocheck GmbH, Munster, Germany) were recently introduced with good performances [6, 9, 10]. However, to the best of our knowledge, comparison of performances of those assays and analysis of concordance with ImmunoCAP system has not been performed. The aim of this study was to compare the performance of 3 MAST assays: RIDA Allergy Screen (R-Biopharm, Darmstadt, Germany), MAST Optigen allergy system (Hitachi Chemical Diagnostics, Mountain View, CA, USA), and Polycheck Allergy (Biocheck GmbH, Munster,

Table 1: Comparison of allergens and classes of three MAST assays.

	RIDA Allergy Screen	MAST Optigen	Polycheck Allergy
Inhalant allergens included in common	Soy bean, Milk, Egg White, Crab, Shrimp, Peach, Acacia, Ash mix, Birch-alder mix, Sallow willow, Hazelnut, Cedar Japanese, Oak white, Sycamore mix, Bermuda grass, Orchard grass, Timothy grass, Rye Cultbatd, Goldenrod, Pigweed, Russian thistle, Dandelion, Mugwort, Ragweed short, Alternaria, Aspergillus, Cladosporium, Penicillium, Cat, Dog, Cockroach Mix, House dust, D. farinae, D. pteronyssinus		
Inhalant allergens included only in each reagent	Sweet vernal grass, Reed, Pine, Ox-eye-daisy	Cottonwood East	Redtop, Lilac, Fescue meadow, Latex, Tyrophagus putrescentiae, Ox-eye-daisy
Food allergens included in common	Soy beans, Milk, cheese, Egg white, Crab, Shrimp, Tuna, Codfish, Salmon, Pork, Chicken, Beef, Citrus mix, Wheat flour, Rice, Barley meal, Garlic, Peanut, Yeast bakers, Birch-Alder mix, Oak white, Rye, Mugwort, Ragweed short, Alternaria, Cat, Dog, Cockroach mix, House dust, D. farinae, D. pteronyssinus, Buckwheat meal		
Food allergens included only in each reagent	Aspergillus, Cladosporium, Onion, Acarus siro, Tomato, Candida albicans		Tomato, Timothy grass pollen, Cacao, Mackerel, Potato, Sweet chestnut
Class 0	0.0–0.34	0–26	0.0–0.34
1	0.35–0.69	27–65	0.35–0.69
2	0.7–3.49	66–142	0.7–3.49
3	3.5–17.49	143–242	3.5–17.49
4	17.5–49.99	>242	17.5–49.99
5	50.00–99.99		50.00–99.99
6	>100		>100
Unit	IU/mL	LUs	kU/L

Table 2: Concordance among three MAST assays.

		RIDA		Agreement (%)	kappa	Polycheck		Agreement (%)	kappa
		N*	P†			N	P		
Inhalant panel									
MAST Optigen	N	529	26	87.6	0.59	529	11	86.8	0.51
	P	61	84			79	61		
Polycheck	N	574	54	89.9	0.55				
	P	17	55						
Food panel									
MAST Optigen	N	600	23	91.3	0.60	552	32	90.6	0.61
	P	40	57			32	64		
Polycheck	N	572	31	88.3	0.46				
	P	51	46						

RIDA: RIDA Allergy Screen, Polycheck: Polycheck Allergy, N: negative, P: positive. *Number of tests with negative results was shown. †Number of tests with positive results was shown.

Germany) compared to ImmunoCAP system as a reference method.

2. Material and Methods

2.1. Patients. Forty sera that tested positive with the RIDA Allergy Screen (20 for the food panel and 20 for the inhalant panel) in immunology laboratory of Seoul National University Hospital from October to December 2010 were stored in −70°C until thawing for MAST Optigen and Polycheck Allergy assays. Allergens and classifications of results of three MAST assays are summarized in Table 1. Specific IgE assay with ImmunoCAP FEIA system (Phadia, Uppsala, Sweden) as a reference method was performed on 26 available residual sera out of 32 sera showing discrepant results (0 class in one assay and ≥2 class in another assay) among three MAST assays. The Institutional Review Board of Seoul National University Hospital approved this study (IRB no. 1-2011-0038).

2.2. RIDA Allergy Screen. Two hundred and fifty *u*L of patient serum were added to reaction wells of each of inhalant and

Table 3: Antigen panels with discrepant results among three MAST assays.

RIDA	MAST Optigen	Polycheck	Antigen panel*
		Inhalant panel	
+	+	−	Rye cultbatd, Cockroach mix, Birch-alder mix, Orchard grass, Timothy grass, Goldenrod, Dandelion, Mugwort
+	−	−	Sycamore mix (4), Goldenrod
−	+	+	House dust (4), D. farinae
−	+	−	Peach (5), Pigweed (4), Mugwort (3), Dandelion, Cockroach Mix, Milk, Crab, Birch-alder mix,
−	−	+	Hazelnut
+	NT	−	Ox-eye-daisy (4)
		Food panel	
+	+	−	Beef (3), Milk
+	−	−	Alternaria, Pork
−	+	+	Peanut, Soy beans, Birch-alder mix, Yeast bakers, Cat
−	+	−	Cheese
−	−	+	House dust (4)

RIDA: RIDA Allergy Screen, Polycheck: Polycheck Allergy. NT: not tested. *Antigen panels with ≥2 discrepant samples were shown. Number of samples was shown in parenthesis when it was ≥3.

food panels which contain 39 kinds of allergens. After 45 min of incubation at room temperature and wash, 250 uL of Biotin tagged anti-IgE were added. After 45 minutes of incubation at room temperature and wash, 250 uL of streptavidin conjugate were added. Twenty minutes of incubation at room temperature and wash, 250 uL of luminescent reagent were added. After 20 minutes of incubation, results were scanned with CCD camera (RIDA X-Screen Reader) and interpreted as class 0–6. Class ≥1 was interpreted as positive.

2.3. Polycheck Allergy. After washing of inhalant and food cassette which contain 39 kinds of allergens, 250 uL of start solution were added. After 60 seconds of incubation, 200 uL of patient sera were added. After 1 hour of incubation on shaker, 6 times of washes were performed. Anti-IgE was added and 45 minutes of incubation on shaker was performed. After 3 times of washes, 250 uL of enzyme tagged conjugate were added. After 20 minutes of incubation and washes, 250 uL of luminescent reagent were added. After 20 minutes of incubation, results were scanned and interpreted with Biocheck Image Software as class 0–6. Class ≥1 was interpreted as positive.

2.4. MAST Optigen. Patient sera were added to MASTpette chambers which contain 35 kinds of allergens. After 2 hours of incubation and washes, enzyme-tagged anti-IgE was added. After 2 hours of incubation and washes, luminescent reagent was added. After 10 minutes of incubation, results were interpreted as class 0–4 with MAST Optigen luminometer. Class ≥1 was interpreted as positive.

2.5. ImmunoCAP System Allergen-Specific IgE. All procedures were performed following the manufacture's instruction. The detection range of ImmunoCAP FEIA was 0.1 to 100 kU/L. The sIgE classification scales were as follows: class 0: under 0.35 kU/L, class 1: 0.35–0.7 kU/L, class 2: 0.7–3.5 kU/L, class 3: 3.5–17.5 kU/L, class 4: 17.5–50 kU/L, class 5: 50–100 kU/L, class 6: over 100 kU/L. Class ≥1 was interpreted as positive.

2.6. Statistical Analysis. Agreement of detection results (Cohen's kappa analysis) was analyzed. We assessed and categorized Kappa value as almost perfect (0.8–1.0), substantial (0.6–0.8), moderate (0.4–0.6), fair (0.2–0.4), and poor (below 0.2) [11]. We calculated three different agreement percentages (positive, negative, and total agreement percentage). The positive and negative agreement percentages were calculated with the proportions of agreement for the average of their positive and negative responses. The total agreement percentage was calculated following: (total number of results − number of discrepancies) × 100/total number of results [12].

3. Results

For each of the MAST inhalant and food panels, percent agreements (kappa value) were 87.6% (0.59) and 91.3% (0.60) between RIDA Allergy Screen and MAST Optigen; 89.9% (0.55) and 88.3% (0.46) between RIDA Allergy Screen and Polycheck Allergy; and 86.8% (0.51) and 90.6% (0.61) between MAST Optigen and Polycheck Allergy (Table 2).

Among the 20 sera tested by inhalant panel, for House-dust, most common inhalant allergen in Korean population [7], RIDA Allergy Screen was negative but MAST Optigen and Polycheck Allergy were positive on 4 sera (Table 3). Out of those 4 sera, 3 (with available residual sera) were tested by ImmunoCAP specific IgE. All of them showed positive results with ImmunoCAP (Table 4). Agreements of RIDA Allergy Screen, MAST Optigen, and Polycheck Allergy with

Table 4: Concordance of three MAST assays with ImmunoCAP according to antigen panels.

	Agreement with ImmunoCAP(+)			Agreement with ImmunoCAP(−)		
	RIDA	MAST Optigen	Polycheck	RIDA	MAST Optigen	Polycheck
Inhalant panel*						
House dust	0/3 (0%)†	3/3 (100%)	3/3 (100%)	NA	NA	NA
Milk	NA	NA	NA	2/3 (66.7%)	0/3 (0%)	3/3 (100%)
Mugwort	1/1 (100%)	1/1 (100%)	0/1 (0%)	1/1 (100%)	0/1 (0%)	1/1 (100%)
Crab	1/1 (100%)	1/1 (100%)	0/1 (0%)	1/1 (100%)	0/1 (0%)	1/1 (100%)
Timothy grass	1/1 (100%)	1/1 (100%)	0/1 (0%)	0/1 (0%)	1/1 (100%)	1/1 (100%)
Dandelion	NA	NA	NA	0/1 (0%)	0/1 (0%)	1/1 (100%)
Peach	0/3 (0%)	3/3 (100%)	0/3 (0%)	1/1 (100%)	0/1 (0%)	1/1 (100%)
Cockroach mix	NA	NA	NA	1/1 (100%)	0/1 (0%)	1/1 (100%)
Birch-alder mix	NA	NA	NA	1/2 (50%)	0/2 (0%)	2/2 (100%)
Hazelnut	NA	NA	NA	1/1 (100%)	1/1 (100%)	0/1 (0%)
Alternaria	1/1 (100%)	0/1 (0%)	1/1 (100%)	0/1 (0%)	1/1 (100%)	1/1 (100%)
Rye, cultbatd	1/1 (100%)	1/1 (100%)	0/1 (0%)	NA	NA	NA
Aspergillus	NA	NA	NA	0/1 (0%)	1/1 (100%)	1/1 (100%)
Sycamore mix	NA	NA	NA	0/1 (0%)	1/1 (100%)	1/1 (100%)
Cedar Japanese	NA	NA	NA	0/1 (0%)	1/1 (100%)	1/1 (100%)
Ox-eye-daisy	1/1 (100%)	NA	0/1 (0%)	NA	NA	NA
Orchard grass	1/1 (100%)	1/1 (100%)	0/1 (0%)	NA	NA	NA
Food panel*						
D. pteronyssinus	0/1 (0%)	1/1 (100%)	1/1 (100%)	NA	NA	NA
House dust	NA	NA	NA	2/2 (100%)	2/2 (100%)	0/2 (0%)
Milk	1/3 (33.3%)	3/3 (100%)	1/3 (33.3%)	0/1 (0%)	0/1 (0%)	1/1 (100%)
Mugwort	NA	NA	NA	0/1 (0%)	1/1 (100%)	1/1 (100%)
Dog	1/1 (100%)	1/1 (100%)	0/1 (0%)	0/1 (0%)	1/1 (100%)	1/1 (100%)
Egg white	0/2 (0%)	2/2 (100%)	1/2 (50%)	NA	NA	NA
Soy beans	0/1 (0%)	1/1 (100%)	1/1 (100%)	NA	NA	NA
Shrimp	0/1 (0%)	1/1 (100%)	0/1 (0%)	NA	NA	NA
cheese	1/3 (33.3%)	3/3 (100%)	0/3 (0%)	0/1 (0%)	1/1 (100%)	1/1 (100%)
Garlic	1/1 (100%)	0/1 (0%)	0/1 (0%)	NA	NA	NA
Alternaria	1/2 (50%)	1/2 (50%)	1/2 (50%)	0/1 (0%)	1/1 (100%)	1/1 (100%)
Cat	0/1 (0%)	1/1 (100%)	1/1 (100%)	NA	NA	NA
Codfish	1/1 (100%)	1/1 (100%)	0/1 (0%)	NA	NA	NA
Salmon	1/2 (50%)	2/2 (100%)	0/2 (0%)	NA	NA	NA
Pork	NA	NA	NA	0/2 (0%)	2/2 (100%)	2/2 (100%)
Chicken	1/2 (50%)	1/2 (50%)	0/2 (0%)	NA	NA	NA
Beef	NA	NA	NA	0/2 (0%)	0/2 (0%)	2/2 (100%)
Citrus mix	1/1 (100%)	1/1 (100%)	0/1 (0%)	NA	NA	NA

RIDA: RIDA Allergy Screen, Polycheck: Polycheck Allergy, NA: not available. *Antigen panels were shown in the order of decreasing positive rate in Korean population [7]. †Number of positive results/number tested (%).

ImmunoCAP-positive results for House dust were 0% (0/3), 100% (3/3), and 100% (3/3), respectively (Table 4).

For Peach, three MAST assays showed highest number of discrepant sera (On 5 sera, MAST Optigen Screen was positive but and RIDA Allergy Screen and Polycheck Allergy were negative.) (Table 3). Three of them, tested by ImmunoCAP specific IgE, showed positive results. Agreements of Allergy Screen, MAST Optigen, and Polycheck Allergy with ImmunoCAP-positive results for Peach were 0% (0/3), 100% (3/3), and 0% (0/3), respectively (Table 4).

Compared with the 62 ImmunoCAP allergen-specific IgE test results for 26 discrepant sera, agreements (kappa value) of inhalant and food panels were 51.7% (0.04) and 33.3% (−0.38) for RIDA Allergy Screen; 60.7% (0.27) and 81.8% (0.59) for MAST Optigen; and 65.5% (0.26) and 45.5% (0.07) for Polycheck Allergy (Table 5). The agreements between RIDA Allergy Screen, MAST Optigen, and Polycheck Allergy results and ImmunoCAP-positive results were 53.8%, 91.7%, and 30.8% for inhalant panel; 40.9%, 86.4%, and 27.3% for food panel, respectively (Table 5). The agreements between

Table 5: Concordance of three MAST assays with ImmunoCAP on discrepant sera among three MAST assays.

		ImmunoCAP		Agreement (%)		
		N*	P†	Total (kappa)	ImmunoCAP(+)	ImmunoCAP(−)
Inhalant panel						
RIDA	N	8	6	51.7 (0.04)	53.8	50.0
	P	8	7			
MAST Optigen	N	6	1	60.7 (0.27)	91.7	37.5
	P	10	11			
Polycheck	N	15	9	65.5 (0.26)	30.8	93.8
	P	1	4			
Food panel						
RIDA	N	2	13	33.3 (−0.38)	40.9	18.2
	P	9	9			
MAST Optigen	N	8	3	81.8 (0.59)	86.4	72.7
	P	3	19			
Polycheck	N	9	16	45.5 (0.07)	27.3	81.8
	P	2	6			

RIDA: RIDA Allergy Screen, Polycheck: Polycheck Allergy, N: negative, P: positive. *Number of tests with negative results was shown. †Number of tests with positive results was shown.

RIDA Allergy Screen, MAST Optigen, and Polycheck Allergy results and ImmunoCAP-negative results were 50.0%, 37.5%, and 93.8% for inhalant panel; 18.2%, 72.7%, and 81.8% for food panel, respectively (Table 5).

4. Discussion

Although, most of evaluations of performance of MAST assays were performed compared to allergen skin test [6, 13–16], comparisons with ImmunoCAP assay have been performed [5, 8, 17] considering the limitation of allergen skin test as a reference method due to the difference of principle of in vivo test from in vitro test [1]. ImmunoCAP assay has been known to have established performance [2]. Our study was also performed compared to ImmunoCAP assay.

In this study, 3 MAST assays showed moderate agreement (86.8–91.3%, kappa 0.46–0.61) among them (Table 2). In comparison with ImmunoCAP, three MAST assays showed similar agreements for Inhalant panel (51.7–65.5%, kappa 0.04–0.27), and MAST Optigen showed better agreement (81.8%, kappa 0.59) than Polycheck Allergy (45.5%, kappa 0.07) or RIDA Allergy Screen (33.3%, kappa −0.38) for food panel (Table 4). In previous reports, the agreement between RIDA Allergy Screen and ImmunoCAP has been reported as 29.1% (kappa −0.303) on 633 discrepant sera between RIDA Allergy Screen and another MAST assay, AdvanSure system (LG Life Science, Seoul, Korea) [8]. Among 115 allergic patients, RIDA Allergy Screen showed 83.1% of agreement with ImmunoCAP for 10 common allergens [17]. Our result is similar to former one [8] because we also performed ImmunoCAP assays only on sera with discrepant results among three MAST assays.

In our study, the agreement of MAST Optigen with ImmunoCAP-positive results was best (91.7% for inhalant panel and 86.4% for food panel) among 3 MAST assays (Table 5), implicating better sensitivity than other two assays. MAST CLA, previous version of MAST Optigen, has been reported to have slightly lower sensitivity (44.5%) than RIDA Allergy Screen (55.8%) or Polycheck Allergy (55.6%) [6]. The performance of MAST Optigen might be improved compared to MAST CLA as previous report [17].

The agreement of Polycheck Allergy with ImmunoCAP-negative results was best (93.8% for inhalant panel and 81.8% for food panel) among 3 MAST assays, implicating better specificity than other two assays (Table 5). Polycheck Allergy has been reported to have similar specificity (93.5%) with an RIDA Allergy Screen (90.0%) or MAST CLA (96.0%) [6]. In our study, ImmunoCAP assay was performed only on discrepant sera, which could make some different results from previous study [6].

For individual allergens, on House dust, which is most common allergen in Korean population [7] and on Peach, which showed most common discrepant results in our study, better sensitivities of MAST Optigen were suspected (Table 4). From previous study, when compared to allergen skin test, MAST CLA showed best performance on D. farinae [6]. However, because of the retrospective design of our study, the small number of ImmunoCAP assay results due to shortage of residual sera is a limitation to see the performance of MAST assays on individual allergens. Further studies are needed on larger number of samples to compare the performance of MAST assays on individual allergens.

5. Conclusions

The 3 MAST assays: RIDA Allergy Screen, MAST Optigen, and Polycheck Allergy showed moderate agreements among them. In comparison with ImmunoCAP allergen-specific IgE test, MAST Optigen showed better agreement than other

assays in the food panel. Better sensitivity of MAST Optigen and better specificity of Polycheck Allergy were suspected. Further studies are needed in larger number of samples to know the performance of MAST assays for individual allergens.

Authors' Contribution

M. Han and S. Shin share first authorship in this study.

Conflict of Interests

The authors declare that they have no conflict of interests.

References

[1] L. Cox, B. Williams, S. Sicherer et al., "Pearls and pitfalls of allergy diagnostic testing: report from the American College of Allergy, Asthma and Immunology/American Academy of Allergy, Asthma and Immunology Specific IgE Test Task Force," *Annals of Allergy, Asthma and Immunology*, vol. 101, no. 6, pp. 580–592, 2008.

[2] P. Williams, W. A. C. Sewell, C. Bunn, R. Pumphrey, G. Read, and S. Jolles, "Clinical Immunology Review Series: an approach to the use of the immunology laboratory in the diagnosis of clinical allergy," *Clinical and Experimental Immunology*, vol. 153, no. 1, pp. 10–18, 2008.

[3] D. R. Ownby, "Allergy testing: in vivo versus in vitro," *Pediatric Clinics of North America*, vol. 35, no. 5, pp. 995–1009, 1988.

[4] M. Ollert, S. Weissenbacher, J. Rakoski, and J. Ring, "Allergen-specific IgE measured by a continuous random-access immunoanalyzer: interassay comparison and agreement with skin testing," *Clinical Chemistry*, vol. 51, no. 7, pp. 1241–1249, 2005.

[5] J. H. Lee, K. H. Park, H. S. Kim et al., "Specific IgE measurement using AdvanSure system: comparison of detection performance with ImmunoCAP system in Korean allergy patients," *Clinical Chimica Acta*, vol. 413, no. 9-10, pp. 914–919, 2012.

[6] W. R. Jang, C. H. Nahm, J. H. Kim et al., "Allergen specific IgE measurement with polycheck allergy: comparison of three multiple allergen simultaneous tests," *Korean Journal of Laboratory Medicine*, vol. 29, no. 5, pp. 465–472, 2009.

[7] S. E. Yang, H. B. Oh, S. J. Hong, D. H. Moon, and H. S. Chi, "Analysis of MAST Chemiluminescent Assay (MAST CLA) results performed in Asan Medical Center: suggestion for the improvement of MAST CLA performance," *The Korean Journal of Clinical Pathology*, vol. 18, no. 4, pp. 660–666, 1998.

[8] E. J. Oh, S. A. Lee, J. Lim, Y. J. Park, K. Han, and Y. Kim, "Detection of allergen specific IgE by AdvanSure allergy screen test," *Korean Journal of Laboratory Medicine*, vol. 30, no. 4, pp. 420–431, 2010.

[9] D. S. Park, J. H. Cho, K. E. Lee et al., "Detection rate of allergen-specific IgE by multiple antigen simultanesou test-immunoblot assay," *The Korean Journal of Laboratory Medicine*, vol. 24, no. 2, pp. 131–138, 2004.

[10] S. Lee, H. S. Lim, J. Park, and H. S. Kim, "A new automated multiple allergen simultaneous test-chemiluminescent assay (MAST-CLA) using an AP720S analyzer," *Clinica Chimica Acta*, vol. 402, no. 1-2, pp. 182–188, 2009.

[11] J. R. Landis and G. G. Koch, "The measurement of observer agreement for categorical data," *Biometrics*, vol. 33, no. 1, pp. 159–174, 1977.

[12] Clinical Laboratory Standards Institute, "Method comparison and bias estimation using patient samples," *Approved Guideline*, vol. 22, no. 19, 2nd edition, 2008.

[13] A. Linneberg, L. L. N. Husemoen, N. H. Nielsen, F. Madsen, L. Frølund, and N. Johansen, "Screening for allergic respiratory disease in the general population with the ADVIA Centaur Allergy Screen Assay," *Allergy*, vol. 61, no. 3, pp. 344–348, 2006.

[14] N. Ballardini, C. Nilsson, M. Nilsson, and G. Lilja, "ImmunoCAP™ Phadiatop® Infant—a new blood test for detecting IgE sensitisation in children at 2 years of age," *Allergy*, vol. 61, no. 3, pp. 337–343, 2006.

[15] C. Contin-Bordes, A. Petersen, I. Chahine et al., "Comparison of ADVIA Centaur® and Pharmacia UniCAP® tests in the diagnosis of food allergy in children with atopic dermatitis," *Pediatric Allergy and Immunology*, vol. 18, no. 7, pp. 614–620, 2007.

[16] C. M. Cobbaert and G. J. Jonker, "Allergy testing on the IMMULITE 2000 random-access immunoanalyzer—a clinical evaluation study," *Clinical Chemistry and Laboratory Medicine*, vol. 43, no. 7, pp. 772–781, 2005.

[17] J. K. Kim, Y. M. Yoon, W. J. Jang, Y. J. Choi, S. C. Hong, and J. H. Cho, "Comparison study between MAST CLA and OPTIGEN," *American Journal of Rhinology and Allergy*, vol. 25, no. 4, pp. e156–e159, 2011.

Hindawi Publishing Corporation
BioMed Research International
Volume 2013, Article ID 213109, 6 pages
http://dx.doi.org/10.1155/2013/213109

Research Article

Comparison of International Normalized Ratio Measurement between CoaguChek XS Plus and STA-R Coagulation Analyzers

Mina Hur,[1] Hanah Kim,[1] Chul Min Park,[1] Antonio La Gioia,[2] Sang-Gyu Choi,[1] Ju-Hee Choi,[1] Hee-Won Moon,[1] and Yeo-Min Yun[1]

[1] *Department of Laboratory Medicine, School of Medicine and Konkuk University Hospital, Konkuk University, 120-1 Neungdong-ro, Hwayang-dong, Gwangjin-gu, Seoul 143-729, Republic of Korea*
[2] *Italian Society of Clinical Biochemistry and Molecular Biology, Rome, Italy*

Correspondence should be addressed to Mina Hur; dearmina@hanmail.net

Received 22 August 2012; Accepted 10 October 2012

Academic Editor: Andrew St. John

Background. Point-of-care testing (POCT) coagulometers are increasingly being used in the hospital setting. We investigated whether the prothrombin time international normalized ratio (INR) results by CoaguChek XS Plus (Roche Diagnostics GmbH, Mannheim, Germany) can be used reliably without being confirmed with the INR results by STA-R system (Diagnostica Stago S.A.S, Asnières sur Seine, France). *Methods*. A total of 118 INR measurements by CoaguChek XS Plus and STA-R were compared using Passing/Bablok regression analysis and Bland-Altman plot. Agreement of the INR measurements was further assessed in relation to dosing decision. *Results*. The correlation of INR measurements between CoaguChek XS Plus and STA-R was excellent (correlation coefficient = 0.964). The mean difference tended to increase as INR results increased and was 0.25 INR in the therapeutic range (2.0-3.0 INR). The overall agreement was fair to good (kappa = 0.679), and 21/118 (17.8%) INR measurements showed a difference in dosing decision. *Conclusion*. The positive bias of CoaguChek XS Plus may be obvious even in the therapeutic INR range, and dosing decision based on the CoaguChek XS Plus INR results would be different from that based on the STA-R results. The INR measurements by POCT coagulometers still need to be confirmed with the laboratory INR measurements.

1. Introduction

High-quality anticoagulation management is necessary to keep the narrow therapeutic index medications as effective and safe as possible. Oral anticoagulation therapy should be managed in a systematic and coordinated fashion, incorporating patient education, systematic international normalized ratio (INR) testing, tracking, followup, and good patient communication of results and dosing decisions. Prothrombin time (PT) INR is fundamental to prevent bleeding complications or thrombotic events during oral anticoagulation therapy [1, 2]. The target range for INR is dependent on the clinical condition being monitored. For example, targeting an INR of 2.0 to 3.0 for patients with atrial fibrillation, deep vein thrombosis, pulmonary embolism, and heart valves on vitamin K antagonist therapy is one of the strong recommendations of the American College of Chest Physicians [3].

Point-of-care testing (POCT) coagulometers are increasingly being used in the general practice setting by primary healthcare providers and by patients and have the potential to improve management of anticoagulation therapy. However, there have been several documented limitations regarding the accuracy and precision of these devices, including greater differences compared with a standard plasma-based methodology as INRs increase above the therapeutic range [4–7]. Given that INR methods are not harmonized, when monitoring patients on warfarin it is best to keep to one method, and swapping between different laboratory methods or going from laboratory methods to POCT should be discouraged. Nevertheless, using POCT coagulometers is beneficial in that INR results are readily available using capillary blood from a fingertip or untreated venous whole blood instead of citrated venous blood for standard laboratory analyzers [8, 9]. Accordingly, the need for implementing these POCT

coagulometers has increased even in the tertiary care hospitals by the clinicians as well as by the patients.

There have been limited comparisons between CoaguChek XS Plus (Roche Diagnostics GmbH, Mannheim, Germany) and STA-R automated coagulation system (Diagnostica Stago S.A.S, Asnières sur Seine, France) [10]. In this study, we compared the INR results between CoaguChek XS Plus and STA-R to know how interchangeable both INR results are and whether the CoaguChek XS Plus INR results can be used reliably for following up the patients without being confirmed or validated with the results of standard laboratory analyzer.

2. Materials and Methods

2.1. Study Population and INR Measurements. A total of 118 patients were enrolled in this study. They were 70 males and 48 females, and their median age was 68 years (range, 5–87 years). During the period between May and July in 2011, they presented to the outpatient clinic of Konkuk University Medical Center, Seoul, Korea, for the baseline screening of their coagulation system or for the routine monitoring of oral anticoagulation therapy. They were recruited from the departments of cardiovascular surgery ($n = 50$), cardiology ($n = 42$), neurology ($n = 19$), and others ($n = 7$). All blood samples were obtained in the blood collection room for outpatients by one certified phlebotomist, who had about 15-year experience for the blood collection and clinical laboratory tests. Each patient was scheduled to draw the venous blood and gave informed consent to participate in this study. Because either capillary blood or venous blood can be used for the analysis in the CoaguChek XS Plus, to avoid dual sampling, venous blood was used for the comparison. This study was approved by the institutional review board.

From a venipuncture approximately 5 mL of blood was drawn into a syringe. The 2.7 mL venous blood was put into a tube containing 3.2% buffered sodium citrate and was sent to the laboratory for the INR measurement using STA-R system. The remaining blood in the syringe was used for the INR measurement by CoaguChek XS Plus without delay. CoaguChek XS Plus was operated by the same phlebotomist. The preanalytical conditions (differences) were thought to be not influential. The CoaguChek XS Plus uses a human recombinant thromboplastin (ISI = 1.01) and employs electrochemical current detection to measure clot formation. In whole blood testing the mean coefficient of variation of the CoaguChek XS Plus PT determination was claimed to be in the range of 1.3% to 1.6% by the manufacturer. The citrated venous blood samples for STA-R were processed and analyzed immediately after collection according to the routine procedures of the laboratory. The laboratory measurements using STA-Neoplastine CI Plus kit (Diagnostica Stago S.A.S) were considered the reference standard method.

2.2. Statistical Analysis. The INR measurements were analyzed using Pearson's correlation coefficient, Passing/Bablok regression analysis, and Bland-Altman plot. Bland-Altman plot was used to identify mean difference and 95% limits of agreement of the INR results between CoaguChek XS Plus and STA-R. The overall correlation and difference were compared in a total of 118 measurements and were further compared in two INR ranges (1.0-2.0 INR and 2.0-3.0 INR). Agreement of INR measurements was also assessed according to the three ranges of dosing decision (subtherapeutic, therapeutic, and supratherapeutic ranges) with cut-off values of 2.0 INR and 3.0 INR, respectively. Cohen's Kappa value was used for assessing agreement (<0.4, poor; 0.4–0.75, fair to good; >0.75, excellent). Statistical analysis was performed using MedCalc Statistical Software (version 12.3.0, MedCalc Software, Mariakerke, Belgium), and P values less than 0.05 were considered statistically significant.

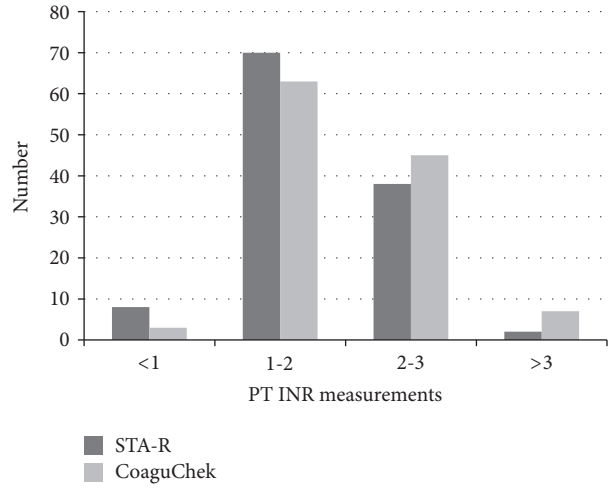

Figure 1: The distribution of prothrombin time (PT) international normalized ratio (INR) measurements by CoaguChek XS Plus and STA-R.

3. Results

Based on the STA-R system, the INR measurements ranged from 0.95 INR to 4.95 INR. The distribution of INR measurements by CoaguChek XS Plus and STA-R is presented in Figure 1. The overall correlation of the INR measurements between CoaguChek XS Plus and STA-R was excellent without significant deviation from linearity. The Pearson's correlation coefficient in all 118 measurements was 0.964 (95% confidence interval [CI], 0.948–0.975; $P < 0.0001$). When the correlation was further assessed in the ranges of 1.0-2.0 INR ($n = 70$) and 2.0-3.0 INR ($n = 38$), the Pearson's correlation coefficient was 0.940 (95% CI, 0.906–0.963; $P < 0.0001$) and 0.759 (95% CI, 0.580–0.868; $P < 0.0001$), respectively (Figure 2).

The mean difference between the INR measurements by STA-R and CoaguChek XS Plus was −0.13 INR. For differences with 95% limits of agreement (1.96 standard deviations [SD] of the mean difference), the STA-R INR measurements differed from the CoaguChek XS Plus INR measurements by −0.54 INR to 0.28 INR. The mean difference of INR measurements tended to increase as INR values increased, and CoaguChek XS Plus exhibited increasing

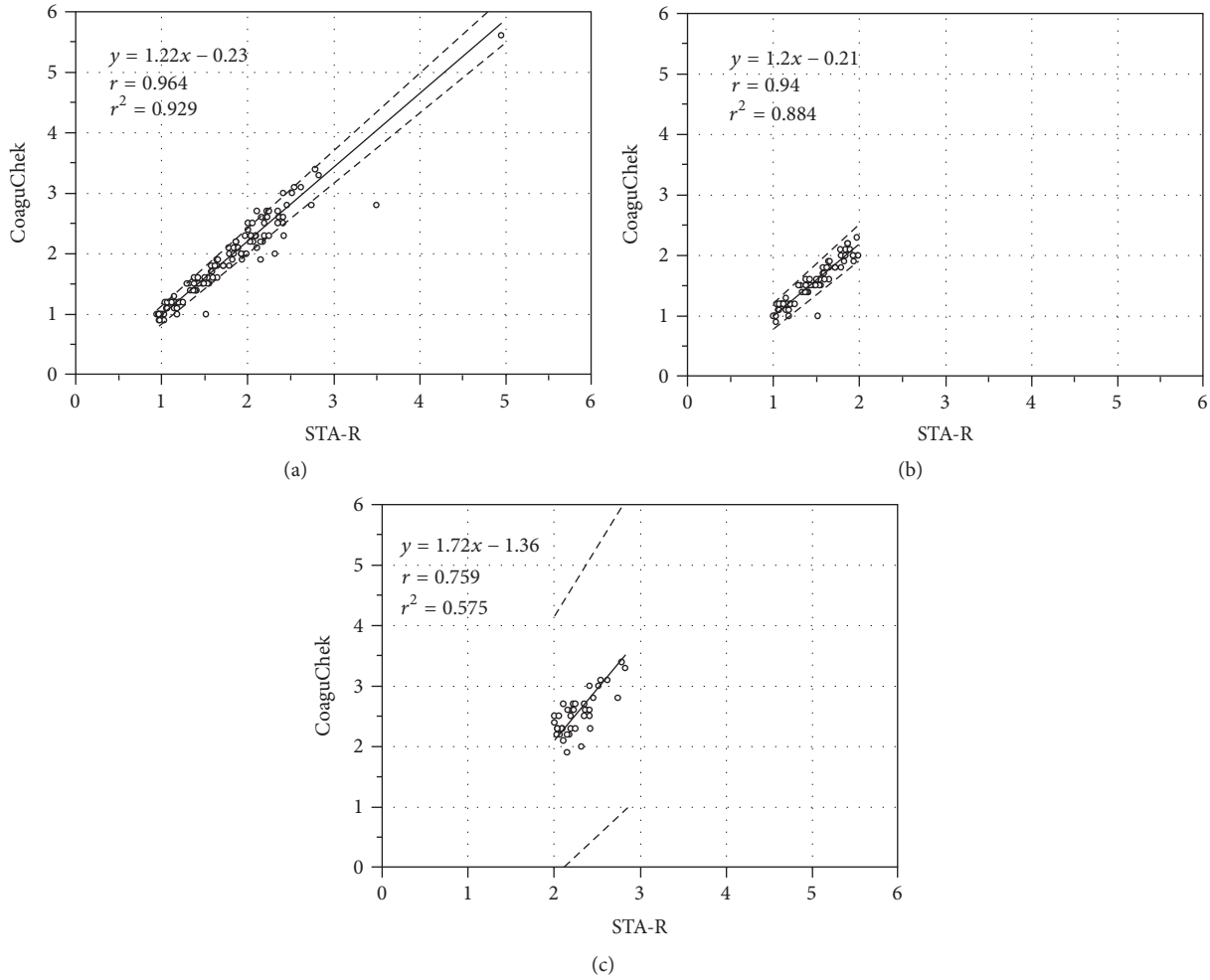

Figure 2: Comparison of INR measurements between the CoaguChek XS Plus and the STA-R using Passing/Bablok regression analysis. The solid lines indicate the regression lines, and the dashed lines indicate the 95% confidence interval (CI). (a) In a total of 118 measurements, Passing-Bablok regression analysis gave a slope of 1.22 (95% CI, 1.16–1.28) and an intercept of −0.23 (95% CI = −0.32–0.14). (b) In the range of INR 1.0-2.0 (n = 70), it gave a slope of 1.20 (95% CI, 1.11 to 1.30) and an intercept of −0.21 (95% CI, −0.35 to −0.9). (c) In the range of INR 2.0-3.0 (n = 38), it gave a slope of 1.72 (95% CI, 1.33 to 2.31) and an intercept of −1.36 (95% CI, −2.36 to −0.48).

Table 1: Agreement of INR measurements between CoaguChek XS Plus and STA-R.

	CoaguChek XS Plus			Total (%)
	INR < 2	INR 2.0-3.0	INR > 3	
STA-R				
INR < 2	65	13	0	78 (66.1)
INR 2.0-3.0	1	31	6	38 (32.2)
INR > 3.0	0	1	1	2 (1.7)
Total (%)	66 (55.9)	45 (38.1)	7 (5.9)	118

Kappa value was 0.679 (95% CI, 0.569–0.790).

positive bias compared with STA-R at higher INR measurements. The mean difference of the INR measurements was −0.08 (±1.96 SD, −0.34–0.18) in the lower range (1.0-2.0 INR) and −0.26 (±1.96 SD, −0.71–0.19) in the higher range (2.0-3.0 INR), respectively (Figure 3).

The agreement of INR measurements between CoaguChek XS Plus and STA-R was further assessed according to the three INR ranges (subtherapeutic, therapeutic, and supratherapeutic ranges) related to dosing decision. The overall agreement was fair to good (kappa = 0.679; 95% CI, 0.569–0.790), and 21/118 (17.8%) INR measurements showed a difference in dosing decision between the two instruments (Table 1).

4. Discussion

Although there have been numerous studies on POCT coagulometers, they were all different in the study designs and statistical analyses, leading to diverse conclusions regarding the precision and accuracy of POCT coagulometers [4, 6, 11, 12]. In a recent review, the precision and accuracy of POCT coagulometers were regarded as generally acceptable for clinical use [11]. On the contrary, another systematic

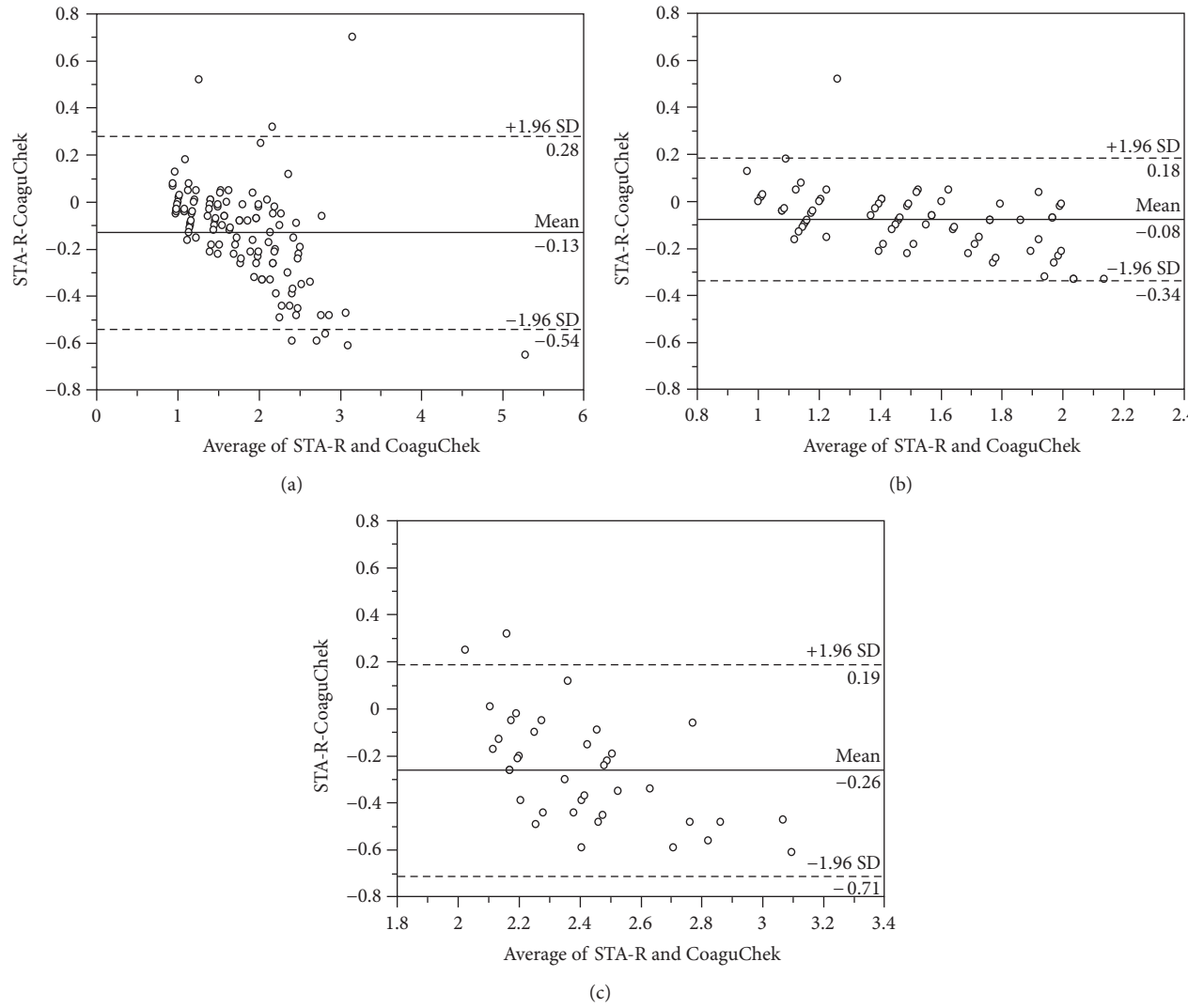

Figure 3: Comparison of INR measurements between the CoaguChek XS Plus and STA-R using Bland-Altman plots in a total of 118 measurements (a), in the range of INR 1.0-2.0 (b), and in the range of INR 2.0-3.0 (c). The difference between two values in the y-axis is plotted against the average of STA-R and CoaguChek XS Plus results in the x-axis. The solid lines represent the mean differences in INR measurements between the two methods, and the dashed lines represent mean difference ±1.96 standard deviation (SD).

review did not provide robust evidence that POCT in general practice improves patient health outcomes and that it has comparable analytical quality to pathology laboratory testing. That review also stated that drawing firm conclusions are also difficult because of the different measurement technologies used for both POCT and in the laboratory [7].

The CoaguChek XS Plus system was designed for use in the professional setting, differently from the CoaguChek XS system designed for use in patient-self testing [13]. Several studies have evaluated the clinical use of the CoaguChek XS Plus system [10, 13–17]. Those studies were performed in different clinical settings using different laboratory-based tests, and only one of them compared the CoaguChek XS Plus system with the Stago coagulation system (Table 2).

Given these various and questionable conclusions in relatively limited literature on the CoaguChek XS Plus, we wanted to get more insight into the issues how interchangeable the INR results by CoaguChek XS Plus and STAR-R are and whether the INR results by CoaguChek XS Plus are reliable enough for monitoring the patients without being confirmed with the laboratory-based test. We found that INR values measured by CoaguChek XS Plus exhibited positive bias as INR values increased. Our results are in line with the previous findings that showed an increased INR difference at higher INR values [10, 18]. In addition to the overall correlation and agreement, we further compared the INR results in the lower INR (1.0-2.0 INR) and higher INR (2.0-3.0 INR) ranges and found profound difference or bias even in the therapeutic INR range (Figures 2 and 3).

Whether POCT INR measurement should be confirmed by the laboratory method or not is still debatable. Some studies insisted that the CoaguChek XS Plus is a reliable tool and dosing decision for vitamin K antagonist therapy may be safely made based on its INR results [13, 16]. On the contrary,

Table 2: Previous studies on the performances of CoaguChek XS Plus system.

Study	Number of measurements	Setting	Laboratory-based system	Comparison using Bland-Altman plot, mean bias (95% limit of agreement)
Deom et al. (2009) [13]	259	Community setting (38 doctor's offices)	Innovin (Siemens/Dade-Behring)	0.03 INR (−0.67 INR ~ 0.74 INR)
Urwyler et al. (2009) [14]	227	Perioperative setting	Innovin (Siemens/Dade-Behring)	2.3% (95% CI = −20.3% ~ 24.9%)
Donaldson et al. (2010) [10]	52	Pharmacist-managed anticoagulation clinic	Stago (Diagnostica-stago)	0.27 INR (−0.33 INR ~ 0.88 INR)
Celenza and Skinner (2011) [15]	293	Emergency department	Not specified	−0.0 INR (−1.1 INR ~ 1.1 INR)
Lawrie et al. (2012) [16]	168 for innovin and 115 for PT-Fib HS+	Overanticoagulated (INR > 4.5) patients in anticoagulation clinic	Innovin (Siemens/Dade-Behring) on CA-7000 analyzer (Sysmex) and PT-Fib HS+ (Instrumentation Laboratory) on CA-1500 analyzer (Sysmex)	Innovin: −0.1% (−22.0% ~ 22.1%) PT-Fib HS+: 8.2% (−21.4% ~ 37.9%)
Urwyler et al. (2012) [17]	73	Pediatric intensive care unit setting	Innovin (Siemens/Dade-Behring)	1.22% (−27% ~ 56%)

Abbreviations: INR: international normalized ratio; SD: standard deviation; CI: confidence interval; PT-Fib HS+: HemosIL PT-Fibrinogen HS Plus.

Celenza and Skinner [15] concluded that although POC INR testing is sufficiently accurate to exclude clinically significant coagulopathy, laboratory-based INR measurements are still required to confirm nonnormal POC INR results, particularly in the supratherapeutic range. One study performed in the setting of anticoagulation clinic also showed that 33% (17/52) of INR measurements with the CoaguChek XS Plus was sufficiently different from the Stago-measured INR values to have resulted in a different therapeutic decision [10]. Noticeably, in the present study, 21/118 (17.8%) INR measurements showed a difference in dosing decision for the anticoagulation therapy between CoaguChek XS Plus and STA-R. Statistically, the agreement between the two instruments was not excellent but just fair to good, with kappa value of 0.679 (95% CI, 0.569–0.790) (Table 1). Our data supports the finding by Donaldson et al. (2010) and implies that dosing decision based on the INR results by CoaguChek XS Plus would be different from that based on the laboratory-based INR results.

In summary, we compared the PT INR results generated by the CoaguChek XS Plus and the STA-R to know how comparable the results would be in the professional hospital setting. This study is limited in that the sample size in the >3.0 INR range was very small. Nevertheless, we observed that the positive bias of CoaguChek XS Plus was obvious even in the therapeutic INR range and dosing decision based on the INR results by CoaguChek XS Plus would be different from that based on the INR results by STA-R. Our data does not support the assumption that POCT coagulometers can be used reliably and safely without being validated with the standard laboratory INR measurements. Even though the use of POCT coagulometers is getting increased in the professional setting, the INR measurements by POCT coagulometers, especially higher INR measurements, still need to be confirmed regularly with the laboratory INR measurements. Further studies with larger sample size and broad INR values would be necessary to confirm our findings.

References

[1] J. Hirsh, J. E. Dalen, D. R. Anderson et al., "Oral anticoagulants: mechanism of action, clinical effectiveness, and optimal therapeutic range," *Chest*, vol. 114, no. 5, supplement, pp. 445S–469S, 1998.

[2] J. R. Petersen, H. M. Vonmarensdorf, H. L. Weiss, and M. T. Elghetany, "Use of error grid analysis to evaluate acceptability of a point of care prothrombin time meter," *Clinica Chimica Acta*, vol. 411, no. 3-4, pp. 131–134, 2010.

[3] A. Holbrook, S. Schulman, D. M. Witt et al., "Evidence-based management of anticoagulant therapy: antithrombotic therapy and prevention of thrombosis, 9th ed: American College of Chest Physicians evidence-based clinical practice guidelines," *Chest*, vol. 141, no. 2, supplement, pp. e152S–e184S, 2012.

[4] R. Loebstein, D. Kurnik, A. Lubetsky, D. Ezra, and H. Halkin, "Potential dosing errors using portable prothrombin time monitoring devices," *Blood Coagulation and Fibrinolysis*, vol. 14, no. 5, pp. 479–483, 2003.

[5] R. D. McBane II, C. L. Felty, M. L. Hartgers, R. Chaudhry, L. K. Beyer, and P. J. Santrach, "Importance of device evaluation for point-of-care prothrombin time international normalized ratio testing programs," *Mayo Clinic Proceedings*, vol. 80, no. 2, pp. 181–186, 2005.

[6] G. W. Moore, A. Henley, S. S. Cotton, S. Tugnait, and S. Rangarajan, "Clinically significant differences between point-of-care analysers and a standard analyser for monitoring the international normalized ratio in oral anticoagulant therapy: a multi-instrument evaluation in a hospital outpatient setting," *Blood Coagulation and Fibrinolysis*, vol. 18, no. 3, pp. 287–292, 2007.

[7] A. Gialamas, A. St John, C. O. Laurence, and T. K. Bubner, "Point-of-care testing for patients with diabetes, hyperlipidaemia or coagulation disorders in the general practice setting: a systematic review," *Family Practice*, vol. 27, no. 1, pp. 17–24, 2010.

[8] J. E. Ansell and K. E. Leaning, Eds., *Capillary Whole Blood Prothrombin Time Monitoring: Instrumentation and Methodologies*, Aspen, New York, NY, USA, 1997.

[9] W. Ageno, A. S. Gallus, A. Wittkowsky, M. Crowther, E. M. Hylek, and G Palareti, "American college of chest physicians. Oral anticoagulant therapy: antithrombotic therapy and prevention of thrombosis, 9th ed: american college of chest physicians evidence-based clinical practice guidelines," *Chest*, vol. 141, no. 2, supplement, pp. e44S–e88S, 2012.

[10] M. Donaldson, J. Sullivan, and A. Norbeck, "Comparison of international normalized ratios provided by two point-of-care devices and laboratory-based venipuncture in a pharmacist-managed anticoagulation clinic," *American Journal of Health-System Pharmacy*, vol. 67, no. 19, pp. 1616–1622, 2010.

[11] T. D. Christensen and T. B. Larsen, "Precision and accuracy of point-of-care testing coagulometers used for self-testing and self-management of oral anticoagulation therapy," *Journal of Thrombosis and Haemostasis*, vol. 10, no. 2, pp. 251–260, 2012.

[12] C. Heneghan, A. Ward, R. Perera et al., "Self-monitoring of oral anticoagulation: systematic review and meta-analysis of individual patient data," *The Lancet*, vol. 379, no. 9813, pp. 322–334, 2012.

[13] A. Deom, G. Reber, D. A. Tsakiris, F. M. Hannes, and W. Plesch, "Evaluation of the CoaguChek XS plus system in a swiss community setting," *Thrombosis and Haemostasis*, vol. 101, no. 5, pp. 988–990, 2009.

[14] N. Urwyler, L. P. Staub, D. Beran et al., "Is perioperative point-of-care prothrombin time testing accurate compared to the standard laboratory test?" *Thrombosis and Haemostasis*, vol. 102, no. 4, pp. 779–786, 2009.

[15] A. Celenza and K. Skinner, "Comparison of emergency department point-of-care international normalised ratio (INR) testing with laboratory-based testing," *Emergency Medicine Journal*, vol. 28, no. 2, pp. 136–140, 2011.

[16] A. S. Lawrie, J. Hills, I. Longair et al., "The clinical significance of differences between point-of-care and laboratory INR methods in over-anticoagulated patients," *Thrombosis Research*, vol. 130, no. 1, pp. 110–114, 2012.

[17] N. Urwyler, E. Staub, L. P. Staub et al., "Point-of-care prothrombin time testing in paediatric intensive care: an observational study of the ease of use of two devices," *European Journal of Anaesthesiology*, vol. 29, no. 2, pp. 75–81, 2012.

[18] C. R. Shiach, B. Campbell, L. Poller, M. Keown, and N. Chauhan, "Reliability of point-of-care prothrombin time testing in a community clinic: a randomized crossover comparison with hospital laboratory testing," *British Journal of Haematology*, vol. 119, no. 2, pp. 370–375, 2002.